Stochastic theory of nonequilibrium steady states and its applications. Part I

Xue-Juan Zhang [a,*], Hong Qian [b,*], Min Qian [c]

[a] Department of Mathematics, Zhejiang Normal University, Jinhua, 321004, Zhejiang, PR China
[b] Department of Applied Mathematics, University of Washington, Seattle, WA 98195, USA
[c] School of Mathematical Sciences, Peking University, Beijing, 100871, PR China

A R T I C L E   I N F O

A B S T R A C T

The concepts of equilibrium and nonequilibrium steady states are introduced in the present review as mathematical concepts associated with stationary Markov processes. For both discrete stochastic systems with master equations and continuous diffusion processes with Fokker–Planck equations, the nonequilibrium steady state (NESS) is characterized in terms of several key notions which are originated from nonequilibrium physics: time irreversibility, breakdown of detailed balance, free energy dissipation, and positive entropy production rate. After presenting this NESS theory in pedagogically accessible mathematical terms that require only a minimal amount of prerequisites in nonlinear differential equations and the theory of probability, it is applied, in Part I, to two widely studied problems: the stochastic resonance (also known as coherent resonance) and molecular motors (also known as Brownian ratchet). Although both areas have advanced rapidly on their own with a vast amount of literature, the theory of NESS provides them with a unifying mathematical foundation. Part II of this review contains applications of the NESS theory to processes from cellular biochemistry, ranging from enzyme catalyzed reactions, kinetic proofreading, to zeroth-order ultrasensitivity.

© 2011 Elsevier B.V. All rights reserved.

Contents

* Corresponding authors.

E-mail addresses: xuejuanzhang@gmail.com (X.-J. Zhang), hqian@u.washington.edu (H. Qian), qianpku@gmail.com (M. Qian).

1. Introduction

Based on the three fundamental laws and the concept of temperature (sometime defined through the zeroth law) classical thermodynamics provides a complete and concise description of the equilibrium state of a closed molecular system — be it a box of gases, a collection of electrons confined in a block of metal, or a test tube of biological macromolecules in aqueous solution [1]. With atoms and molecules in mind, more precisely, according to Gibbs' theory there are several thermodynamically equivalent ways to set up a molecular system: the ensembles [2]. An isolated system has no exchange of energy nor material with its surrounding. A canonical system exchanges energy with its environment at a constant temperature via heat. A grand canonical system can exchange both energy, via heat, and materials with its surrounding at a constant temperature and a constant chemical potential. One example for the last is a dialysis tube with a semi-permeable membrane that contains proteins [3–6].

All the above systems are thermodynamically closed. One essential feature of a closed thermodynamic system is the monotonic increase (or decrease) of its entropy (free energy). This is a hallmark of the destruction of order in a system spontaneously approaching to its equilibrium [7,8]. However, in a real life, especially in biological organisms, many systems

are actually open to exchange of energy and materials with their environment.[1] In contrast to a closed system, an open system exists in a state away from equilibrium even when it reaches its steady state. As has been articulated in I. Prigogine's seminal text [9], nonequilibrium systems can generate self-organized order even without introducing external mechanical forces. While it does not require external *mechanical* force, it is necessary to have an external chemical driving force. This thermodynamic necessity is at the heart of the problem: We are accustomed to macroscopic organization due to mechanical forces; but somehow infinitely surprised by mesoscopic organization due to chemical forces.

Nonequilibrium phenomena are ubiquitous and widely present in physics, chemical reactions, cellular activities and biological systems. We would like to make a clear distinction, however, at the on-set of this review: A significant portion of nonequilibrium phenomena being studied in the literature are "time-dependent" phenomena: There, one is interested in the system's dynamics on its way toward equilibrium. This is not the focus of this review. Rather, we are interested in systems with "driving forces". Further more, we will be mainly interested in the time-invariant stationary behavior of such systems. Two examples, one electrical and one thermal, immediately come to mind: A copper wire connecting a constant electrical battery and an iron bar under a constant temperature gradient across its two ends. A bacteria cell is the chemical version of these two examples: glucose goes in and carbon dioxide and water come out.

What systems are far from equilibrium? What are the basic rules that govern these systems and phenomena? How do we mathematically characterize them? With respect to the first question, Prigogine and the Brussels school have long regarded a stationary nonequilibrium system as a time-invariant open system with positive entropy production rate. However, such a definition is only descriptive. How to measure the entropy production rate? Not satisfied with the above descriptive definition of the so-called nonequilibrium steady state, one of us (M.Q.) and his colleagues at Peking University began to develop a rigorous mathematical treatment shortly after the publication of the celebrated book *Self-Organization in Nonequilibrium Systems: From dissipative structure to order through fluctuations* in 1977 [9]. Now after more than thirty years of effort and endeavor, several basic concepts and rules have been clarified. A comprehensive, but rather mathematical monograph has already been published [10]. The present review is written with the aim of being more accessible to a wider audience in physical and biological sciences.

We assume that a molecular system can be mathematically characterized by a stochastic model: This can be a master equation, a Fokker–Planck equation, or a Markov chain, depending on the nature of the molecular system under study. Within this mathematical framework, the first concept is the distinction between detailed balance that is a consequence of an equilibrium state and nonequilibrium steady state (NESS) in terms of their different mathematical assumptions. In fact, Kolmogorov has already indicated, as early as 1935 [11], the equivalence between the concept of detailed balance originated in physics and the mathematical concept of reversibility of a Markov chain. This deep relation even had been hinted in the original work of Maxwell and Boltzmann. Inspired by this, M. Qian and his colleagues proposed that a nonequilibrium steady state is actually a stationary, irreversible Markov process in mathematical terms.[2]

The second concept emerged from this study reveals the origin of all nonequilibrium phenomena: Dissipation lies in the appearance of *circulation* in a stochastic sense. Cyclic dynamics with rhythms play important roles in a wide range of engineering and biological systems, see texts such as [14,15]. However, to be able to identify such dynamics as a fundamental aspect of any nonequilibrium system in steady state is a very significant insight.

A third theoretical result that is particularly important is the quantification of entropy production rate via a rigorous mathematical formula. One is able to prove that positive entropy production rate is the sufficient and necessary condition for unbalanced circulation. Recall that the Second Law of Thermodynamics has always been an inequality only. Hence, being able to provide a quantitative supplement to the Second Law should have a long-lasting consequence in physics and biology. We shall also point out that the recent development of fluctuation theorems is precisely along a similar line [16]. See also the work of Zia and Schmittmann [17].

All the above mentioned results have been published in research papers and recently summarized in a Springer Lecture Notes in Mathematics (LNM) [10]. However, the LNM has put its main emphasis on the mathematical rigor; the physical meaning of the entire theory of nonequilibrium steady states, thus, is obscured in the logical deductions for the mathematical theorems. Furthermore, the LNM does not contain any example for the applications of the theory in analyzing nonequilibrium phenomena.

The present review, thus, is designed to amend the shortcomings of the LNM. With the recently emerging interests in computational systems biology at cellular level, it is now timely to have a text for physicists, biochemists and applied mathematicians interested in the subject that is mathematically not too involved but at the same time with some detailed applications of theory of NESS. This sets the tone of the review in which we mainly emphasize the mathematical expressions of the theory of NESS as well as its applications in physics and biochemistry. Readers with a minimal amount of background in probability theory and stochastic processes will be easy to follow the physical ideas in mathematical terms.

As in the equilibrium theory of matters where the deeper understanding of thermodynamics relies on a molecular view of fluctuations, the nonequilibrium phenomena can only be fully understood in terms of fluctuations. Therefore, the more

---

[1] Another often made statement is that complex systems are open to information exchange with their surrounding. However, information is only an abstract term; as far as we know its physical bases have to be either energy or material.

[2] In a recent publication [12], a more refined distinction between *mathematical detailed balance* and *chemical detailed balance* of Lewis [13] is introduced and discussed.

effective, probably the best, way to study nonequilibrium systems is to use the method of stochastic processes. After all, this was the choice of Gibbs. There exist several excellent books that deal with nonequilibrium phenomena or the method of stochastic processes, but none of them has combined the two as one coherent theory. For example, Risken, van Kampen, and Gardiner's books are all excellent texts for applying stochastic methods in physics and chemistry [18–20], but there are no focused discussions on nonequilibrium phenomena. The books by Nicolis and Prigogine, Keizer, and Ross [9,21,22], on the other hand, contain a great deal of related materials; but they did not present their theories with a coherent mathematical framework. The recently published *Computational Cell Biology* [23] aims to discuss nonequilibrium phenomena at the cellular level, but it is mainly based on deterministic dynamical systems rather than stochastic mathematics.

Since 1970s, there has been a growing fascination toward driven phenomena in stochastic systems sustained in NESS. H. Haken and his colleagues have developed a successful program for laser physics, which were further developed into the general theory of synergetics [24,25]. The Brussels school's approach has been more rooted in physical chemistry. Two of the most widely studied NESS systems in recent years, stochastic resonance (SR) [26] and molecular motors [27], have their theoretical origins in the earlier work [28]. There are many other systems to which the theory of NESS can be applied; but stochastic resonance and molecular motors are two areas with which we are most familiar. Thus they are the main examples for the applications in the Part I of this review. In the Part II, applications of the theory of NESS to problems in chemical biophysics, via enzyme kinetics, will be presented.

This review is organized as follows. In Section 2, we introduce the background material needed for and the foundations of the theory of NESS. Section 2.1 illustrates the concept of a *mesoscopic system* using an enzymatic reaction as an example. Section 2.2 discusses the equilibrium and nonequilibrium steady state properties of a mesoscopic system from a statistical thermodynamic point of view. Section 2.3 presents the mathematical background for mesoscopic systems in terms of a discrete Markov jump (Q) process (i.e., master equation). It derives the basic properties of equilibrium state and NESS through a more rigorous mathematical treatment. In Section 2.4, the discussion is extended to diffusion processes and NESS in continuous stochastic systems. In particular, we discuss one-dimensional stochastic dynamics on a circle. This is a very unique topic which offers a great deal of insights to the general problem of NESS. All the materials in Section 2 provide the theoretical foundations for the applications in the subsequent Sections 3 and 4.

In Section 3, we study the coherence resonance (CR), also widely known as SR without forcing. As we shall show, the theory of NESS indeed sets the mathematical foundation for the exciting phenomenon. In Section 3.1, we first give a general introduction that distinguishes the two types of SR: the traditional SR which occurs under the interplay of noise and a weak deterministic periodic forcing, and the CR which occurs with only noise perturbation. In Section 3.2, the nonequilibrium nature of CR is investigated in several excitable systems that include a simple phase model, the integrate-and-fire model, as well as the FitzHugh–Nagumo model. We shall also discuss CR in a single Hodgkin–Huxley neuron with intrinsic noises aroused from the stochastic opening and closing of membrane channels. We show that the phenomena of CR, whether the noise is from external environmental perturbations or intrinsic molecular fluctuations, is always originated in the nonequilibrium circulation in a NESS. In Section 3.3, we investigate the traditional SR in a typical bistable system and a periodically driven overdamped pendulum model. We show that one can map a non-autonomous periodically driven system to a high-dimensional autonomous one. Therefore, there is no fundamental difference between SR and CR. We further explore the phenomena of CR and SR in coupled oscillators in Section 3.4. It is found that both CR and SR are greatly enhanced in the coupled systems.

Section 4 is devoted to the application of the NESS theory to Brownian motors. In Section 4.1, we presented a brief introduction of the noise-induced unidirectional transport in a spatially periodic but asymmetric potential. Due to the periodic nature of the problem, the dynamical framework of the Brownian ratchet is stochastic dynamics on the torus, as illustrated in Section 4.2. The relationship between probability flux, rotation number, and the mean velocity of a Brownian ratchet are discussed in Section 4.3. These sections prepare us for Section 4.4, which investigates the unidirectional transport of a Brownian ratchet in a spatially periodic but asymmetric potential and its corresponding dynamics. It is shown that the direction and velocity of the unidirectional movement are closely related to the relative position of stable and unstable limit cycles on a cylinder. Section 4.4 studies the unidirectional transport in coupled diffusion systems, which model motor proteins, such as a kinesin moving along a microtubule with conformational transitions. In the presence of both periodic driving and white noise forces, the motor undergoes either positive unidirectional transport or negative unidirectional transport, depending on the amplitude of the driving force. In Section 4.6, we study the efficiency of energy transduction by Brownian ratchet. It is illuminating to discover that the efficiency of free energy transduction can be expressed exactly in terms of the entropy production rate of a Brownian ratchet during the process of transport against a load. This demonstrates the fundamental role the NESS theory plays in Brownian motors. Section 5 provides some concluding remarks and outlook. In the Appendices, some detailed mathematical materials are presented.

2. An introduction to nonequilibrium steady states

2.1. Microscopic, macroscopic and mesoscopic systems

We assume our readers have some familiarity with the terminology of *macroscopic world* and *microscopic world*: The former usually refers to material in our daily life that is described by a handful of variables (e.g., volume, temperature, total

internal energy), even though it consists a large number of particles (10^{19}–10^{23}!). The latter usually refers to a complete molecular (or atomic) description of all the particles in the system, in terms of their positions and momenta. To some other authors, these two terms are related to the classical world and the quantum world. In recent years, one often hears also the term *mesoscopic*. The prefix *meso-* means "middle" or "intermediate" [29]. First introduced by van Kampen [30], physicists now use mesoscopic systems to describe a physical world that is between classical and quantum physics [31], or between the few-variable description and the complete molecular description.

In this review, our usage of the term "mesoscopic" is in line with Laughlin et al. [29]. What we are concerned with is a class of molecular systems widely observed in biology, whose configurational states change with the evolution of time. For example, in biochemical reactions, an enzyme can exist in either a state that without binding anything or in a state that binding a substrate (or a product) molecule. The latter is widely known as enzyme–substrate (-product) complex. In cell membrane, almost all the ion channel proteins switch between open and close states that allow or forbid specific ion passing through. These systems cannot be simply categorized as macroscopic or microscopic: They are not macroscopic since it is only one or few protein molecules; they are not microscopic since the proteins are immersed in aqueous fluid or sea of lipids; there are very large number of atoms in the molecular systems. We, thus, prefer to call these systems mesoscopic. We shall further clarify this concept below. Perhaps the best known theory of mesoscopic systems, according to our usage, is the polymer theory developed by P.J. Flory, B.H. Zimm, and P.-G. de Gennes [32].

Let us first review the concepts of *microscopic states* and *macroscopic states* which can be found in any textbook on statistical physics [33]. In principle, the true dynamics of a microscopic system follows quantum mechanics. To avoid unnecessary additional knowledge of quantum mechanics, however, we shall confine ourselves to consider only classical physics. Consider a system consisting of r, an enormous number (on the order of 10^{23}) of particles such as molecules and atoms. From the standpoint of classical mechanics, the state of each individual particle can be represented by its three-dimensional coordinate $\vec{q}$ and momentum $\vec{p}$. If we know the mechanical states of each individual particle at any fixed time t, then the state of such a system can be determined by the values of r generalized coordinates $\vec{q}_1, \vec{q}_2, \ldots, \vec{q}_r$ and r generalized momenta $\vec{p}_1, \vec{p}_2, \ldots, \vec{p}_r$ at this time. Hence, **a microscopic state** of a multiple-particle system is a representative point in a $6r$-dimensional phase space.

According to the laws of classical mechanics, the microscopic evolution of a macroscopic system can be described by a trajectory in the $6r$-dimensional phase space. However, due to the extremely complex and intractable motions of the many-body system, it is impossible to describe the microscopic motion of such a system just by applying the classical mechanical theory which requires solving an enormous number of differential equations.[3] The behaviors and properties of a macroscopic system we observed in daily life are basically the consequences of the interacting microscopic particles. It is sufficient to give a macroscopic description of the system by statistically averaged method based on the fundamental mechanical properties such as positions and momenta of microscopic particles [34,35]. This is the subject of statistical physics, which connects the macroscopic quantities with the microscopic states of a multi-particle system. In statistical physics, **a macroscopic state** of a system is a *complete* macroscopic description in terms of temperature, pressure and internal energy etc., under some thermodynamical assumptions. A macroscopic state corresponds to many microscopic states. A "complete description" is determined depending upon the particular problems to be studied [33]. Classical statistical mechanics, however, can only deal with systems that are under thermodynamic equilibrium. In the language of systems biology, equilibrium statistical physics is about the intrinsic properties of macroscopic matters; it is not about a functional system.

To illustrate the concept of mesoscopic state, let us consider the biochemical reaction of adenosine triphosphate (ATP) hydrolysis. Inside living cells this reaction is the central energy generator for all the other processes [36]. In terms of atoms, ATP is a nucleotide formed by attaching three phosphate groups at the 5' carbon atom of a pentose sugar. It is an extremely important molecule since its hydrolysis reaction powers the gene expression, cell division, biosynthesis, signal transduction, etc. In Section 4, we shall study a nonequilibrium phenomenon of how ATP providing chemical energy to drive a class of proteins called molecular motor that, by a single molecule, moves unidirectional along its linear track.

To fulfill all the important functions of ATP in a living cell, however, the hydrolysis reaction has to have the participation of the enzyme called ATPase and/or kinase. They are macromolecules (biopolymers). In the presence of the enzyme, ATP in aqueous solution is quickly hydrolyzed into ADP (adenosine diphosphate) plus Pi (inorganic phosphate), and free energy in the "chemical gradient" (see below) is released. For simplicity, we write the ATP hydrolysis process as follows:

$$M + ATP \underset{\beta_1}{\overset{\alpha_1}{\rightleftharpoons}} M \cdot ATP, \tag{1a}$$

$$M \cdot ATP \underset{\beta_2}{\overset{\alpha_2}{\rightleftharpoons}} M \cdot ADP \cdot Pi, \tag{1b}$$

$$M \cdot ADP \cdot Pi \underset{\beta_3}{\overset{\alpha_3}{\rightleftharpoons}} M \cdot ADP + Pi, \tag{1c}$$

$$M \cdot ADP \underset{\beta_4}{\overset{\alpha_4}{\rightleftharpoons}} M + ADP. \tag{1d}$$

---

[3] Nevertheless, such an approach is one way to study mesoscopic systems. The method is called *molecular dynamic* (MD) simulations which have enjoyed a great deal of applications in molecular biophysics and material sciences.
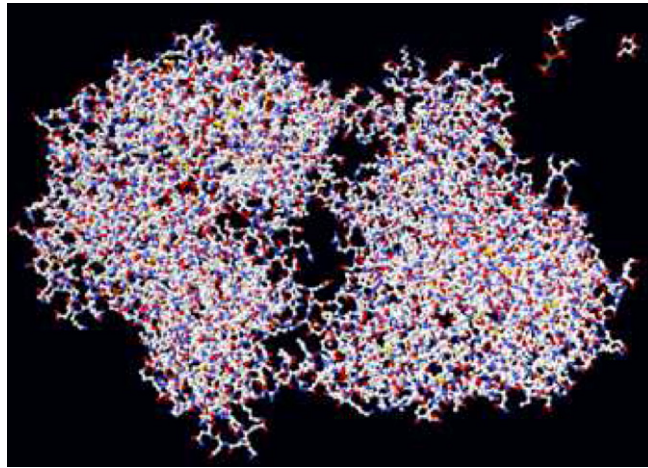
Fig. 1. An image of a structural model, made of balls and sticks, of protein molecule *hexokinase*, a key enzyme in cellular glycolysis process. On the top right-hand corner are ATP and glucose, two small molecules which are substrates of the enzyme. Carbon atoms are in white, oxygens are in red, nitrogens are in blue, and phosphorus atoms are in orange. (For interpretation of the references to colour in this figure legend, the reader is referred to the web version of this article.)
Source: Copied from online Wikipedia http://en.wikipedia.org/wiki/Protein.

In the first equation, the forward direction says that the enzyme M is associated with ATP to form a complex M·ATP, while the backward direction refers to the dissociation of the enzyme M and ATP. The second reaction represents the catalyzed hydrolysis of ATP into ADP plus Pi when they are bound with the enzyme. The third reaction is for the Pi to leave the ternary complex M·ADP·Pi. In the last reaction the ADP is dropped off from the complex M·ADP, and the enzyme is recovered to its original state. The parameters α_i and β_i ($1 \leq i \leq 4$) refer to the forward and backward chemical reaction rate constants according to the Law of Mass Action. Some of them, the first-order rate constants, have a dimension of $[\text{time}]^{-1}$, and other, the second-order rate constants, have a dimension of $[\text{concentration}]^{-1}[\text{time}]^{-1}$. Chemical rate constants are different from the transition probability rates in a Markov model (see below).

Inside a cell there are many copies of the enzyme M, some of which are by itself, while others are in the ternary complex with ADP and Pi. We shall regard M, M·ATP, M·ADP·Pi and M·ADP as four different "conformational states" of an enzyme molecule, denoted as M_1, M_2, M_3, M_4, respectively. This definition is motivated by well-established biophysical studies of enzyme kinetics of ATP hydrolysis. Fig. 1 shows that each state of the enzyme is a collection of large number of atoms. Furthermore, all the atoms, as well as water molecules around the enzyme, are in constant thermal motion. Therefore, we can treat the "ensemble" as a macroscopic system. This can be done for each of the four states.

If the concentrations of ATP, ADP, and Pi are much greater than that of the concentration of the enzyme, then each copy of the enzyme is essentially independent of other copies. In this case, we only have to track one enzyme. Its dynamics is stochastic due to all the microscopic motions of the atoms within. In fact, it is impossible to determine completely the positions and the momenta of all the atoms at time t from only knowing that the enzyme being in mesoscopic conformational state i ($1 \leq i \leq 4$) at time zero; neither can we know for certain what the conformational state of the enzyme is at time t. However, both empirical evidences and Kramers' theory for chemical reactions [37] state that the enzyme conformation changes by "jumping" from one of the four possible states to another with certain transition probability. We, thus, can write the conformational dynamics of a single enzyme as

$$\boxed{1}_{\substack{k_{+1} \\ \text{M} \underset{k_{-1}}{\rightleftharpoons}}} \boxed{2}_{\substack{k_{+2} \\ \text{M·ATP} \underset{k_{-2}}{\rightleftharpoons}}} \boxed{3}_{\substack{k_{+3} \\ \text{M·ADP·Pi} \underset{k_{-3}}{\rightleftharpoons}}} \boxed{4}_{\substack{k_{+4} \\ \text{M·ADP} \underset{k_{-4}}{\rightleftharpoons}}} \boxed{1}_{\text{M}}, \tag{2}$$
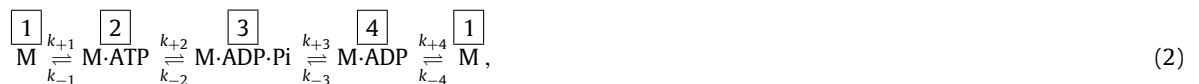
where $k_{\pm i}$ are the transition probability rates.

The "chemical kinetic scheme" in Eq. (2) is in fact a stochastic Markov model for the conformational transition of a single enzyme.[4] We know the probability of the occurrence of each conformational state if we know the probability of its initial state. A macromolecule such as an enzyme that consists of a large number of atoms can be understood in the macroscopic terms. For this reason, we call such a system a mesoscopic system, and the conformational states are correspondingly called mesoscopic states. The mesoscopic system is interpreted in a probability sense, which exhibits certain degree of uncertainty of the occurrence of the system's conformational states. **A mesoscopic system** will undergo different conformational states with the evolution of time, stochastically. We can study this dynamics from the transition rates between these conformational states, and its statistical properties from the time evolution of the probability distribution of the system being in different states.

---

[4] A more fundamental approach that justifies this entire mesoscopic approach is the theory of Kramers [37,38].

2.2. Equilibrium and nonequilibrium properties of mesoscopic systems

In this section, we shall explore the equilibrium and nonequilibrium properties of mesoscopic systems from two different angles, but both reach the same conclusions at the end. Let us first consider a liquid system containing N different components e.g. $M_1, M_2, \ldots, M_N$. Suppose that the system keeps in a close contact with a large heat bath with constant temperature T and pressure P, i.e., the system considered is in an isothermal and isobaric surrounding. For simplicity, the concentration of every substance is assumed to be independent of its position, and there is no external input or output of mechanical energy.

In classical thermodynamics, one frequently talks about *reversible processes*. These are processes that can be "reversed" by means of infinitesimal rate of change in some property of the system without loss or dissipation of energy [39]. Due to these infinitesimal rate of change, the system is in equilibrium throughout the entire process. All the properties of a reversible process are derived from the Laws of Thermodynamics. The First Law is about the conservation of energy in a physical system. For a single-component system, it is stated as

"The increment of the internal energy of a system is equal to the amount of energy added by heating the system, minus the amount of lost as a result of the work done by the system on its surroundings."

Mathematically, the First Law is expressed in the following equation

$$dU = \delta Q - \delta W, \tag{3}$$

where U is the internal energy, and dU is the infinitesimal increase of the internal energy. As one knows that the internal energy U is a state function while heat Q and work W are not. The latter are dependent upon a physical process. We using δQ to represent the infinitesimal amount of heat obtained by the system, and δW the infinitesimal amount of work done by the system, through the process.

When a system is doing work against its surrounding only in the form of volume change, $\delta W = PdV$ where P is the pressure on the system. For a system at temperature T and when an amount of heat δQ is absorbed, Clausius introduced a quantity $dS \overset{\triangle}{=} \delta Q/T$, and gave S a name called *entropy*. S is a state function which is central to the Second Law of Thermodynamics. The Second Law tells us about the time evolution of thermodynamic systems. It is stated as

"The total entropy of an isolated thermodynamic system tends to increase over time, until reaching a maximum. For a thermodynamic system exchanging heat with its surrounding at temperature T, $dS \geq \delta Q/T$."

Combining the First and the Second Laws gives us an important thermodynamics equation for the state variables:

$$dU + PdV - TdS \leq 0. \tag{4}$$

A process is reversible if and only if the equality holds in the above equation.

A system undergoing reversible processes has a well defined characteristic function called Gibbs function, or *Gibbs free energy*, which is a thermodynamic potential expressed as

$$G = U + PV - TS. \tag{5}$$

Then the total differential of G

$$dG = dU + PdV + VdP - TdS - SdT. \tag{6}$$

If the thermodynamic system is under constant T and P, then $dT = dP = 0$ and

$$(dG)_{T,P} = dU + PdV - TdS \leq 0. \tag{7}$$

That is, a spontaneous irreversible process of any macroscopic system under constant T, P intends to decrease the value of G:

$$(dG)_{T,P} \leq 0, \quad \text{and} \quad (dG)_{T,P} = 0 \quad \text{iff the process is reversible.} \tag{8}$$

Eq. (5) is valid only for systems with single component and constant number of particles. For a multi-component system, the number of particles of each component in the system may not be constant. Let n_i be the number of particles in the ith component, then the system's volume V, internal energy U, and entropy S are all functions of the temperature T, pressure P and the number of molecules n_i:

$$V = V(T, P, n_1, \ldots, n_N),$$
$$U = U(T, P, n_1, \ldots, n_N),$$
$$S = S(T, P, n_1, \ldots, n_N).$$

The First Law is then expressed as:

$$dU = \delta Q - \delta W + \sum_{i=1}^{N} \mu_i dn_i. \tag{9}$$

Each component has a chemical potential μ_i (see Eq. (12) below), and the internal energy changes when the number of particles change. The Gibbs free energy of an equilibrium state can be expressed as $G = G(T, P, n_1, \ldots, n_N)$. In such a case,[5]

$$dG = -SdT + VdP + \sum_i \mu_i dn_i. \tag{10}$$

For an isothermal and isobaric system, the increment of the Gibbs free energy is:

$$(dG)_{T,P} = \sum_i \mu_i dn_i, \tag{11}$$

where $\mu_i = (\partial G/\partial n_i)_{T,P,n_j}$ is called the chemical potential of the ith component [40]. It represents the increment of Gibbs free energy of the system as the number of particles of the ith component increases by 1 but all other variables such as the temperature, the pressure and the molecule numbers of other components are kept constant. In other words, the "chemical potential" μ_i is a measure of how much the free energy of a system changes if one adds or removes one particle of the ith component.

A macroscopic system is said to reach a thermodynamic equilibrium if the system reaches thermal equilibrium (i.e., the temperatures of different parts are the same), mechanical equilibrium (i.e., all the parts have the same pressure) and chemical equilibrium (i.e., all the components in exchange reaches same chemical potential) [40]. For a system which keeps in close contact with a heat bath and excludes any work done due to volume change, it naturally satisfies thermal equilibrium as well as mechanical equilibrium. Hence as long as a macroscopic system reaches a chemical equilibrium, then it is in thermodynamic equilibrium. When a system reaches chemical equilibrium, the chemical potentials of different components are the same, i.e.,

$$\mu_i = \mu_j, \quad \forall \ i \neq j. \tag{12}$$

The equilibrium characteristics of a system with components $M_1, M_2, M_3, \ldots, M_N$ can be discussed in the framework of a multi-component single-phase system.

According to physical chemistry theory [40], we have[6]

$$\mu_i = \mu_i^0 + k_B T \ln[M_i], \quad i = 1, 2, 3, 4, \tag{13}$$

in which $[M_i]$ is the concentration of the ith component, μ_i^0 is the standard chemical potential which is independent of the concentration of the ith component. k_B is Boltzmann's constant and T is temperature in Kelvin. Actually, μ_i^0 is a basic free energy which can be understood as the Gibbs free energy per particle when the system consists only one component. Hence if an aqueous system contains only M_i, the Gibbs free energy of the system is just the basic free energy multiplied by the concentration of the component, i.e., $G_i = [M_i] \cdot \mu_i^0$.

It follows from formulas (12) and (13) that at chemical equilibrium:

$$\mu_i^0 + k_B T \ln[M_i] = \mu_j^0 + k_B T \ln[M_j], \quad \forall i \neq j. \tag{14}$$

Hence for an macroscopic system in equilibrium, the ratio of concentrations of any two different components satisfies

$$\frac{[M_i]}{[M_j]} = e^{-\frac{\mu_i^0 - \mu_j^0}{k_B T}}. \tag{15}$$

It is worth mentioning that in equilibrium, it is still possible for chemical reactions between different components to take place. Considering a chemical reaction between reactants M_i and M_j, let r_{ij} and r_{ji} be the reaction rate constants of $M_i \rightarrow M_j$ and $M_j \rightarrow M_i$, respectively. Then the number of particles transferring from M_i to M_j in unit time is $r_{ij}[M_i]$, and that from M_j to M_i is $r_{ji}[M_j]$. Hence the net number of particles from $M_i \rightarrow M_j$ is

$$r_{ij}[M_i] - r_{ji}[M_j].$$

According to the Law of Mass Action in chemical kinetics [41], the concentration $[M_i]$ of the ith component satisfies the following differential equation

$$\frac{d[M_i]}{dt} = \sum_{j \neq i} (-r_{ij}[M_i] + r_{ji}[M_j]). \tag{16}$$

---

[5] From Eq. (6), it should be clear that the term $(dG)_{T,P}$ in Eq. (7) is for a *nonequilibrium changing* system under constant T, P. However, in Eq. (7), dG is the difference of G for two *equilibrium states* of the system with different T and P. The former is about irreversibility, the latter is about equilibrium states.

[6] The hidden assumption of the following equation is that the M_i are ideal solution in a liquid system. This poses no problem for all the applications to mesoscopic systems with dilute macromolecular concentrations.

If $\frac{d[M_i]}{dt} = 0$ ($i = 1, 2, \ldots$), then the concentration of every component of the considered system is invariant with the evolution of time. Such a system is said to be in a steady state. However, a real equilibrium state should be such a state that not only the concentration $[M_i]$ is invariant with time, but also there is no net current of particles, i.e., besides satisfying

$$\frac{d[M_i]}{dt} = 0, \tag{17}$$

the system is required to obey the following condition

$$r_{ij}[M_i] = r_{ji}[M_j], \quad \forall\, i, j. \tag{18}$$

In statistical physics, such a system is said to be in equilibrium, and Eq. (18) is known as detailed balance. The concept of detailed balance was first introduced by Boltzmann [42] as a way of maintaining thermodynamic equilibrium.

A steady state with $\frac{d[M_i]}{dt} = 0$ is still possible for a net current between states i and j to exist. *We call a state that satisfies*

$$\frac{d[M_i]}{dt} = 0, \quad \forall\, i$$

but for some i, j,

$$r_{ij}[M_i] \neq r_{ji}[M_j]$$

a nonequilibrium steady state (NESS). More detailed discussions of the NESS will be presented later.

For the ATP hydrolysis process discussed before, we have studied the equilibrium and nonequilibrium characteristics of the system from the viewpoint of classical thermodynamics by treating the system as a multi-component system. In the following, however, we will take the enzyme M as a *single molecule*. We regard the M, M·ATP, M·ADP·Pi and M·ADP as four possible states of an enzyme, denoted as 1, 2, 3, 4. From this point of view, the state of the system (i.e., the state of a mesoscopic single particle M) at time t is one of these four states. The system is stochastic. If the state of the enzyme M at time t is realized for a large number of times, then the concentration of the component M_i mentioned above corresponds to the probability distribution of the enzyme at state i. In this way, one can describe the chemical reactions in an aqueous system from the viewpoint of a mesoscopic system and its probability distribution among different states, and how the system transforms, i.e., moves, from one state to another. This in fact is what single-molecule chemical kinetics about [43].

For the sake of generality, we consider a mesoscopic system with N possible states $1, 2, \ldots, N$ and an initial distribution $\{p_1(0), \ldots, p_N(0)\}$. Suppose that the probability density of the system in state i at time t is $p_i(t)$, and the transition probability from state i to j in unit time is q_{ij}, then corresponding to the chemical reaction described by Eq. (16), we have the following master equation concerning the probability distributions of the states

$$\frac{dp_i(t)}{dt} = \sum_{j \neq i} \left(-p_i(t) q_{ij} + p_j(t) q_{ji} \right). \tag{19}$$

Parallel to the detailed balance condition in (18) for a macroscopic system, a mesoscopic system is said to be in equilibrium if and only if there exists an invariant distribution $\vec{\pi} = (\pi_1, \ldots, \pi_N)$ and the system satisfies the detailed balance condition: $\pi_i q_{ij} = \pi_j q_{ji}$. If a mesoscopic system has an invariant distribution $\vec{\pi}$, but for some i, j, $\pi_i q_{ij} \neq \pi_j q_{ji}$, then it is said to be in a nonequilibrium steady state (NESS).

An equilibrium mesoscopic system fixed in a certain state i can be considered as a "pure, homogeneous" solution, hence it can be endowed with relevant thermodynamical quantities such as Gibbs free energy. Parallel to Eq. (13), the Gibbs free energy of a mesoscopic system in a given state consists of two parts: a basic free energy term μ_i^0, which is determined by the molecular structure of state i, and an entropy contributed from the probability. Note that logarithm of the probability is precisely the Boltzmann's entropy. Thus, the Gibbs free energy of state i

$$\mu_i = \mu_i^0 + k_B T \ln(\pi_i). \tag{20}$$

Because the free energies of different states in an equilibrium mesoscopic system are equal, i.e., $\mu_i = \mu_j$, then

$$\frac{\pi_i}{\pi_j} = e^{-\frac{\mu_i^0 - \mu_j^0}{k_B T}}. \tag{21}$$

Eq. (21) shows that the equilibrium distribution of a mesoscopic system obeys Boltzmann distribution, i.e.,

$$\pi_i = \frac{e^{-\mu_i^0 / k_B T}}{\sum_i e^{-\mu_i^0 / k_B T}}. \tag{22}$$

In statistical physics, the theory of equilibrium systems has been well established with wide and successful applications to nontrivial problems such as complex fluids and critical phenomena. Nonequilibrium studies in general focus on fluctuations and relaxations near equilibrium state. For a very long time, researchers mainly focused on closed systems, i.e. the dynamical

processes approaching an equilibrium. Along this line, L. Onsager's work on linear irreversibility is particularly worth noting [44]. However, it becomes clear in recent years that the more interesting systems are in fact those that are far from equilibrium state.

In this section, we shall give a probabilistic description of mesoscopic systems in terms of Markov chains with discrete states and continuous time parameters. This is widely known as master equation in physics literature. We apply the theory of Markov chains to discuss the basic, statistical properties of equilibrium and nonequilibrium states of mesoscopic systems. The discussion then will be further extended to diffusion processes, Markov processes with continuous states and time, on a circle. Studying one-dimensional dynamics on a circle rather than on $\mathbb{R}^1$ is an approach first taken in the theory of nonlinear dynamical systems. As we shall see, it offers greater insights with less amount of mathematics.

Let $\xi(t)$ be the state of a mesoscopic system at time t. At any given time only the probabilities of the system being in different states are known; $\xi(t)$ is a random variable taking discrete values in $\{1, 2, \ldots, N\}$. Following the evolution of time, one observes a stochastic process $\{\xi(t)\}_{t\geq 0}$ with state space $\{1, 2, \ldots, N\}$. For most applications, $\{\xi(t)\}_{t\geq 0}$ is a process without long memory. Taking the state transitions of a single enzyme M in an aqueous solution for example, the particle M in a ATP hydrolysis reaction will undergo the following states:

$$\boxed{1} \qquad \boxed{2} \qquad \boxed{3} \qquad \boxed{4} \qquad \boxed{1}$$
$$\mathrm{M} \rightleftharpoons \mathrm{M \cdot ATP} \rightleftharpoons \mathrm{M \cdot ADP \cdot Pi} \rightleftharpoons \mathrm{M \cdot ADP} \rightleftharpoons \mathrm{M} \ .$$

When M is in state i (e.g. state M·ADP), it can only transfer to state $i - 1$ (M·ADP·Pi) or state $i + 1$ (M), here states -1 and $N + 1$ correspond to states N and 1, respectively. Let $t_1, t_2, \ldots,$ be the time that the particle M switches its states. Generally, we suppose that the state of M at time t_{n+1} only depends on the state at time t_n, but not on the ones before time t_n. Such a property is called Markov property, i.e., knowing the current state, the statistical law of the future of a system is independent of its past.[7] Rigorous definition will be presented in the subsequent section.

We shall discuss exclusively stochastic dynamics following Markov processes. There is also a large literature on non-Markov dynamics with applications to, among other subjects, enzyme dynamics [45]. Semi-Markov processes, also known as continuous time random walk (CTRW), has also been extensively studied in the past. The reversibility of semi-Markov processes, however, is not as completely developed as for Markov processes. Thus we shall not present the non-Markov models. Interested readers are referred to [46,47] and cited references within.

In the following sections, we shall see that the NESS of a mesoscopic system and the irreversibility of a Markov process are in fact two representations of the same entity. Markov theory is the appropriate mathematical framework for nonequilibrium mesoscopic systems.

2.3. Description of a mesoscopic system in terms of a continuous time Markov (Q) process

2.3.1. Preliminary material

In the mathematical theory of probability, a stochastic process is defined on a suitable probability space $(\Omega, \mathcal{F}, P)$. To have an intuitive understanding of the space $(\Omega, \mathcal{F}, P)$, let us take the previously mentioned single enzyme molecule M as an example. It is treated as a *mesoscopic system* whose dynamics is stochastic due to its incessant random collisions with the aqueous solvent. The state of M changes with time stochastically, and there are different probabilities for the occurrence, i.e., realization, of different trajectories. The time-dependent random states of the molecule M is a *stochastic process*. All the possible trajectories form a sample space Ω. Clearly, the dimension of this space is infinite since the trajectories are infinitely long. For a given trajectory $\omega \in \Omega$ space, its state at time t is $\xi_t(\omega)$: It is a *deterministic* function of ω with parameter t; the randomness is only in the ω. The trajectory ω here is the elementary random event, and $\Omega = \{\omega\}$. The stochastic process defined on Ω is $\{\xi_t(\omega)\}_{t\in R}$: For a fixed time t, $\xi_t(\cdot)$ is a random variable; with the evolution of time, one observes the trajectory $\xi_\cdot(\omega)$.

The sample space can be understood in a more intuitive way. Consider there are a large number of independent enzyme copies, each of which is jumping among the four different states. If the state of every enzyme can be written down at any time t, then with time evolution, we observe many different trajectories in t–ξ plane. They are discontinuous with respect to time t. The set of all trajectories, extending to time infinity, is the sample space Ω.

A.N. Kolmogorov has proved that if $\forall t_1 < t_2 < \cdots < t_n$, and the joint probability distribution of any finite random variables $(\xi_{t_1}(\omega), \xi_{t_2}(\omega), \ldots, \xi_{t_n}(\omega))$ are known, then one can obtain all statistical laws of the stochastic process $\{\xi_t(\omega)\}_{t\in R}$. The $\mathcal{F}$ in the triplet $(\Omega, \mathcal{F}, P)$ is a set whose elements are all the Ω's subsets that can be furnished reasonably with a probability, and P is a probability measure defined on such subsets.

2.3.2. Q-process description of mesoscopic systems

In the previous section, we have established a Markov jump process as the mathematical representation of a mesoscopic system with finite states. In the following, we shall discuss the characteristics of NESS of mesoscopic systems in terms of Q-processes.

---

[7] Markov property is the stochastic version of first-order dynamical systems. As in the case of a differential equation with higher order but finite, it can always be transformed into a first-order system in a space with higher dimension.

2.3.2a. Basic expressions for equilibrium and nonequilibrium steady states. When a mesoscopic system reaches equilibrium, it has a steady distribution

$$\pi_i = \frac{e^{-\mu_i^0/k_BT}}{\sum_i e^{-\mu_i^0/k_BT}}, \quad i = 1, 2, \ldots, N, \tag{23}$$

and it satisfies the detailed balanced condition

$$\pi_i q_{ij} = \pi_j q_{ji}, \quad \forall\, i \neq j. \tag{24}$$

It follows from Eq. (23) that $\pi_i/\pi_j = \exp[-(\mu_i^0 - \mu_j^0)/k_BT]$, together with condition (24), we have

$$\frac{q_{ij}}{q_{ji}} = e^{\frac{\mu_i^0 - \mu_j^0}{k_BT}}. \tag{25}$$

Let $\mu_{ij}^0 \overset{\triangle}{=} k_BT \ln(q_{ij}/q_{ji})$, which is called the chemical force associated with transition from state i to state j. Eq. (25) states that $\mu_{ij}^0 = \mu_i^0 - \mu_j^0$. Hence for an equilibrium mesoscopic system,

$$\mu_{i_1 i_2}^0 + \mu_{i_2 i_3}^0 + \cdots + \mu_{i_s i_1}^0 = 0, \tag{26}$$

which means that μ_{ij}^0 corresponds to a potential function. In general, we say a chemical force having a potential if there exists a function Φ defined on a state space, such that $\mu_{ij}^0 = \Phi(i) - \Phi(j)$. It can be proved that **a mesoscopic system reaches equilibrium if and only if the chemical force μ_{ij}^0 corresponds to a potential, and if and only if μ_{ij}^0 satisfies** Eq. (26).

We now consider the situation of NESS. It should be kept in mind that the concept of free energy of a state for an equilibrium system is no longer valid now, i.e. $\mu_{ij}^0 \neq \mu_i^0 - \mu_j^0$. Nevertheless, there is free energy difference $\Delta\mu_{ij}$ between any two states i and j:

$$\Delta\mu_{ij} = \mu_{ij}^0 + (k_BT \ln \pi_i - k_BT \ln \pi_j) = \mu_{ij}^0 + k_BT \ln \frac{\pi_i}{\pi_j}. \tag{27}$$

This corresponds to a non-gradient force field in the classical calculus. The first term in the right-hand-side of Eq. (27) is caused by the transition between states due to the chemical force, while the second term is contributed by the change of entropy. Furthermore, as $\mu_{ij}^0 = k_BT \ln(q_{ij}/q_{ji})$, then

$$\Delta\mu_{ij} = k_BT \ln \frac{q_{ij}}{q_{ji}} + k_BT \ln \frac{\pi_i}{\pi_j} = k_BT \ln \frac{\pi_i q_{ij}}{\pi_j q_{ji}}.$$

Therefore, for a nonequilibrium mesoscopic system, we have

$$\frac{\pi_i q_{ij}}{\pi_j q_{ji}} = e^{\Delta\mu_{ij}/k_BT}. \tag{28}$$

We emphasize again that $\Delta\mu_{ij}$ is the free energy *difference* resulted from the transition from state i to j. Single-step transition like such in a NESS requires energy input, but can also result in an release of energy, for example the phenomenon of fluorescence. We refer readers to H. Qian's work [48–50] for detailed discussions on free energy difference associated with equilibrium fluctuations and nonequilibrium deviations.

Eqs. (25) and (28) are basic expressions for a mesoscopic system in equilibrium and nonequilibrium steady states, respectively. From Eq. (28), one knows that the necessary and sufficient condition for a mesoscopic system in equilibrium is

$$\Delta\mu_{ij} = 0, \quad \forall\, i \neq j,$$

i.e., the free energy difference $\Delta\mu_{ij}$ between any two states is zero.

2.3.2b. Free energy dissipation and entropy production. The Second Law of Thermodynamics tells us that the increment in the entropy of an isolated, macroscopic system undergoing a spontaneous change is impossible to be negative. For a closed, canonical system the statement becomes the impossibility of free energy increment being positive. However, for an open system, the increment of entropy may be negative (and free energy increment may be positive) because the system is driven by the environment: energy is pumped into the system. In the steady state of an open system, it is now the *entropy production rate* (e.p.r) that must be nonnegative. The concept of entropy production was articulated by Prigogine [9,51] to describe phenomena far from equilibrium. Since then, a great deal of interests has been aroused in understanding the concept, from both mathematics and physics perspectives [10,52–56]. A deep insight in recent years on the entropy production and free energy dissipation is the fluctuation theorems [57,58,10].

Intuitively, the concept of entropy production can be introduced from the following non-mathematical discussion. Suppose that the distribution of a mesoscopic system at time t is $P(t) = (p_1(t), \ldots, p_N(t))$, then the Gibbs entropy of the system is

$$S(t) = -\sum_i p_i(t) \ln p_i(t). \tag{29}$$

Taking the total derivative of Gibbs entropy with respect to t and noting that $\sum_i p_i(t) = 1$, we have

$$\begin{aligned}
\frac{dS(t)}{dt} &= -\sum_i p_i'(t) \ln p_i(t) \\
&= -\sum_{i \neq j} \left(p_j(t) q_{ji} - p_i(t) q_{ij} \right) \ln p_i(t) \quad \text{(according to Eq. (19))} \\
&= -\frac{1}{2} \sum_{i \neq j} \left(p_j(t) q_{ji} - p_i(t) q_{ij} \right) \ln \frac{p_i(t)}{p_j(t)}.
\end{aligned}$$

$dS(t)/dt$ should be considered as the increment of entropy during the evolution of a mesoscopic system. Entropy is an extensive quantity, its time derivative and its production rate are two different concepts.

In a steady state, $dS(t)/dt = 0$, and $p_i(t) = \pi_i$. Hence

$$\begin{aligned}
0 &= \frac{1}{2} \sum_{i \neq j} \left(\pi_i q_{ij} - \pi_j q_{ji} \right) \left(\ln \pi_i - \ln \pi_j \right) \\
&= -\frac{1}{2} \sum_{i \neq j} \left(\pi_i q_{ij} - \pi_j q_{ji} \right) \ln \frac{q_{ij}}{q_{ji}} + \frac{1}{2} \sum_{i \neq j} \left(\pi_i q_{ij} - \pi_j q_{ji} \right) \ln \frac{\pi_i q_{ij}}{\pi_j q_{ji}} \\
&\stackrel{\Delta}{=} -h_d + e_p, \tag{30}
\end{aligned}$$

where

$$h_d \stackrel{\Delta}{=} \frac{1}{2} \sum_{i \neq j} \left(\pi_i q_{ij} - \pi_j q_{ji} \right) \ln \frac{q_{ij}}{q_{ji}} \tag{31}$$

reflects the heat dissipation of the system. We call h_d the heat dissipation rate (h.d.r). Furthermore,

Definition 2.1. We call

$$e_p \stackrel{\Delta}{=} \frac{1}{2} \sum_{i \neq j} \left(\pi_i q_{ij} - \pi_j q_{ji} \right) \ln \frac{\pi_i q_{ij}}{\pi_j q_{ji}} \tag{32}$$

the entropy production rate of a mesoscopic system in a steady state.

Since every term in the right-hand-side of Eq. (32) is nonnegative, $e_p \geq 0$, and

$$e_p = 0 \Leftrightarrow \left(\pi_i q_{ij} - \pi_j q_{ji} \right) \ln \frac{\pi_i q_{ij}}{\pi_j q_{ji}}, \quad \forall \, i \neq j \Leftrightarrow \pi_i q_{ij} = \pi_j q_{ji}, \ i \neq j.$$

Hence a mesoscopic stationary system is in detailed balance if and only if the entropy production rate is zero.

Eq. (30) shows that in a NESS, the entropy production rate equals to the heat dissipation rate of the system. Terms in both formulas for h_d and e_p contain the product of currents and the forces. $\ln(q_{ij}/q_{ji})$ is a deterministic force having to do with the "internal energy" of the system, while $\ln(\pi_i q_{ij}/\pi_j q_{ji})$ is a statistical force with contributions from the "entropy terms". One can consider the deterministic force $\ln(q_{ij}/q_{ji})$ as the molecular driving force (non-conservative) of the system, then it is the force that drives the system to a nonequilibrium steady state.

From the above discussion, one knows that after realizing a transition from state i to j in a steady state, the free energy change of the system is $\Delta \mu_{ij} = k_B T \ln \frac{\pi_i q_{ij}}{\pi_j q_{ji}}$. Since the probability current caused by the transition $i \to j$ in unit time is $J_{ij} = \pi_i q_{ij} - \pi_j q_{ji}$, then the free energy dissipation in unit time caused by the state transition of $i \to j$ is

$$\Pi_{ij} = k_B T J_{ij} \ln \frac{\pi_i q_{ij}}{\pi_j q_{ji}} = k_B T \left(\pi_i q_{ij} - \pi_j q_{ji} \right) \ln \frac{\pi_i q_{ij}}{\pi_j q_{ji}}.$$

Thus, the total free energy dissipation of the system in unit time is

$$\Pi^{ss} = k_B T \sum_{i > j} J_{ij} \ln \frac{\pi_i q_{ij}}{\pi_j q_{ji}} = k_B T \sum_{i > j} \left(\pi_i q_{ij} - \pi_j q_{ji} \right) \ln \frac{\pi_i q_{ij}}{\pi_j q_{ji}}. \tag{33}$$

This is exactly Eq. (32).

Hence the essence of the entropy production is actually the free energy dissipation. Noticing that every term on the right-hand-side of (33) is nonnegative, thus a system is in equilibrium if and only if the free energy dissipation is zero.

2.3.2c. Calculating free energy dissipation along a stochastic trajectory. In this section, we will demonstrate a very significant fact that, in a steady state, the free energy dissipation rate (or the entropy production rate) of a mesoscopic system, is in fact the time-averaged free energy dissipation along a realization of the corresponding Q-process provided that the Q is communicative, as described in Appendix A. This fact implies that the concept of entropy production could be in fact defined as a stochastic quantity associated with a sample path.

Let us observe a sample path ω of the Q-process starting from time $t_0 = 0$. Suppose that the particle transits from its initial state i_0 to i_1, and then to $i_2, \ldots, i_k, \ldots$ at time $t_1, t_2, \ldots, t_k, \ldots$, respectively. Let n be the total times of the particle changing its states during time interval $[0, t]$. One knows from the above discussion that each transition between any two different states will lead to a free energy dissipation. Then during $[0, t]$, the averaged free energy dissipation of the system along this trajectory is

$$\frac{1}{t} \sum_{k=1}^{n} \ln \frac{\pi_{i_k} q_{i_k i_{k+1}}}{\pi_{i_{k+1}} q_{i_{k+1} i_k}}. \tag{34}$$

In the following, as a main result that cannot easily be found in standard textbooks, we shall prove that for almost every trajectory, the above time-averaged value of free energy dissipations along the trajectory equals to the entropy production rate of the system in steady state.

Lemma 2.2. *Suppose that $\{\zeta_k(\omega)\}_{k \geq 1}$ is an embedded Markov chain of a stationary and communicative Q-process, then*

$$\lim_{n \to \infty} \frac{1}{n} \sum_{k=1}^{n} \ln \frac{\pi_{\zeta_k} q_{\zeta_k \zeta_{k+1}}}{\pi_{\zeta_{k+1}} q_{\zeta_{k+1} \zeta_k}} = \frac{\frac{1}{2} \sum_{i \neq j} (\pi_i q_{ij} - \pi_i q_{ji}) \ln \frac{\pi_i q_{ij}}{\pi_j q_{ji}}}{\sum_i \pi_i q_i}, \ a.e. \ \widehat{P}(d\omega), \tag{35}$$

where a.e. means for almost every trajectory ω.

Proof. Let $G_{ij} = \ln(\pi_i q_{ij} / \pi_j q_{ji})$, which is a two-variable function defined on the state space $E \times E$ with $E = \{1, 2, \ldots, N\}$.

Since the embedded Markov chain of a stationary communicative Q-process is irreducible and positive recurrent (i.e., ergodic), then it follows from the strong Birkhoff ergodic theorem that

$$\lim_{n \to \infty} \frac{1}{n} \sum_{k=1}^{n} \ln \frac{\pi_{\zeta_k} q_{\zeta_k \zeta_{k+1}}}{\pi_{\zeta_{k+1}} q_{\zeta_{k+1} \zeta_k}} = \lim_{n \to \infty} \frac{1}{n} \sum_{k=0}^{n-1} G_{\zeta_k(\omega) \zeta_{k+1}(\omega)}$$

$$= \sum_{i \neq j} G_{ij} \widehat{P}(\zeta_0 = i, \zeta_1 = j) \quad \text{(ergodic theorem)}$$

$$= \sum_{i \neq j} G_{ij} \widehat{\pi}_i \widehat{p}_{ij}$$

$$= \sum_{i \neq j} \ln \frac{\pi_i q_{ij}}{\pi_j q_{ji}} \cdot \frac{\pi_i q_i}{\sum \pi_i q_i} \cdot \frac{q_{ij}}{q_i}$$

$$= \sum_{i \neq j} \ln \frac{\pi_i q_{ij}}{\pi_j q_{ji}} \cdot \frac{\pi_i q_{ij}}{\sum \pi_i q_i}$$

$$= \frac{1}{\sum \pi_i q_i} \cdot \sum_{i \neq j} \pi_i q_{ij} \ln \frac{\pi_i q_{ij}}{\pi_j q_{ji}}$$

$$= \frac{1}{\sum \pi_i q_i} \cdot \frac{1}{2} \sum_{i \neq j} (\pi_i q_{ij} - \pi_i q_{ji}) \ln \frac{\pi_i q_{ij}}{\pi_j q_{ji}}.$$

That is,

$$\lim_{n \to \infty} \frac{1}{n} \sum_{k=1}^{n} \ln \frac{\pi_{\zeta_k} q_{\zeta_k \zeta_{k+1}}}{\pi_{\zeta_{k+1}} q_{\zeta_{k+1} \zeta_k}} = \frac{1}{\sum \pi_i q_i} \cdot \frac{1}{2} \sum_{i \neq j} (\pi_i q_{ij} - \pi_i q_{ji}) \ln \frac{\pi_i q_{ij}}{\pi_j q_{ji}}, \ a.e. \ \widehat{P}(d\omega). \quad \square$$

For the original process $\{\xi_t(\omega)\}_{t \in R}$, we note that the sojourn time for each step is $\left(\sum \pi_i q_i \right)^{-1}$, then the limit of the time-averaged quantity in (34) becomes the entropy production rate e_p. We have the following theorem.

Theorem 2.3. *Suppose that $\{\xi_t(\omega)\}_{t \in R}$ is a stationary communicative Q-process with jumping time t_k, $k = 1, 2, \ldots$, then for almost every trajectory ω, we have*

$$\lim_{t \to \infty} \frac{1}{t} \sum_{0 \leq t_k \leq t} \ln \frac{\pi_{\xi_{t_k}} q_{\xi_{t_k} \xi_{t_{k+1}}}}{\pi_{\xi_{t_{k+1}}} q_{\xi_{t_{k+1}} \xi_{t_k}}} = \frac{1}{2} \sum_{i \neq j} \ln \frac{\pi_i q_{ij}}{\pi_j q_{ji}} (\pi_i q_{ij} - \pi_i q_{ji}). \quad a.e. \ P(d\omega). \tag{36}$$

Proof. Let $n_i(\omega)$ be the times of the particle transiting to state i during $[0, t]$, and $t_i(\omega)$ be the corresponding sojourn time in state i, then $n(\omega) = \Sigma_i n_i(\omega)$ is the total jumping times of the process $\{\xi_t(\omega)\}_{t \in R}$ before time t, and $\frac{t_i(\omega)}{n_i(\omega)}$ is the averaged sojourn time at state i during this time interval.

Since the Q-process we consider is communicative, then the corresponding embedded Markov chain $\{\zeta_k(\omega)\}_{k \geq 1}$ ($\zeta_k(\omega) \triangleq \xi_{t_k}(\omega)$) is irreducible and positive recurrent. Hence starting from any state i, $\{\zeta_k(\omega)\}_{k \geq 1}$ will come back to this state after a certain random time. Actually, the process $\{\zeta_k(\omega)\}_{k \geq 1}$ will come back to state i for infinite times with probability 1. Hence, we have

$$\lim_{t \to \infty} n_i(\omega) = \infty, \qquad \lim_{t \to \infty} t_i(\omega) = \infty \ a.e. \ \widehat{P}(d\omega).$$

And

$$\lim_{t \to \infty} \frac{t_i(\omega)}{t} = \pi_i, \qquad \lim_{t \to \infty} \frac{t_i(\omega)}{n_i(\omega)} = \frac{1}{q_i} \ a.e. \ \widehat{P}(d\omega).$$

As a result,

$$\lim_{t \to \infty} \frac{n(\omega)}{t} = \sum_i \pi_i q_i, \ a.e. \ \widehat{P}(d\omega).$$

So

$$\lim_{t \to \infty} \frac{1}{t} \sum_{0 \leq \tau_k \leq t} G_{\xi_{t_k}(\omega)\xi_{k+1}(\omega)} = \lim_{t \to \infty} \frac{n(\omega)}{t} \frac{1}{n(\omega)} \sum_{k=0}^{n(\omega)-1} G_{\zeta_k(\omega)\zeta_{k+1}(\omega)}$$

$$= \lim_{t \to \infty} \frac{n(\omega)}{t} \cdot \lim_{n \to \infty} \frac{1}{n} \sum_{k=0}^{n-1} G_{\zeta_k(\omega)\zeta_{k+1}(\omega)}$$

$$= \left(\sum_{i=1} \pi_i q_i \right) \lim_{n \to \infty} \frac{1}{n} \sum_{k=1}^{n} \ln \frac{\pi_{\zeta_k} q_{\zeta_k \zeta_{k+1}}}{\pi_{\zeta_{k+1}} q_{\zeta_{k+1} \zeta_k}}.$$

Therefore, it follows from Lemma 2.2 that

$$\lim_{t \to \infty} \frac{1}{t} \sum_{0 \leq t_k \leq t} \ln \frac{\pi_{\xi_{t_k}} q_{\xi_{t_k}\xi_{k+1}}}{\pi_{\xi_{k+1}} q_{\xi_{k+1}\xi_k}} = \frac{1}{2} \sum_{i \neq j} \ln \frac{\pi_i q_{ij}}{\pi_j q_{ji}} (\pi_i q_{ij} - \pi_i q_{ji}), \ a.e. \ P(d\omega). \quad \square$$

2.3.2d. Entropy production and the theorem of circulation distribution. Theorem 2.3 shows that the entropy production rate of a Q-process $\{\xi_t(\omega)\}_{t \in R}$ can be calculated along any sample path, and the value is $\frac{1}{2} \sum_{i \neq j} \ln \frac{\pi_i q_{ij}}{\pi_j q_{ji}} (\pi_i q_{ij} - \pi_j q_{ji})$. In this probabilistic interpretation, $\ln(\pi_i q_{ij}/\pi_j q_{ji})$ is the chemical potential difference between states i and j (an analogue to a force in a continuous system), and $J_{ij} = (\pi_i q_{ij} - \pi_j q_{ji})$ is the net current from i to j. In the derivation of the formula, we only consider the current and the "force" between each two states. Actually, along a trajectory of the Q-process, some states will be visited more than one time. For example, In a realization of the process, the mesoscopic particle may undergo a sequence of ordered states like $\ldots, i_1, i_2, \ldots, i_k, i_1, \ldots$. For simplicity, we let $c = (i_1, i_2, \ldots, i_k, i_1)$ represent a directed cycle starting from state i and then come back to it after visiting states $i_2, i_3, \ldots, i_k$ in order, and $c^- = (i_1, i_k, i_{k-1}, \ldots, i_1)$ represent the reverse cycle obtained by reversing the time in cycle c.

For a Q-process in a steady state, it follows from the master Eq. (19) that $\sum_{j \neq i}(\pi_i q_{ij} - \pi_j q_{ji}) = 0$. This means that the total probability influx to state i equals to the total outflow from the state i. We classify the visited states of a mesoscopic particle along a trajectory into different directed cycles, and can endow each cycle with a probability current J_c. There is an analogy between the chemical potential and current in the probability model and the voltage and current in an electrical circuit. If one looks for the Kirchhoff's loop expression of the total power for the electrical circuit in the case of Markov master equation, then the entropy production rate is analogous to the electric power. It has been proved that the entropy production can be calculated by considering the probability current on each and every directed cycle [10]. The result is stated in the following theorem.

Theorem 2.4. *For a mesoscopic system in a NESS, the e.p.r can be expressed as*

$$e_p = \sum_{c \in C_\infty} (J_c - J_{c^-}) \ln \frac{J_c}{J_{c^-}}, \tag{37}$$

where C_∞ is the collection of directed cycles occurring along almost all the sample paths and c_- is the reversed cycle of c. Actually, we should write $C_\infty(\omega)$, but by ergodicity they can be proved to be ω independent, a.e., $P(d\omega)$.

The proof is mathematically sophisticated, but the theorem demonstrates that a mesoscopic system is in detailed balance if and only if the system maintains a balance within each and every cycle, i.e., $J_c = J_{c^-}$.

2.3.2e. Equivalent conditions for detailed balance.　With the above discussion concerning a mesoscopic system, we are now in a position to state the relationship between NESS, the irreversibility of a Markov process, the positivity of entropy production rate, and unbalanced circulations (NBC) [10,59]. We have

Theorem 2.5. *Let* $\{\xi_t\}_{t \in R}$ *be a stationary and irreducible communicative Q-process with a state space* $E = \{1, 2, \ldots, N\}$ *and an invariant distribution* $\vec{\pi} = (\pi_1, \ldots, \pi_N)$. *Let* $p_{ij}(t) = \Pr\{\xi_t = j | \xi_0 = i\}$. *Then the following conditions are equivalent:*

(1) *The process* $\{\xi_t\}_{t \in R}$ *is detail balanced, i.e.,* $\pi_i q_{ij} = \pi_j q_{ji}, \forall i \neq j$.
(2) $\pi_i p_{ij}(t) = \pi_j p_{ji}(t), \forall t > 0, \forall i \neq j$.
(3) $\{\xi_t\}_{t \in R}$ *satisfies the following Kolmogorov cycle criteria*

$$q_{i_1 i_2} q_{i_2 i_3} \cdots q_{i_{s-1} i_s} q_{i_s i_1} = q_{i_2 i_1} q_{i_3 i_2} \cdots q_{i_s i_{s-1}} q_{i_1 i_s}. \tag{38}$$

(4) $\{\xi_t\}_{t \in R}$ *is time reversible.*
(5) *The entropy production rate of the process* $\{\xi_t\}_{t \in R}$ *is zero, i.e.,* $e_p = 0$.
(6) *The process maintain circulation balance, i.e.,* $J_c = J_{c^-}$, *for all* $c \in C_\infty$.
(7) *The chemical force* $\mu_{ij}^0 = \ln(q_{ij}/q_{ji})$ *between any two states* i, j *can be expressed as the difference of values of a potential function in these two states, i.e., there exists a function* $\Phi(\cdot)$, *such that* $q_{ij}/q_{ji} = \exp(\Phi(i) - \Phi(j))$.

The following proof is provided for readers who are interested in the mathematics. Readers who are only interested in the physics of the problem can simply skip the entire proof.

Proof. (1) $\Leftrightarrow$ (2). First, (2) $\Rightarrow$ (1): Given the statement in (2), assertion (1) is obvious since $\forall i \neq j$, $\lim_{t \to 0} P_{ij}(t)/t = q_{ij}$. Now (1) $\Rightarrow$ (2): Let

$$\mathbf{M} \triangleq \begin{bmatrix} \sqrt{\pi}_0 & & \\ & \ddots & \\ & & \sqrt{\pi}_N \end{bmatrix}, \qquad \mathbf{U} \triangleq \mathbf{M}^2 = \begin{bmatrix} \pi_0 & & \\ & \ddots & \\ & & \pi_N \end{bmatrix},$$

and $\bar{\mathbf{Q}} \triangleq \mathbf{M} \cdot \mathbf{Q} \cdot \mathbf{M}^{-1}$. Then condition (1) implies that $\bar{\mathbf{Q}}$ is a symmetric matrix. Hence there exists an orthonormal matrix $\boldsymbol{\Gamma} = (\Gamma_{ij})$ such that $\bar{\mathbf{Q}} = \boldsymbol{\Gamma} \cdot \mathbf{A} \cdot \boldsymbol{\Gamma}^T$, where

$$\mathbf{A} \triangleq \begin{bmatrix} -a_0 & & \\ & \ddots & \\ & & -a_N \end{bmatrix},$$

in which a_i is determined by the eigenvalue of the matrix $\bar{\mathbf{Q}}$.
　　Obviously, $\mathbf{Q} = \mathbf{M}^{-1} \cdot \bar{\mathbf{Q}} \cdot \mathbf{M}$, and $\exp(\mathbf{Q}t) = \mathbf{M}^{-1} \cdot \exp(\bar{\mathbf{Q}}t) \cdot \mathbf{M}$, then

$$\mathbf{P(t)} = \exp(\mathbf{Q}t) = \mathbf{M}^{-1} \cdot \exp(\bar{\mathbf{Q}}t) \cdot \mathbf{M},$$
$$\mathbf{U} \cdot \exp(\mathbf{Q}t) = \mathbf{M} \cdot \exp(\bar{\mathbf{Q}}t) \cdot \mathbf{M}.$$

So

$$(\mathbf{U} \cdot \exp(\mathbf{Q}t))^T = (\mathbf{U} \cdot \exp(\mathbf{Q}t)).$$

Since the element of $(\mathbf{U} \cdot \exp(\mathbf{Q}t))$ is $\pi_i p_{ij}(t)$, then

$$\pi_i p_{ij}(t) = \pi_j p_{ji}(t), \quad \forall i \neq j.$$

Therefore (1) $\Rightarrow$ (2).
　　(1) $\Leftrightarrow$ (3). First, (1) $\Rightarrow$ (3): Suppose that the Q-process $\{\xi_t\}_{t \in R}$ is in detailed balance, then for $\forall i \neq j$, $\pi_i q_{ij} = \pi_j q_{ji}$. Hence for any cyclic path $i_1 \to i_2 \to \cdots \to i_s \to i_1$, we have

$$\pi_{i_1} q_{i_1 i_2} q_{i_2 i_3} \cdots q_{i_{s-1} i_s} q_{i_s i_1} = q_{i_2 i_1} \cdot \pi_{i_2} q_{i_2 i_3} \cdots q_{i_{s-1} i_s} q_{i_s i_1} = \cdots = q_{i_2 i_1} q_{i_3 i_2} \cdots q_{i_s i_{s-1}} q_{i_1 i_s} \cdot \pi_{i_1}.$$

Subsequently,

$$q_{i_1 i_2} q_{i_2 i_3} \cdots q_{i_{s-1} i_s} q_{i_s i_1} = q_{i_2 i_1} q_{i_3 i_2} \cdots q_{i_s i_{s-1}} q_{i_1 i_s}.$$

Thus, the Kolmogorov criteria is satisfied.
　　Now (3) $\Rightarrow$ (1): Suppose that $\{\xi_t\}_{t \in R}$ satisfies the Kolmogorov criteria, i.e, for any cyclic path $i_1 \to i_2 \to \cdots \to i_s \to i_1$, we have

$$q_{i_1 i_2} q_{i_2 i_3} \cdots q_{i_{s-1} i_s} q_{i_s i_1} = q_{i_2 i_1} q_{i_3 i_2} \cdots q_{i_s i_{s-1}} q_{i_1 i_s}.$$

First, let us fix a state i_0, and suppose that $\mu_{i_0} = 1$. Since the process is communicative, then for $\forall i \neq i_0$, there exists $i_1, i_2, \ldots, i_n$, such that $q_{i i_n} q_{i_n i_{n-1}} \cdots q_{i_2 i_1} q_{i_1 i_0} > 0$, i.e., $q_{i_1 i_0} q_{i_2 i_1} \cdots q_{i i_n} > 0$. We thus define

$$\mu_i = \frac{q_{i_0 i_1} q_{i_1 i_2} \cdots q_{i_n i}}{q_{i_1 i_0} q_{i_2 i_1} \cdots q_{i i_n}}.$$

It can be proved that the value of μ_i is independent of the selection of $i_1, i_2, \ldots, i_n$ and the number n of jumping times. Actually, suppose that there is another path $i'_1, i'_2, \ldots, i'_m$, such that $q_{i i'_m} q_{i'_m i'_{m-1}} \cdots q_{i'_2 i'_1} q_{i'_1 i_0} > 0$, i.e., $q_{i'_1 i_0} q_{i'_2 i'_1} \cdots q_{i i'_m} > 0$, then $\widetilde{\mu}_i = \frac{q_{i_0 i'_1} q_{i'_1 i'_2} \cdots q_{i'_m i}}{q_{i'_1 i_0} q_{i'_2 i'_1} \cdots q_{i i'_m}}$ makes sense. It follows from the Kolmogorov criteria that

$$q_{i_0 i_1} q_{i_1 i_2} \cdots q_{i_n i} \cdot q_{i i'_m} \cdots q_{i'_2 i'_1} q_{i'_1 i_0} = q_{i_1 i_0} q_{i_2 i_1} \cdots q_{i i_n} \cdot q_{i'_m i} \cdots q_{i'_1 i'_2} q_{i_0 i'_1}.$$

This shows that $\mu_i / \widetilde{\mu}_i = 1$, which demonstrates that the value of μ_i is independent of n and the path $i_1, i_2, \ldots, i_n$.

In the following, we will apply the Kolmogorov criteria to prove that $\{\mu_i\}$ satisfies

$$\mu_i q_{ij} = \mu_j q_{ji}, \quad \forall i \neq j.$$

Actually,

$$\mu_i q_{ij} = \frac{q_{i_0 i_1} q_{i_1 i_2} \cdots q_{i_n i} q_{ij}}{q_{i_1 i_0} q_{i_2 i_1} \cdots q_{i i_n}}, \qquad \mu_j q_{ji} = \frac{q_{i_0 j_1} q_{j_1 j_2} \cdots q_{j_m j} q_{ji}}{q_{j_1 i_0} q_{j_2 j_1} \cdots q_{j j_m}}.$$

where $\mu_j = \frac{q_{i_0 j_1} q_{j_1 j_2} \cdots q_{j_m j}}{q_{j_1 i_0} q_{j_2 j_1} \cdots q_{j j_m}}$, in which $j_1, j_2, \ldots, j_m$ are arbitrarily selected such that $q_{j_1 i_0} q_{j_2 j_1} \cdots q_{j j_m} > 0$.

According to the Kolmogorov criteria, we have

$$q_{i_0 i_1} q_{i_1 i_2} \cdots q_{i_n i} q_{ij} \cdot q_{j j_m} q_{j_m j_{m-1}} \cdots q_{j_2 j_1} q_{j_1 i_0} = q_{i_1 i_0} q_{i_2 i_1} \cdots q_{i i_n} q_{ji} \cdot q_{j_m j} q_{j_{m-1} j_m} \cdots q_{j_1 j_2} q_{i_0 j_1}.$$

Hence

$$\mu_i q_{ij} = \mu_j q_{ji}, \quad \forall i \neq j.$$

Let $\pi_i = \frac{\mu_i}{\Sigma_i \mu_i}$, then $(\pi_1, \ldots, \pi_N)$ is a probability measure which is determined uniquely by the Q-matrix.

(2) $\Leftrightarrow$ (4). First (2) $\Rightarrow$ (4): For any $t > 0$, and $t_1 \leq t_2 \leq \cdots \leq t_k \leq t$, then conditioning on (2), we have

$$\begin{aligned}
\Pr\{\xi_{t_1} = i_1, \xi_{t_2} = i_2, \ldots, \xi_{t_k} = i_k\} &= \pi_{i_1} p_{i_1 i_2}(t_2 - t_1) \cdots p_{i_{k-1} i_k}(t_k - t_{k-1}) \\
&= p_{i_2 i_1}(t_2 - t_1) \pi_{i_2} \cdot p_{i_2 i_3}(t_3 - t_2) \cdots p_{i_{k-1} i_k}(t_k - t_{k-1}) \\
&= \cdots = p_{i_2 i_1}(t_2 - t_1) p_{i_3 i_2}(t_3 - t_2) \cdots p_{i_k i_{k-1}}(t_k - t_{k-1}) \pi_{i_k} \\
&= \pi_{i_k} p_{i_k i_{k-1}}(t_k - t_{k-1}) \cdots p_{i_3 i_2}(t_3 - t_2) p_{i_2 i_1}(t_2 - t_1).
\end{aligned}$$

On the other hand,

$$\Pr\{\xi_{-t_1} = i_1, \xi_{-t_2} = i_2, \ldots, \xi_{-t_k} = i_k\} = \pi_{i_k} p_{i_k i_{k-1}}(t_k - t_{k-1}) \cdots p_{i_3 i_2}(t_3 - t_2) p_{i_2 i_1}(t_2 - t_1).$$

Hence

$$\Pr\{\xi_{t_1} = i_1, \xi_{t_2} = i_2, \ldots, \xi_{t_k} = i_k\} = \Pr\{\xi_{-t_1} = i_1, \xi_{-t_2} = i_2, \ldots, \xi_{-t_k} = i_k\},$$

which manifests that the process is reversible.

Now (4) $\Rightarrow$ (2): If the process $\{\xi_t\}_{t \in R}$ is reversible, then for $\forall h > 0$, $\forall i \neq j$, we have

$$\Pr\{\xi_t = i, \xi_{t+h} = j\} = \Pr\{\xi_{t+h} = i, \xi_t = j\}.$$

i.e.,

$$\pi_i p_{ij}(h) = \pi_j p_{ji}(h).$$

(2) is proved.

(1) $\Leftrightarrow$ (5). Noticing that every term in the formula of e_p is nonnegative, then the equivalence between (1) and (5) is obvious.

(5) $\Leftrightarrow$ (6). This follows immediately from the definition of e_p given in Eq. (37).

(1) $\Leftrightarrow$ (7). The proof is straightforward if one starts with the fact that a force doing work but independent of the path implies the existence of a potential function. This is a standard result in multivariate calculus. We omit the details here. $\quad\square$

2.3.3. Measure theoretical basis of time-reversal and entropy production

In the previous sections, we have discussed the entropy production rate (e.p.r) of a mesoscopic system from the standpoint of free energy dissipation and probabilistic circulation distribution. We have provided a physical meaning to the entropy production rate. In this section, we shall further provide a more general mathematical definition for the entropy production in terms of the probability measure of a Q-process and its time-reversed process. The significance of this abstract definition is that it can be applied to a much broader class of dynamical systems. It also implies that e_p is the quantity to capture all the irreversibility in a stochastic Markov process.

First, we consider the embedded Markov chain $\{\zeta_n\}_{n \in Z}$ of $\{\xi_t\}_{t \in R}$ and its reversed process $\{\zeta_n^-\}_{n \in Z}$. Let $\widehat{P}^+$ be the probability measure of $\{\zeta_n(\omega)\}_{n \in Z}$ along time-increasing direction, and $\widehat{P}^-$ be the one along time-decreasing direction, then

$$\widehat{P}^+(\zeta_0 = i_0, \zeta_1 = i_1, \ldots, \zeta_N = i_N) = \widehat{\pi}_{i_0} \widehat{p}_{i_0 i_1} \cdots \widehat{p}_{i_{N-1} i_N},$$

$$\widehat{P}^-(\zeta_0 = i_0, \zeta_1 = i_1, \ldots, \zeta_N = i_N) = \widehat{P}^+(\zeta_{-N} = i_N, \zeta_{-(N-1)} = i_{N-1}, \ldots, \zeta_{-1} = i_1, \zeta_0 = i_0)$$

$$= \widehat{\pi}_{i_N} \widehat{p}_{i_N i_{N-1}} \cdots \widehat{p}_{i_1 i_0}.$$

The last equation is based on the stationarity of the process (the initial time is $-N$). Then we have

Lemma 2.6. *For the embedded Markov process $\{\zeta_n\}_{n \in Z}$ of a Q-process $\{\xi_t\}_{t \in R}$,*

$$\left. \frac{d\widehat{P}^+_{[1,N]}(\omega)}{d\widehat{P}^-_{[1,N]}(\omega)} \right|_{\zeta_0 = i_0, \zeta_1 = i_1, \ldots, \zeta_N = i_N} = \frac{\widehat{\pi}_{i_0} \widehat{p}_{i_0 i_1} \cdots \widehat{p}_{i_{N-1} i_N}}{\widehat{\pi}_{i_N} \widehat{p}_{i_N i_{N-1}} \cdots \widehat{p}_{i_1 i_0}} = \frac{\pi_{i_0} q_{i_0 i_1} \cdots q_{i_{N-1} i_N}}{\pi_{i_N} q_{i_N i_{N-1}} \cdots q_{i_1 i_0}}. \quad \square \tag{39}$$

Furthermore, according to Lemma 2.2, we have the following theorem

Theorem 2.7. *For the embedded Markov process $\{\zeta_n\}_{n \in Z}$ of a Q-process $\{\xi_t\}_{t \in R}$,*

$$\lim_{N \to \infty} \frac{1}{N} E\left[\ln \frac{d\widehat{P}^+_{[1,N]}(\omega)}{d\widehat{P}^-_{[1,N]}(\omega)} \right] = \frac{1}{\sum_i \pi_i q_i} \cdot \frac{1}{2} \sum_{i \neq j} \ln \frac{\pi_i q_{ij}}{\pi_j q_{ji}} (\pi_i q_{ij} - \pi_j q_{ji}), \quad a.e. \ \widehat{P}(d\omega). \tag{40}$$

Proof. It follows from Lemma 2.6 that

$$\frac{1}{N} \ln \frac{dP^+_{[1,N]}(\omega)}{dP^-_{[1,N]}(\omega)} = \frac{1}{N} \sum_{k=0}^{N-1} \ln \frac{\pi_{\zeta_k} q_{\zeta_k \zeta_{k+1}}}{\pi_{\zeta_{k+1}} q_{\zeta_{k+1} \zeta_k}}.$$

Calculating the limit of the above lemma according to Lemma 2.2, we have

$$\lim_{N \to \infty} \frac{1}{N} \ln \frac{d\widehat{P}^+_{[1,N]}(\omega)}{d\widehat{P}^-_{[1,N]}(\omega)} = \frac{1}{\sum_i \pi_i q_i} \cdot \frac{1}{2} \Sigma_{i \neq j} \ln \frac{\pi_i q_{ij}}{\pi_j q_{ji}} (\pi_i q_{ij} - \pi_i q_{ji}).$$

Therefore

$$\lim_{N \to \infty} \frac{1}{N} E\left[\ln \frac{d\widehat{P}^+_{[1,N]}(\omega)}{d\widehat{P}^-_{[1,N]}(\omega)} \right] = E\left[\lim_{N \to \infty} \frac{1}{N} \ln \frac{d\widehat{P}^+_{[1,N]}(\omega)}{d\widehat{P}^-_{[1,N]}(\omega)} \right]$$

$$= \frac{1}{\sum_i \pi_i q_i} \cdot \frac{1}{2} \sum_{i \neq j} \ln \frac{\pi_i q_{ij}}{\pi_j q_{ji}} (\pi_i q_{ij} - \pi_i q_{ji}). \quad \square$$

Let us further consider the Q-process $\{\xi_t(\omega)\}_{t \in R}$ and its time-reversed process $\{\xi_t^- : \xi_t^-(\omega) = \xi_{-t}(\omega), \forall t \in R\}$. Let

$$t_0(\omega) = 0,$$

$$t_{k+1}(\omega) = \inf\{t > t_k(\omega); \xi_t(\omega) \neq \xi_{t_k}(\omega)\}, \quad k = 0, 1, 2, \ldots$$

and

$$\tau_k(\omega) = t_{k+1}(\omega) - t_k(\omega), \quad k = 0, 1, 2, \ldots.$$

For $T > 0$, denote $N_T(\omega)$ as the number of the total transition times of an trajectory ω during $[0, T]$, it is also a stochastic variable. Furthermore, let

$$A_{i_0 i_1 \cdots i_n} = \{\omega : N_T(\omega) = n, \xi_{t_0(\omega)} = i_0, \xi_{t_1(\omega)} = i_1, \ldots, \xi_{t_n(\omega)} = i_n\},$$

then $A_{i_0, i_1, \ldots, i_n}$ is the collection of those trajectories ω that transfer their states for n times until time T with $t_0(\omega) = 0$ and transition times $t_1(\omega), t_2(\omega), \ldots, t_n(\omega)$.

We have the following Lemma

Lemma 2.8. *Let* $\{\xi_t(\omega)\}_{t\in R}$ *be a stationary communicative Q-process on space* $(\Omega, \mathcal{F}, P)$*, then for* $\forall T > 0$*,*

$$\frac{dP^+_{[0,T]}(\omega)}{dP^-_{[0,T]}(\omega)}\bigg|_{A_{i_0 i_1 \cdots i_n}} = \frac{\pi_{i_0} q_{i_0 i_1} \cdots q_{i_{n-1} i_n}}{\pi_{i_n} q_{i_n i_{n-1}} \cdots q_{i_1 i_0}}. \tag{41}$$

Proof.

$$P^+_{[0,T]}\left(\omega : \omega \in A_{i_0 i_1 \cdots i_n}; s_1 \le t_1(\omega) \le s_1 + \Delta s_1, \ldots, s_n \le t_n(\omega) \le s_n + \Delta s_n\right)$$
$$= P^+_{[0,T]}\left(\xi_{t_0} = i_0, \xi_{t_1} = i_1, \ldots, \xi_{t_n} = i_n; s_1 \le t_1 \le s_1 + \Delta s_1, \ldots, s_n \le t_n \le s_n + \Delta s_n; N_T(\omega) = n\right)$$
$$= \int_{s_1}^{s_1 + \Delta s_1} q_{i_0} e^{-q_{i_0} \tau_1} d\tau_1 \int_{s_2 - \tau_1}^{s_2 - \tau_1 + \Delta s_2} q_{i_1} e^{-q_{i_1} \tau_2} d\tau_2 \cdots \int_{s_n - \sum_{i=1}^{n-1} \tau_i}^{s_n - \sum_{i=1}^{n-1} \tau_i + \Delta s_n} q_{i_{n-1}} e^{-q_{i_{n-1}} \tau_n} d\tau_n$$
$$\times \int_{T - \sum_{i=1}^{n} \tau_i}^{\infty} q_{i_n} e^{-q_{i_n} \tau} d\tau \, \pi_{i_0} \frac{q_{i_0 i_1}}{q_{i_0}} \cdots \frac{q_{i_{n-1} i_n}}{q_{i_{n-1}}}$$
$$= \pi_{i_0} q_{i_0 i_1} \cdots q_{i_{n-1} i_n} q_{i_n} \int_{s_1}^{s_1 + \Delta s_2} d\tau_1 \int_{s_2 - \tau_1}^{s_2 - \tau_1 + \Delta s_1} d\tau_2 \cdots \int_{s_n - \sum_{i=1}^{n-1} \tau_i}^{s_n - \sum_{i=1}^{n-1} \tau_i + \Delta s_n} d\tau_n \int_{T - \sum_{i=1}^{n} \tau_i}^{\infty} d\tau_{n+1} \prod_{i=0}^{n+1} e^{-q_i \tau_{i+1}}.$$

On the other hand, we have

$$P^-_{[0,T]}\left(\omega : \omega \in A_{i_0 i_1 \cdots i_n}; s_1 \le t_1(\omega) \le s_1 + \Delta s_1, \ldots, s_n \le t_n(\omega) \le s_n + \Delta s_n\right)$$
$$= P^-_{[0,T]}\left(\xi_{t_0} = i_0, \xi_{t_1} = i_1, \ldots, \xi_{t_n} = i_n; s_1 \le t_1 \le s_1 + \Delta s_1, \ldots, s_n \le t_n \le s_n + \Delta s_n; N_T(\omega) = n\right)$$
$$= \tilde{\pi}_{i_0} \tilde{q}_{i_0 i_1} \cdots \tilde{q}_{i_{n-1} i_n} \tilde{q}_{i_n} \int_{s_1}^{s_1 + \Delta s_2} d\tau_1 \int_{s_2 - \tau_1}^{s_2 - \tau_1 + \Delta s_2} d\tau_2 \cdots \int_{s_n - \sum_{i=1}^{n-1} \tau_i}^{s_n - \sum_{i=1}^{n-1} \tau_i + \Delta s_n} d\tau_n \int_{T - \sum_{i=1}^{n} \tau_i}^{\infty} d\tau_{n+1} \prod_{i=0}^{n+1} e^{-\tilde{q}_i \tau_{i+1}}$$
$$= \pi_{i_0} \frac{\pi_{i_1}}{\pi_{i_0}} q_{i_1 i_0} \frac{\pi_{i_2}}{\pi_{i_1}} q_{i_2 i_1} \cdots \frac{\pi_{i_n}}{\pi_{i_{n-1}}} q_{i_n i_{n-1}} \int_{s_1}^{s_1 + \Delta s_2} d\tau_1 \int_{s_2 - \tau_1}^{s_2 - \tau_1 + \Delta s_2} d\tau_2 \cdots \int_{s_n - \sum_{i=1}^{n-1} \tau_i}^{s_n - \sum_{i=1}^{n-1} \tau_i + \Delta s_n} d\tau_n \int_{T - \sum_{i=1}^{n} \tau_i}^{\infty} d\tau_{n+1} \prod_{i=0}^{n+1} e^{-q_i \tau_{i+1}}$$
$$= q_{i_1 i_0} q_{i_2 i_1} \cdots q_{i_n i_{n-1}} \pi_{i_n} \int_{s_1}^{s_1 + \Delta s_1} d\tau_1 \int_{s_2 - \tau_1}^{s_2 - \tau_1 + \Delta s_2} d\tau_2 \cdots \int_{s_n - \sum_{i=1}^{n-1} \tau_i}^{s_n - \sum_{i=1}^{n-1} \tau_i + \Delta s_n} d\tau_n \int_{T - \sum_{i=1}^{n} \tau_i}^{\infty} d\tau_{n+1} \prod_{i=0}^{n+1} e^{-q_i \tau_{i+1}}.$$

Hence

$$\frac{dP^+_{[0,T]}(\omega)}{dP^-_{[0,T]}(\omega)}\bigg|_{A_{i_0 i_1 \cdots i_n}} = \frac{\pi_{i_0} q_{i_0 i_1} \cdots q_{i_{n-1} i_n}}{\pi_{i_n} q_{i_n i_{n-1}} \cdots q_{i_1 i_0}}. \quad \square$$

Based on Lemma 2.8, the following theorem can be obtained:

Theorem 2.9.

$$\lim_{T \to \infty} \frac{1}{T} E\left[\ln \frac{dP^+_{[0,T]}(\omega)}{dP^-_{[0,T]}(\omega)}\right] = \frac{1}{2} \sum_{i \ne j} \ln \frac{\pi_i q_{ij}}{\pi_j q_{ji}} (\pi_i q_{ij} - \pi_j q_{ji}). \quad \square \tag{42}$$

Rigorous mathematical proof of the above theorem was first presented in [60]. Detailed mathematical discussion of the relationship between the reversibility of a Q-process and entropy production can be found in [10].

2.4. Diffusion processes on a circle

One of the most fundamental insights from the theory of NESS is the existence of circular fluxes in a stationary Markov process without detailed balance, and its intimate relation to free energy dissipation and entropy production. In recent years, a connection between this mesoscopic cyclic motion and the nonlinear oscillations in non-gradient dynamical systems was also discovered [61]. The most natural mathematical tool for studying this connection is the dynamics, deterministic or stochastic, on a circle. This section focuses on the stochastic (diffusion) processes on the circle.

2.4.1. Dynamics on a circle

We now give a very brief introduction to the nonlinear dynamics on a circle. For a more detailed discussion of the subject, see [62].

The simplest deterministic dynamics on a circle is the uniform rotation: $\frac{d\theta}{dt} = \omega$. Such a motion can be obtained from a linear dynamical system with a center:

$$\frac{dx}{dt} = y, \qquad \frac{dy}{dt} = -\frac{1}{m}\{kx + \eta y\}.$$

When applied to a harmonic oscillator, the three parameters, m, k, and η are the mass, spring constant, and frictional coefficient, respectively. If we transform this pair of differential equations into the polar coordinate system:

$$r^2 = kx^2 + my^2, \qquad \tan\theta = \sqrt{\frac{m}{k}}\frac{y}{x},$$

then we have

$$\frac{dr}{dt} = -2ar\sin^2\theta, \qquad \frac{d\theta}{dt} = -\omega - a\sin 2\theta, \tag{43}$$

where $a = \eta/(2m)$ and $\omega = \sqrt{k/m}$. We note that the rotational dynamics is independent of the radial component, as is expected for a harmonic oscillator.

The θ component in Eq. (43) is a nonlinear dynamical system on a circle. It undergoes in fact a saddle–node bifurcation when $\omega = a$: For $\omega > a$, the right-hand-side of Eq. (43) is always negative. Hence the particle has a continuous, clockwise rotation with non-uniform angular velocity. However, then $\omega < a$, the system has four fixed points within $[0, 2\pi]$ interval, located at $\frac{\pi}{2} + \theta^*$ (unstable), $\pi - \theta^*$ (stable), $\frac{3\pi}{2} + \theta^*$ (unstable), and $2\pi - \theta^*$ (stable) where $\theta^* = \frac{1}{2}\arcsin(\omega/a)$.

We note that the critical condition for the saddle–node bifurcation in θ is when $\omega = a$. That corresponds to $\eta^2/(4mk) = 1$, the same critical condition for under- to over-damped oscillation. We thus see that the underdamped oscillation, $\eta^2/(4mk) < 1$, corresponds to a continuous rotation of θ; and the overdamped oscillation, $\eta^2/(4mk) > 1$, corresponds to an asymptotic relaxation to the origin with a fixed angular value.

We are now in a position to compute the long-time average

$$Rot = \lim_{t\to\infty}\frac{\theta(t)}{t}. \tag{44}$$

Rot is called rotation number. It is easy to show that for $\omega > a$, we have $Rot = 2\pi/T$ where T is the period of the rotation [62].

$$T = \int_0^{2\pi}\frac{d\theta}{\omega + a\sin 2\theta} = \frac{2\pi}{\sqrt{\omega^2 - a^2}}. \tag{45}$$

The rotation number is the imaginary part of the eigenvalues of a underdamped harmonic oscillation. For $\omega < a$, we have $Rot = 0$.

Therefore, for deterministic nonlinear dynamics on the circle, having fixed points and having nonzero rotation are mutually exclusive scenarios. As we shall see, when there is noise present, this is no longer the case. In fact, the coexistence of nonzero rotation and "stochastic fixed points" gives rise to one kind of coherent resonance.

A clarification on harmonic oscillations, or Hamiltonian dynamics in general, and the stochastic circulation extensively discussed in the present review is in order: Throughout the present review, all the dynamics considered are overdamped. Thus, any oscillation in dynamics is in the "position space", and it is not a consequence of classical conservative dynamics but due to active forcing. For stochastic dynamics of an underdamped system, dynamics in the phase space of (p, q) can have rotation even in equilibrium without entropy production. In the latter cases, the time reversal is defined as $(p, q, t) \to (-p, q, -t)$. See [63] for more discussions and references cited within.

2.4.2. Entropy production, circulation and rotation number

We are now ready to discuss the relationship between entropy production and circulation of a useful but simple stochastic dynamics on a circle. This is actually the noisy phase equation of Eq. (43). We consider the following stochastic differential equation (SDE) with a constant diffusion

$$dx(t) = b(x) + AdB(t), \tag{46}$$

where $b(x)$ satisfies $b(x + L) = b(x)$, $B(t, \omega)$ is a Brownian motion, and A is a constant representing the strength of noise.

The corresponding Fokker–Planck equation (FPE) to the SDE in Eq. (46) is

$$\frac{\partial}{\partial t}p(t, x) = -\frac{\partial}{\partial x}(b(x)p(t, x)) + \frac{A^2}{2}\frac{\partial^2}{\partial x^2}p(t, x) = -\frac{\partial}{\partial x}J(t, x), \tag{47}$$

where $p(t, x)$ is the probability density of the particle in position x at time t, and

$$J(t, x) \overset{\triangle}{=} b(x)p(t, x) - \frac{A^2}{2} \frac{\partial}{\partial x} p(t, x).$$

If one views Eq. (47) as a continuity equation for the probability density (as analogous to a fluid), then the $J(t, x)$ is the corresponding probability flux.

If we consider the dynamics of system (46) on a real line, then there is no invariant probability density $p(x)$, that is $p(t, x) \to p(x)$, as $t \to \infty$. However, due to the periodicity of $b(x)$, the solution to Eq. (46) can be winded on a circle $\mathbb{S}^1$ with radius $L/(2\pi)$. Hence, let

$$\widetilde{x}(t) = x(t) \pmod L,$$

then $\{\widetilde{x}(t)\}_{t \geq 0}$ is a diffusion process on $\mathbb{S}^1$ satisfying

$$d\widetilde{x}(t) = b(\widetilde{x})dt + Ad\widetilde{B}(t), \qquad \widetilde{x}(t) \in \mathbb{S}^1, \tag{48}$$

where $\{\widetilde{B}(t)\}_{t \geq 0}$ is a Brownian motion on $\mathbb{S}^1$. The FPE corresponding to Eq. (48) is

$$\frac{\partial}{\partial t} \widehat{p}(t, \widetilde{x}) = -\frac{\partial}{\partial x} \widehat{J}(t, \widetilde{x}), \quad (\widetilde{x} \in [0, L)), \tag{49}$$

where $\widehat{p}(t, \widetilde{x}) = \sum_{n=-\infty}^{\infty} p(t, \widetilde{x} + nL)$ is a probability density of the system in position $\widetilde{x} \in \mathbb{S}^1$ at time t, it is smooth on $\mathbb{S}^1$, and the corresponding probability current is

$$\begin{aligned}
\widehat{J}(t, \widetilde{x}) &= b(x)\widehat{p}(t, \widetilde{x}) - \frac{A^2}{2} \frac{\partial}{\partial x} \widehat{p}(t, \widetilde{x}) \\
&= \left[b(\widetilde{x}) - \frac{A^2}{2} \frac{\partial}{\partial \widetilde{x}} \ln \widehat{p}(t, \widetilde{x}) \right] \widehat{p}(t, \widetilde{x}).
\end{aligned} \tag{50}$$

Since $\widetilde{J}$ is defined on a circle, it is also called the circulation of the stochastic motion. It is more directly to be visualized than the same object in a Markov chain.

With Eqs. (48)–(50), there is a unique invariant probability distribution $\nu(d\widetilde{x}) = \widehat{p}(\widetilde{x})d\widetilde{x}$ for system (48), where $\widehat{p}(\widetilde{x})$ is the solution to the equation

$$b(x)\widehat{p}(\widetilde{x}) - \frac{A^2}{2} \frac{\partial}{\partial x} \widehat{p}(\widetilde{x}) = \widehat{J}, \tag{51}$$

in which $\widehat{J}$ is a constant. The process $\{\widetilde{x}(t)\}_{t \in R}$ is ergodic on $\mathbb{S}^1$. For more related discussions on diffusion processes on a manifold, see [64,65].

The Gibbs entropy associated with the probability density $\widehat{p}(t, x), x \in \mathbb{S}^1$ is

$$S(t) = -\int_0^L \widehat{p}(t, x) \ln \widehat{p}(t, x)dx.$$

Differentiating $S(t)$ with respect to t, we have

$$\begin{aligned}
\frac{dS(t)}{dt} &= -\int_0^L [\ln \widehat{p}(t, x) + 1] \frac{\partial \widehat{p}(t, x)}{\partial t} dx \\
&= -\int_0^L \ln \widehat{p}(t, x) d\widehat{J}(t, x) \\
&= -\int_0^L 2A^{-2}b(x)\widehat{J}(t, x)dx + \int_0^L 2A^{-2}b(x)\widehat{J}(t, x)dx - \int_0^L \frac{\partial}{\partial x} \ln \widehat{p}(t, x)\widehat{J}(t, x)dx \\
&= -\int_0^L 2A^{-2}b(x)\widehat{J}(t, x)dx + \int_0^L 2A^{-2} \left[b(x) - \frac{A^2}{2} \frac{\partial}{\partial x} \ln \widehat{p}(t, x) \right] \widehat{J}(t, x)dx \\
&= -\int_0^L 2A^{-2}b(x)\widehat{J}(t, x)dx + \int_0^L 2A^{-2} \left[b(x) - \frac{A^2}{2} \frac{\partial}{\partial x} \ln \widehat{p}(t, x) \right]^2 \widehat{p}(t, x)dx.
\end{aligned} \tag{52}$$

In the above equation, we introduce

$$h_d \overset{\triangle}{=} \int_0^L 2A^{-2}b(x)\widehat{J}(x)dx, \tag{53}$$

which should be interpreted as the *heat dissipation rate (h.d.r)* of the system; and

$$e_p \triangleq \int_0^L 2A^{-2} \left[b(x) - \frac{A^2}{2} \frac{d}{dx} (\ln \widehat{p}(x)) \right]^2 \widehat{p}(x) dx, \tag{54}$$

which should be interpreted as the *entropy production rate (e.p.r)* of the system. Then Eq. (52) can be again written as

$$\frac{dS}{dt} = e_p - h_d. \tag{55}$$

This is the celebrated entropy balance equation in nonequilibrium thermodynamics [66]. An alternative definition for the e.p.r in terms of time irreversibility will be given by the theorem below.

If a system starts from the invariant distribution $\widehat{p}(x)dx$, i.e., it is in a NESS, then Eq. (55) becomes

$$e_p = h_d. \tag{56}$$

In a NESS, the amount of entropy created is precisely balanced by the amount of dissipation, while the entropy of the system remains constant.

In Section 2.3.3, we have discussed the e.p.r of a Markov process with discrete states and continuous time. There we had

$$e_p = \lim_{T \to \infty} \frac{1}{T} E \left[\ln \left(\frac{dP_{[0,T]}^+(\omega)}{dP_{[0,T]}^-(\omega)} \right) \right] = \frac{1}{2} \sum_{i \neq j} (\pi_i q_{ij} - \pi_j q_{ji}) \ln \frac{\pi_i q_{ij}}{\pi_j q_{ji}}.$$

For a diffusion process $\{x(t)\}_{t \geq 0}$, we in fact can have a similar result expressed in the following Theorem 2.10:

Theorem 2.10. *The entropy production rate of diffusion process on a circle is*

$$e_p = \lim_{T \to \infty} \frac{1}{T} E \left[\ln \left(\frac{dP_{[0,T]}^+(\omega)}{dP_{[0,T]}^-(\omega)} \right) \right]$$

$$= \int_0^L 2A^{-2} \left[b(x) - \frac{A^2}{2} \frac{d}{dx} (\ln \widehat{p}(x)) \right]^2 \widehat{p}(x) dx. \tag{57}$$

Proving formula (57) requires the application of Cameron–Martin–Girsanov theorem and the mathematical details are rather involved. We shall skip the proof here; readers who are interested in the mathematics are referred to Chapter 4 of Ref. [10].

As in the deterministic case, for a diffusion process $\{x(t, \omega)\}_{t \geq 0}$ defined on a circle, the rotation number $Rot = \lim_{t \to \infty} \frac{x(t, \omega)}{L\, t}$ (if it exists) describes the average number of turns a trajectory winding around the circle. It characterizes the circulations in a diffusion process. In generally, Rot is a stochastic quantity, a function of ω. However, by applying the ergodicity of system (48) on $\mathbb{S}^1$, we shall demonstrate in the following that the value of Rot is independent of the sample path ω.

Following the integral formula given in Appendix B, Eq. (B.5), we have

$$\frac{x(t, \omega)}{t} = \frac{1}{t} \int_0^t b(x(s)) ds + \frac{1}{t} \int_0^t A dB(s). \tag{58}$$

Using the law of logarithm of the Brownian motion [67]:

$$\Pr \left\{ \liminf_{t \to \infty} \frac{B(t, \omega) - B(0)}{\sqrt{2t \log \log t}} = -1 \right\} = 1,$$

$$\Pr \left\{ \limsup_{t \to \infty} \frac{B(t, \omega) - B(0)}{\sqrt{2t \log \log t}} = 1 \right\} = 1,$$

thus

$$\lim_{t \to \infty} \frac{A(B(t, \omega) - B(0, \omega))}{t} = 0, \quad a.e. \, P(d\omega). \tag{59}$$

Since the process $\{\widetilde{x}(t)\}_{t \geq 0}$ is ergodic on $\mathbb{S}^1$, then for almost all $\omega \in \Omega$, we have

$$(a.e.) \lim_{t \to \infty} \frac{x(t, \omega)}{t} = \quad (a.e.) \lim_{t \to \infty} \frac{1}{t} \int_0^t b(x) ds$$

$$\overset{\text{see Eq. (48)}}{=} (a.e.) \lim_{t \to \infty} \frac{1}{t} \int_0^t b(\widetilde{x}) ds$$

$$= \int_0^L b(\widetilde{x}) \widehat{p}(\widetilde{x}) d\widetilde{x}; \tag{60}$$

The last equality is ensured by the Birkhoff ergodic theorem. Therefore

$$Rot = \frac{1}{L} \int_0^L b(x)\widehat{p}(x)dx. \tag{61}$$

We now establish the relationship between the e.p.r and the rotation number using a rather elementary method [68]. A system in a steady state implies that $\frac{\partial \widehat{p}}{\partial t} = 0$, and since $\frac{\partial \widehat{p}(x)}{\partial t} + \frac{\partial \widehat{J}(x)}{\partial x} = 0$, then

$$\widehat{J}(x) = b(x)\widehat{p}(x) - \frac{A^2}{2}\widehat{p}'(x) = \text{Constant} \stackrel{\triangle}{=} J_c, \quad x \in \mathbb{S}^1. \tag{62}$$

As $\widehat{p}(x)$ is continuous on $\mathbb{S}^1$, then

$$J_c = \frac{1}{L} \int_0^L (b(x)\widehat{p}(x) - \frac{A^2}{2}\widehat{p}'(x))dx = \frac{1}{L} \int_0^L b(x)\widehat{p}(x)dx = Rot.$$

Therefore

$$
\begin{aligned}
e_p &= \int_0^L 2A^{-2}\left[b(x) - \frac{A^2}{2}\frac{d}{dx}\ln\widehat{p}(x)\right]^2 \widehat{p}(x)dx \\
&= \int_0^L 2A^{-2}\left[b(x)\widehat{p}(x) - \frac{A^2}{2}\widehat{p}'(x)\right]\left[b(x) - \frac{A^2}{2}\frac{d}{dx}\ln\widehat{p}(x)\right]dx \\
&= Rot \int_0^L 2A^{-2}\left[b(x) - \frac{A^2}{2}\frac{d}{dx}\ln\widehat{p}(x)\right]dx \quad \text{(see Eq. (62))} \\
&= Rot \int_0^L 2A^{-2}b(x)dx = Rot \times W, \quad \text{(Note } \widehat{p}(x) > 0 \text{ on } \mathbb{S}^1\text{)}
\end{aligned}
\tag{63}
$$

where $W = \int_0^L 2A^{-2}b(x)dx$ is the work done by the force $F(x) = 2A^{-2}b(x)$ winding around the circle $\mathbb{S}^1$.

The above result shows that the entropy production rate e_p is just equal to the rotation number Rot multiplying the total work per cycle, W. The rotation number of the system is a manifestation of the circulation. Hence the entropy production is due to the existence of circulations. In fact $e_p = 0$ if and only if $Rot = 0$. But also, $Rot = 0$ if and only if $W = 0$, i.e., the $b(x)$ has a potential on $\mathbb{S}^1$.

2.4.3. Equivalent conditions for a diffusion process in equilibrium

Similar to the case of discrete-state Markov chains, we have the following theorem for diffusion processes on a circle [10].

Theorem 2.11. *Let $\{\xi_t\}_{t\in R}$ be a stationary diffusion process on a circle described by Eq. (46), with state space $\mathbb{S}^1$ and an invariant distribution $\nu(dx)$, then the following conditions are equivalent:*

(1) *$\{\xi_t\}_{t\in R}$ is detail balanced, i.e.,*

$$\int_D \nu(dx) \int_{D'} P(t; x, dy) = \int_{D'} \nu(dy) \int_D P(t; y, dx),$$

$D, D' \subset \mathbb{S}^1$, in which $P(t; x, dy)$ represents transition probability.
(2) *The process $\{\xi_t\}_{t\in R}$ is reversible.*
(3) *The entropy production rate of $\{\xi_t\}_{t\in R}$ is zero, i.e., $e_p = 0$.*
(4) *the rotation number vanishes, i.e., $Rot = 0$.*
(5) *The force $F(x) \stackrel{\triangle}{=} 2A^{-2}b(x)$ has a potential function, i.e., there exists a continuous $U(x)$ such that $F(x) = -U'(x)$, and $\int_{S^1} e^{U(x)}dx = 1$.* $\square$

3. Coherent resonance in stochastic nonlinear systems with circulations

Uncertainty is an inevitable part of mathematical models of natural phenomena. The rise of statistical thinking testifies the importance of dealing with randomness, or noise, in modern science, be it physical, biological or social, and engineering. However, deeply rooted in Newtonian–Laplacian tradition of classical mechanics, noise has long been thought to be a nuisance, playing only a destructive role. It supposedly hinders the transmission and detection of signals, and causing the behavior of a system irregular and uncontrollable. However, during the past two decades, it has been discovered that under certain nonlinear conditions, an extra dose of noise can actually play a "constructive" rather than a "destructive" role. For example, in signal processing, noise can help enhancing the transmission of signal! The recently emerged area of research on stochastic resonance (SR) has become a paradigm for illustrating this seemingly counter-intuitive role of

noise [26]. In fact, we are witnessing an increasing list of phenomena due to the positive effect of noise: coherence resonance (CR) [69–71], noise-induced transport (which includes Brownian motor) [28], stochastic focusing [72], noise suppressing noise [73], stochastic induced bifurcation and bistability [74,75], and stochastic synchronization [76]. The list is rapidly growing. We now realize that all these phenomena occur only in systems that are far from equilibrium; all these phenomena are behavior of driven systems. Borrowing the concepts from Section 2, it is not the noise *per se*, but the "energy" carried by an irreversible stationary stochastic process that does the job.

Recall that in Section 2, nonequilibrium steady state (NESS) is characterized by the following properties [10]:

(i) the underlying stochastic process is irreversible with respect to time;
(ii) the entropy production of the system is positive;
(iii) there appears clockwise and counterclockwise nonbalanced circulations (NBC) in the system.

Recent studies have further shown that NESS also exhibits nonmonotonic power spectrum due to the property (iii). Mathematically, this is a consequence of complex eigenvalues associated with irreversible Markov processes [59,77] (Q matrix with detailed balance has all eigenvalues being real).

In the following two sections, we shall discuss the noise-induced phenomena within the framework of the theory of NESS. The present Section 3 focuses on stochastic and coherence resonance. Section 4 will be dedicated to Brownian ratchet models for molecular motors. We refer the readers to two previous reviews published by the *Review of Modern Physics*, on the two subjects [26,27]. The unique feature of our review is treating these two subjects as applications of the theory of NESS.

This section starts with a general introduction to two types of SR: those with a deterministic, periodic driving force and those without. The latter, also known as SR without forcing, is now widely called CR. Then in Section 3.2 we discuss the phenomenon of CR and its nonequilibrium nature in terms of a one-dimensional stochastic model on a circle (the phase model), the two-dimensional FitzHugh–Nagumo (FHN) model, and (Section 3.2.5) the stochastic Hodgkin–Huxley (HH) model. The last one is the most natural way of attacking a system with internal noise, which is quite novel. Section 3.3 studies the phenomena of SR, starting with the periodically driven one-dimensional system on the circle with a bistable potential. We note that by mapping a non-autonomous, periodically driven system to a high-dimensional autonomous one, there is essentially no difference between SR and CR. Furthermore, using an embedding-based description, the bistable system is shown to exhibit SR in the super-threshold regime. Section 3.4 is devoted to explore the phenomena of CR and SR in coupled systems where one has the interplay among noise, nonlinearity, and "spatial" coupling, which often considered as a model for flocking behavior.

3.1. Brief introduction

3.1.1. Stochastic resonance (SR)

The phenomenon of SR was first discovered independently in 1981 by Benzi et al. [78,79] and Nicolis et al. [80,81] in studying the problem of periodically recurrent ice ages. Through analyzing the historical records of 700,000 years of the climate change, it was discovered that there is an approximately 100,000 year cycle between two successive ice ages. Analyzing the power spectrum of the time series for the ice volume, inferred from oxygen isotope data, revealed a clear frequency peaking. At the same time, one also discovered that the earth's motion around the sun experiences a 100,000 year periodic influence, due to the perturbation of other planets. This influence, however, is rather weak. This led to a proposal that the weak periodic influence to the earth's motion can be "boosted" by a random forcing inherently present in the planetary motion. A typical model in studying the SR phenomenon, thus, is the following equation which contains bistability:

$$\frac{dx}{dt} = -\frac{dV(x)}{dx} + a\sin(\omega t + \varphi) + D\xi(t), \tag{64}$$

where $V(x) = \frac{x^4}{4} - \frac{x^2}{2}$ is a potential function with two wells, a, ω and φ are the magnitude, frequency and initial phase of the periodic driving force, respectively. $\xi(t)$ is a white noise, i.e., the "derivative" of a Brownian motion that satisfies

$$\langle \xi(t) \rangle = 0, \quad \langle \xi(t)\xi(t') \rangle = \delta(t - t'), \tag{65}$$

and D is the noise intensity.

With respect to the climate dynamics, the two stable states correspond to an ice state and a warm state; the weak periodic influence in planetary motion is represented by a sinusoidal function $a\sin(\omega t + \varphi)$; and the white noise represents the random forcing. One can intuitively understand the following: If without the external periodic force, then the random forcing will make the system stochastically transit between the two (ice and warm) states. But the oscillatory cycle will not be periodic. The weak periodic influence makes the stochastic transition more periodic. On the other hand, without the white noise, the periodic force is too weak to be able to push the system over the energy barrier.

In fact, from the power spectrum of the signal $x(t)$, one finds a peak, located at the frequency of the external drive. Furthermore, the height of the peak changes with the noise intensity, and the height reaches a maximum at an intermediate noise level. This resonance-like optimal behavior is called SR. Note that unlike the traditional resonance of deterministic

systems in which there is a "frequency matching", here the term "resonance" emphasizes the greatest response of the system to an optimal noise intensity. The traditional resonance, in the contrary, is weaken by the presence of noise. Still, SR and the traditional resonance share a common feature: Both represent an enhancement of the output signal of a system.

Since the original development of the concept of SR thirty years ago, the SR phenomenon has been extensively observed in controlled experiments. Fauve and Helslot first realized the SR in an electronic device called Schmitt trigger system [82]. Later, McNamara et al. also observed SR in a bistable ring laser [83]. Today, SR has grown into an exciting, highly interdisciplinary area of research that involves both theories and experiments. SR phenomena have been observed in superconducting device [84–86], magnetic systems [87], optics [88–92], quantum systems [93,94], chemical reactions [95,96,61], neurophysiology [97–101], and biological evolutionary systems [102]. For a comprehensive discussion of the applications of SR, see reviews [26,103].

On the theoretical side, it has been shown that beside bistability, uni-stable systems with excitability can also exhibit SR. In contrast to a bistable system, an excitable system has a single stable state (called resting state) but also a threshold. When a relatively large perturbation passes the threshold, the system undergoes a large excursion (called excited state, or "firing"). Driven by a noise together with a periodic force, excitable systems can exhibit SR phenomenon [104–106]. The canonical example of excitability is the Hodgkin–Huxley (HH) equation for the dynamics of neuronal membrane potential [107–111]. Its simplified version is the FitzHugh–Nagumo (FHN) equation [112–115]. Several other systems: Hindmarsh–Rose model [116,117], Morris–Lecar model [118], integrate-and-fire (IF) mode [110,119,120], and the phase mode (i.e., dynamics on the circle) [121–123] all have been studied in connection to SR.

3.1.2. Coherence resonance (CR)

With the SR understood as above, it comes as a surprise that even without a periodic drive, excitable systems can still exhibit coherent oscillation in the presence of noise (or more precisely a stochastic driving force). This phenomenon has also been called stochastic limit cycle in phase space [124]. The system also shows the property of "resonance": There is an optimal noise intensity at which the noise-sustained oscillations become most regular. To distinguish this type of phenomena from SR, it has been termed as coherence resonance (CR).

Originally, CR was found in a simple dynamical system [125] in the vicinity of a saddle–node bifurcation. Hu et al. called the phenomenon "SR without forcing". The history of CR, however, is much longer. It is interesting to note that it had been discussed in the enzyme reaction literature by Chen in 1973 [126], for a linear reaction, and Hahn et al. in 1974 for a nonlinear reaction [127].

The canonical model for the CR is the following Adler's one-dimensional system on a circle:

$$\frac{dx}{dt} = b - \sin x + D\xi(t), \quad x \in \mathbb{S}^1, \tag{66}$$

where $b > 0$ is a control parameter, $\xi(t)$ is a white noise satisfying Eq. (65), and D is the intensity of noise.

Pikovsky and coworkers investigated CR in the FitzHugh–Nagumo (FHN) model near a Hopf bifurcation [71]. The corresponding equation can be written as [128]

$$\begin{cases} \dfrac{du}{dt} = u(a - u)(u - 1) - v + b + D\xi(t), \\ \dfrac{dv}{dt} = \varepsilon(u - \gamma v), \end{cases} \tag{67}$$

where u is the fast, voltage-like variable and v is the slow recovery variable. $\epsilon \ll 1$ is a small parameter allowing one to separate all motions into the fast and slow ones. The parameter b controls the firing behavior of a neuron in deterministic case. The noise term stands for external perturbations from other neurons as well as intrinsic noise sources.

CR can be expected in systems near its dynamical bifurcation point [129–131]. It is now a sub-field of the stochastic resonance research. Through exploring different mathematical models (see review [132]), the mechanism of CR has also been extensively discussed in the literature. Statistically speaking, CR is explained as the result of difference in the noise dependences of activation time and excursion time [71,132]. Dynamically, it is regarded as due to the noise precursor of bifurcation [129–131]. Qian and Qian [61] first pointed out that, as a nonequilibrium phenomenon, the occurrence of CR is a consequence of the unbalanced circulation in the stochastic dynamics. The NESS approach to CR in terms of the one-dimensional dynamics on a circle, Eq. (66), and two-dimensional FitzHugh–Nagumo model (Eq. (67)) will be presented in Section 3.2.4.

The above discussed SR and CR are all in the context of ordinary differential equations. With many potential applications in physics, chemistry, and life sciences (see reviews [26,133,132]), both SR and CR have been extended into coupled systems with spatial dimension, i.e., lattice and partial differential equations. One of the earliest report on the subject is [134]. Later, spatiotemporal order and array enhanced SR were introduced by Lindner et al. [69]. Their work was further carried to two-dimensional systems [135]. These work has shown that the occurrence of SR is due to a cooperation between a periodic driving force, white noise, and the coupling. There is a sizable literature on the subject [136–142]. SR has also been extended to chaotic systems and quantum systems. See the reviews [26,103] for more details.

The distinction between the SR and CR is only a mathematical one. Consider the system in Eq. (64) which contains an external periodic drive. This is a non-autonomous differential equation. However, it is equivalent to the following autonomous system:

$$\frac{dx}{dt} = -V'(x) + a \sin(\theta + \phi) + D\xi(t), \qquad \frac{d\theta}{dt} = \omega,$$

(68)

where $\theta \in \mathbb{S}^1$. The second equation is defined on a cycle. Thus, (x, θ) is defined on a cylinder. As we shall show, this dynamics on a cylinder's point of view is very natural to the SR problem. We believe the key to understand SR is to understand CR. The present review reflects this believe of ours.

3.1.3. The characterization of CR

One of the standard methods for analyzing CR is the power spectrum. Suppose that $\{x(t)\}_{t \geq 0}$ is a solution to an excitable system driven by a white noise but without a periodic force, then in the long time limit $x(t)$ is a stationary stochastic process (the solution to SDE). The power spectrum of the stochastic process $\{x(t)\}_{t \geq 0}$ is defined as

$$S(\omega) = \int_{-\infty}^{\infty} E\left[x(t)x(t + \tau)\right] e^{-i\omega\tau} d\tau.$$

(69)

Here, to be consistent with Section 2, we use the $E[\cdots]$ to denote the expectation instead of the $\langle \cdots \rangle$. Alternatively, because of the Wiener–Khinchin theorem, one has

$$S(\omega) = \lim_{T \to \infty} \frac{1}{T} E\left[\left|\int_{-T}^{T} e^{-i\omega t} x(t) dt\right|^2\right].$$

(70)

The equivalence between Eqs. (69) and (70) is due to the ergodicity of the stationary process. Since function $S(\omega)$ is an expectation, it is a deterministic function.

In numerical simulations, we need to take the time sequence sufficiently long. Equivalently, we can take adequate number of identical, independent realizations of $\{x(t)\}_{t \geq 0}$ and obtain the average of their power spectrum.[8] From N identical, independent time series $\{x_k(t)\}$ according to certain numerical algorithm, such as Runge–Kutta or simply Euler forward method, one can compute the corresponding Fourier transforms $\hat{S}_k(\omega)$, which is an approximation of $S_k(\omega)$ defined by formula Eq. (70) ($k = 1, \ldots, N$). Then the power spectrum we need is:

$$S(\omega) = \frac{1}{N} \sum_{k=1}^{N} \left|\hat{S}_k(\omega)\right|^2.$$

(71)

For CR, Hu et al. [125] introduced a quality factor β to quantify the influence of noise on the output signal:

$$\beta = \omega_p h / W,$$

(72)

where h and ω_p are the peak height and location of the power spectrum, and W is the width of the power spectrum at height $h/\sqrt{e}$. Therefore, W/ω_p is the relative sharpness of the power spectrum peak. Hence large h and small W/ω_p indicates a more deterministic like periodic oscillation. Another way to look at the β is that h and ω_p reflect noise's positive contributions to the periodic motion, while W reflects its destructive role.

Beside the spectral method, the phenomenon of CR can also be studied by statistical analysis. Taking the FHN model (67) as an example, one can define a threshold level u_{th} in the voltage variable u. Suppose that $\tau_0 = 0$, $u(\tau_0) = u_{th}$, let

$$\tau_i = \inf\{t > \tau_{i-1} : u(t) = u_{th}, \dot{u}(t) > 0\},$$

(73)

which corresponds to, because of the threshold phenomenon, the onset of a spike at the time τ_i, then $T_i = \tau_i - \tau_{i-1}, i \geq 1$ is a sequence of the interspike interval (ISI) time. It is easy to see that $\{T_i, i \geq 1\}$ is an i.i.d. sequence and has the identical distribution density as T, a continuous non-negative random variable, defined as

$$T = \inf\{t > 0 : u(t) = u_{th}, \dot{u}(t) > 0\}.$$

Then CR can be measured by the coefficient of variation (CV) of T, defined as

$$\rho = \frac{\sqrt{Var\,(T)}}{E[T]}$$

(74)

where $E[T]$ is the mean of the ISI T, and $Var\,(T) = E[T^2] - E[T]$ is the variance of T. Smaller the ρ is, more periodically regular the spiking will be.

---

[8] In practice, the difference between these two methods is due to a very slowly varying component in the time series. In that case, the shorter realizations serve as a "filter" for the low frequency signal.

3.1.4. The characterization of SR

For a periodically driven system, the time correlation function of the process

$$E[x(t)x(t+\tau)] \tag{75}$$

is a function of both t and τ. Ref. [26] suggested a phase-averaged power spectral density defined as

$$S(\omega) = \int_{-\infty}^{\infty} \langle E[x(t)x(t+\tau)]\rangle e^{i\omega\tau} d\tau, \tag{76}$$

where the $E[\cdots]$ denote the ensemble average over the realizations of the noise and $\langle \cdots \rangle$ stands for $\frac{1}{T}\int_0^T [\ldots]dt$, where T is the period of the driving force.

The standard method for quantifying SR is to compute signal-to-noise ratio (SNR) or response amplitude (RA). The SNR is defined as

$$SNR = \frac{2}{S_N(\omega)} \left[\lim_{\Delta\omega \to 0} \int_{\omega-\Delta\omega}^{\omega+\Delta\omega} S(\omega')d\omega' \right], \tag{77}$$

where $S(\omega)$ is the power spectrum of the signal, and $S_N(\omega)$ is the power spectrum of the noise itself. The RA is defined as

$$RA = \frac{R_1}{R_0}, \tag{78}$$

where R_0 is the peak height of the power spectrum of the output signal in the absence of the noise (i.e., $D = 0$), and R_1 is the height in the presence of noise. We say that an SR occurs when RA as a function of D shows a maximum RA_{max}. Larger the value of RA_{max}, stronger the effect of SR.

Both SNR and RA characterize the enhancement of the output periodic signal due to the presence of the noise in the frequency domain. In addition, parallel to the ISI distribution for excitable systems, another method to quantify SR is done in time domain. For the bistable system (64), one can calculate the residence distribution of two successive switches between the two potential wells. More precisely, we set two crossing levels, for instance at $x_\pm = \pm c$ with $0 \le c \le 1$. Suppose that at time $t_0 = 0$, $x(0) = -c$, $\dot{x} < 0$, let

$$t_{2k+1} = \inf\{t > t_{2k}, x(t) = c, \dot{x}(t) > 0\},$$
$$t_{2k} = \inf\{t > t_{2k-1}, x(t) = -c, \dot{x}(t) < 0\}, \quad k = 1, 2, \ldots,$$

then the quantity $T_i = t_i - t_{i-1}$ represents the residence time between two subsequently switching events. If the distribution of the residence time has peaks at $\left(n - \frac{1}{2}\right) T_\omega$, where $T_\omega = 2\pi/\omega$ is the period of the driving force and $n = 1, 2, \ldots$, with the peak at $\frac{1}{2}T_\omega$ being dominant, then this can be considered as a signature of SR. For more discussions on this method, see [143–145].

For systems exhibiting CR and SR, the above mentioned characteristics all share a common feature: With the increase of the noise intensity, they all increase first, but at some particular noise intensities, begin to decrease. There is an optimal noise intensity. This is the hallmark of SR.

In general, the methods used in studying SR are based on theoretical analysis, numerical computation, and experiments. So far, the theoretical studies are based on the FPE or associated SDE. Unfortunately, as a second-order partial differential equation, the FPE with two energy wells is notoriously difficulty to be integrated numerically due to its stiffness. Hence, a large amount of literature focuses on the adiabatic approximation ($b \ll 1$, $\omega \ll 1$, $D \ll 1$). This regime has provided many useful results [146–151]. However, the approach is not very effective for systems with strong noise or strong periodic drive. We shall not follow this direction in the review; for applying adiabatic method to this type of problems, see [18].

3.2. Nonequilibrium nature of coherence resonance in excitable systems

In this section, we take the one-dimensional phase model, the IF single neuron model, as well as the two dimensional FHN model (67), as examples for explaining how nonequilibrium circulation plays it organizational role in the occurrence of CR in excitable systems. In these models, both the dynamical and physical mechanisms of CR will be elucidated. In particular, the FHN system motivates the novel concept of stochastic limit cycle [124] which is intimately related to the nonequilibrium circulations we discussed in Section 2. The discussions of the nonequilibrium characteristic of CR in these models are representative for all other excitable systems, where NBC can be described in terms of the statistical properties of the stochastic limit cycle, and the rotation number introduced in Section 2.4.2.

3.2.1. Coherence resonance in a simple phase model

We first investigate the phenomenon of CR in a phase model whose dynamics is characterized by the one-dimensional Adler equation (66): $\dot{x} = b - \sin x + D\xi(t)$, $x \in \mathbb{S}^1$ [152,153].
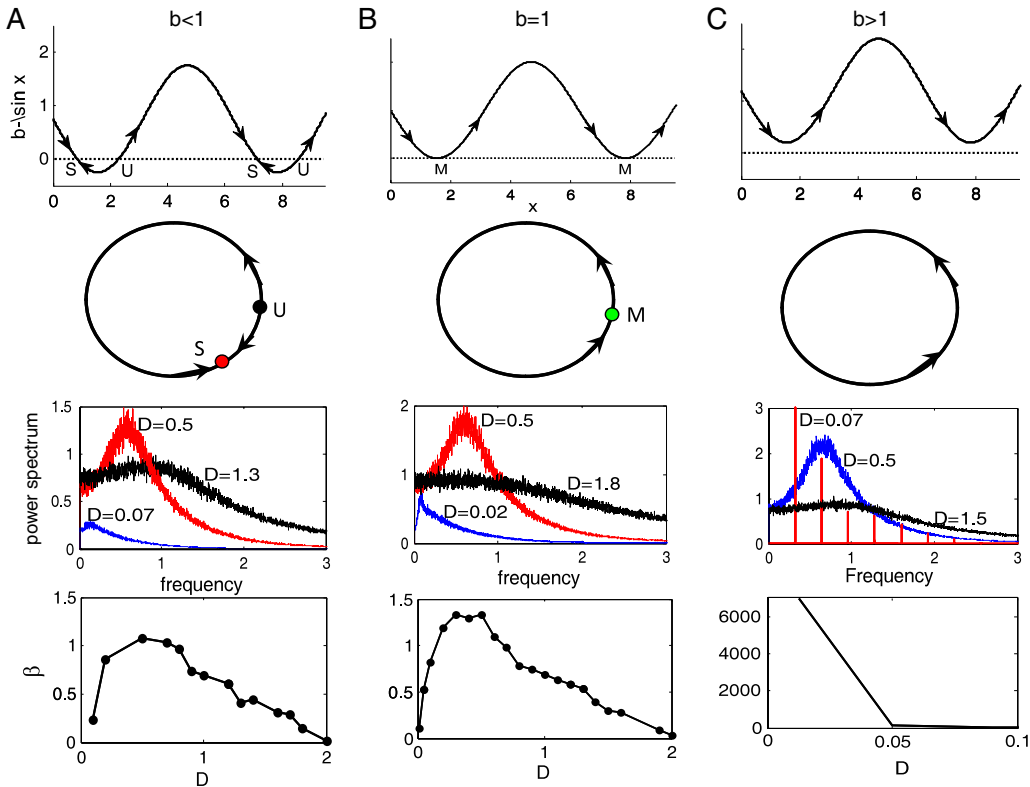
Fig. 2. From top to bottom traces: the phase curves of system (79), the fixed points shown on a circle (S: stable, U: unstable, M: marginal stable), the average power spectra of $\sin\{x(t)\}_{t\geq 0}$, and the quality factors β of Eq. (66) as functions of the noise intensity D. Column (A) is for $0 < b < 1$, column (B) is for $b = 1$ and column (C) is for $b > 1$.

The deterministic equation corresponding to Eq. (66) is

$$\dot{x} = b - \sin x, \quad x \in \mathbb{S}^1. \tag{79}$$

The dynamics of Eq. (79) is properly defined on the unit circle $\mathbb{S}^1$. There are two fixed points (one is a stable node and the other is an unstable saddle) of Eq. (79) on the circle for $0 < b < 1$. When b increases to 1, these two fixed points collide into a saddle–node point which is marginal stable. In these two cases, the particle starting from a point different from the fixed points eventually stays close to the stable fixed point S (for $0 < b < 1$) or the semistable fixed point M (for $b = 1$). So the rotation number is just zero. When $b > 1$, the fix point disappears and the particle starting from any point will rotate periodically around the circle forever. This gives a nonzero rotation number for $b > 1$ even without noise.

Let us investigate the situation when white noise is present. For the case $0 < b < 1$, instead of staying motionless at the stable fixed point S, the particle will wander in the neighborhood of the stable fixed point S for some time. However, there is a positive probability that the noise produces a sufficiently large positive force, which pushes the particle to overcome the threshold U (i.e., the energy barrier). Therefore, at a certain random time, it escapes from the attraction of S and reaches the position where the unstable fixed point is located and then completes a full counter-clockwise to be back into the basin of attraction of S again. The normal distribution of the noise term ensures that this process is recurrent. Thus a coherent, noise-induced rotation on the circle appears. This motion can be quantified by a nonzero rotation number. With the increase of noise strength, such a circular motion occurs more frequently. It is easy to see that the rotation number also becomes larger (see the dashed curves with open circles in Fig. 7). However, if the noise intensity is too large, then both clockwise and counter-clockwise cycling occur, and the coherent motion is destroyed.

Numerical computations are used to obtain the power spectrum of the stochastic dynamics of Eq. (66). The third panel of Fig. 2(A) shows the power spectra of the system with $b = 0.98$ and three different values of D. As usually, we consider the power spectrum of $\{\sin x(t)\}_{t\geq 0}$ [equivalent to $x(t)\mod(2\pi)$]. One sees that for small noise (for example $D = 0.007$), a small spectrum peak occurs at a low frequency (curve a1). As the strength of noise increases, the peak moves toward a higher frequency, meanwhile the height of the spectrum peak increases until reaching a maximum at a certain value of D (about $D = 0.5$). After that, the peak height decreases with the further increase of the noise intensity. If the strength of noise becomes sufficiently large, no distinct peak in the power spectrum can be observed (see the curve for $D = 1.3$). Thus the strongest coherent oscillation occurs at an intermediate value of D. To further confirm the above observation, we also plot the quality factor β versus D in the bottom panel of Fig. 2(A). The figure shows that as a function of D, β has a maximum. In

the region with positive slope, the enhancement of the quality factor indicates that the coherent motion becomes stronger as the noise intensity D increases. The negative slope tells us that the noise is gradually destroying the coherent motion when its strength increases. The fact that the quality factor passing through a maximum at a certain value of noise intensity announces the existence of coherence resonance.

As can be seen from Fig. 2(B), $b = 1$ is a critical case in which S and U coincide at the point M and the deterministic system is marginal stable. Then even a slight perturbation can motivate the particle to move away from the semistable fixed point M (a saddle–node). But the particle will still oscillate near M for a certain random time before rotating around the circle and then entering the neighborhood of M again. Hence in this case, the system also occurs CR at a certain noise intensity. And since the threshold is greatly decreased, one can expect a better effect of CR than in the case $0 < b < 1$ (compare the bottom panels in Fig. 2(A) and (B)).

As for the case $b > 1$, since the particle without noise perturbation is already rotating periodically on the circle in one direction, the presence of noise can only destroy such a periodic motion. The destruction of the coherent motion of the system by noise can be clearly seen in the last two panels in Fig. 2(C) for $b = 1.05$, where the height of the spectrum peak and the value of the quality factor β both decrease with the increase of the noise intensity. There is no CR in this case.

3.2.2. Coherence resonance in an integrate-and-fire single neuron

Both SR and CR have been successfully demonstrated in mathematical models of neural systems and laboratory neurophysiological experiments [98,154,132,99,155,156]. Applications of SR and CR have been enthusiastically anticipated. In fact, several successful biomedical applications have been achieved. For a comprehensive review, see [157].

In mathematical modeling of single neuron, integrate-and-fire (IF) model has been widely used by computational neuroscientists due to its simplicity [158]. Even though this simple model often is not sufficient in describing the dynamics of a real neuron [159,160], it is expected to provide great insights for dynamics of neural networks where emergent properties are usually insensitive to the details of underlying single neurons. In this section, we shall consider the single IF neuron driven by Gaussian white noise. The source of the noise is assumed to be "external": It represents the synaptic inputs from many other neurons [101,161,162]. In more realistic biological applications, the noise is often assumed to be a Poisson process or more generally a renewal process [163,164].

The dynamics of a single IF neuron subject to a Gaussian white noise is given by the following threshold equation

$$
\begin{cases}
C_m \cdot dV = -g_L \cdot V dt + I dt + \sigma_c dB_t, & V \leq V_{th} \\
V = V_{rest}, & V > V_{th}.
\end{cases} \tag{80}
$$

Here g_L is the leaky conductance, and an artificial threshold is added to say that once $V(t)$ crosses the threshold V_{th} from below, a spike is generated and $V(t)$ is reset to the resting state V_{rest}. Without noise, the neuron stays at $V = I/g_L$ if $I \leq g_L \cdot V_{th}$, and generates spikes periodically for $I > g_L \cdot V_{th}$.

Actually, the dynamics of the system can again be considered on a circle by wiring the solution on a circle and regarding V_{rest} and V_{th} as being identical (modul 2π). Let $\mathbb{S}^1_{[V_{rest},V_{th}]}$ be the circle. The model is then simply written as

$$
C_m \cdot dV = -g_L \cdot V dt + I dt + \sigma_c dB_t, \quad V \in \mathbb{S}^1_{[V_{rest},V_{th}]}. \tag{81}
$$

This model is now equivalent to the phase model discussed in the previous subsection. Corresponding to each value of $V \in (V_{rest}, V_{th})$, we can define a phase on the circle $\mathbb{S}^1_{[V_{rest},V_{th}]}$, with $\theta_{rest} = 0$ which corresponds to $V = V_{rest}$, and $\theta_{th} = 2\pi$ corresponding to $V = V_{th}$. When $I < g_L \cdot V_{th}$, the deterministic system without noise has two fixed points on the circle, one is located at θ_s corresponding to $V = I/g_L$. It is stable. The other is located at θ_{th}, which is unstable.

By defining the deterministic picture of model (80) on the circle $\mathbb{S}^1_{[V_{rest},V_{th}]}$, the effect of noise on a single IF neuron can be explored in the same way as in the phase model. For simulation, we take $C_m = 1 nF, V_{th} = 20$ mV, $g_L = 0.05 \,\mu S, V_{rest} = 0$ mV. The time evolutions of the membrane potentials without noise (red) and in the presence of noise (blue) are plotted in the second panel of Fig. 3, the power spectra for different noise intensities are depicted in the third panel, and the curves of the quality factor β and the coefficient of variance (CV) vs. the noise intensity are plotted in the bottom panel. It is shown that for $I < g_L \cdot V_{th}$ (it is equal to 1 in the above given values of parameters), CR occurs at an intermediate noise intensity, and coherent spiking is induced at this noise intensity. This is similar to the phase model in the case $b < 1$. Furthermore, once the quality factor reaches a maximum, the CV reaches a minimum which indicates the best coherence of the firing.

As expected, there is no CR for $I > g_L \cdot V_{th}$, because the neuron already fires regularly even without noise, adding noise only destroys such a periodic firing behavior. Therefore, the quality factor β decreases, while the CV increases with the increase of the noise intensity (see Fig. 3(C)).

What is different from the phase model is for the critical case $I = g_L \cdot V_{th}$. In both models, no rotating motion occurs on the circle without noise, and the corresponding spectrum, obtained as the Fourier transform of a transient trajectory is of Lorentz type centered at zero frequency. In the presence of noise, the peak of the spectrum peak first increases with increasing noise intensity, reaching a maximum and then decreases with the further increase of the noise perturbation. This characterizes the occurrence of CR in the phase model for the critical case $b = 1$ (see Fig. 2(B)). However, for the IF neuron, even a very weak noise perturbation (for example $D = 0.0001$) can induce the neuron to fire quite coherently. However, increasing the noise intensity destroys the coherence in the firings, which can be seen from the decreasing of the power
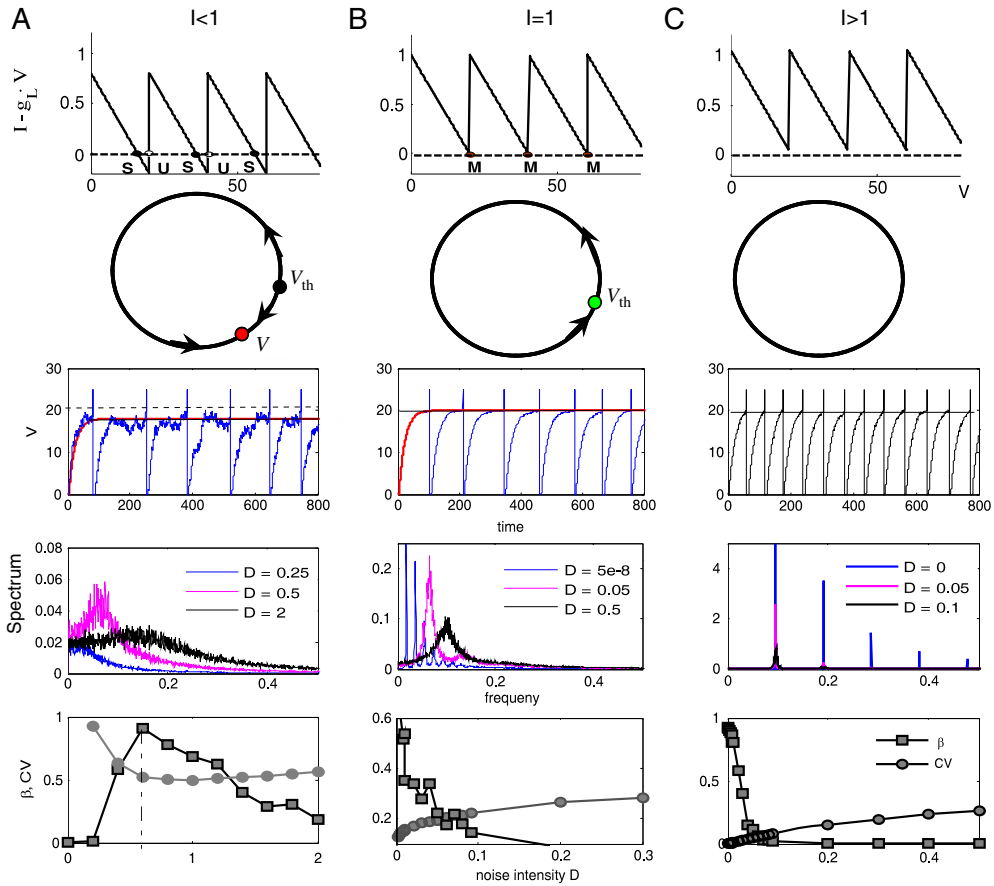
Fig. 3. From top to bottom traces: the phase curves of $\dot{V}$ vs. V, the fixed points (S: stable, U: unstable, M: marginal stable) shown on the circles, the time course of the membrane potential of system (80), the average power spectrum of $\{V(t)\}_{t\geq 0}$, and the quality factor β (square) and the CV (circle) as functions of THE noise intensity D. (A) $0 < I < g_L \cdot V_{th} (= 1)$. (B) $I = g_L \cdot V_{th} (= 1)$. (C) $I > g_L \cdot V_{th} (= 1)$. (For interpretation of the references to colour in this figure legend, the reader is referred to the web version of this article.)

spectrum peak as well as the quality factor. To understand the reason for this difference between the two models in the critical case, let us first have a look of the dynamics of the particle (single neuron in the IF model) in a small neighborhood of the fixed point (see the upper panel of Fig. 2(B) and the upper panel of Fig. 3(B)). For the phase model, $\dot{x}$ looks parabolic near its minimum, thus the velocities in the left and right neighborhoods of the fixed point are both very small, but with opposite directions. In the presence of noise, though the particle can be perturbed to escape the semistable fixed point and rotates around the circle, the fixed point still makes itself feel through a saddle–node ghost [62], if the noise intensity is very weak. On the other hand too strong noise totally makes the system behave randomly. This is why one sees similar pictures of the power spectra for the cases of $b < 1$ and $b = 1$ in the presence of noise. For the IF model, $\dot{V}$ is not continuous near its minimum, it linearly decreases to zero below the threshold, and once it reaches V_{th}, it "spontaneously" re-starts from a large positive value I. Under such a deterministic dynamics, even a very weak noise can easily induce the neuron fire regularly, while further increasing the noise intensity destroys the coherence of the firing gradually. This explains a decreasing quality factor with the increasing noise, but with a sharp jump between the deterministic and stochastic cases.

3.2.3. Coherence resonance in FitzHugh–Nagumo system

In this subsection, we take the well known FitzHugh–Nagumo (FHN) equation (67) from neuroscience as a typical mathematical model to further investigate how nonequilibrium, unbalanced circulation (NBC) plays the essential role in the occurrence of CR in excitable systems. We will first give a more precise description of a *stable stochastic limit cycle* (SSLC) than one finds in the literature. We then describe the probability localization behavior of NBC intuitively in terms of the statistical properties of the SSLC. And finally we shall present our point of view: the occurrence of CR is not only due to the existence of NBC, but more crucially, it is a result of sufficient localization of NBC along the SSLC [165].

Through out the discussion, all computations and graphings are based on system (67) with parameters fixed as $a = 0.14$, $\gamma = 2.54$, $\epsilon = 0.005$. The nullclines of the deterministic system plotted in Fig. 4 show that the system is excitable for
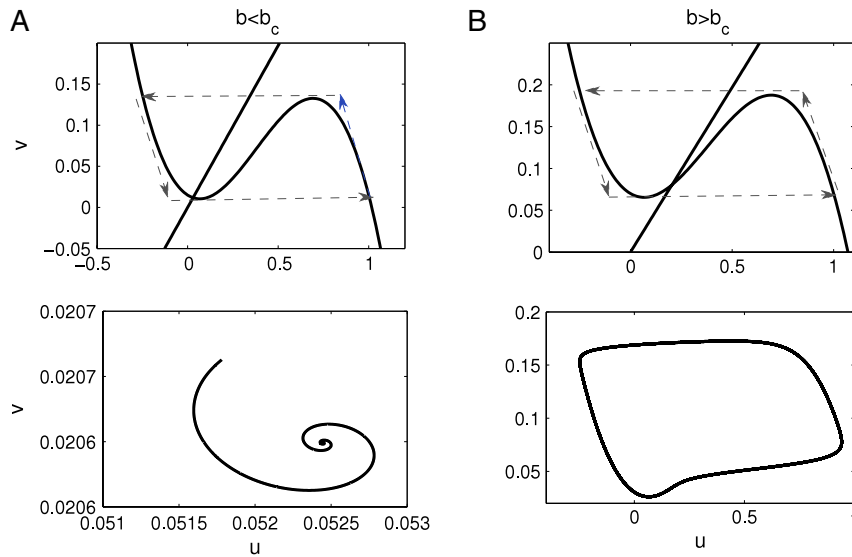
Fig. 4. Top trace: The nullclines (solid lines) of the FHN system (67) in the absence of noise (i.e., $D = 0$). Bottom trace: The corresponding phase portraits: (A) $b < b_c$, (B) $b > b_c$.
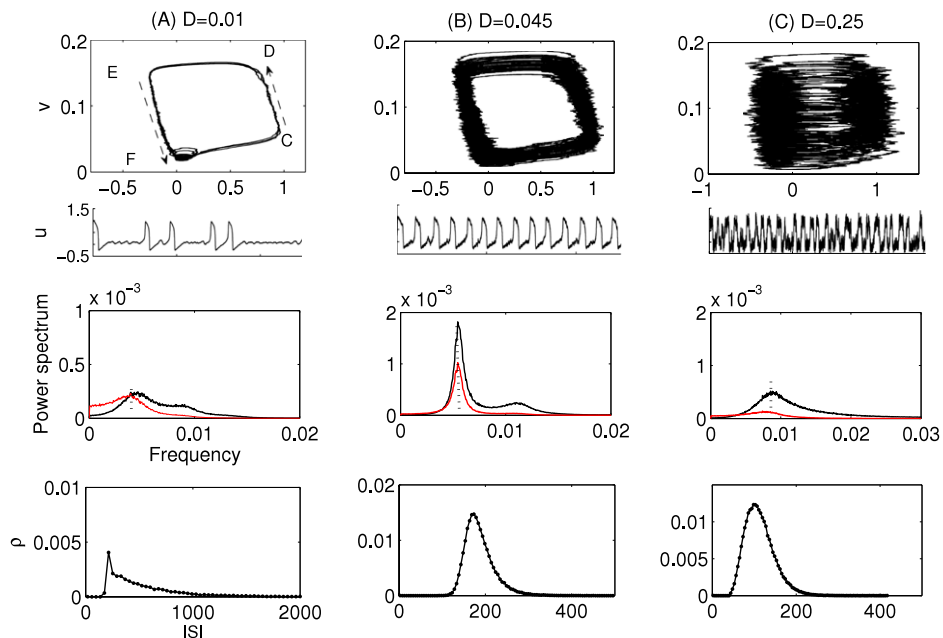
Fig. 5. Effect of noise. The first and second traces: The phase portraits of the FHN system (67) in the presence of noise and the corresponding trajectories of $\{u(t)\}_{t \geq 0}$. The third trace: The power spectra of $\{u(t)\}_{t \geq 0}$ (black) and $\{v(t)\}_{t \geq 0}$ (red). Bottom trace: The probability densities of ISI. Column (A) is for weak noise. Column (B) is for intermediate noise perturbation. Column (C) is for strong noise perturbation. (For interpretation of the references to colour in this figure legend, the reader is referred to the web version of this article.)

$b < b_c \approx 0.0334$ and is excited for $b > b_c$. In numerical integration, we implement the 4th-order Runge–Kutta algorithm with a time step $\Delta t = 0.01$.

The effects of noise perturbation in these two parameter regimes are quite different. In the excited regime, the deterministic system already exhibits periodic firings, then adding noise only plays a destructive role. However, in the excitable regime, moderate perturbations of noise can induce regular firing, while too weak or too strong noise cannot result in such effects (see the first and second traces in Fig. 5). To quantify the degree of such a noise-induced coherence, we depict the profiles of power spectra of both $\{u(t)\}_{t \geq 0}$ and $\{v(t)\}_{t \geq 0}$ to different noise intensities in the third trace of Fig. 5. The quality factor β of the power spectrum is further calculated. The bell-shaped curve of β vs D in Fig. 6 reveals that the CR occurs at an optimal noise intensity (about $D \approx 0.045$).
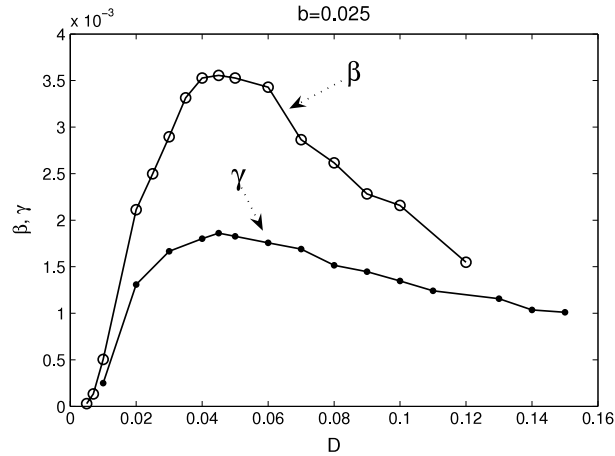
Fig. 6. The variations of the quality factor β of the power spectrum and the regularity factor γ of the FHN system (67) with the increase of the noise intensity D.

A nonzero peak frequency in the power spectrum manifests that the excitable FHN system driven by noise exhibits noise-sustained oscillations which are usually identified with the so-called SSLC [124,132]. Based on this, the state of the system can be described by the phase along the SSLC. Such a treatment is useful in studying the synchronization phenomena of coupled oscillators [166]. Not only this, we shall show in the following that the SSLC is directly related to the NBC which we think is the physical origin of CR.

Dynamically, since the name of SSLC, stable stochastic limit cycle, is transplanted from the concept of deterministic limit cycle, it should inherit (in a weaker sense) the main characteristics of a stable limit cycle: (1) It displays a certain degree of attraction; (2) it appears sustained circular motion on the attractor, i.e., a ring-shaped region which is localized to a limit cycle. Viewing with these two features in mind, both too weak and too strong noise cannot support a SSLC. In fact, it is seen from the upper trace in Fig. 5 that for weak noise, the system behaves as switching between two basins of attraction, one stable focus which exists before bifurcation, and another stable limit cycle which occurs after bifurcation (the upper-left panel). For strong noise, the rotation around the limit cycle becomes totally irregular (the upper-right panel). Hence the concept of a SSLC is confined to a certain range of noise intensity, where the limit-cycle like oscillation is optimally supported by the noise (the upper-middle panel).

We can further give a quantitative description of the SSLC; or more widely, noise-sustained oscillations. Let random variable T be the ISI (interspike interval) between two successive firings of u. If the SSLC is supported, we can define $E[T]$ as the mean period of the SSLC. In the bottom row of Fig. 5, we show the probability density function ρ of the time interval T normalized from the histograms of ISIs. We define the regularity factor of the noise-sustained oscillations as

$$\gamma = \rho_{max}/W, \tag{82}$$

where ρ_{max} is the maximum of the probability density of T, W is the width of the curve at half value of ρ_{max}. The larger the value of ρ_{max} is (or the smaller W is), the more regular the oscillations are. The most concentrated NBC in the phase portrait of Fig. 5(B) may be defined as the SSLC when γ reaches its maximum value: For too weak noise, the neuron spends most of the time near its resting state with some occasional and random firings, then ρ_{max} is small and W is large, which gives rise to small value of γ. For too strong noise perturbation, the neuron fires very randomly. Certainly, γ is also small. For moderate noise, the spikes are rather regular which implies that the ISIs do not differ much. Then the density curve is centered near a large value of ρ_{max} with narrow width W, which provides the optimal γ_{opt}. So γ is a quality factor to measure the concentration of NBC.

Thus a noise-induced cycle can be characterized by its mean period $E[T]$ and the regularity factor γ. Fig. 6 shows the variation of the regularity factor γ with the increase of the noise intensity D. One can see that the value of γ first increases with the increase of D, reaches a maximum at a critical value of D, and then decreases with further increasing D. This means that the noise-induced oscillations obtain the best degree of regularity at a critical value of D. We prefer to name the ring-shaped region at this critical value of D as a SSLC, and γ_{opt} its characteristic value.

We further compare the variation of the regularity factor γ of the SSLC versus the noise intensity D with that of the quality factor β of the power spectrum versus D. From Fig. 6, one can see that these two quantities undergo similar increasing manners, and almost at the same critical value of D, both γ and β reach a maximum. This means that when CR occurs, the ring-shaped region has its most preferable profile, which also announces the existence of the SSLC. Therefore, the SSLC and CR in the excitable regime share a common feature: both are related to the best degree of noise-induced regularity of an excitable system.
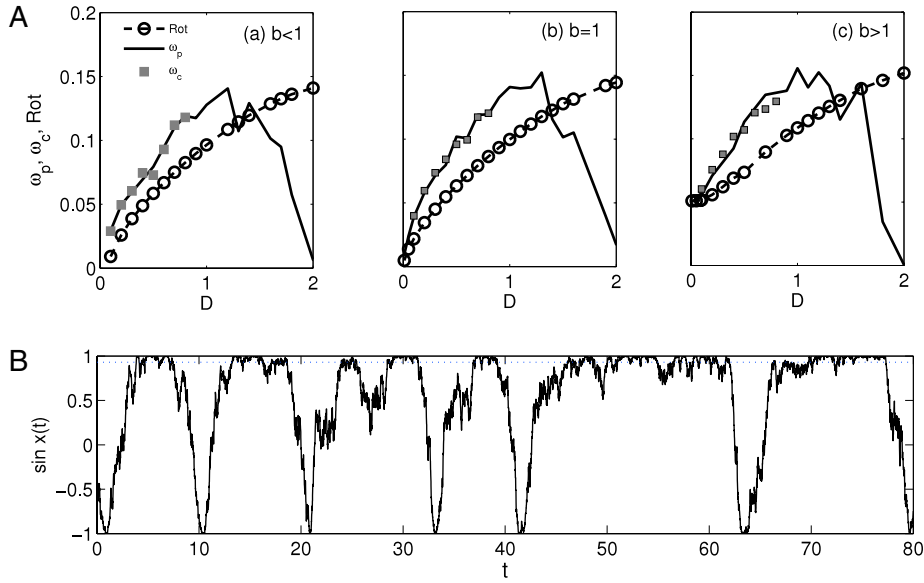
Fig. 7. (A) Variations of the peak frequency of the power spectrum ω_p, the calculated frequency ω_c, and the rotation number *Rot* with the increase of the noise intensity for (a) $b < 1$; (b) $b = 1$; and (c) $b > 1$. (B) The time series of $\{\sin x(t)\}_{t \geq 0}$ of the Adler equation (66) vs. time t in the presence of noise perturbation.

3.2.4. Nonequilibrium origins of CR phenomena

Earlier work relating power spectrum with nonequilibrium circulations can be traced back to the work of Hill, Chen, and their colleagues [167,168], who constructed a general mesoscopic model for the associations and conformational changes of biopolymers in open systems and applied their results on cycle kinetics in elucidating the mechanism of muscle contractions and the power spectrum "peaking" of membrane channel current in the Hodgkin–Huxley type model [126,169]. In 2000, H. Qian and M. Qian, using a toy model of cyclic chemical reaction in terms of a master equation with five states, presented a concrete bridge between CR and NESS [61]. Later, it was further shown that, in terms of finite state Q-processes, the power spectrum of any equilibrium mesoscopic system is necessary of Lorentzian type [59], a consequence of the Q-matrix being similar to a symmetric matrix. Since a continuous diffusive process can be approximated via discretization by a Q-process, the above results imply that CR is impossible to occur in an equilibrium system. Both CR and SR are driven phenomena.

Let us now discuss this nonequilibrium origin of CR in the above mentioned Adler's phase model. The materials presented in Section 2 will be used. For system (66), the condition $b > 0$ is crucial for the existence of CR. When $b = 0$, the stationary distribution of the system obeys Boltzmann's distribution, and the system is in equilibrium steady state.

Considering system (66) on the circle $\mathbb{S}^1$, from Section 2 we know that $b > 0$ implies a positive entropy production rate (e.p.r) for the diffusive process on a circle, and the entropy production rate (e.p.r) is linearly proportional to the rotation number. The rotation number quantifies the circular motion of the system (i.e., circulation). To demonstrate the relation of nonequilibrium circulation and CR in this system, let us first establish the relationship between the rotation number *Rot* and the peak frequency of the power spectrum ω_p. Fig. 7(A) shows the variations of *Rot* and ω_p with the increase of the noise intensity. One can see that in a certain range of noise intensity, the peak frequency ω_p is close to the rotation number of the system (the relative error is about 25%), and they both increase with the increase of the noise intensity. This fact further confirms that CR is indeed due to the appearance of non-equilibrium circulations.

The reason for the 25% difference between *Rot* and ω_p can be explained as follows. One knows that the power spectrum of a time sequence is the composition of different harmonic signals. The spectrum analysis is to display the amplitude of every harmonic component in the composed signal. The larger the amplitude is, the stronger the corresponding harmonic signal will be. Obviously, the periodic component corresponding to the peak frequency is the most prominent. As for the rotation number, it reflects the mean number of the particle winding around the circle. Therefore, ω_p generally does not equal to the value of *Rot*. In a nutshell, it is a matter of mean value versus peak value in a distribution. Generally, ω_p should be larger than *Rot*. In the phase model, excluding the fluctuating motions near the stable fixed point S (the part near the dashed line in Fig. 7(B)), the remaining motion could more accurately determine the peak frequency of the power spectrum. To be more precise, we denote T as the total time for the particle to move around the unit circle and T_0 as the time the particle fluctuating near the stable fixed point S, and $T_1 = T - T_0$. Let $N_r(b, D)$ count the total number of times that the particle complete rotates around the whole circle. Then $\omega_c \approx N_r(b, D)/T_1$ measures the frequency of the particle moving coherently on the circle excluding the fluctuation near S. Comparing ω_c with the peak frequency ω_p of the power spectrum, we find that they are in a good agreement if the noise intensity is not too large (compare the gray squares in Fig. 7(A) and

the solid curve). This tells us that the peak frequency ω_p may reflect the periodicity of the excursion motion of the particle outside the attracting basin.

The nonequilibrium mechanism of CR can be further clarified from quantifying CR and SSLC in FHN system. Actually, the nonzero frequency in the power spectrum implies the existence of NBC, a probability flow [59–77]. Intuitively, in analogous to an electrical current density, a probability flow, a vector field, has a density. In FHN model, the NBC is localized at a ring-shaped region. This localized probabilistic behavior is directly reflected by the regularity of the dynamic motion. For weak noise, the NBC is "blocked" frequently at certain positions (see the top panel in Fig. 5(A)). Increasing the noise level helps eliminating the "blockage" of the NBC. But of course at the meantime the increase of the noise intensity results in the scattering of the NBC. For too strong noise, the NBC is widely de-localized. Thus, only for a moderate level of noise, the NBC "flows smoothly" and is localized along a ring-shaped region. This is reflected by a maximum value of regularity factor γ of the SSLC, which indicates the occurrence of CR at an optimal noise level. The effect of CR, therefore, is the result of optimal localization of NBC along the SSLC.

Based on the close relationship between CR, SSLC and NBC we have discovered, we suggest that the SSLC in excitable systems exists only when the noise-sustained oscillations exhibit a sufficient degree of regularity. CR exists when noise supports such a SSLC in excitable systems. In fact, CR occurs when NBC is localized along the SSLC. We have presented the novel regularity factor γ to describe a SSLC. It can also be taken as a measurement of CR.

Previously in the literature, CR is usually measured by the inverse of CV (see Eq. (74) for its definition) which quantifies the ratio $R = E[T]/\sqrt{Var(T)}$ of the ISI in time domain. Or equivalently, it is measured by the quality factor β of the power spectrum in the frequency domain. Here γ measures CR in terms of the probability density of the ISIs. All these share a common feature of CR, and all are due to the existence of localized NBC.

The mechanism of NBC playing a role in CR of FHN model is a general one. It can be used to explain CR in other excitable systems, such as phase model, IF model, and Hodgkin–Huxley model, etc. It provides a nonequilibrium-physics insight into discussing noise-induced phenomena, e.g., stochastic synchronization, coherence transport. Elucidating the relationship between SSLC, NBC and CR helps scientists and engineers to better understand the physical origin of the regularity in stochastic, nonlinear systems. For example, the occurrence of nearly periodic oscillations in the biochemical system P53/Mdm2 has recently become a focus of interest in molecular systems biology [170,171].

3.2.5. Coherence resonance in Hodgkin–Huxley equation with intrinsic channel noise

In the above sections, we have shown CR in simple neuronal systems in terms of IF and FHN models. So far, the noises considered are all "external". Can intrinsic thermal fluctuations also give rise to CR? In this section, we will show that while internal thermal fluctuations, when a system is left alone, have to satisfy Gibbs–Boltzmann distribution in an equilibrium steady state, when it is coupled to a time-dependent deterministic dynamics, unbalanced circulation (NBC) also arises. Again, the NBC leads to CR.

We shall study the Hodgkin–Huxley (HH) model for single neurons, in which the membrane electrical potential is characterized by a deterministic variable V. V changes according to stochastic open and close of membrane channels for sodium (Na) and potassium (K) ions. This type of stochastic processes that couple deterministic dynamics with Markov jump processes are called *random evolution* in probability theory [172]. While the membrane channel sub-system satisfies detailed balance at all time without internal circulations, channel states and voltage together as a whole still exhibit NBC. The significance of the present model is demonstrating the possibility of CR using purely internal equilibrium fluctuations in the sub-system.

In the literature, channels' open and close were treated as deterministic rate equations in the past. Due to the finite size of the cell membrane, however, the number of ion channels is finite, and the role of intrinsic channel noise on the firing behavior should not be neglected. Indeed, it has been suggested that voltage-sensitive spontaneous conformational transitions of ion channels can give rise to spontaneous firing of the membrane potential of a single neuron, even without any external driving [173]. Hänggi and coworkers [111] have also studied CR due to the intrinsic channel noise. However, in the earlier work, the treatment of the channel fluctuation is approximated by Langevin equations. Here, we investigate the phenomenon of CR in the original HH model with a finite number of sodium and potassium channels according to a discrete Markov description [174–176], with voltage-dependent transition rates.

A few words on the equation for the dynamics of membrane potential in the HH model is in order. The traditional equation is given by

$$C_m \frac{dV}{dt} = -[g_L(V - V_L) + g_K(V, t)(V - V_K) + g_{Na}(V, t)(V - V_{Na})], \tag{83}$$

in which C_m is the capacity per unit area of membrane. Therefore, both sides of Eq. (83) are intensive quantities: g_L, g_K and g_{Na} are all conductances per unit area. It is important to point out that deterministic equations like (83) should *not* be considered as the mean value of a stochastic dynamics; rather it is the infinite population limit of the corresponding stochastic dynamics, expressed in terms of intensive quantities. Thus, to consider the corresponding stochastic dynamics for finite membrane area A_{rea}, one needs to consider the A_{rea} explicitly:

$$A_{rea} \cdot C_m \frac{dV}{dt} = -A_{rea} \left[\text{right-hand-side of (83)}\right],$$

Table 1
Parameters for the stochastic HH model (83).

Symbol	Definition	Values, units
C_m	Unit area membrane capacitance	$1\,\mu\text{F/cm}^2$
V_L	Leaky reversal potential	$-54.4\,\text{mV}$
V_{Na}	Sodium reversal potential	$50\,\text{mV}$
V_{K}	Potassium reversal potential	$-77\,\text{mV}$
$\hat{g}_L$	Leaky conductance	$0.3\,\text{mS/cm}^2$
$\hat{g}_{\text{Na}}$	Sodium channel conductance	$120\,\text{mS/cm}^2$
$\hat{g}_{\text{K}}$	Potassium channel conductance	$36\,\text{mS/cm}^2$
ρ_{Na}	Sodium channel density	$60\,\text{channels}/\mu\text{m}^2$
ρ_{K}	Potassium channel density	$18\,\text{channels}/\mu\text{m}^2$

in which, $A_{rea} \cdot g(V, t) = $ total number of open channels $\times$ conductance per open channel. That is,

$$g(V, t) = \frac{\text{tot. \# of open chann.}}{\text{tot. \# of chann.}} \times \frac{\text{tot. \# of chann.} \times \text{conduct. per open chann.}}{A_{rea}}.$$

Therefore, we have that in Eq. (83),

$$g_K(V, t) = \left(\frac{O_K(V, t)}{N_k}\right)\hat{g}_{\text{K}}, \qquad g_{Na}(V, t) = \left(\frac{O_{Na}(V, t)}{N_{Na}}\right)\hat{g}_{\text{Na}}. \tag{84}$$

In Eq. (84), $O_K(V, t)$ and $O_{Na}(V, t)$ are the numbers of potassium and sodium channels in their respective "open" states. They are discrete random variables following time-inhomogeneous Markov process, through $V(t)$. $N_K = \rho_K A_{rea}$ and $N_{Na} = \rho_{\text{Na}} A_{rea}$ are the total numbers of potassium and sodium channels, with ρ_{K} and ρ_{Na} being the number densities of the two channels, respectively. Parameter values used in computations are given in Table 1.

Each sodium channel is composed of three identical m-gates and one h-gate, and each potassium is composed of four identical n-gates. Only when all of the constituent gates are in the open states, a given channel is said to be open. The state evolution of each individual channel can be described by a Markov process, with kinetics given by

$$
\begin{array}{ccccccc}
m_0h_0 & \underset{\beta_m}{\overset{3\alpha_m}{\rightleftharpoons}} & m_1h_0 & \underset{2\beta_m}{\overset{2\alpha_m}{\rightleftharpoons}} & m_2h_0 & \underset{3\beta_m}{\overset{\alpha_m}{\rightleftharpoons}} & m_3h_0 \\
\alpha_h \updownarrow \beta_h & & \alpha_h \updownarrow \beta_h & & \alpha_h \updownarrow \beta_h & & \alpha_h \updownarrow \beta_h \\
m_0h_1 & \underset{\beta_m}{\overset{3\alpha_m}{\rightleftharpoons}} & m_1h_1 & \underset{2\beta_m}{\overset{2\alpha_m}{\rightleftharpoons}} & m_2h_1 & \underset{3\beta_m}{\overset{\alpha_m}{\rightleftharpoons}} & m_3h_1
\end{array} \tag{85}
$$
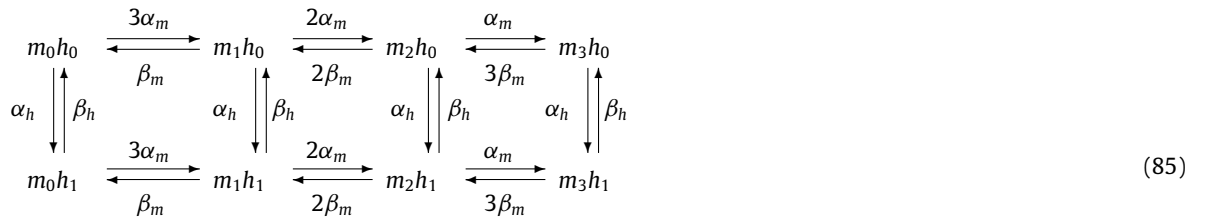
for the sodium channel, and

$$n_0 \underset{\beta_n}{\overset{4\alpha_n}{\rightleftharpoons}} n_1 \underset{2\beta_n}{\overset{3\alpha_n}{\rightleftharpoons}} n_2 \underset{3\beta_n}{\overset{2\alpha_n}{\rightleftharpoons}} n_3 \underset{4\beta_n}{\overset{\alpha_n}{\rightleftharpoons}} n_4, \tag{86}$$

for the potassium channel.

The voltage-dependent transition rates are given as in the literature [173]

$$\alpha_n = \frac{0.01(V + 55)}{1 - e^{-(V+55)/10}}, \qquad \beta_n = 0.125e^{-(V+65)/80},$$

$$\alpha_m = \frac{0.1(V + 40)}{1 - e^{-(V+40)/10}}, \qquad \beta_m = 4e^{-(V+65)/18},$$

$$\alpha_h = 0.07e^{-(V+65)/20}, \qquad \beta_h = \frac{1}{1 + e^{-(V+35)}}.$$

The dependence of these transition rates on the membrane voltage V is depicted in Fig. 8.

Different from the traditional treatment, we consider a membrane patch consist of N_{Na} sodium channels and N_K potassium channels. These channels, instead of behaving independently, are controlled by a common voltage $V(t)$ varying with time.

In simulating the dynamics of the stochastic HH equation with intrinsic Markovian channel kinetics, there are two alternative methods: the Gillespie algorithm [178–180] that tracks the number of channels in each state, or a Monte Carlo algorithm that tracks the state of each channel. Computationally, the former one is more efficient with large number of channels, while the later gives the state of each channel, which can be helpful in explaining the mechanism for the spontaneous firing.
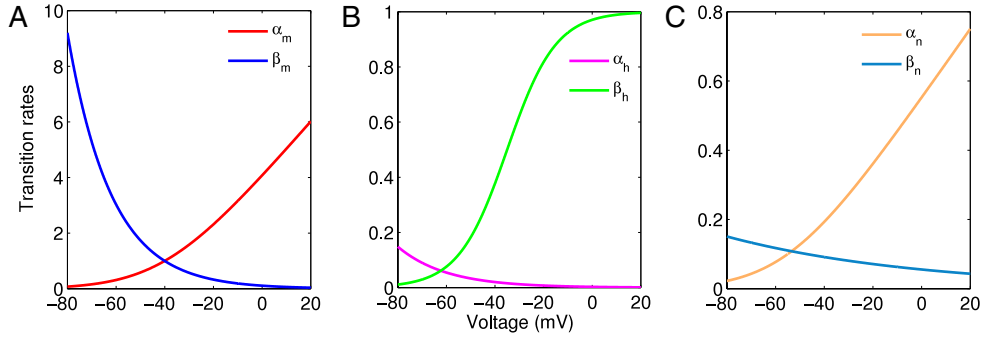
Fig. 8. Dependence of the transition rates of the ion channels on the membrane voltage V. (A) is for m gate of the sodium channel, (B) is for h gate of the sodium channel, and (C) is for n gate of the potassium channel. (For interpretation of the references to colour in this figure legend, the reader is referred to the web version of this article.)
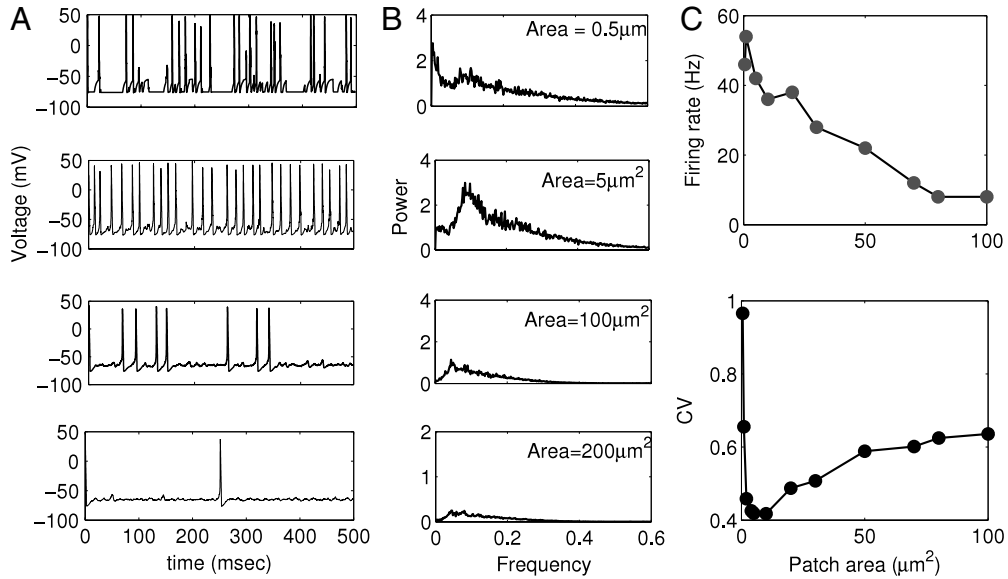
Fig. 9. (A) Time courses of the membrane voltage of the stochastic HH model (83) and (84), with different patch sizes, 0.5, 5, 100, and 200, in μm^2, from top to bottom. The densities for the sodium and potassium channels are 60 and 18 per μm^2. (B) The corresponding power spectra. (C) The firing rate and the CV of the ISI vs. the area of the membrane patch.

We use the Gillespie method to see how the intrinsic channel noise affects the dynamics of the membrane potential in a single neuron. We plot the membrane potentials for different sizes of a membrane patch, and the corresponding power spectra (Fig. 9A and B). It is shown that if the patch area is very small (0.5 μm^2), the neuron fires very irregularly, and the height of the spectrum is very low; on the other hand, if the area of the membrane patch is too big (e.g. 200 μm^2), the action potential is rarely generated. However, for an intermediate patch area (5 $\sim$ 20 μm^2), the neuron produces action potentials relatively regularly, compared with the case in a small patch area. Viewing from the profile of the power spectrum, there is a distinguish peak at a nonzero frequency, which reflects a certain degree of coherence of the firing of the neuron.

To further show the effect of intrinsic channel noise on the statistic properties of the firing behavior, we calculate the CV of the ISIs of the action potentials. The curves of the firing rate and the CV vs. the area of the membrane patch are depicted in Fig. 9C. It is shown that although the firing rate of a single neuron decreases with increasing the channel number, the CV of the firings reaches the minimum at about $A_{rea} = 5 \mu$ m^2. This further confirms the occurrence of CR.

It is important to point out that, conditioned on a given membrane potential V, the mesoscopic channel fluctuations are strictly equilibrium. However, when coupled to the macroscopic V, there is an unbalanced circulation (NBC) in the "voltage channel-state space" without any externally injected current. We give a more detailed description below.

According to Eqs. (85), (86) and Fig. 8, when the membrane voltage is at $V_1 = V_{rest} \approx -50$ mV, most of the sodium channels are in state (m_0, h_1) and most of the potassium channels are in state n_0. Noticing that the second term in Eq. (83) is nonnegative (i.e., $-g_{Na}(V - E_{Na}) \geq 0$) at $V = V_1$, and the kinetics of n-gate of the potassium channels are much slower than those of m-gate of the sodium channel, there will be an increase in the membrane potential after a short time duration. Since α_m increases and β_m decreases with the increase of V, there will be a net probability flux through
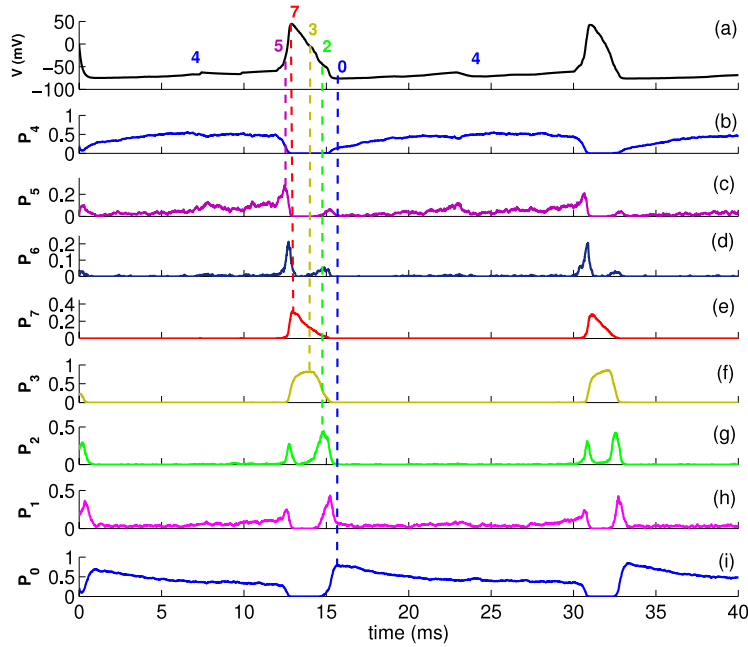
Fig. 10. The coupling between macroscopic dynamics of the membrane potential V and mesoscopic stochastic kinetics of individual channels (sodium). (a) membrane potential $V(t)$. (b–i) The fraction of the channels in different states: $0 := m_0 h_0$, $1 := m_1 h_0$, $2 := m_2 h_0$, $3 := m_3 h_0$, $4 := m_0 h_1$, $5 := m_1 h_1$, $6 := m_2 h_1$ and $7 := m_3 h_1$. There is an emergence of a NBC: The peaks successively occur at states 4, 5, 6, 7 (b–e), which correspond to the depolarizing phase of the membrane voltage in (a), and then to 3, 2, 1, 0 (f–i) corresponding to the hyperpolarizing phase of V. Interestingly, for states 1, 2 and 5, 6, in addition to the high peaks, there are also low peaks. Taking state 1 as an illustration: This is due to the net flux from state $5(m_1, h_1)$ to state $1(m_1, h_0)$, which appears earlier than the major circulation from $5 \rightarrow 6 \rightarrow 7 \rightarrow 3 \rightarrow 2 \rightarrow 1$. This is also the case for state 2. As for state 5 and 6, the low peak should appear later than the major one. In the simulation, the area of the membrane patch is $5 \, \mu m^2$. (For interpretation of the references to colour in this figure legend, the reader is referred to the web version of this article.)

$(m_0, h_1) \rightarrow (m_1, h_1) \rightarrow (m_2, h_1) \rightarrow (m_3, h_1)$: A large fraction of sodium channels open up, which causes the neuron to generate a spike. In Fig. 10a, the positions within one spike is marked. One can clearly see the states of the sodium channel at the rising phase of the membrane potential. After the generation of the spike, V further increases (see the increasing part after state 7 in Fig. 10a), but this will subsequently be shut down by the inactive h-gate, whose backward transition rate $\beta_h(V)$ increases and forward rate $\alpha_h(V)$ decreases with the increase of V. Thus there is a net flux from (m_3, h_1) to (m_3, h_0) during the overshooting phase of the membrane potential. Finally, after the occurring of the peak at state (m_3, h_1), one observes a peak at states (m_3, h_0), and later the peak successively occurs at state (m_2, h_0), (m_1, h_0), and (m_0, h_0), these channel states correspond to the falling phase of the membrane potential (see marked states in Fig. 10a).

During the changes of the membrane potential, there also occurs a net flux of the potassium channel (see the successive peaks at states $n_0, n_1, \ldots, n_4$ in Fig. 11a). Because the forward transition rate α_m of the sodium channel is much greater than the rate α_n of the potassium channel (compare Fig. 8A and C), the opening of the potassium channels has a time lag to the sodium channels (compare state 7 in Fig. 10a and state 4 in Fig. 11a). Hence during the rising phase of the membrane potential, it is mainly the sodium current that gives rise to the depolarization of the membrane potential. After the firing, however, the net flux in the potassium channel population results in a large fraction of the potassium channels to open and an opposite current, which leads to the polarization of the membrane potential, and the net flux from n_4 to n_0. The neuron is then hyperpolarized, and the net flux of the sodium is then going toward to state (m_0, h_1) to complete a circle and allows the neuron back to the resting state, ready for the next spike generation.

With the coupling of "equilibrium channel" with the macroscopic V, there is a time-irreversible circulation in the phase space. Such a circular motion is spontaneous and stochastic; leading to a nonequilibrium phenomenon in the HH model (83). To mathematically prove asymptotic stationarity of the stochastic process is outside the scope of the present review. Nevertheless, we believe the physical interpretation in terms of NESS is still valid. It is also important to point out that the thermodynamic driving force in the present model is from the macroscopic dynamics, i.e., the sustained sodium and potassium ion gradients across the membrane due to the Na–K-ATPase pumps, which is implicitly assumed in the HH model. It is not from the breakdown of detailed balance in the mesoscopic part.

With respect to SR, the central question is why the spontaneous firings disappear when the number of channels, together with the membrane area, becomes too large? The reason for this can be clearly found in Eq. (84): For the potassium channels, note that with increasing the membrane patch area, both the random variable $O_K(V, t)$ the total channel number N_K increase proportionally. Hence, by the probability law of large numbers and the central limit theorem, their ratio tends to a deterministic value with variance proportional to N_K^{-1}. The same is true for sodium channel fluctuations. Hence, with increasing membrane area, the channel noise levels are decreasing.
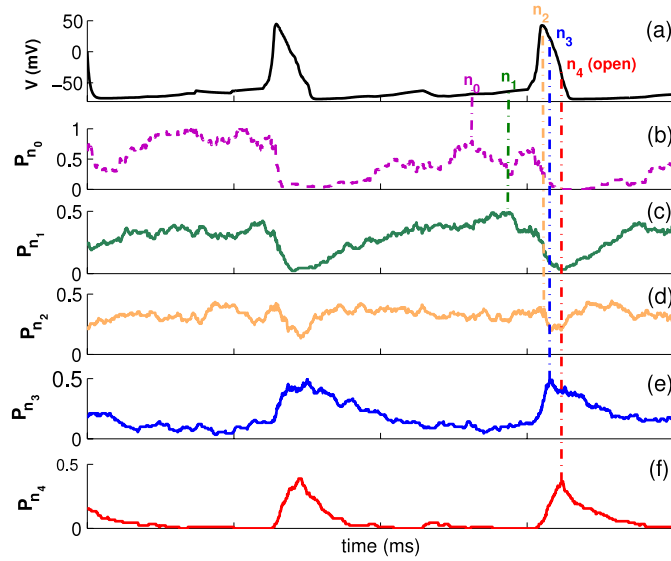
Fig. 11. The coupling between the macroscopic dynamics and the mesoscopic kinetics of individual channels (potassium). Due to the emergence of NBC, there are peaks successively occurring at states n_0, n_1, n_2, n_3 and n_4 (b–f). The corresponding phases of these states can be clearly seen in (a). Here the area of the membrane patch is the same as Fig. 10. (For interpretation of the references to colour in this figure legend, the reader is referred to the web version of this article.)

Based on Kramers–Moyal expansion, Fox and Lu [177] have shown that the effect of randomly opening and closing of independent individual channels can be approximated by three independent, standard Gaussian white noise terms added to the traditional HH equation for gating variables m, n and h:

$$\frac{dn}{dt} = \alpha_n(1 - n) - \beta_n n + \sqrt{\frac{2\alpha_n \beta_n}{N_{Na}(\alpha_n + \beta_n)}}\xi_n(t),$$
(87a)

$$\frac{dm}{dt} = \alpha_m(1 - m) - \beta_m m + \sqrt{\frac{2\alpha_m \beta_m}{N_K(\alpha_m + \beta_m)}}\xi_m(t),$$
(87b)

$$\frac{dh}{dt} = \alpha_h(1 - h) - \beta_h h + \sqrt{\frac{2\alpha_h \beta_h}{N_{Na}(\alpha_h + \beta_h)}}\xi_h(t).$$
(87c)

They obtained this set of equations based on the *diffusion approximation* of the underlying discrete Markov process: The latter approach preserves the independence of the gates within a channel while in the former this independence is lost due to terms like $n^4(t)$ and $m^3(t)h(t)$. Using the approximated Eq. (87) but consider $n^4(t)$ as a product of four independent processes, Hänggi et al. discovered CR in a moderate area of membrane patch. Further injection of external periodic current passing through the cell membrane does not have a significant effect on such a CR originated from the intrinsic channel noise [111].

Recently it has also been reported that, in comparison to the Markov model, the Langevin approximation, even with the correction introduced in [111], is most of the time inadequate to accurately represent channel dynamics. It underestimates the effect of channel noise contribution, even in simulations with large numbers of ion channels [181,182].

3.3. Stochastic resonance in the presence of periodic driving and its relation with coherence resonance

In this section, we will explore the phenomena of SR, which occurs usually in nonlinear systems owing a certain energy threshold and driven by a periodic force plus noise perturbation. Traditionally, the phenomena of CR and SR were considered different. In this section, by treating the periodically driven SR model as an autonomous system based on an embedding-based description, we shall show that both SR and CR actually have the same essence; both are intimately related to NESS.

3.3.1. Stochastic resonance in a periodically driven phase model

We first investigate the interplay between noise and periodic excitation in the simple Adler's phase model [183]

$$\dot{x} = b - \sin x + A\cos \omega t + D\xi(t).$$
(88)

It is obligatory to first study the deterministic dynamics of Eq. (88) without noise:

$$\dot{x} = b - \sin x + A\cos \omega t.$$
(89)
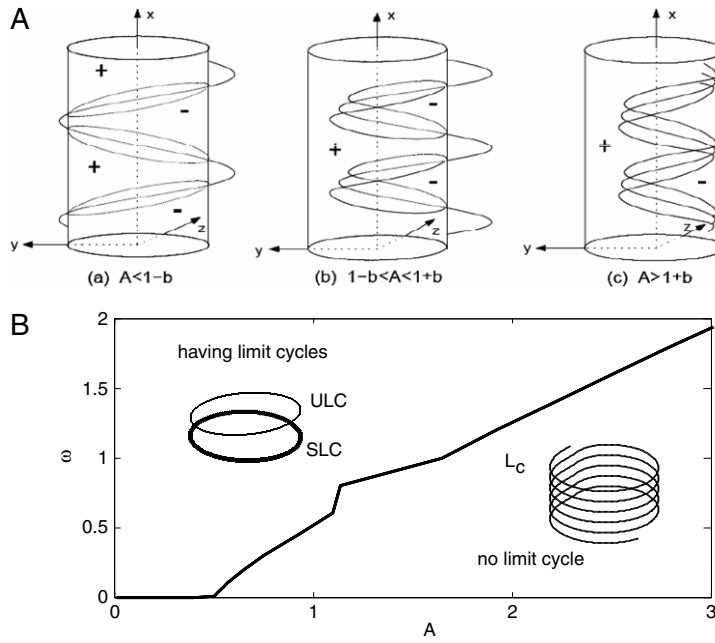
Fig. 12. (A) The intersections of the surface $y = \sin x - b$ with the cylinder E^2 for (a) $0 < A < 1 - b$, (b) $1 - b < A < 1 + b$, and (c) $A > 1 + b$, where the sign "+" represent $\dot{x} > 0$, while "−" represents $\dot{x} < 0$. (B) The bifurcation curve L_c of Eq. (90): above L_c, there are one SLC and one ULC on the cylinder in every strip $2k\pi - \pi/2 < x \le 2k\pi + 3\pi/2$, while below L_c, no limit cycle exists.

In the literature, the traditional way to explore the existence of periodic solutions in such a system is to take the signal term as a small perturbation. However, for large values of A, the perturbation theory is no longer valid. To explore the dynamical behavior of system (89) both for small and large periodic modulations, we transform Eq. (89) into an autonomous system by setting $y = A\cos\omega t$ and $z = A\sin\omega t$, then Eq. (89) equivalently becomes:

$$\begin{cases} \dot{x} = b - \sin x + y, \\ \dot{y} = -\omega z, \\ \dot{z} = \omega y. \end{cases} \tag{90}$$

Because of the periodicity in x, a solution to Eq. (90) can either be regarded as a curve winding on a cylinder $E^2 : y^2 + z^2 = A^2$ or on a torus $\mathbb{T} = \mathbb{S}^1 \times \mathbb{S}^1$.

Let $\dot{x} = 0$, one has $b - \sin x + y = 0$, i.e. $y = \sin x - b$. Considering the intersection of the surface $y = \sin x - b$ with E^2 for $b < 1$. We shall first learn to visualize the interaction(s) between the two surfaces and its relation to the system of differential equations. As in the case of intersections between the two nullclines in the system of two differential equations, such intersection(s) provides a basic understanding of the dynamics on a cylinder.

Let the coordinate system satisfies the right-hand rule: $\hat{x} \times \hat{y} = \hat{z}$. The equations $\dot{y} = \omega z$ and $\dot{z} = -\omega y$ means that the trajectory is rotating on the front face (to the reader) of the cylinder from right to left in Fig. 12A. It does not stop nor turn back since the angular velocity is constant. Now combining the rotation with the movement in vertical x direction, we notice that the x component has to change direction across the null cline surface.

We now see that there are two different cases that deserve attention separately:

Case 1: $A \le 1 - b$. In every strip $(2k\pi - \pi/2, 2k\pi + 3\pi/2)$ of x, the surface $y = \sin x - b$ divides the cylinder into three parts. In each two neighboring parts, $\dot{x}$ changes sign (see Fig. 12A (a)).

Case 2: $A > 1 - b$. in every strip $(2k\pi - \pi/2, 2k\pi + 3\pi/2]$, the surface $y = \sin x - b$ divides the cylinder into two sections. Fig. 12 A(b) shows the intersection for $1 - b < A < 1 + b$, and Fig. 12A(c) shows the intersection for $A > 1 + b$.

The dynamics of the deterministic system (90) on the cylinder for the above two cases are discussed in Appendix C. It is shown that for every fixed value of b, there exists a critical function $\omega = \omega_c(A)$ such that for $\omega > \omega_c(A)$, system (90) has two limit cycles, while for $\omega \le \omega_c(A)$, no limit cycle exists (see Fig. 12B). Note that no limit cycle means that x continuously increases.

Except a stable limit cycle that is perfectly perpendicular to the cylinder, there is an oscillation in x in system (88) even without noise. To measure noise-induced enhancement of the amplitude of the periodic signal x, we average the power spectra of 50 runs of the time series of $\{\sin x(t)\}_{t \ge 0}$. We then calculate the response amplitude RA, defined by Eq. (78) in Section 3.1.4, which characterizes the occurrence of SR. Let us first investigate the influence of noise in the regime for $\omega > \omega_c(A)$.
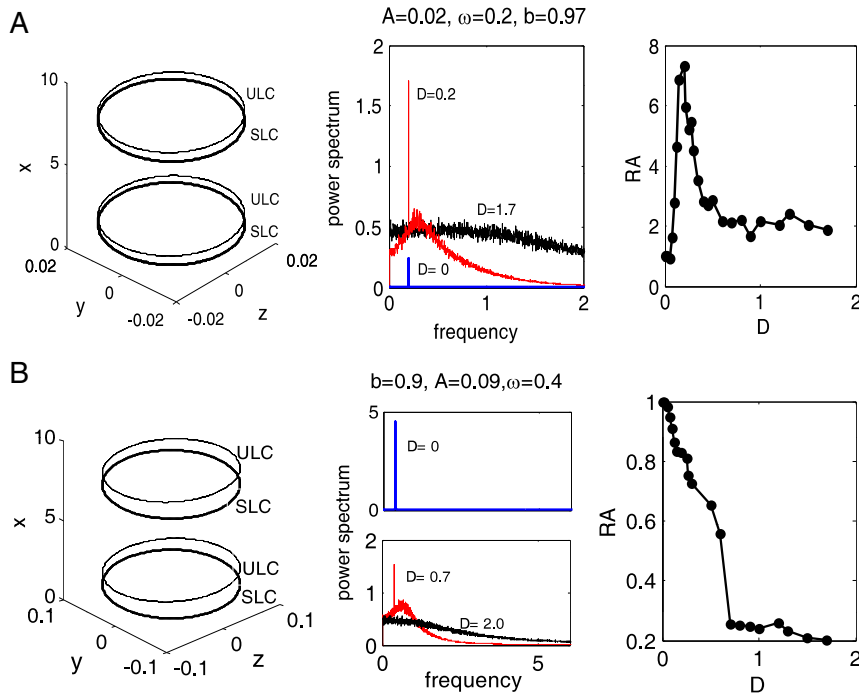
Fig. 13. The effects of noise for two different phase portraits under the case of $A \leq 1 - b$. Left column: the phase portraits; middle column: the power spectra for different noise intensities; right column: the response amplitude as a function of noise. Parameters used in (A): $b = 0.97$, $A = 0.02$, $\omega = 0.2$; and in (B): $b = 0.9$, $A = 0.09$, $\omega = 0.4$. (For interpretation of the references to colour in this figure legend, the reader is referred to the web version of this article.)

3.3.1a. $\omega > \omega_c(A)$ *and* $A \leq 1 - b$. In this parameter regime, for every driving frequency ω, the deterministic system (90) has a stable limit cycle (SLC) and an unstable limit cycle (ULC) on every strip $(2k\pi - \pi/2, 2k\pi + 3\pi/2]$ ($k = 0, \pm1, \pm2, \ldots$). Motions on the limit cycles have the same frequency ω. To investigate the behavior of the system in the presence of noise perturbation, we consider two different sets of system parameters.

Firstly, let us see the situation for a weak periodic drive, with $b = 0.97$, $A = 0.02$, $\omega = 0.2$ for illustration. The phase portrait of the deterministic system in Fig. 13A shows that both the SLCs and the ULCs are very flat, i.e., almost perpendicular to the cylinder, and the distance of the SLC to one ULC is much closer than to another ULC (This is due to the parameter b is very near 1.) Correspondingly, there is a low spectrum peak centered at the driving frequency in the power spectrum (blue in the middle panel of Fig. 13A). When noise is included, hopping motion from one SLC to the next SLC on the cylinder, crossing the ULC, occurs. Reflected in the power spectrum is an enhanced spectrum peak at the driving frequency. With the noise intensity D increasing, the height of this peak increases correspondingly until reaching a maximum at about $D = 0.2$, which indicates the maximal degree of coherence of the hopping motion (red spectrum in the middle panel of Fig. 13A). After that, the spectrum peak decreases with further increasing D. This means that in system (88) the conventional SR occurs as an optimal "cooperation" between a weak periodic signal and white noise.

We point out that by treating the periodically driven SR model as an autonomous system according to the embedding-based description, this traditional SR can be regarded as the coherent hopping motion between the two SLCs on the cylinder. It is essentially a type of CR.

We now explore the situation when the amplitude of the driving signal is relatively larger. For illustration, we use $b = 0.9$, $A = 0.09$ and $\omega = 0.4$. It is seen in the left panel of Fig. 13B that the smallest distance between the SLC and the ULC is now much larger than that in Fig. 13A. Although the effect of noise is more or less the same to the case in (A), the deterministic case has a much stronger peak in (B) compared that in (A). One therefore sees that the height of the spectrum peak at the driving frequency is decreasing with the increase of the noise intensity (middle panels of Fig. 13B). So for this set of parameters, no conventional SR is judged by the *RA* curve shown in the right panel of Fig. 13B.

3.3.1b. $\omega > \omega_c(A)$ *and* $A > 1 - b$. The case of $A \leq 1 - b$ is called subthreshold. We proceed to investigate the case of superthreshold periodic modulations: $A > 1 - b$, $\omega > \omega_c(A)$. Again, we take two sets of parameters for illustration: One is $b = 0.9$, $A = 0.3$, $\omega = 0.423$, and another is $b = 0.5$, $A = 0.6$, $\omega = 0.131$. From the phase portrait shown in Fig. 14A with $b = 0.9$, $A = 0.3$, $\omega = 0.423$, one sees that the neighboring SLC and ULC are very close to each other. In such a situation, even a weak perturbation of noise can easily induce coherent switching between the stable limit cycles. Correspondingly, from the power spectrum in the presence of noise (middle panels in Fig. 14A), one sees that noise can boost the signal that is very weak in the deterministic case. Furthermore, the background in the spectrum is much smaller than that in Fig. 13.
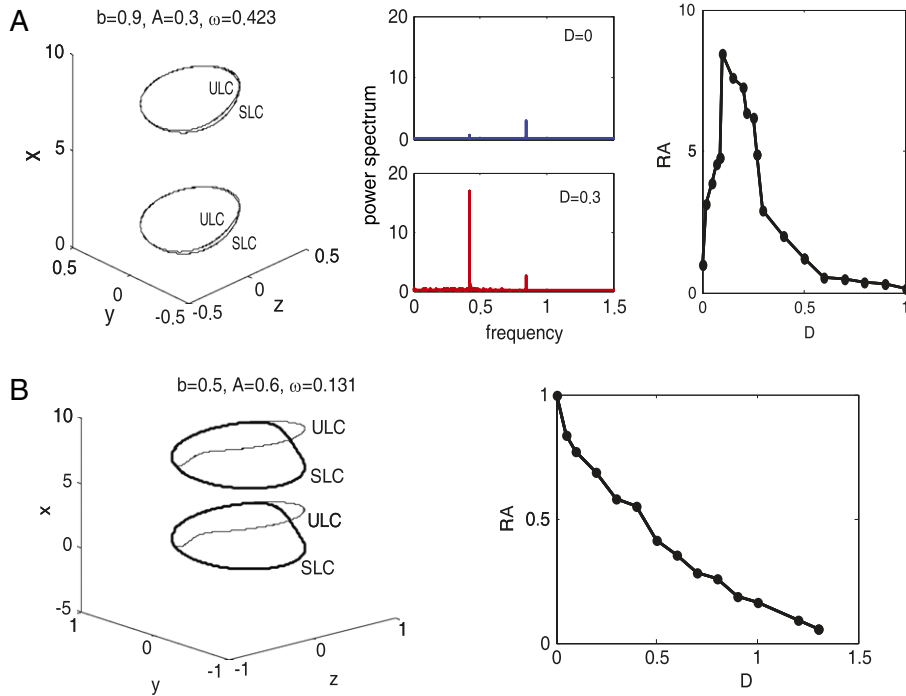
Fig. 14. The effects of noise for two different phase portraits under the case of $A > 1 - b$: (A) $b = 0.9$, $A = 0.3$, $\omega = 0.423$, (B) $b = 0.5$, $A = 0.6$, $\omega = 0.131$. The phase portraits are shown in the left column, the curves of the response amplitude *RA* vs. the noise intensity *D* are shown in the right column. The middle panel in (A) gives the comparison of the power spectrum in the absence and presence of noises. Note that the noise-induced motion peaks at a different frequency.

The occurrence of conventional SR in this scenario is characterized in the right panel of Fig. 14A, where *RA* vs. *D* displays an optimum.

Fig. 14B shows the results for $b = 0.5$, $A = 0.6$, $\omega = 0.131$. It is seen that although the SLC and the ULC are still close to each other, including noise does not facilitate the response amplitude any more. This is because the deterministic motion already has a periodic rotation around the SLC with large amplitude even in the absence of noise. Thus even though adding noise can easily induce switching between stable limit cycles, it can only cause irregularity. These results tell us why noise can detect weak period signal, but certainly can only cause deterioration for strong periodic signal.

3.3.1c. $\omega < \omega_c(A)$. In the above sections, we have illustrated different consequences of the interplay between noise and the periodic driving in the situation where the deterministic system (90) exhibits two SLCs with an ULC in between. In the absence of noise, if the periodic motion on a SLC has a very small amplitude, noise will increase the amplitude as well as induce coherent hopping motions between the two SLCs.

Let us now consider the situation when the deterministic system (90) has no limit cycle on the cylinder. Fig. 15a is the phase portrait of system (90) for $b = 0.9$, $A = 0.4$, and $\omega = 0.2$. It is shown that without any noise perturbation, the solution to the deterministic system is already periodically running around the cylinder E^2 with a large amplitude. Then it is easy to conclude that adding noise can only destroy such a regular motion. This is confirmed in Fig. 15b, where the response amplitude of the output is decreasing with the increase of the noise level. Numerical simulations for other sets of parameters, with which the deterministic system has no limit cycle, all give the same result. Therefore SR is impossible to exist when system (90) has no limit cycle.

In conclusion, SR in a periodically driven nonlinear, stochastic system is essentially the same as the phenomenon of CR. SR exists only when the deterministic system has two SLCs and one ULC on the cylinder, and the mechanism of SR/CR is attributed to the coherent hopping between stable limit cycles. The occurrence of CR depends on the relative position of the SLC to its neighboring ULC as well as the amplitude of the SLC itself, as shown in Figs. 13 and 14.

3.3.2. Stochastic resonance in a bistable system

In this subsection, we will apply the same idea of embedding an non-autonomous system to an autonomous one to investigate the phenomenon of SR in system (64) with a bistable $V(x)$. The conventional results on SR in such systems require the amplitude of the driving force not exceeding a threshold value of $A_c = 2\sqrt{3}/9$ (subthreshold regime). For $A > A_c$ (superthreshold regime), SR was declared as impossible [184] because the double-well profile of the potential is no longer preserved. Recently, Apostolico et al. [185] pointed out that SR can also occur in superthreshold regime, but via a mechanism called "noise failure" which is essentially different from the one in the subthreshold regime (see Fig. 16).
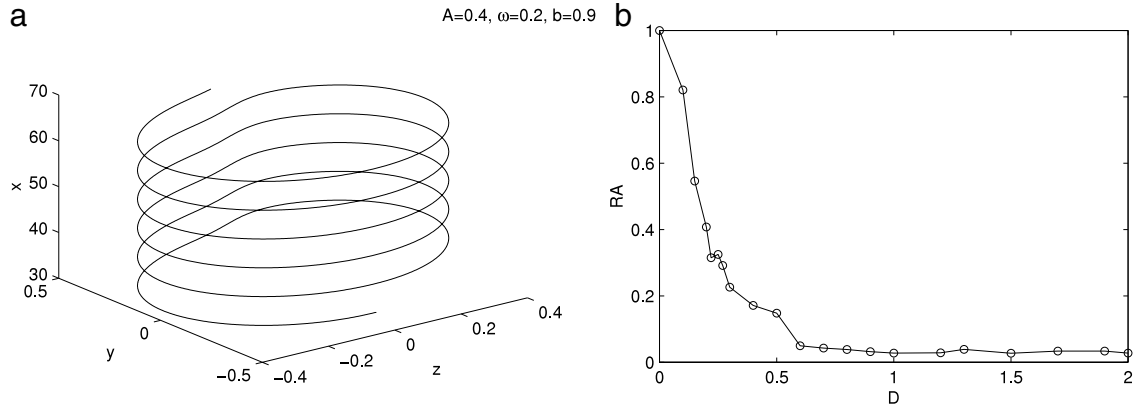
Fig. 15. (a) The phase portrait of system (90) for $b = 0.9$, $A = 0.4$, $\omega = 0.2$. (b) The response amplitude *RA* vs. the increase of the noise intensity *D*.
Source: Reproduced with permission from X. J. Zhang, J. Phys. A: Math. Gen. 37(2004) 7473.
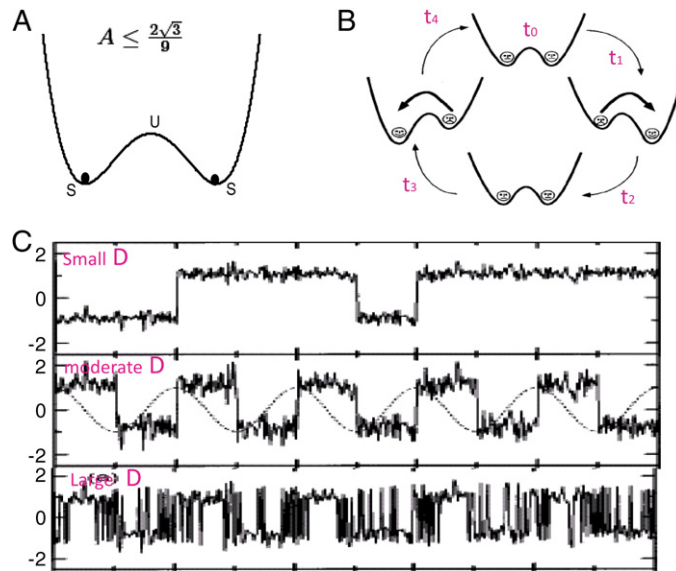
Fig. 16. (A) The sketch of the effective potential $V(x)$ of Eq. (64) in the absence of a periodic driving. (B) Periodic rocking of the potential under a subthreshold periodic driving ($A < 2\sqrt{3}/9$) at different time points. (C) Trajectories of the system in the presence of a subthreshold drive and noise fluctuation with different intensities. In the subthreshold regime ($A \leq 2\sqrt{3}/9$), SR was found to occur for moderate strength noise perturbation; however, in the superthreshold regime ($A > 2\sqrt{3}/9$), SR was usually thought to be impossible because of loosing bistability.
Source: Figure reproduced from L. Gammaitoni et al., Rev. Mod. Phys. 70, 224 (1998) with permission.

Actually, using the idea of embedding the non-autonomous equation into an autonomous system [186–188], we will further show the existence of SR in the superthreshold regime via numerical computations. We will demonstrate two SLCs of the deterministic system above a bifurcate curve. From this perspective, the mechanisms of SR in both subthreshold and superthreshold cases are essentially the same.

By setting $y = A \sin(\omega t + \varphi)$, $z = A \cos(\omega t + \varphi)$, Eq. (64) in the absence of noise is equivalent to the following autonomous system on a cylinder $E^2 : y^2 + z^2 = A^2$ (see Fig. 17A)

$$\begin{cases} \dot{x} = x - x^3 + y, \\ \dot{y} = \omega z, \\ \dot{z} = -\omega y. \end{cases} \tag{91}$$

Applying the same method used in Section 3.3.1, we have the following results for the two-dimensional system on a cylinder:

(i) For $A \leq A_c$ and all $\omega > 0$, Eq. (91) has and only has three limit cycles with two stable and the other one unstable.
(ii) For $A > A_c$ and $\omega \ll 1$, there exists only one SLC on the cylinder for Eq. (91).
(iii) For $A > A_c$ and $\omega \gg 1$, Eq. (91) has and only has three limit cycles with two stable and the other one unstable.

A detailed mathematical proof of the above assertions, which we shall not present here, can be found in [189].
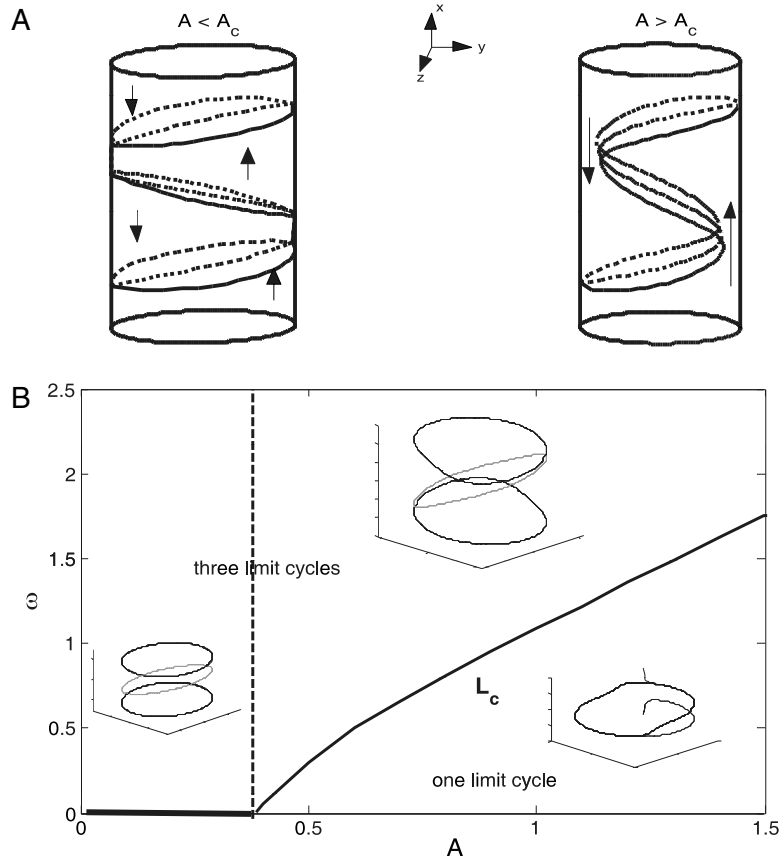
Fig. 17. (A) The intersection of $y = x^3 - x$ with the cylinder for $A < A_c$ and $A > A_c$. (B) The bifurcation curve L_c of Eq. (91): Above L_c, there are two SLCs and one ULC on the cylinder; while below L_c, only one SLC exists on the cylinder. The left side of the dashed line is for the subthreshold parameter regime ($A \leq A_c = \frac{2\sqrt{3}}{9}$), and the right side is for the superthreshold regime ($A \leq A_c$).

According to the above statements, it is expected that for $A > A_c$ and with any ω, there still exists a critical curve L_c: $\omega = \omega_c(A)$, for $\omega \geq \omega_c(A)$, Eq. (91) has three limit cycles, while for $\omega < \omega_c(A)$, only one SLC exists on the cylinder. Fig. 17B is a plot of such a bifurcation curve.

From the standpoint of the embedded autonomous system, the bistability of the system in a subthreshold regime referred in the literature corresponds to the existence of two SLCs on the cylinder. As for the superthreshold regime, the system can still exhibit bistability if the driving frequency ω is larger than a critical value ω_c (see Fig. 17B). Then in the presence of noise, the motion will no long be confined on one SLC. Rather, it will switch between the two SLCs randomly. Such a motion can result in SR in system (64). Thus, for $A > A_c$, SR can still occur for suitable driving frequencies, and the mechanism will be essentially the same as that for $A < A_c$. We suggest that SR is easy to occur when the driving parameters (A, ω) is close to the bifurcation curve L_c. To confirm this, in Fig. 18A and B, we plot the power spectra and the corresponding response amplitudes for values of (A, ω) that are close to the curve L_c and also values that are far from L_c, respectively. As for $\omega < \omega_c$, since there is only one SLC, introducing the noise destroys the periodic motion along the limit cycle. Hence no SR is observed (see Fig. 18C).

Similar to what we have presented for the periodically driven phase model with noise, the occurrence of SR depends upon the relative position of the SLC and the ULC as well as upon the amplitude of the SLC itself in the absence of noise. In order for SR to occur, the distance between the SLC and the ULC has to be small, and the amplitude of the stable periodic motion should also be small. Note that these two quantities do not simultaneously increase or decrease with varying the parameters of the system. Decreasing the distance between the SLC and the ULC till they almost collide should optimize the switching motion and hence the SR. However at the meantime it might increase the amplitude of the SLC and boost the deterministic spectrum peak, which reduces the response amplitude. Overall, the occurrence of SR is a competition between these opposite effects (see Fig. 19). SR thus can only be observed in a certain parameter regime in the A–ω plane (see Fig. 20). For a more detailed discussion of the dependence of SR on these two ingredients, see [190].

3.4. Array-enhanced coherence resonance and stochastic resonance in coupled systems

For systems with a single oscillator, we have elucidated the mechanism(s) of CR and SR in the previous sections. The question naturally comes next is what the situations will be in systems with many degrees of freedom? In this section, we
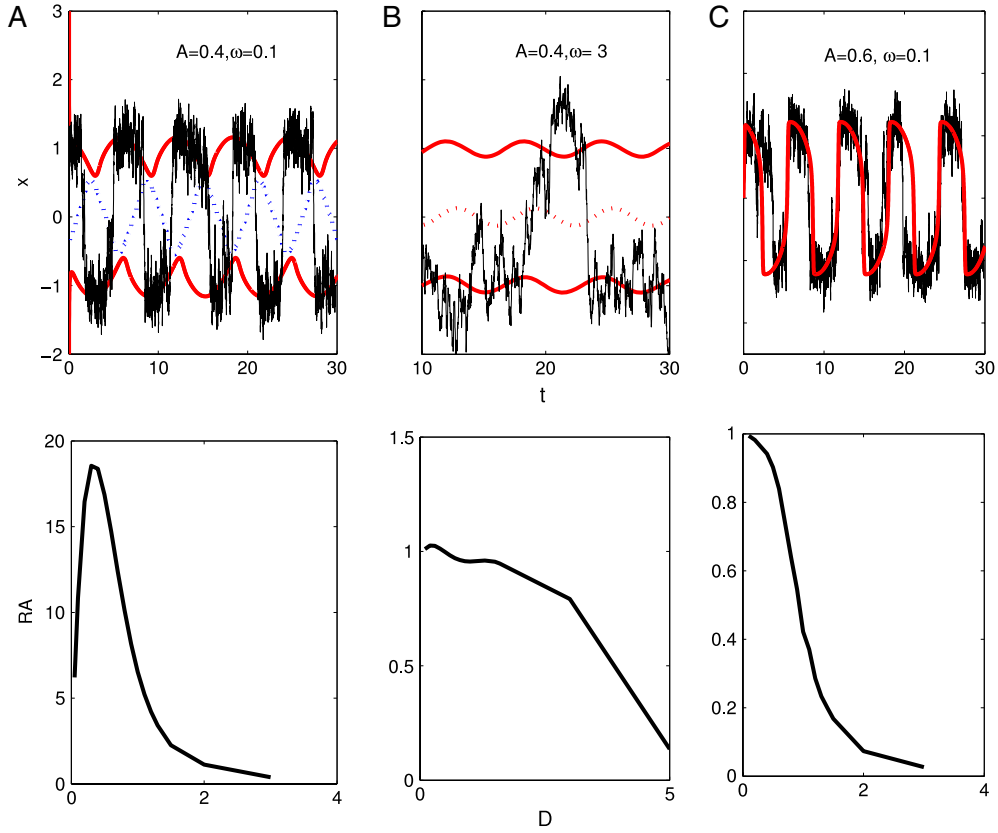
Fig. 18. The effects of noise in the superthreshold regime: Top panel: The trajectories in the absence (red for stable and blue for unstable) and in the presence of noise (black). Bottom panel: The response amplitude vs. the noise intensity. Column (A) is for $A = 0.4$, $\omega = 0.1$, column (B) is for $A = 0.4$, $\omega = 3$, and column (C) is for $A = 0.6$, $\omega = 0.1$. (For interpretation of the references to colour in this figure legend, the reader is referred to the web version of this article.)

further investigate the phenomenon of CR as well as SR in coupled systems, where one sees that the interaction between noise, nonlinearity, and the coupling will result in much more pronounced CR and SR.

3.4.1. CR in a coupled phase model without periodic driving force

Let us now investigate the influence of noise on a system of $N \times N$ identical overdamped oscillators with nearest neighbor-coupling on a square lattice, without an external periodic driving [191]. The model in dimensionless form is characterized as

$$\dot{u}_{i,j} = b_{i,j} - \sin u_{i,j} + K \left(u_{i-1,j} + u_{i+1,j} + u_{i,j+1} + u_{i,j-1} - 4u_{i,j} \right) + D_{i,j}\xi_{i,j}(t), \tag{92}$$

$$(\vec{u} = (u_{i,j}, i, j = 1, 2, \ldots, N) \in \mathbb{T}^{N^2} \triangleq \underbrace{\mathbb{S}^1 \times \mathbb{S}^1 \times \ldots \times \mathbb{S}^1}_{N^2})$$

in which $u_{i,j}$ represents the phase of the oscillator on the lattice (i, j), it is a time-varying variable; $b_{i,j} \geq 0$ is the control parameter, $K > 0$ is the coupling coefficient, and $\xi_{i,j}(t) > 0$ is Gaussian white noise satisfying: $\langle \xi_{i,j}(t) \rangle = 0$, $\langle \xi_{i,j}(t)\xi_{i',j'}(t') \rangle = \delta_{i,i'}\delta_{j,j'}\delta(t - t')$. We use free boundary conditions at the edges of the array. Such a system was introduced to describe the real physical phenomena such as the motion of squid arrays [192]; they were also used to model oscillating chemical reaction [193] and neural networks in biology [194]. In our computations, the array size is taken as 10×10 and the coupling constant $K = 1$.

Even without any noise, system (92) displays interesting dynamical behaviors. Numerical simulations show that whenever the coupling $K > 0$, it may alternatively rest near a stable state or has a unique running periodic solution. And if there are fixed points, their numbers will be about e^{N^2} [195]. These fixed points form a vast majority of metastable states of the system. Taking $\mathbb{T}^{N^2}$ (the production of N^2 unit circles $\mathbb{S}^1$) as the phase space, then the rotation numbers for different components of the solution are either zero or nonzero. Further calculations show that they are all equal even when the values of $b_{i,j}$'s are different: There is a phase-locking phenomenon. Thus, we define the rotation number of the deterministic system as $R_{det} = \lim_{t \to \infty} u_{1,1}(t)/2\pi t$. One will see in the following that for the cases of $R_{det} = 0$ and $R_{det} \neq 0$, the noise
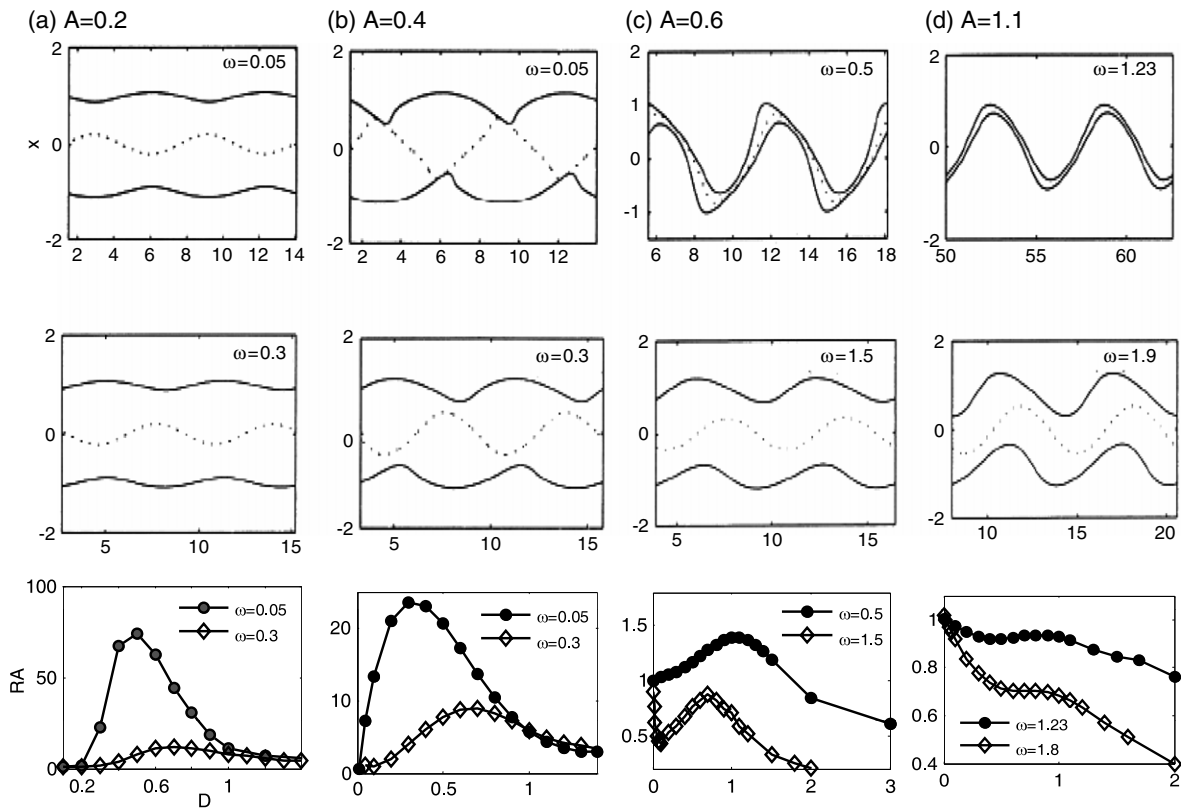
Fig. 19. Dependence of SR on the relative position of the SLC and the ULC. By varying the driving amplitude and frequency, the relative position of the SLC and the ULC changes accordingly. (a) corresponds to the subthreshold regime, (b–d) correspond to the superthreshold regime. The top panels are plotted from the parameters that are close to the bifurcation curve L_c in Fig. 17, while the middle panels are from the parameters that are not close to L_c. It is seen that (i) the effect of SR in the subthreshold parameter regime is much more significant than in the superthreshold regime. (ii) For a fixed driving amplitude, the effect of SR decreases with the increase of the driving frequency. (iii) For a fixed driving frequency, increasing the driving amplitude destroys the phenomenon of SR (see the bottom panels).
Source: Reproduced with permission from M. Qian and X. Zhang, PRE 65, 011101 (2001).
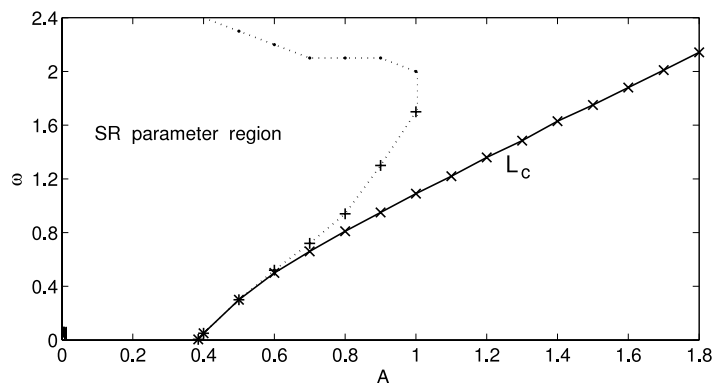
Fig. 20. The parameter regime where SR can occur in system (64).
Source: Reproduced with permission from M. Qian and X. Zhang, PRE 65, 011101 (2001).

plays very different roles for the behavior of the corresponding system. Actually, for $R_{det} > 0$, every oscillator in the absence of noise already rotates periodically on the circle, introducing noise only destroys such a nice periodic motion. Hence no CR can occur. We therefore need only to consider the effect of noise for the case of $R_{det} = 0$.

3.4.1a. Homogeneous driving with global noise perturbation. For $0 < b_{ij} = b < 1$, all the oscillators are driven by the same constant forces. Here we set $b_{i,j} = b = 0.98$ for illustration. Without any noise, the system has two spatially homogeneous stationary solutions: $u_{i,j}^s = \arcsin b$ (stable) and $u_{i,j}^u = \pi - \arcsin b$ (unstable) ($i, j = 1, 2, \ldots, N$). We speculate that with
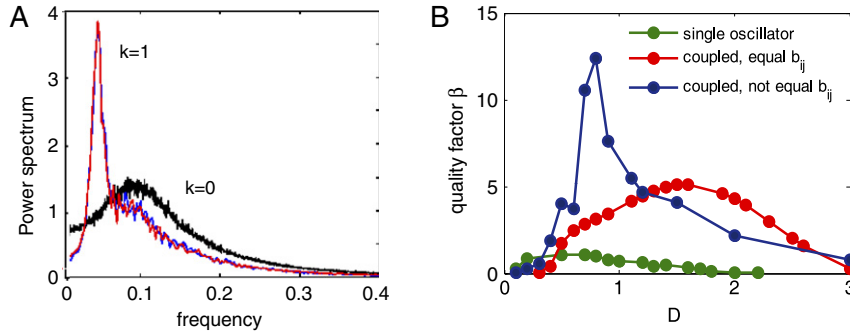
Fig. 21. (A) The power spectrum of $\{\sin u(t)\}$ for the single oscillator system (66) and for the coupled system (92) with $K = 1$ on lattices $(1, 5)$ and $(2, 7)$. Here $b_{i,j} = b = 0.98$, $D_{i,j} = D = 0.5$ $(i, j = 1, 2, \ldots, N)$. (B) The quality factor β vs. D for $b_{i,j} = 0.98$, $K = 0$, $b_{i,j} = 0.98$, $K = 1$, and $b_{i,j} = 0.98 + 0.2 \times (-1)^i$, $K = 1$ $(i, j = 1, 2, \ldots, N)$. Here $D_{i,j} = D$ $(i, j = 1, 2, \ldots, N)$. (For interpretation of the references to colour in this figure legend, the reader is referred to the web version of this article.)

the increase of the noise strength, the quality factor (see Eq. (72)) of the power spectrum for every oscillator will exhibit similar increase property to that in the uncoupled case (i.e., system (66)). Numerical simulations confirm this speculation (see Fig. 21A). It turns out that the profile of the power spectrum as well as the D–β curve are independent of the lattice sites. The coupled system exhibits nice, coherent behavior: First of all, for every oscillator, the height of the spectrum peak is increased, meanwhile, the width of the spectrum becomes much narrower. As a result, the maximum of the quality factor is significantly (about five times) higher than that of the uncoupled case (see Fig. 21B, the green and red curves). Secondly, as shown in Fig. 21A, all the oscillators have exactly the same peak frequency, even when the values of $D_{i,j}$ are different). This means that all the units oscillate in synchrony. From these two facts, we say that even without any external periodic driving, bona fide CR actually occurs in system (92) as a mutually cooperative phenomenon.

3.4.1b. Heterogeneous driving with global noise perturbation. As an illustration, we take $b_{i,j} = 0.98 + (-1)^i \times 0.2$, $(i, j = 1, 2, \ldots, N)$. It is shown in Fig. 21B (the blue curve) that though the averaged force is $\Sigma b_{i,j}/N^2 = 0.98$, the effect of array-enhanced CR is much better than that in the case $b_{i,j} = 0.98$. This shows that heterogeneous driving forces can result in a better array-enhanced CR than homogeneous driving.

3.4.1c. Local noise perturbation. In the above two cases, independent noises are applied to the lattice points. What will be the result if only a fraction of the sites are perturbed with noise? For illustration, we use $b_{i,j} = 0.9$ $(i, j = 1, 2, \ldots, N)$ and subject only the single middle oscillator to noise: $D_{5,5} = 9$ and all other $D_{i,j} = 0$. In such a situation, it requires relatively stronger noise perturbation to promote the running motion than in the globally perturbed cases. In Fig. 22, we plot the phase trajectories of the oscillators at lattices $(5, 5)$, $(6, 5)$ and $(4, 8)$ and the corresponding power spectra of $\{\sin u_{5,5}(t)\}$, $\{\sin u_{6,5}(t)\}$, $\{\sin u_{4,8}(t)\}$. One sees that although only one element is subjected to the noise perturbation, the phases of all the oscillators increase in a phase-locking manner, but the motion of the oscillator at lattice $(5, 5)$ is severely disturbed by the noise and there is only a low peak in its power spectrum. For its neighboring oscillators, c.f. at $(6, 5)$, the noise disturbance is not so great, and there is in fact a significantly higher spectrum peak than at lattice $(5, 5)$. As for other oscillators, say the one at $(4, 8)$, the noise disturbance is further reduced. In fact, it is the coupling which plays a dominant role in promoting the oscillator to skip cycles. Consequently, for these sites, there is a higher spectrum peak than the middle two layers. In the bottom trace of Fig. 22, we plot the curves of the quality factors vs. D of these oscillators, one can clearly see different effects induced by the noise. The above observations show that for SR, it is not necessary to subject every oscillator to noise. Suitable localized noise perturbation can have global effect on the whole dynamics of the system, and cause most of the oscillators undergo SR.

3.4.2. Stochastic frequency resonance in a coupled phase model with a periodic driving force

Introducing a periodic driving to system (92), we have the following periodically driven coupled phase model

$$\dot{u}_{i,j} = b_{i,j} - \sin u_{i,j} + K \left(u_{i-1,j} + u_{i+1,j} + u_{i,j+1} + u_{i,j-1} - 4u_{i,j} \right) + A \sin \omega t + D\xi_{i,j}(t), \qquad (93)$$

$$(\vec{u} = (u_{i,j}, i, j = 1, 2, \ldots, N) \in \mathbb{T}^{N^2} \stackrel{\triangle}{=} \underbrace{\mathbb{S}^1 \times \mathbb{S}^1 \times \cdots \times \mathbb{S}^1}_{N^2})$$

In the previous sections, through numerical computations, we have shown that pure noise can already induce the occurrence of CR in system (93) with $A = 0$. Such a CR phenomenon is usually characterized by the appearance of a nonzero-frequency peak in the power spectrum, and by a nonmonotonic increasing of the quality factor with increasing noise intensity. The off-zero power spectral peak in such systems reflects an intrinsic periodicity of the noisy system [125]. One could say that such a system has an intrinsic frequency. A natural question then is: If the frequency of an external
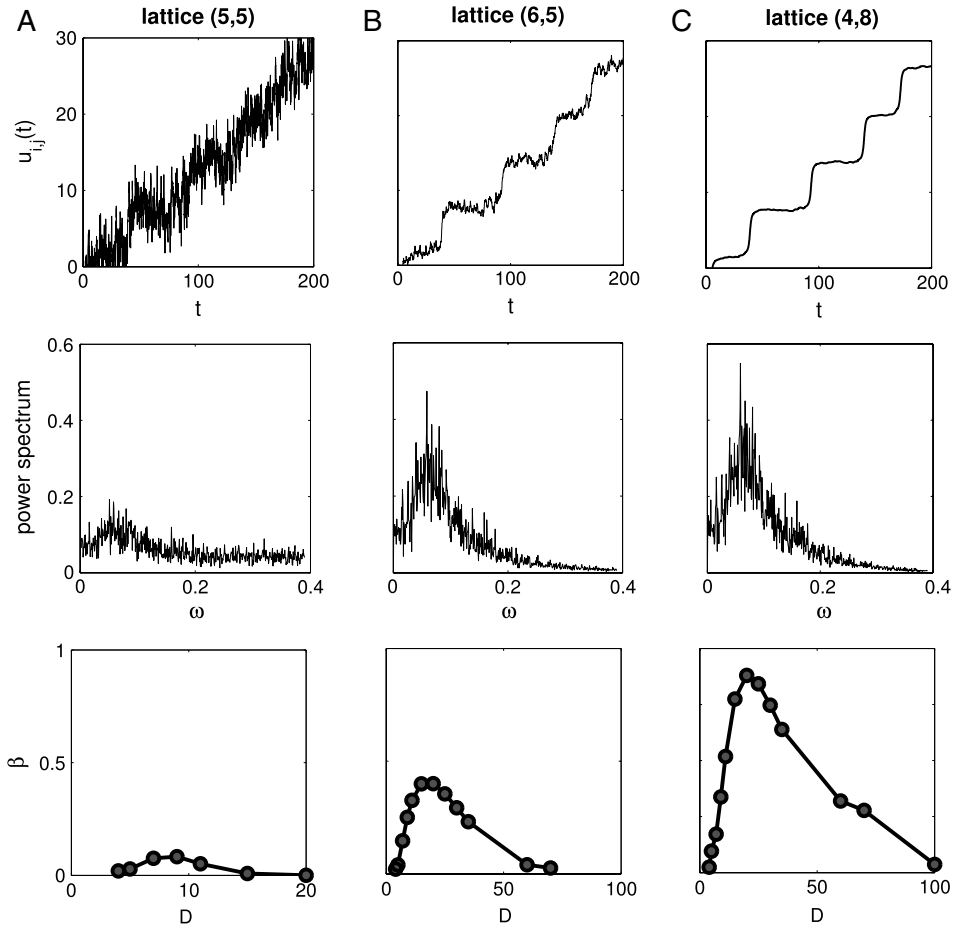
Fig. 22. Top trace: Time courses of the phase $u_{i,j}(t)$ of the oscillator on lattices (5, 5), (6, 5) and (4, 8). Middle trace: The corresponding power spectra. Bottom trace: The quality factor β calculated from the power spectrum vs. the noise intensity D. Here the external constant forces are added homogeneously with $b_{i,j} = 0.9$, $(i, j = 1, 2, \ldots, 10)$; and the noise perturbation is added only on the lattice (5, 5), with $D_{5,5} = D > 0$ and $D_{i,j} = 0$ $(i \neq 5$ or $j \neq 5)$.

periodic forcing matches the intrinsic one, will the periodic signal of the system be significantly higher than adding signals with "non-resonance" frequencies? In 1998, Hu and coworkers [141] considered this interesting problem and obtained an affirmative answer in a globally coupled spatial system, near a bifurcate point, with both activating and inhibitory terms. Similar result was later reported by Plesser and Geisel in an IF neuron model [196]. Here we shall use the model in (93) to see such an effect.

As a control, we first consider the case of a single oscillator with Eq. (88). We fix the parameters $b = 0.98$ and $D = 0.7$. Without the periodic force, the peak frequency of the power spectrum is at $\omega_0 \approx 0.7095$ (see inset in Fig. 23A). To investigate the effect of a periodic modulation on the output of the stochastic system, we use $A = 0.1$ and plot the power spectra with different driving frequencies in Fig. 23A. One indeed sees that the output of system (88) reaches a maximum when the external modulation frequency is varied to match the noise-induced "intrinsic" frequency ω_0. This is the characteristics of traditional "resonance" with matching frequencies in deterministic physics systems.

To distinguish this novel resonance phenomenon in stochastic systems from the better-known SR which emphasizes the noise influence on the output of a system, we suggest to call it stochastic frequency resonance (SFR).

We now further investigate the effect of spatial coupling. To compare with the uncoupled case, we still use $b_{i,j} = b = 0.98$ and $D = 0.7$. Without periodic forcing $(A = 0)$, the power spectrum of system (93) is shown in the inserted in Fig. 23B, where noise-induced peak frequency $\omega_0 \approx 0.3336$. With periodic forcing using $A = 0.1$, the power spectra for various driving frequencies are shown in Fig. 23B. One sees that when the frequency of the periodic driving matches ω_0, the spectral peak is again much higher than the ones for other driving frequencies. This indicates that SFR also occurs in the locally coupled system (93). One also notices that the noise-induced spectrum shown in Fig. 23A is significantly "cleaned" in the coupled system. When further plot the height of the spectrum peak h vs. the driving frequency ω in Fig. 24A, it is seen that the coupled system exhibits much better SFR than the single-oscillator system. For the case we considered with $D = 0.7$, the SFR output of coupled system (93) is almost 7 times larger than that of single-oscillator system (88).
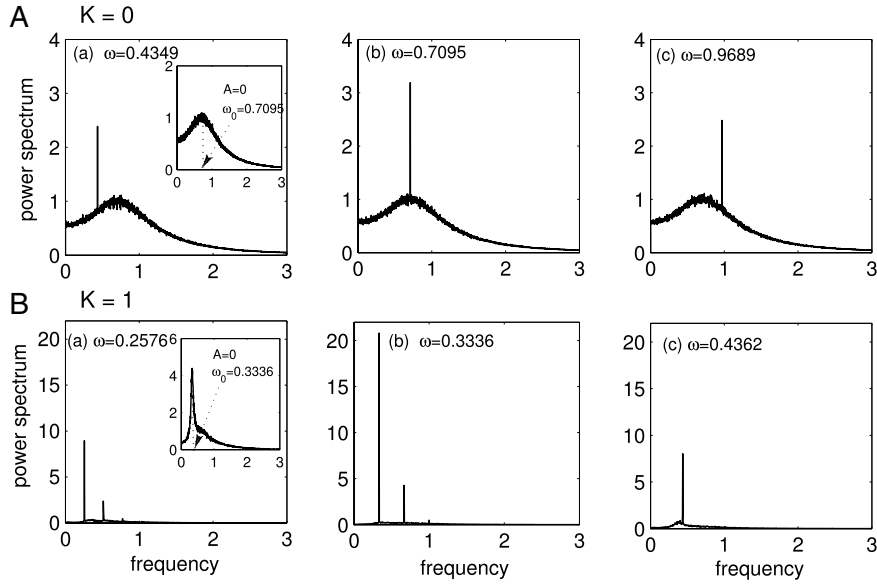
Fig. 23. The power spectra of (A) the single oscillator system (88), and (B) the coupled phase model (93) for different values of the driving frequency stated in the figures. Here $b = 0.98$, $A = 0.1$, $D = 0.7$. The inserted figure is for $A = 0$.
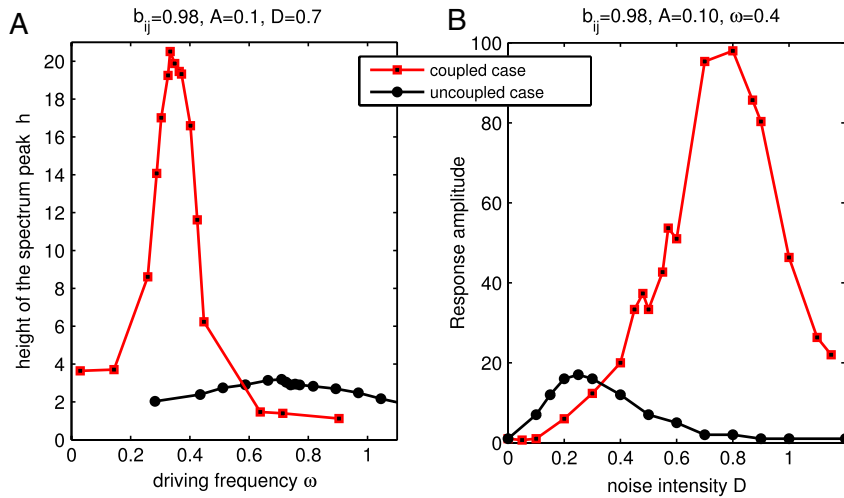
Fig. 24. (A) Array-enhanced FSR, where the height of the spectrum peak h vs. the driving frequency ω with fixed a noise intensity $D = 0.7$. (B) Array-enhanced SR, where the response amplitude vs. the noise intensity D with a fixed driving frequency $\omega = 0.4$. In both figures, $b_{ij} = b = 0.98$, $A = 0.1$. (For interpretation of the references to colour in this figure legend, the reader is referred to the web version of this article.)

The mechanism of the amazing array-enhanced SFR can be elucidated from the different interactions between the noise and the periodic forcing in these two systems. To distinguish from the motion of a system forced by a periodic signal, here we call the oscillations of a system driven only by white noise self-oscillations. This is really just a highly coherent version of the NESS circulations. For system (88) without a periodic forcing, it is seen from the inserted figure in Fig. 23A(a) that there is a wide range of self-oscillating frequencies. When a weak periodic signal is applied, though the power spectrum is peaked at the driving frequency, the profile of the noise-induced power spectrum is still preserved. This fact tells us that the external periodic signal can barely drive the original self-oscillations to synchronize with itself. The reason system (88) exhibiting SFR, therefore, is mainly due to noise-boosted spectrum peak being preserved under a periodic modulation. However, for the coupled-oscillator system (93), the power spectrum without periodic forcing already exhibits a narrower spectral line with a much higher peak than that in the single-oscillator (compare the insets in Fig. 23B(a) and A(a)), for the reason of coupling and synchronization [191]. Without external periodic driving, noise-induced coherent motion has already occurred with frequency partly concentrated at the intrinsic ω_0. Then when an external periodic signal is applied, it drives the noise-induced oscillations to synchronize with itself. So in Fig. 23B(a), the spectrum of the self-oscillation is essentially the entire

spectrum. It is easy to imagine that as a periodic signal with the exact noise-induced central frequency is introduced, it becomes even easier to synchronize the motion of the self-oscillation.

Hence the occurrence of array-enhanced SFR in coupled system (93) is due to the "frequency focusing" twice: the first time due to the coupling in the presence of noise and the second time due to the external periodic driving with matched to the noise-induced frequency.

So far we have shown SFR both in single and coupled oscillator systems. Compared with the phenomenon of SR which emphasizes the optimal level of intensity of the noise to a system, SFR exhibits a real resonance of a stochastic system, as in the classical physics, with stimulus frequency matching the noise-induced intrinsic frequency.

There is also array-enhanced SR in the coupled phase model (93). This can be clearly seen in Fig. 24B, where the response amplitudes of the single oscillator system (88) and of the coupled system (93) are plotted.

3.4.3. Rotation number and stochastic resonance (SR)

From the previous discussion, we have learnt that the rotation number is an essential indicator for nonequilibrium circulation, and it is closely related to the occurrence of CR in stochastic nonlinear systems without a periodic forcing. In this subsection, we shall further discuss the relationship between the rotation number and the SR. Let us first define the rotation number in the coupled system (92). Recall that the rotation number of a single oscillator is defined as $Rot = \lim_{t\to\infty} u(t)/(2\pi t)$. As has been shown in the Fig. 7A, it is an increasing function of noise strength D. Thus, for an $N \times N$ array of uncoupled oscillators, if the noise levels $D_{i,j}$ $(i, j = 1, 2, \ldots, N)$ are different, then the oscillators will all have different values for their rotation numbers. However, when there are coupling between the neighboring oscillators, the rotation numbers of all the oscillators are exactly the same, irrespective whether the $D(i, j)$ are same or different. A rigorous prove of this result can be found in [64]. Thus a rotation number of the coupled stochastic system (92) still makes sense. We therefore define the rotation number of the coupled system simply by

$$Rot = \lim_{t\to\infty} \frac{u_{11}(t)}{2\pi t}. \tag{94}$$

Let us first exam the relationship between the rotation number and the peak frequency of the power spectrum in the absence of an external periodic driving. For single oscillators such as in Eq. (66), Fig. 25A (the same data from the left panel of Fig. 7A) shows a difference between the rotation number and the peak frequency of the power spectrum. There, we argued that the difference is caused by the local fluctuations at the bottom of the potential well. In the coupled system, numerical simulations show that these two quantities now agree with each other very well in a wide range of noise intensity (see Fig. 25B). The close relation between the rotation number and the peak frequency of power spectrum in the coupled oscillators suggests that all the oscillators are frequency-locked and behaves coherently.

Let us further see the situation in the presence of a periodic driving. For illustration, we take $A = 0.1$, $b_{i,j} = b = 0.98$ and $D_{i,j} = D = 0.7$. For the case $K = 0$, i.e., no coupling, Eq. (93) for a single isolated oscillator yields rotation number $Rot = 0.4761$ almost independent of driving frequency ω, as shown in Fig. 26A). This fact means that the external driving can barely change the rotation number of a single oscillator. We have also seen in Fig. 23A that the spectral shape of the noise-sustained oscillations is almost independent of the external driving frequency. However, in sharp contrast, for coupled system (93) with $K = 1$, Fig. 26B shows that the rotation number changes correspondingly with the increase of the driving frequency. In fact, it first increases until reaching a maximal value, but then decreases with the further increase of the driving frequency. Furthermore, when the value of ω is close to the noise-induced intrinsic frequency $\omega_0 = 0.3336$, the rotation number is also close to both, i.e., $Rot \approx \omega = \omega_0$. When the driving frequency ω becomes away from ω_0, the rotation number also departures from the driving frequency. The consistence of the rotation number and the noise-induced internal frequency suggests that the oscillations in the coupled system are localized near this intrinsic frequency ω_0.

The relationship among the rotation number, the peak frequency and the driving frequency motivates us to further investigate the relationship between SR and the rotation number. We surmise that for a fixed periodic driving, SR occurs just when the rotation number of the system increases to a value that equals to the driving frequency ω. Numerical simulations confirm this: We use $A = 0.1$, $\omega = 0.4$ and $\omega = 0.6136$ for illustration. In Fig. 27A and B, one sees that with increasing noise intensity A, the value of the rotation number Rot is also increasing; and when Rot increases to the value that equals to the driving frequency ω, the corresponding spectrum peak reaches its maximum compared with both those for $Rot < \omega$ and $Rot > \omega$. This shows that for the coupled system, SR indeed occurs just when the value of Rot matches the driving frequency.

4. Unidirectional motion and energy transduction efficiency of molecular motors

4.1. Brief introduction

In addition to stochastic/coherence resonance (SR/CR) discussed in the previous section, another nonequilibrium system in which thermal "noise" plays a striking constructive role is molecular motor, also called Brownian ratchet. This is a mesoscopic, stochastic system that is capable of carrying out unidirectional transport in a spatially periodic but asymmetric potential, in the absence of any macroscopic force or mean potential gradient [27,197]. The connection between
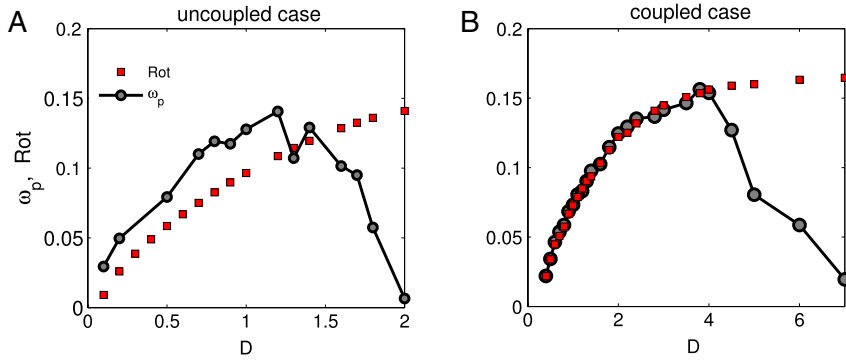
Fig. 25. The relationship between the peak frequency of the power spectrum and rotation number. (A) For a single oscillator in Eq. (66) with $b = 0.98 < 1$. There is about 25% difference between the two quantities. This is the same data from Fig. 7A. (B) The coupled system (92) with $b_{i,j} = b = 0.98$ and $D_{i,j} = D$ ($i, j = 1, 2, \ldots, 10$). It is seen that in the coupled case, these two quantities agree with each other very well in a wide range of noise intensity. This announces the coherent synchronization among all the coupled oscillators. (For interpretation of the references to colour in this figure legend, the reader is referred to the web version of this article.)
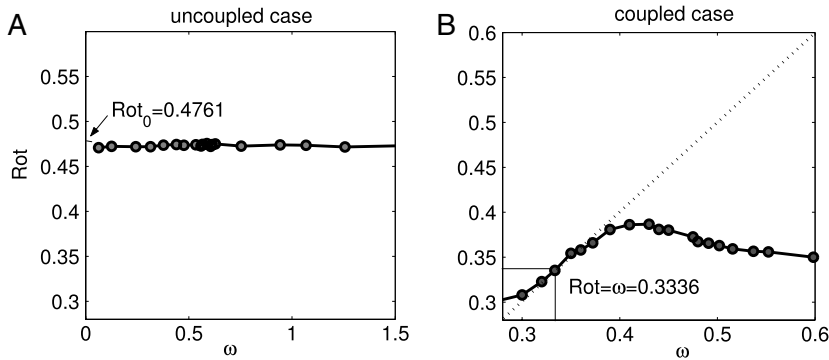
Fig. 26. The variation of the rotation number Rot with the increase of the driving frequency ω. (A) The single oscillator system (88). (B) The coupled oscillator system (93). Both are with $b = 0.98$, $A = 0.1$ and $D = 0.7$. The value of Rot_0 gives the rotation number in the absence of a periodic driving. It is seen that in the uncoupled case, the rotation number in the presence of a periodic driving is kept almost unchanged, irrespective of the increase of the driving frequency; while in the coupled case, the rotation number changes accordingly with the driving frequency.
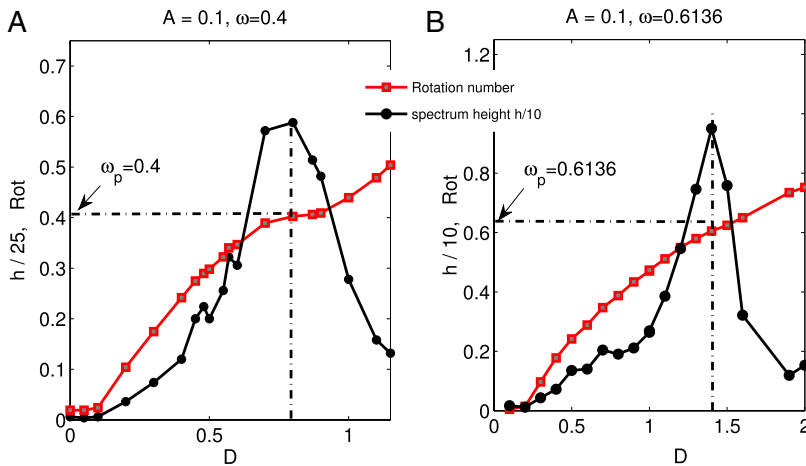
Fig. 27. The maximal spectrum height h vs. the noise intensity D (black curve with circles), and the rotation number Rot vs. D (red curve with squares). The horizontal dashed line marks the driving frequency (also equals to the peak frequency, ω_p, of the power spectrum). (A) is for $\omega = 0.4$, (B) is for $\omega = 0.6136$. Both are with $b_{ij} = b = 0.98$, $A = 0.1$. It is seen that with increasing D, the value of h obtains its maximum when the rotation number Rot equals to the external driving frequency ω. (For interpretation of the references to colour in this figure legend, the reader is referred to the web version of this article.)

stochastic, nonequilibrium fluctuations and unidirectional motion was extensively studied in the physics literature in [28]. In biophysics, the theory of muscle contraction pioneered by Huxley and further developed by Hill had predated all the recent

work on Brownian ratchets [198,199], though the theory developed from 1950s to 1970s was not formulated at single-molecules level. It was formulated in terms of the so called "sliding filament" and "cross-bridge". In modern terms, the Huxley–Hill theory is based on a randomly positioned linear array of identical single motors (cross-bridges). Their chemical kinetics are independent; but they are mechanically constrained to a rigid filament: They can only move in unison [172].

Such a mesoscopic transport phenomenon is now understood to occur under two crucial conditions, namely, outside a thermal equilibrium (i.e., breakdown of detailed balance and time reversibility) and an one-dimensional spatial asymmetry. It is called *a Brownian ratchet*, or *a molecular motor*, which has received considerable attention in recent years. In addition to muscle contraction, there are other biophysical motivation to study such a phenomenon [200]: Many active processes in biological systems are carried out by enzymes, often ATPases, which can move, linearly or circularly, biased toward one direction by converting the chemical energy from ATP hydrolysis to mechanical work [201].

Therefore, the physics of a Brownian ratchet, especially its free energy transduction, is of considerable interest to biologists, physicists and chemists [202–204]. In general, a motor protein functions by moving along a certain type of macromolecular filament. The latter plays the role of a track to guide the motion of the motor protein. In cell biology, there are mainly four different families of motor proteins: kinesins, myosins, dyneins, and polymerases. Kinesins and dyneins move along tubulin filaments, while myosins move along actin filaments. The primary biological functions of polymerases are not mechanical movement *per sc*. However, they move along their templates (DNA for replication and transcription, RNA for protein biosynthesis) nevertheless.

Though the detailed atomic structures are very different, common to all molecular motors is a tail domain that attaches to a cargo and a head domain that binds the track and hydrolyzes ATP and/or GTP [202]. The basic ingredients for kinetic modeling are essentially the same for all molecular motors. The underlying biochemical reaction cycle occurs at the ATP (or GTP) binding site is as the following:

$$\overset{1}{M} \;\rightleftharpoons\; \overset{2}{M \cdot ATP} \;\rightleftharpoons\; \overset{3}{M \cdot ADP \cdot Pi} \;\rightleftharpoons\; \overset{4}{M \cdot ADP} \;\rightleftharpoons\; \overset{1}{M}. \tag{95}$$

In which state 1 represents the head of the motor being attached to the filament but without anything else bound to it. Transition to state 2 represents the binding of one ATP molecule. Transition to state 3 represents the chemical transformation of ATP being decomposed into ADP and Pi. In many cases, the same step is simultaneously the motor head detaching from the filament. Transition to state 4 represents the release of Pi and the affinity between the motor head and filament becomes high again, resulting in the motor attaching to the filament after a certain amount of random diffusion. Inside a living cell the concentration ratio of ATP to ADP/Pi is about 10 decades above its thermal equilibrium value. Thus macroscopically it is essentially impossible for ADP and Pi to be transformed back into ATP. This is the driven force of the molecular motor.

If the motion in the $3 \rightarrow 4$ is not a random diffusion, but rather a definitive tight coupling between the Pi release and motor head stepping forward a period along the filament, then the motor protein has a tightly coupled hydrolysis and mechanical movement. The chemical models for motor proteins can be developed along this line. The ratchet model we shall discuss in the present section, however, assumes that the mechanical movement can be decoupled from the hydrolysis. Thus, the random diffusion can be in both directions, with of course a bias for the forward direction.

The filaments are spatially periodic with a period on the order of nanometers or tens of nanometers. Moreover, it has a polarity which means that its mechanical potential within a period is asymmetric. This feature is very important since the chemical transition in a ratchet model is completely "orthogonal" to the mechanical axis. On the other hand, the interaction energy between a molecule protein and the filament is on the order $k_B T$, where k_B is the Boltzmann constant and T is temperature in Kelvin. The influence of thermal fluctuations, thus, is not negligible. The directional motion of a single motor protein is caused by the nonequilibrium fluctuations and the asymmetry of the filament [197,27]. This is the reason why it is also called a Brownian motor.

Various models have been proposed in the literature in studying the mechanism of molecular motor movement. The first step in modeling the dynamics of a motor enzyme is to regard it as a single particle characterized by its position, say the center of mass, in an overdamping continuous medium.[9] The general form of this type of models is given by the following SDE

$$\dot{x}(t) = -V'(x(t), f(t)) + y(t) + F(x(t)) + D\xi(t), \tag{96}$$

where $V'(x, f) = \partial V(x, f)/\partial x$, $V(x, f)$ is a periodic, but asymmetric potential function satisfying $V(x+L, f(t)) = V(x, f(t))$, in which $f(t)$ is a time periodic with zero time average; $y(t)$ can either be a time-periodic force or an external stochastic force; $F(x)$ is an external load, it is required to be zero in deciding whether the system exists directed motion and to be nonzero in calculating the efficiency of the transport; the noise term $\xi(t)$ is assumed to be Gaussian white noise satisfying $\langle \xi(t) \rangle = 0$, $\langle \xi(t)\xi(t') \rangle = \delta(t-t')$. According to different forms of the functions $V(x(t), f(t))$ and $y(t)$, the model is classified as flashing ratchet ($y(t) = 0$) [205–208], tilting ratchet ($f(t) = 0$) [209,210], etc.

For a Brownian ratchet, the occurrence of directed transport requires the presence of a nonequilibrium forcing. To understand this necessary condition [59,202,211,172], let us first consider the following simple ratchet system

$$\dot{x} = -V'(x) + A \sin \Omega t + D\xi(t). \tag{97}$$

---

[9] More precisely, for an overdamped mechanical system, it should be the *center of friction*.

In the case $A = 0$, system (97) becomes

$$\dot{x} = -V'(x) + D\xi(t). \tag{98}$$

The term $D\xi(t)$ is assumed to represent equilibrium thermal fluctuations. Hence, the stationary system (98) is an equilibrium system with a stationary distribution

$$\pi(x) = \frac{e^{-V(x)/k_BT}}{\int_0^L e^{-V(x)/k_BT}dx},$$

which dictates $D^2 = 2k_BT$. The probability flux in stationary state $J = 0$, which implies no macroscopic current in the system. From the viewpoint of thermodynamics, directed transport in an equilibrium thermal bath violates Kelvin–Planck's version of the Second Law: It is impossible for any cyclic device to convert heat from a single bath into work.

Besides noise-induced unidirectional transport, unbiased deterministic force with time or spatial symmetric breaking can also result in directed motion of the particle. Such a phenomenon is called deterministic ratchet. If one further takes into account the mass of the particle in the underdamped regime, then the corresponding unidirectional transport is call inertia ratchet. It has been shown that besides regular or chaotic transport, an inertia ratchet may exhibit inverse transport. As the direction of the current depends on the mass of the particle and the damping coefficient of the system [212], applications of inertial ratchets in particle separation based on mass is expected. Since we are primarily concerned with the phenomenon aroused by nonequilibrium fluctuations, we will not discuss inertia ratchets. Readers who are interested in this topic can refer to the Refs. [212,202,213,214].

When applying a Brownian motor with Eq. (96) to a motor protein, the variable x represents the center of friction of the macromolecule with respect to its track; it is a geometric point. Conformational changes of the macromolecular structure, including association with ATP, ADP, and Pi, are characterized by discrete biochemical states i. A unified working model describing the dynamics of a single-head motor protein with N different chemical states is governed by the following coupled diffusion model [206,207,215]

$$\dot{x}(t) = -V_i'(x) + D_i\xi_i(t), \quad (i = 1, 2, \ldots, N) \tag{99}$$

To fix our terminology, we call $x(t)$ the mechanical position of the motor at time t, and $i = i(t)$ ($i = 1, 2, \ldots, N$) the chemical state of the motor. They are both stochastic processes, i.e., $x = x(t, \omega)$, $i = i(t, \omega)$, in which ω gives rise to randomness.

The first important issue in studying Brownian motors is to understand, without net external mechanical work done to the system, how it can break down symmetry and thermochemical equilibrium, resulting in a net unidirectional transport. The second important problem concerns the determination of the direction, and its reversal, of a ratchet with the various system's parameters.

A third important issue, naturally, is about the efficiency of Brownian motors when it is used as an "engine" to pull an external load [216,217]. With respect to the over-damped, one-dimensional Brownian ratchet system (97), the motor efficiency can be calculated by thermodynamic efficiency or alternative, Stokes efficiency. Thermodynamic efficiency defines how well a motor converts chemical free energy into useful work [218,215,27]

$$\eta_{therm} \overset{\triangle}{=} \frac{\langle\dot{x}\rangle F}{P_{in}}, \tag{100}$$

where $\langle\dot{x}\rangle$ is the mean velocity of the motor, F is the external load, and P_{in} is the total input power. An alternative measure, Stokes efficiency, has been devised for purely viscous loads such as a motor encounters in normal transport. Stokes efficiency is defined as [219,220]

$$\eta_{stokes} \overset{\triangle}{=} \frac{\langle\dot{x}\rangle F + \langle\dot{x}\rangle^2}{P_{in}}, \tag{101}$$

where the term $\langle\dot{x}\rangle^2$ reflects the power working against the viscous drag. In both cases, the input power must be formulated to ensure that the defined efficiencies are bounded by 1.

In this section, we confine our discussion to models (97) and (99). We investigate the dynamics of unidirectional movement, the efficiency of a Brownian motor and the corresponding nonequilibrium origin.

4.2. Nonlinear, stochastic dynamics on a torus

4.2.1. Diffusion processes on a torus

$$\frac{d\phi}{dt} = -\Omega_e + a\sin(\psi - \phi) + A_1\xi_1(t),$$
$$\tag{102}$$
$$\frac{d\psi}{dt} = -\Omega_d + A_2\xi_2(t),$$

in which Ω_e represents the external resistant force, Ω_d represents the driving force. One should compare this equation with Eq. (68) and realize that Brownian motors and SR are indeed intimately related problems [221,222]. Now if we introduce a phase difference $\theta = \phi - \psi$, then

$$\frac{d\theta}{dt} = \Delta\Omega - a\sin\theta + A\xi(t) \tag{103}$$

where $\Delta\Omega = \Omega_d - \Omega_e$ and $A^2 = A_1^2 + A_2^2$. This is the exactly the same equation of Adler phase model! In fact, it is tempting, not unreasonably, to consider the $a > \Delta\Omega$ case (i.e., phase locking) related to "power stroke" and $a < \Delta\Omega$ case to "Brownian ratchet" [211].

4.3. Mean velocity, probability flux and rotation number of Brownian motors

The most important and widely studied quantity that characterizes the unidirectional motion of a molecular motor is its mean velocity $\langle\dot{x}\rangle$, where $\langle\cdot\rangle$ denotes the statistical ensemble average. There is a well-established relationship between the mean velocity, the probability flux (or current) J, and the time-averaged velocity (also known as rotation number) [202]:

$$\langle\dot{x}\rangle = L \cdot J = \lim_{t\to\infty} \frac{x(t)}{t}, \tag{104}$$

where L is the length of the period of a linear track along which the motor moves. Intuitively, Eq. (104) is understood as a consequence of the ergodicity of a stochastic process. However, a more careful examination shows that it requires some mathematical explanations. First, the continuous stochastic motion of the motor, $x(t)$, is nowhere smooth, just as Brownian motion $B(t)$; the limit of $\frac{x(t+h)-x(t)}{h}$ when h tends zero does not exist. Hence the meaning of the very notation $\langle\dot{x}\rangle$ remains to be clarified. Second, a molecular motor moving along a periodic linear track never reaches a true stationarity, just as a biased Brownian motion. The $x(t)$ has no invariant probability distribution; The ergodicity, i.e., the ensemble average being the same as the time average, in principle does not apply.

Therefore, for further in-depth studies of the Brownian ratchet mechanism of molecular motors, it is of essential importance to give a precise definition for the mean velocity $\langle\dot{x}\rangle$, and provide a mathematically justified derivation for Eq. (104). In Section 4.3.1, based on a properly defined *conditional forward random velocity* (CFRV), we will give a mathematically sensible definition for $\langle\dot{x}\rangle$ while maintaining its explicit physical meaning. After defining $\langle\dot{x}\rangle$ as the expected value of the CFRV, we shall discuss in Section 4.3.2 the relationship between the mean velocity, the time-averaged velocity and the probability current, in various Brownian ratchet systems.

4.3.1. A clarification of the definition of mean velocity

To clarify the definition of $\langle\dot{x}\rangle$, let us start by considering the stochastic process characterized by the equation

$$dx(t) = -\frac{\partial}{\partial x}V(t,x)dt + DdB(t), \tag{105}$$

whose solution $\{x(t)\}_{t\geq 0}$ is a Markov process on the Wiener space $(\Omega, \mathcal{F}, \mu)$. More precisely, as discussed in Appendix A, $x(t)$ should be written as $x(t,\omega)$, where the randomness of the trajectory is inherited in $\omega \in \Omega$. One sometimes uses $x(t)$ to represent $x(t,\omega)$. For convenience, we shall in the following write $x(t)$, but $x(t,\omega)$ when the context is necessary. Let $p(s,t;x,y)$ be the transition probability density of $\{x(t,\omega)\}_{t\geq 0}$ from position x at time s to position y at time t.

To keep the original physical meaning of the velocity but at the same time overcome the mathematical difficulty, we define the CFRV $v(t,x(t))$ for the stochastic process $\{x(t)\}_{t\geq 0}$ as

$$v(t,x(t)) \triangleq \lim_{h\to 0^+} E\left[\frac{x(t+h)-x(t)}{h}\bigg|\mathcal{F}_t\right], \tag{106}$$

where $\mathcal{F}_t = \sigma\{x(s), 0 \leq s \leq t\}$ which contains all the information before time t. It follows from the Markovian property of the process that

$$v(t,x(t)) = \lim_{h\to 0^+} E\left[\frac{x(t+h)-x(t)}{h}\bigg|x(t)\right]. \tag{107}$$

To see the existence of the above limit, suppose that the position of a particle at time t is at x, then the CFRV at time t is

$$v(t,x) = \lim_{h\to 0^+} \frac{1}{h}E\left[x(t+h)-x(t)\bigg|x(t)=x\right]$$

$$= \lim_{h\to 0^+} \frac{1}{h}\int (y-x)p(t,x;t+h,y)dy$$

$$= \frac{\partial}{\partial x}V(t,x). \tag{108}$$

So we see that conditioning on $x(t) = x$, the CFRV $v(t, x)$ is just the drift of the diffusion process corresponding to Eq. (105). While this result appears intuitive to physicists, we have not found the rigorous mathematical justification, as given here, in the literature. Since $\{x(t)\}_{t\geq 0}$ is a stochastic process, then $v(t, x(t))$ changes correspondingly along with $x(t)$, i.e. it is a random function $v(t, x(t, \omega))$. So we can define the mean velocity of system (105), denoted as $\langle \dot{x} \rangle$, as the expectation of the CFRV, i.e.,

$$\langle \dot{x} \rangle \overset{\triangle}{=} E[v(t, x(t, \omega))] = E\left[\frac{\partial}{\partial x}V(t, x(t, \omega))\right]. \tag{109}$$

The definition given by formula (109) has a very explicit physical meaning: It is the mean transport (drift) velocity of a diffusing process. This is completely consistent with the intuitive concept referred to in the literature.

In the following section, we shall prove the equivalence between mean velocity, probability flux, and the rotation number. The material is essentially mathematical in nature; hence for readers who are not interested in the mathematical rigor, he/she can skip this section and go to Section 4.4.

4.3.2. Relationship between mean velocity, probability current and time-averaged velocity

4.3.2a. One-dimensional time-homogeneous Brownian ratchet. The first problem we shall study is a ratchet-like mesoscopic system with a non-zero force [223]

$$dx(t) = (F - V'(x))dt + DdB(t), \qquad x(t) \equiv x(t, \omega), \tag{110}$$

where F is a constant and $V(x)$ is a periodic potential satisfying $V(x + L) = V(x)$. By time-homogeneous, we mean neither the diffusion D or drift $(F - V'(x))$ is an explicit function of time. Note that any periodic force $F(x)$ can be always decomposed into the form:

$$F(x) = \overline{F} - \frac{d}{dx}V(x), \quad \text{where } \overline{F} = \frac{1}{L}\int_0^L F(x)dx. \tag{111}$$

Eq. (110) is not a correct model for a motor protein *per se*, since the mean velocity arises from a nonzero mechanical force F. Still, its mathematical analysis will provide clarifications for the relationships in Eq. (104). We shall point out, however, that several correct models for motor proteins can be mathematically simplified into this form, in particular when one evokes the "rapid biochemical cycle approximation" [27,172].

The periodicity of $V'(x)$ with respect to x suggests that we can represent the solution to Eq. (110) on a circle $\mathbb{S}^1$ with radius $L/(2\pi)$. To do this, let

$$\widetilde{x}(t) = x(t) \pmod{L},$$

then $\{\widetilde{x}(t)\}_{t\geq 0}$ is a diffusion process on $\mathbb{S}^1$ satisfying

$$d\widetilde{x}(t) = (F - V'(\widetilde{x}))dt + Dd\widetilde{B}(t), \quad \widetilde{x}(t) \in \mathbb{S}^1, \tag{112}$$

where $\{\tilde{B}(t)\}_{t\geq 0}$ is a Brownian motion on the circle. The FPE corresponding to Eq. (112) is

$$\frac{\partial}{\partial t}\hat{p}(t, \widetilde{x}) = -\frac{\partial}{\partial x}\hat{J}(t, \widetilde{x}), \quad (\tilde{x} \in [0, L]), \tag{113}$$

where

$$\hat{p}(t, \widetilde{x}) = \sum_{n=-\infty}^{\infty} p(\widetilde{x} + nL, t)$$

is the probability density in position $\widetilde{x} \in \mathbb{S}^1$ at time t with periodic boundary condition $\hat{p}(t, \widetilde{x}) = \hat{p}(t, \widetilde{x} + L)$, and

$$\hat{J}(t, \widetilde{x}) = (F - V'(\widetilde{x}))\hat{p}(t, \widetilde{x}) - \frac{D^2}{2} \cdot \frac{\partial}{\partial x}\hat{p}(t, \widetilde{x})$$

is the probability flux (current). The diffusion process on the circle, Eq. (112), has a unique invariant distribution [64] and the process $\{\widetilde{x}(t)\}_{t\geq 0}$ is ergodic on $\mathbb{S}^1$. By solving the equation $\partial\hat{p}(t, \widetilde{x})/\partial t = 0$, we obtain a unique invariant probability density of $\{\widetilde{x}(t)\}_{t\geq 0}$, denoted as $\hat{p}(\widetilde{x})$.

According to formula (108), the CFRV of $\{x(t)\}_{t\geq 0}$ is

$$v(x(t)) = F - V'(x(t)) = F - V'(\widetilde{x}(t)) = v(\widetilde{x}(t)); \qquad v(x(t)) \equiv v(x(t, \omega)).$$

Since in the long-time run, the process $\{\widetilde{x}(t)\}_{t\geq 0}$ will approach stationarity, we can reasonably take the invariant distribution $\hat{p}(\widetilde{x})d\widetilde{x}$ as the initial distribution of $\{\widetilde{x}(t)\}_{t\geq 0}$ and obtain a stationary process. So by (109), in the steady state, the mean velocity of $\{x(t)\}_{t\geq 0}$ is

$$\langle \dot{x} \rangle = E[v(\widetilde{x}(t))] = \int_0^L (F - V'(x))\hat{p}(x)dx. \tag{114}$$

Next, applying Itô's integral to Eq. (110), we have

$$\frac{x(t)}{t} = \frac{1}{t} \int_0^t (F - V'(x))ds + \frac{DB(t) - DB(0)}{t}. \tag{115}$$

According to the iterated-logarithm theorem of Brownian motion [224], we obtain

$$(a.e.) \lim_{t \to \infty} \frac{D(B(t) - B(0))}{t} = 0, \tag{116}$$

here $(a.e.)$ means for almost all trajectories ω. As $V(x)$ is periodic in x, it is a continuous function on $\mathbb{S}^1$. It follows from the ergodicity of the process $\{\widetilde{x}(t)\}_{t \geq 0}$ on $\mathbb{S}^1$ that for almost all $\omega \in \Omega$

$$(a.e.) \lim_{t \to \infty} \frac{x(t, \omega)}{t} = (a.e.) \lim_{t \to \infty} \frac{1}{t} \int_0^t (F - V'(x(s)))ds$$

$$= (a.e.) \lim_{t \to \infty} \frac{1}{t} \int_0^t (F - V'(x(s)))ds$$

$$= \int_0^L (F - V'(\widetilde{x}))\hat{p}(\widetilde{x})d\widetilde{x}; \tag{117}$$

the existence of the limit and the last equality are ensured by Birkhoff ergodic theorem [225].

Finally, in the steady state, the probability flux in one-dimension

$$\hat{J}(\widetilde{x}) = (F - V'(\widetilde{x}))\hat{p}(\widetilde{x}) - \frac{D^2}{2} \cdot \frac{\partial}{\partial x}\hat{p}(\widetilde{x}) \tag{118}$$

is a constant. We shall denote it as $\hat{J}^{ss}$ since $\partial \hat{J}/\partial \widetilde{x} = -\partial \hat{p}/\partial t = 0$. Then integrating the two sides of Eq. (118), we have

$$\int_0^L (F - V'(\widetilde{x}))\hat{p}(\widetilde{x})d\widetilde{x} = L \cdot \hat{J}^{ss}. \tag{119}$$

Therefore, according to (114), (117) and (119), we have

Theorem 4.1. *For time-homogeneous Eq.* (110)*, the mean velocity* $\langle \dot{x} \rangle$*, the time-averaged velocity and the steady state probability flux of system* (112) *on the* $\mathbb{S}^1$ *are all equivalent to each other, i.e.,*

$$\langle \dot{x} \rangle = L \cdot J^{ss} = (a.e.) \lim_{t \to \infty} \frac{x(t, \omega)}{t}, \quad (for\ \omega\ a.e.). \tag{120}$$

Remark. Since $\widetilde{x}$ is a point on the circle $\mathbb{S}^1$, $x(t)/t$ is the mean angle swept during $[0, t]$. Thus.

$$\lim_{t \to \infty} \frac{x(t)}{L \cdot t}$$

is just the rotation number we have discussed in the previous sections, where one has learned that there is a deep connection between the nonequilibrium circulation and the rotation number.

Applying the ideas for proofing Eq. (120) to the more general Eq. (105), similar relationship between the mean velocity and the rotation number can be established. However the same result could be obtained only with much more sophisticated mathematical techniques, which we shall give in the subsequent section.

4.3.2b. One-dimensional time-inhomogeneous Brownian motor. Let us now consider a diffusion with a time-dependent potential, or mathematically called time-inhomogeneous Brownian motor with an external load. The corresponding SDE is

$$dx(t) = [F - V'(x, f(t))]dt + DdB(t), \tag{121}$$

where the time-varying potential $V(x, f(t))$ satisfies $V(x + L, f(t)) = V(x, f(t))$ and $V(x, f(t + T)) = V(x, f(t))$. This type of Brownian ratchets was widely discussed in the literature, but there have been only few mathematical investigations into its dynamics [226,227].

Since the potential $V(x, f(t))$ is periodic with respect to the position x, Eq. (121) can be again considered as a diffusion process on $\mathbb{S}^1$. But due to the explicit external time-varying modulation, the system considered now no longer reaches stationarity. This makes the mean velocity $\langle \dot{x}(t) \rangle = E[v(t, x(t))]$ time-dependent. Nevertheless, for every fixed $s \in [0, T]$, the subprocess $\{x(s + k \cdot T)\}_{k \geq 0}$ is a homogeneous Markov chain with continuous states in $\mathbb{S}^1$. Since $D > 0$ and the state space $\mathbb{S}^1$ is compact, then similar to the case in a finite Markov chain, we have

Lemma 4.2. *For the process $\{x(s + kT)\}_{k \geq 0}$ on $\mathbb{S}^1$, there exists an invariant distribution $\nu_s(x)dx$ on $\mathbb{S}^1$, such that*

$$\frac{1}{n} \sum_{k=0}^{n-1} p(s + kT, x)dx \xrightarrow{weakly} \nu_s(x)dx, \quad n \to \infty, \tag{122}$$

i.e., for any continuous function $g(x)$, $x \in [0, L]$,

$$\lim_{n \to \infty} \int_0^L g(x) \cdot \frac{1}{n} \sum_{k=0}^{n-1} p(s + kT, x)dx = \int_0^L g(x)\nu_s(x)dx. \tag{123}$$

Lemma 4.2 reveals that the process $\{x(s + k \cdot T)\}_{k \geq 0}$ on $\mathbb{S}^1$ is asymptotically stationary. According to this property and the ergodicity of $\{x(s + kT)\}_{k \geq 0}$, we can reach the following conclusion:

Theorem 4.3. *For a time-inhomogeneous Brownian motor characterized by Eq. (121), we have*
 (i) *The mean velocity is*

$$\lim_{t \to \infty} \frac{1}{t} \int_0^t \langle \dot{x}(s) \rangle ds = \frac{1}{T} \int_0^T ds \int_0^L \left[F - \frac{\partial}{\partial x} V(x, f(s)) \right] \nu_s(x)dx. \tag{124}$$

We therefore define the mean velocity of a time-inhomogeneous Brownian motor as

$$\langle \dot{x} \rangle \overset{\Delta}{=} \lim_{t \to \infty} \frac{1}{t} \int_0^t \langle \dot{x}(s) \rangle ds. \tag{125}$$

 (ii) *The limit of the time-averaged velocity is*

$$\underset{t \to \infty}{\ell.i.m.} \frac{x(t, \omega)}{t} = \frac{1}{T} \int_0^T ds \int_0^L \left[F - \frac{\partial}{\partial x} V(x, f(s)) \right] \nu_s(x)dx, \tag{126}$$

in which $\ell.i.m.$ means "limit in mean square".

Proof. Part (i) It follows from (109) that

$$\langle \dot{x}(t) \rangle = E(v(t, x(t, \omega))) = \int_0^L \left[F - \frac{\partial}{\partial x} V(x, f(t)) \right] p(t, x)dx, \tag{127}$$

where $p(t, x) = \int_0^L p(0, t; y, x)p(0, y)dy$ is the probability density of $\{x(t)\}_{t \geq 0}$ in position x at time t. Then,

$$\begin{aligned}
\lim_{n \to \infty} \frac{1}{nT} \int_0^{nT} \langle \dot{x}(s) \rangle ds &= \lim_{n \to \infty} \frac{1}{nT} \int_0^{nT} ds \int_0^L \left[F - \frac{\partial}{\partial x} V(x, f(s)) \right] p(s, x)dx \\
&= \lim_{n \to \infty} \frac{1}{T} \int_0^T ds \int_0^L \left[F - \frac{\partial}{\partial x} V(x, f(s)) \right] \cdot \frac{1}{n} \sum_{k=0}^{n-1} p(s + kT, x)dx \\
&= \frac{1}{T} \int_0^T ds \lim_{n \to \infty} \int_0^L \left[F - \frac{\partial}{\partial x} V(x, f(s)) \right] \cdot \frac{1}{n} \sum_{k=0}^{n-1} p(s + kT, x)dx.
\end{aligned}$$

The exchange of the limit and the integral $\int_0^T \cdots ds$ in the last two equations is warranted by the dominated convergence theorem. According to Lemma 4.2, we have

$$\lim_{t \to \infty} \frac{1}{t} \int_0^t \langle \dot{x}(s) \rangle ds = \frac{1}{T} \int_0^T ds \int_0^L \left[F - \frac{\partial}{\partial x} V(x(s), f(s)) \right] \nu_s(x)dx. \tag{128}$$

Now let us prove Part (ii). By Itô's integral, we have

$$\frac{x(t, \cdot)}{t} = \frac{1}{t} \int_0^t \left[F - \frac{\partial}{\partial x} V(x(s, \cdot), f(s)) \right] ds + \frac{DB(t, \cdot) - DB(0, \cdot)}{t}. \tag{129}$$

A stochastic process $\{x(t, \omega)\}_{t \geq 0}$, when considered as a function in $L^2(\Omega, \mathcal{F}, P)$, is denoted as $\{x(t, \cdot)\}_{t \geq 0}$.

Taking $t = nT$, we have

$$\frac{1}{nT} \int_0^{nT} \left[F - \frac{\partial}{\partial x} V(x(s, \cdot), f(s)) \right] ds = \frac{1}{nT} \sum_{k=0}^{n-1} \int_{kT}^{(k+1)T} \left[F - \frac{\partial}{\partial x} V(x(s, \cdot), f(s)) \right] ds$$

$$= \frac{1}{T} \int_0^T \frac{1}{n} \sum_{k=0}^{n-1} \left[F - \frac{\partial}{\partial x} V(x(s + kT, \cdot), f(s)) \right] ds. \tag{130}$$

Since the stationary process $\{x(s + kT)\}_{k \geq 0}$ with the invariant measure $v_s(x) dx$ ($0 \leq s \leq T$) is ergodic on $\mathbb{S}^1$, then it follows from L^p ergodic theorem of Von Neumann that for every fixed $s \in [0, T]$,

$$\ell.i.m._{n \to \infty} \frac{1}{n} \sum_{k=0}^{n-1} \left[F - \frac{\partial}{\partial x} V(x(s + kT, \cdot), f(s)) \right] = \int_0^L \left[F - \frac{\partial}{\partial x} V(x, f(s)) \right] v_s(x) dx. \tag{131}$$

For $E|B(t) - B(0)|^2 = t$, we have

$$\lim_{t \to \infty} \frac{E|B(t) - B(0)|^2}{t^2} = 0. \tag{132}$$

Since the term $\frac{1}{n} \sum_{k=0}^{n-1} [F - \frac{\partial}{\partial x} V(x(s + kT, \cdot), f(s))]$ in the left-hand side of (131) without $\ell.i.m.$ is a function of s taking values in $L^2(\Omega, \mathcal{F}, P(d\omega))$, and its L^2 norm is uniformly bounded with respect to $s \in [0, T]$, then applying the bounded convergent theorem to formulas (129), (130) yields

$$\ell.i.m._{n \to \infty} \frac{x(nT, \cdot)}{nT} = \frac{1}{T} \int_0^T \ell.i.m._{n \to \infty} \frac{1}{n} \sum_{k=0}^{n-1} \left[F - \frac{\partial}{\partial x} V(x(s + kT, \cdot), f(s)) \right] ds$$

$$= \frac{1}{T} \int_0^T ds \int_0^L \left[F - \frac{\partial}{\partial x} V(x, f(s)) \right] v_s(x) dx. \tag{133}$$

Hence

$$\ell.i.m._{n \to \infty} \frac{x(t)}{t} = \ell.i.m._{n \to \infty} \frac{x(nT, \cdot)}{nT} = \frac{1}{T} \int_0^T ds \int_0^L \left[F - \frac{\partial}{\partial x} V(x, f(s)) \right] v_s(x) dx. \quad \square \tag{134}$$

Remark. At a first glance of (131), and following Birkhoff ergodic theorem that for every fixed s,

$$\lim_{n \to \infty} \frac{1}{n} \sum_{k=0}^{n-1} \left[F - \frac{\partial}{\partial x} V(x(s + kT, \cdot), f(s)) \right] = \int_0^L \left[F - \frac{\partial}{\partial x} V(x, f(s)) \right] v_s(x) dx, \quad a.e. \ P(d\omega) \tag{135}$$

one may expect the following a.e. limit,

$$\lim_{n \to \infty} \frac{1}{T} \int_0^T \frac{1}{n} \sum_{k=0}^{n-1} \left[F - \frac{\partial}{\partial x} V(x(s + kT, \omega), f(s)) \right] ds = \frac{1}{T} \int_0^T \lim_{n \to \infty} \frac{1}{n} \sum_{k=0}^{n-1} \left[F - \frac{\partial}{\partial x} V(x(s + kT, \omega), f(s)) \right] ds$$

$$= \frac{1}{T} \int_0^T ds \int_0^L \left[F - \frac{\partial}{\partial x} V(x, f(s)) \right] v_s(x) dx, \quad a.e. \ P(d\omega).$$

However, it should be noticed that the above limit is not valid for almost all ω, since the zero-measure set omitted in formula (135) may depend on the parameter $s \in [0, T]$. And because the measure of the union of uncountable sets with zero measure may be positive, we cannot improve the limit in (134) as

$$\lim_{n \to \infty} \frac{x(nT)}{nT} = \frac{1}{T} \int_0^T ds \int_0^L \left[F - \frac{\partial}{\partial x} V(x, f(s)) \right] v_s(x) dx, \quad a.e. \ P(d\omega).$$

4.3.2c. Brownian motors with coupled diffusions. The previous section on "One-dimensional time-homogeneous Brownian motion" tells us that, when there is no external force F, the one-dimensional time-homogeneous system (110) allows only zero mean velocity. Therefore, a unidirectional moving Brownian motor either is driven by a time-inhomogeneous mechanism, or from chemical reactions such as ATP hydrolysis. In 1957, Andrew F. Huxley first introduced internal conformational states into the mechanical moving particle, called "cross-bridge" at the time, and coupled biochemical reactions with the mechanical movement in a theory. The "sliding filament" model is a mathematical theory for muscle contractions [198]. In 1990s, with the discovery of single motor protein movement, the mechanical movement has shown

to be a Brownian-like motion. This leads to a coupled diffusion system as the mathematical framework for Brownian motor movement [228,61,27]. For generality in mathematics we consider $N + 1$ chemical states: Eq. (110),

$$dx(t) = (F - V_i'(x))dt + D_i dB_i(t), \quad (i = 0, 1, 2, \ldots, N) \tag{136}$$

where $x(t)$ describes the space position of the center of mass of a molecular motor, $i = i(t)$ represents the chemical state of the molecule at time t. Here $\{i(t)\}_{t \geq 0}$ should be understood also as a stochastic process. Suppose that its transition rate is determined by a **Q**-matrix:

$$\mathbf{Q}(x) \stackrel{\triangle}{=} (q_{ij}(x))_{N \times N}, \quad \left(\sum_j q_{ij}(x) = 0\right). \tag{137}$$

Then to be rigorous, the dynamics of the motor is represented by the stochastic process $\mathbf{X}(t) \stackrel{\triangle}{=} (x(t, \omega), i(t, \omega))$, where x and i characterize its position and its internal chemical states, respectively. Then system (136) should be written as the following SDE:

$$dx(t) = \sum_{k=0}^{N} \mathcal{X}_k(\eta(t))[(F - V_k'(x(t)))dt + D_k dB_k(t)], \tag{138}$$

wherein $\eta(t) \stackrel{\triangle}{=} i(t)$.

$$\mathcal{X}_k(i) = \begin{cases} 1, & i = k, \\ 0, & i \neq k. \end{cases}$$

Eq. (138) defines a *coupled diffusion process* $\{(x(t), \eta(t))\}_{t \geq 0}$ on $\mathbb{R} \times \mathbb{E}$. The corresponding PFE is

$$\frac{\partial}{\partial t} p_i(t, x) = -\frac{\partial}{\partial x}(F - V_i'(x))p_i(t, x) + \frac{D_i^2}{2} \cdot \frac{\partial^2}{\partial x^2} p_i(t, x) + \sum_j p_j(t, x)q_{ji}(x)$$

$$= -\frac{\partial}{\partial x}J_i(t, x) + \sum_j p_j(t, x)q_{ji}(x), \tag{139}$$

in which $p_i(t, x)$ is the probability density of the motor with chemical state i locating at position x at time t. $J_i(t, x) = (F - V_i'(x))p_i(t, x) - \frac{D_i^2}{2} \cdot \frac{\partial}{\partial x}p_i(t, x)$ expresses the net probability current of the motor, being in state i, passing through the position x at time t; it shows the spatial movement of the molecule. The last term in the FPE, $\sum_j p_j(t, x)q_{ji} = \sum_j(p_j(t, x)q_{ji} - p_i(t, x)q_{ij})$, represents the net probability current associated with transitions between state i and all other states at position x. This term displays a chemical reaction flux entering and leaving the ith state. Eq. (139) presents a clear physical picture of the two types of the motion, chemical and spatial, of the motor.

Suppose that the stationary distribution of the system is $\pi_i(x)$, and the stationary probability current is $J_i(x)$, then

$$0 = -\frac{d}{dx}J_i(x) + \sum_j(\pi_j(x)q_{ji}(x) - \pi_i(x)q_{ij}(x)),$$

i.e.

$$\frac{d}{dx}J_i(x) = \sum_j \pi_j(x)q_{ji}(x). \tag{140}$$

Let $J(x) = \sum_i J_i(x)$, then it follows from (140) and the property of $\mathbf{Q} = (q_{ij})$ that

$$\frac{d}{dx}J(x) = \sum_i \sum_j \pi_j(x)q_{ji}(x) = \sum_j \sum_i \pi_j(x)q_{ji}(x) = 0. \tag{141}$$

This indicates that in the steady state, $J(x) = \sum_i J_i(x) = \text{Constant} \stackrel{\triangle}{=} J^{ss}$. If the $J^{ss} \neq 0$, then system (136) exhibits a unidirectional transport phenomenon.

Theorem 4.4. *For the coupled diffusion Brownian motor* (136), *the relationship between the mean velocity, the probability flux and the rotation number can be expressed as*

$$\langle \dot{x} \rangle = L \cdot \sum_{i=1}^{N} J_i(x) = L \cdot Rot, \tag{142}$$

where the last equality is valid in an a.e. $P(d\omega)$ sense.

Proof. Let $b(x, i) = \sum_k \mathcal{X}_k(i)(F - V_k'(x)) = F - V_i'(x)$. Conditioning on $x(t) = x$, $\eta(t) = i$, the CFRV $\{(x(t), \eta(t))\}_{t \geq 0}$ of Eq. (138) is

$$
\begin{aligned}
v(x, i) &\triangleq \lim_{h \to 0} \frac{1}{h} E[x(t + h) - x(t)|x(t) = x, \eta(t) = i] \\
&= \lim_{h \to 0} \frac{1}{h} \int_0^h E_{(x,i)} b(x(s), \eta(s)) ds \\
&= \lim_{h \to 0} \frac{1}{h} \int_0^h ds \int_0^L \sum_k b(y, k) p_{ik}(s, x, y) dy \\
&= \int_0^L dy \lim_{h \to 0} \frac{1}{h} \int_0^h \sum_{k \neq i} b(y, k)[q_{ik} \cdot s + o(s)]\delta(y - x) ds \\
&\quad + \int_0^L dy \lim_{h \to 0} \frac{1}{h} \int_0^h b(y, i) \cdot [1 - q_i s + o(s)]\delta(y - x) ds \\
&= \int_0^L b(y, i)\delta(y - x) dy \\
&= b(x, i).
\end{aligned}
\tag{143}
$$

Similar to the case in the time-homogeneous ratchet system, we consider the stationary process starting from the invariant distribution $\pi_i(x)$. Then

$$
\begin{aligned}
\langle \dot{x}(t) \rangle &= E[v(x_t, \eta_t)] = E[b(x_t, \eta_t] = \int_0^L \sum_i b(x, i)\pi_i(x) dx \\
&= \int_0^L \sum_i (F - V_i'(x))\pi_i(x) dx \\
&= \int_0^L \sum_i \left[(F - V_i'(x))\pi_i(x) - \frac{D_i^2}{2} \cdot \frac{\partial}{\partial x}\pi_i(x) \right] dx \\
&= \int_0^L \sum_i J_i(x) dx \\
&= L \cdot J^{ss} \\
&= L \cdot \sum_i J_i.
\end{aligned}
\tag{144}
$$

On the other hand, according to Itô integral, we have

$$
\frac{x(t)}{t} = \frac{1}{t} \int_0^t b(x_u, \eta_u) du + \frac{\sum_i D_i \mathcal{X}_i(\eta_u) B_i(t,)}{t}.
$$

It follows from the ergodicity of the process that

$$
\begin{aligned}
\lim_{t \to \infty} \frac{x(t)}{t} &= \lim_{t \to \infty} \frac{1}{t} \int_0^t b(x(u), \eta(u)) du \\
&\overset{a.e.}{=} E[b(x_t, \eta_t)] \\
&= \int_0^L \sum_i \pi_i(x)(F - V_i'(x)) dx \\
&= L \cdot \sum_i J_i.
\end{aligned}
\tag{145}
$$

Hence, for the coupled diffusion system (138), we obtain the following equalities

$$
\langle \dot{x} \rangle = L \cdot \sum_i J_i \overset{a.e.}{=} \lim_{t \to \infty} \frac{x(t)}{t}. \quad \square
$$
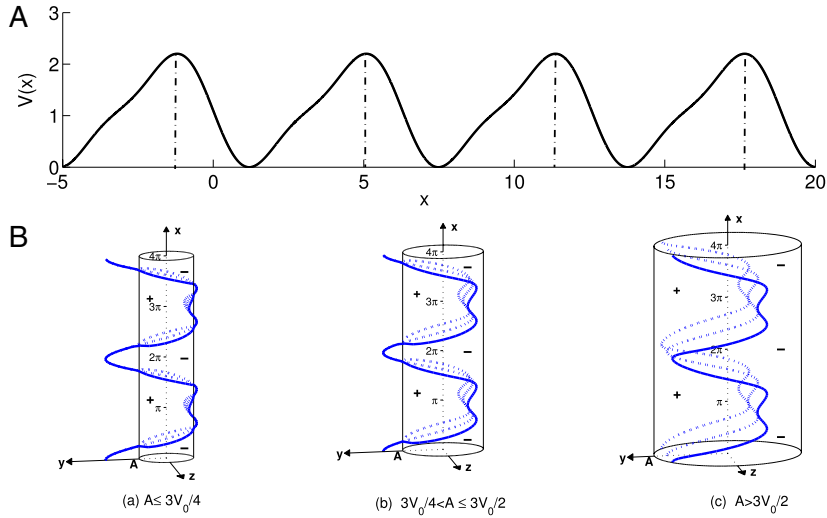
Fig. 28. (A) The potential function $V(x) = -V_0(\sin x + 0.25 \sin 2x) + C$ for given $V_0 = 1$ and $C = 1.1$. (B) The phase space of the system in Eq. (149). Three cases of the intersection of $y = -V_0(\cos x + 0.5 \cos 2x)$ with the cylinder for (a) $A \leq 0.75V_0$, (b) $0.75V_0 < A \leq 1.5V_0$, and (c) $A > 1.5V_0$ are shown. The '+' and '−' signs indicate the x-component of the vector field on the cylinder. (For interpretation of the references to colour in this figure legend, the reader is referred to the web version of this article.)

4.4. Unidirectional movement of Brownian ratchet and dynamical mechanism of symmetry breaking

In this section, we investigate the unidirectional motion in the stochastic, one-dimensional system (97). For concrete computations, we assume that the asymmetric potential shown in Fig. 28(A) takes the form of

$$V(x) = -V_0(\sin x + 0.25 \sin 2x) + C,$$

where C is a constant.

The corresponding SDE is then written as

$$\dot{x} = -V'(x) + A \sin \omega t + D\xi(t). \tag{146}$$

The phenomena of noise-induced transports in such a simple system have been explored in a number of studies in the last decade [209,202]. Many extensions of the simple model have been developed, for instance, inertia ratchets with regular or chaotic transport and coupled ratchets with array-enhanced transport. Still, understanding the simplest model from an alternative viewpoint is very useful. For the specific system in this section, we shall study the current reversal that occurs at a high driving frequency ω.

4.4.1. Deterministic nonlinear dynamics of a system on a cylinder
Let us first study the dynamics without noise perturbation. The nonlinear differential equation is

$$\dot{x} = V_0(\cos x + 0.5 \cos 2x) + A \sin \omega t. \tag{147}$$

Definition 4.5. The solution $\{x(t)\}_{t \geq 0}$ to Eq. (147) with an initial value $x(0) = x_0$ is called a $(p{:}q)$-type phase-locking solution, if

$$x(t + pT) = x(t) + 2\pi q, \quad \forall t \geq 0, \tag{148}$$

where $T = 2\pi/\omega$, p and q are two prime integers.

In Fig. 29, the entire A–ω parameter plane, with $V_0 = 1.5$, is divided into different phase-locking regions. In (1:0) region, no unidirectional transport occurs; while in $(p{:}q)$-type ($p \neq 0$, $q \neq 0$) region, the deterministic system exhibits unidirectional transport with mean velocity $v = \frac{q}{p}\omega$.

By setting $y = A \sin \omega t$, $z = A \cos \omega t$, the deterministic system can be equivalently written as

$$\begin{cases} \dot{x} = V_0(\cos x + 0.5 \cos 2x) + y, \\ \dot{y} = \omega z, \\ \dot{z} = -\omega y, \end{cases} \tag{149}$$

where y, z satisfy: $y^2 + z^2 = A^2$.
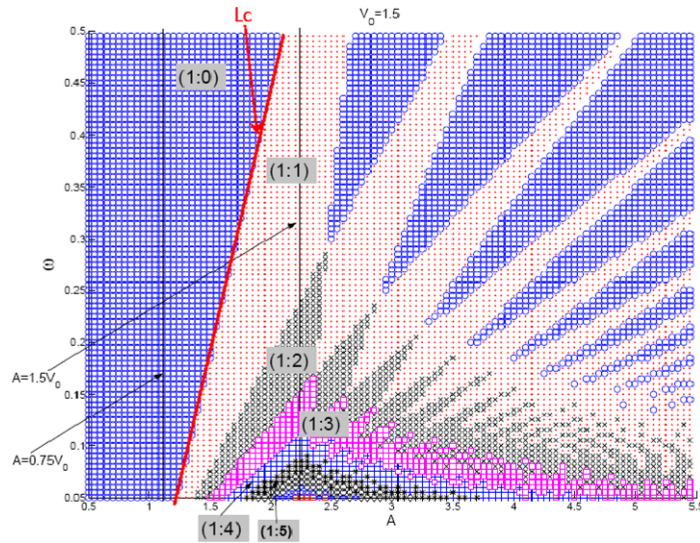
Fig. 29. Different $(p{:}q)$-type phase-locking solutions to Eq. (147) shown in the (A, ω) parameter regime. (For interpretation of the references to colour in this figure legend, the reader is referred to the web version of this article.)

Therefore, (y, z) moves on a circle, and together with x, Eq. (149) is a dynamical system on a cylinder.[10] On the cylinder, as shown in Fig. 28, the (1:0)-type resonance solution means that the particle winds around the cylinder, but it has no movement in x direction. This corresponds to a limit cycle of Eq. (149) on the cylinder. For $(p{:}q)$-type ($p \neq 0, q \neq 0$) phase-locking solution to Eq. (147), the corresponding trajectory to Eq. (149) winds around the cylinder q times with the increment $2\pi q$ in x direction during $p \cdot T$ time. In this situation, there is no limit cycle on the cylinder. These different "topological" scenarios in a molecular motor were first discussed in [216].

Let $\dot{x} = 0$, considering the intersection of the null-cline surface $y = -V_0(\cos x + 0.5 \cos 2x)$ with the cylinder $E^2 : y^2 + z^2 = A^2$. We have the following three different cases for the system in Eq. (149):

Case 1: $0 \leq A \leq 0.75V_0$, where the generatrices $y = -A$ and $y = A$ both intersect with the phase $y = -V_0(\cos x + 0.5 \cos 2x)$. See Fig. 28B(a).

Case 2: $0.75V_0 < A \leq 1.5V_0$, where the generatrix $y = -A$ intersects with the phase $y = -V_0(\cos x + 0.5 \cos 2x)$, while $y = A$ does not. See Fig. 28B(b).

Case 3: $A > 1.5V_0$, where both generatrices $y = -A$ and $y = A$ do not intersect with the phase $y = -V_0(\cos x + 0.5 \cos 2x)$. See Fig. 28B(c).

Corresponding to the above three cases, using qualitatively analysis and numerical simulations, we find that there is no negative, and the velocity of the deterministic unidirectional transport is usually an integral multiple of the driving frequency ω (see Fig. 29). besides, we have:

(i) For every fixed value of $A \in (0, 0.75V_0]$ and any frequency $\omega > 0$, Eq. (149) has one and only one stable limit cycle (SLC) and one unstable limit cycle (ULC) in the region $x \in [k \cdot 2\pi, (k+1) \cdot 2\pi]$. The limit cycles are within in the narrower dashed regions shown in Fig. 28A(a): $+ \backslash -$ (in the x direction) for the stable one and $- \backslash +$ for the unstable one. The conclusions can be rigorously proven mathematically by applying Poincaré–Bendixson theorem on the cylinder.

(ii) For every fixed value of $A \in (0.75V_0, 1.5V_0]$, there exists a critical value of $\omega = \omega_c(A)$ (see the critical line L_c between (1:0)-type motion and (1:1) type motion in Fig. 29), such that for $\omega > \omega_c(A)$, Eq. (149) has a unique SLC and ULC in the region $x \in [k \cdot 2\pi, (k+1) \cdot 2\pi), k \in Z$; while for $\omega < \omega_c(A)$, Eq. (149) has no limit cycle on the cylinder. In conclusion, this critical line $L_c: \omega = \omega_c(A)$ divides the behavior of the system into two different dynamics, above which the system has 1:0 limit cycle; but below which the system has $p{:}q$ ($q \neq 0$), i.e., no limit cycle. These results can all be rigorously proven.

(iii) For $A > 1.5V_0$, Eq. (149) alternatively occurs (1:0)-type solutions, i.e., limit cycles, and $(p{:}q)$-type ($p \neq 0, q \neq 0$) phase-locking solutions (also called periodic running solutions), with the variations of A and ω. A rigorous mathematical treatment of this case is rather difficult.

4.4.2. Noise-induced unidirectional motion in different phase-locking regions

We shall now investigate the effects of noise on the transport behavior of the system in these different phase-locking regions. We shall note that the $(p{:}q)$-type of motion with $q \neq 0$, corresponds to a sustained global mobility in x direction, while (1:0)-type of motion means there is no global mobility in x-direction. The physical significance of $(p{:}q)$, thus, is clear: It corresponds to (chemical cycle:mechanical cycle).

---

[10] If we consider the periodic $x \in \mathbb{S}^1$ as in the previous section, then Eq. (149) is a dynamical system on a torus $\mathbb{S}^2$.
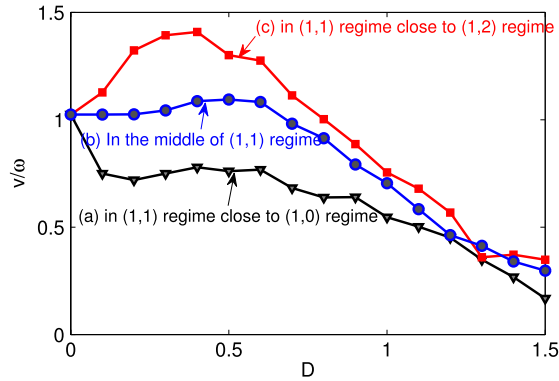
Fig. 30. Noise effects in a (p, q) regime. Here the curves of the mean velocity $v = \langle \dot{x} \rangle$ vs. the noise strength D are plotted for the cases (a) (A, ω) lies in the $(1, 1)$ regime but very near the boundary with the $(1, 0)$ regime, (b) (A, ω) lies in the middle of the $(1, 1)$ regime, and (c) (A, ω) is in the $(1, 1)$ regime but near the boundary with the $(1, 2)$ regime. (For interpretation of the references to colour in this figure legend, the reader is referred to the web version of this article.)

4.4.2a. p:q region with $q \neq 0$. We have learned that when the deterministic system (147) has a $(p{:}q)$-type $(q \neq 0)$ phase locking solution, the particle will undergo unidirectional movement with mean velocity $v = q\omega/p$. In the presence of noise, though the unidirectional motion persists, it is continuously being perturbed by the noise. The question then is, quantitatively, how does the velocity vary with the noise strength? To see the effect of the noise on $(p{:}q)$-type $(q \neq 0)$ phase-locking, we consider the $(1{:}1)$-type motion in Fig. 29 in details.

First, let the parameters (A, ω) lie in the $(1{:}1)$ region, but very near the boundary with the $(1{:}0)$ region. We take $A = 1.55$ and $\omega = 0.2$ for example. Fig. 30a shows that the effect of the noise can reduce the velocity of the unidirectional motion. Numerical simulations for other values of A and ω confirm that in this parameter regime, noise can only play a destructive role.

Now for (A, ω) lies in the middle part of the $(1{:}1)$ region. For example $A = 1.8$ and $\omega = 0.2$. We see from Fig. 30b that, when $0 < D < 0.5$, the velocity of unidirectional transport keeps almost unchanged, and then decreases with further increasing the strength of noise perturbation. This indicates that the phase-locking solution in this case is stable under the small perturbation of noise.

Finally, when (A, ω) lies in the $(1{:}1)$ region but near the boundary with the $(1 : 2)$ region, i.e., $A = 2.0$ and $\omega = 0.2$, we see from Fig. 30c that certain strength of noise perturbation can increase the velocity of unidirectional transport. This result is more interesting, it suggests a "constructive" role of the noise in accelerating the transport.

What is the reason that the noise plays such significantly different roles in different parts of the same phase-locking region? It can be explained from the structure of phase-locking regions shown in Fig. 29. Qualitatively speaking, the noise blurs a boundary between two phase-locking regions. Therefore, when (A, ω) lies at the edge of a boundary, the noise exhibits a more pronounced effect. In fact, the motion of such a particle, in the presence of the noise, actually switches between the two resonance states. The velocity of the transport, then, lies between the velocities of two deterministic resonance states. This explains why in the first case the mean velocity decreases with increasing D while in the third case $\langle \dot{x} \rangle$ increases with the noise strength.

4.4.2b. (1:0) region. We now study the effect of noise to the motion in the $(1{:}0)$ region. Noise can induce a unidirectional motion. But at a first glance, one cannot determine which direction will the particle move in the spatially asymmetric potential $V(x)$, since there is no macroscopic bias force applied nor potential gradient present. Then how and why can the interplay of the asymmetry of $V(x)$, the periodic forcing and white noise result in such a unidirectional transport? In the following, we shall give a dynamical explanation to this problem.

With the modulation of the external periodic driving, we notice that the relative position of the SLC and the ULC varies correspondingly. We denote d_1 the distance between the SLC to its above neighbored ULC, and d_2 the distance between the SLC to its below neighbored ULC. The symmetry breaking of the system can partly be reflected by the difference between d_1 and d_2.

Near the edge of $(1{:}0)$ region closing to $(1{:}1)$ region, $d_1 \approx 0$ and $d_2 > 0$ (see Fig. 31A). In such a situation, the particle moving around the SLC can be easily induced to move around the above copy of SLC by a weak noise perturbation via the ULC. Hence in Fig. 31A, one observes an obvious positive unidirectional motion. Besides, with the increase of noise intensity, the velocity of this unidirectional motion increases until a maximum is reached, and then decreases with further increasing the noise intensity. Here we call such an SR-like behavior velocity-measured SR to distinguish it from the conventional spectrum-measured SR. From Fig. 31A and B, one can see that as d_1 increases together with the decreasing of the difference between d_1 and d_2, the velocity of positive unidirectional motion decreases. And a negative unidirectional transport occurs when difference between d_1 and d_2 further decrease (see Fig. 31C), and this negative velocity also undergoes SR-like
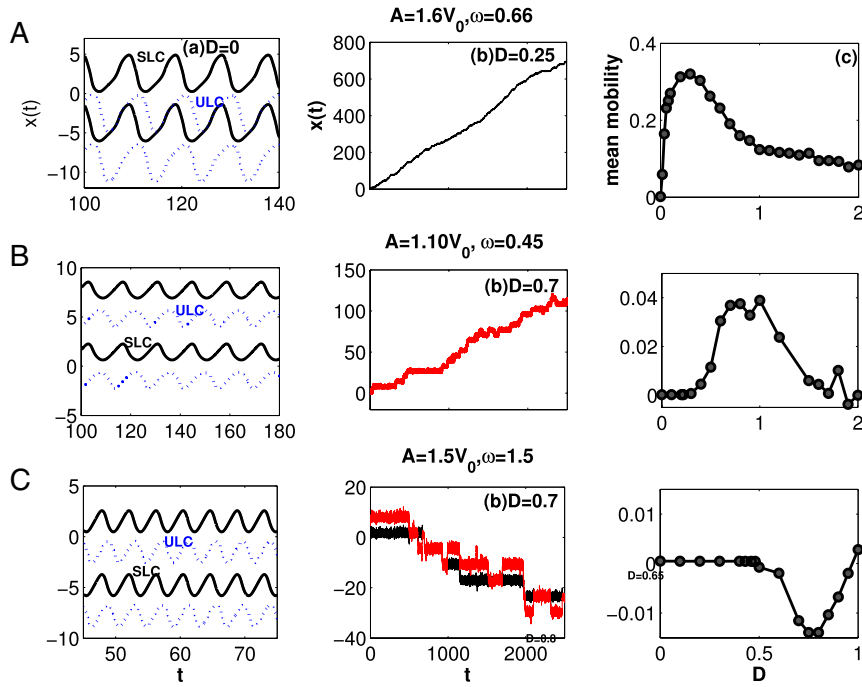
Fig. 31. Dependence of the unidirectional motion on the relative positions of the SLC to its two neighboring ULCs on the cylinder. Left column: Trajectories of the steady-state solutions to Eq. (146) with $D = 0$, which correspond to limit cycles on the cylinder; middle column: the trajectories of system (146) for $D > 0$, where unidirectional movements can be clearly seen; right column: the mean velocity $\langle \dot{x} \rangle$ of the system vs. the noise strength D. Here three different sets of (A, ω) are considered: (A) $A = 1.6V_0$, $\omega = 0.66$; (B) $A = 1.1V_0$, $\omega = 0.45$; (C) $A = 1.5V_0$, $\omega = 1.5$. (For interpretation of the references to colour in this figure legend, the reader is referred to the web version of this article.)

behavior. The result shown in Fig. 31 informs us that the relative position between the SLC to its two neighbored ULC has an important effect on determining the direction of the unidirectional motion of the ratchet system.

4.5. Unidirectional motion in coupled diffusion processes

4.5.1. Time-homogeneous coupled diffusion: a canonical Brownian ratchet

We now turn our attention to unidirectional transports in coupled diffusion systems. This is the canonical mathematical model for Brownian ratchets. For simplicity, we consider the following coupled two-state model

$$\dot{x}(t) = -V_i'(x) + D_i\xi_i(t), \quad i = 1, 2, \tag{150}$$

where $x(t)$ represents the mechanical position of the particle at time t; and $i = i(t)$ ($i = 1, 2$) describes the chemical state of the particle. $i(t)$ is a two-state stochastic jump process with transition rate $\{q_{ij}(x)\}_{2\times2}$ which satisfies $\sum_j q_{ij} = 0$ ($i = 1, 2$). $V_i(x)$ defines the mechanical potential for the particle when in state i ($i = 1, 2$) at point x. We shall choose V_1 to be a flat potential and V_2 an asymmetric function $V_2(x) = -V_0(\sin x + 0.25 \sin 2x) + C$ (see Fig. 32(A)), in which $C = 1.1$ is a constant, $V_0 = 2\pi$. $\xi_i(t)$ ($i = 1, 2$)) are standard white noises satisfying $\langle \xi_i(t) \rangle = 0$, $\langle \xi_i(t)\xi_i(t') \rangle = \delta(t-t')$. The white noise in the two states can either be from two uncorrelated sources, i.e., $\langle \xi_1(t)\xi_2(t') \rangle = 0$, or from the same sources, i.e., $D_1 = D_2$, $\xi_1 = \xi_2$. In this "ratchet" model, we assume that during the transition between the two states, the particle does not change its spatial position.

In numerical simulation, we fix $q_{12} = 3$, $q_{21} = 1$. It is shown that system (150) exhibits a unidirectional transport under the noise perturbation (see Fig. 32B). The direction of the motion, however, is opposite to the one observed in Section 4.4 even though the asymmetric potential function $V_2(x)$ used is the same as the $V(x)$ in Eq. (146). The question naturally arises: Why? And how does the unidirectional motion occur in the coupled diffusion system (150)?

First of all, let us see two extreme cases:

(i) $D_1 = 0$ and $D_2 > 0$. In this case, the particle receives noise perturbation only when it is in state 2. When in state 1, it does not change its position. The random switching between the two states only slows down the time, but contributes no dynamics. Since a Brownian particle in $V_2(x)$ alone does not have unidirectional transport in the long run, the same is true for the present case.

(ii) $D_1 > 0$ and $D_2 = 0$. In this case, the particle only receives perturbations of the noise when it is in state 1. Suppose that the particle is initially at the bottom of the potential V_2. After staying in state 2 for a random amount of time (the mean residence time is $1/q_{21}$), the particle jumps to state 1 and now is in potential V_1. With the presence of Brownian motion, the
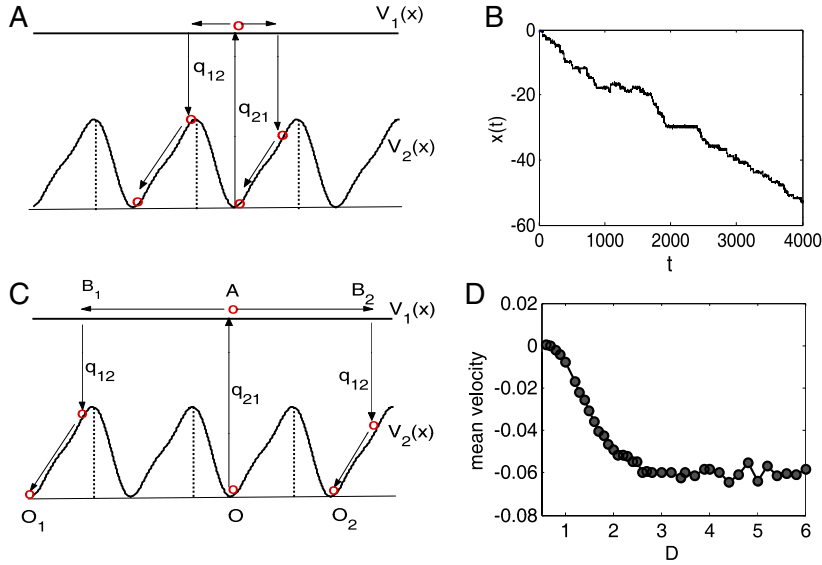
Fig. 32. (A) An example of the two potential functions in system (150): A flat $V_1(x)$ and an asymmetric $V_2(x)$. Also shown is the schematics of the movements of a Brownian motor. (B) A trajectory of the system (150) that undergoes unidirectional motion. (C) Schematics of the motion of the Brownian motor under strong noise perturbation in V_1. (D) The mean velocity $\langle \dot{x} \rangle$ of the system (150) vs. the noise intensity D_1 with fixed $D_2 = 0.05$. (For interpretation of the references to colour in this figure legend, the reader is referred to the web version of this article.)

particle will diffuse in both directions symmetrically with equal probability. And after a certain amount of random time (the mean time duration is $1/q_{12}$), the particle will switch back to the potential V_2. Due to the asymmetry of the $V_2(x)$, the particle has a larger probability of surmounting the left maximum than that of surmounting the right maximum (see Fig. 32A). Hence, macroscopically, the system exhibits a unidirectional motion toward the left. And with the noise intensity D_1 increases, the velocity of the movement increases correspondingly. Fig. 32D shows the mean velocity $\langle \dot{x} \rangle$ as a function of D_1 with fixed $D_2 = 0.1$. Interestingly, one sees that increasing D_1 always increases the mean velocity. As the value of D_1 increases to a sufficiently large value, the mean velocity plateaus. To explain this "noise-induced" ratchet phenomenon, we suppose that the particle is initially at point O of potential V_2 in Fig. 32C. As soon as the particle jumps to state 1, it will diffuse quickly and symmetrically to both sides due to the Brownian motion. If the noise strength is sufficiently strong, as the particle jumps back to state 2, the probability of the particle falling in the $k + 1$ wells leftward is the same as that of falling in the k wells rightward. Hence on average, the system only undergoes the length of one well. This explains why the mean velocity saturates as the noise intensity increases.

From the above discussions, we see that the perturbations of the noise to state 2 does no good for improving the unidirectional motion. In fact it plays a destructive role. Noise to the state 1, however, plays an active role.

Let us further consider the situation with only one noise source, i.e., $D_1 = D_2 \overset{\Delta}{=} D$, $\xi_1(t) = \xi_2(t)$. Increasing the noise intensity D will cause the particle diffuse more quickly along the flat potential V_1, resulting in an increased probability of the particle to fall into the well on the left in the potential V_2. On the other hand, the Brownian motion of the particle in the ratchet-like potential V_2 becomes more "sluggish" with the increasing of the noise strength. As the noise plays these oppo-site roles for a particle in the two potentials, one sees from Fig. 33 that increasing the noise level can accelerate the transport, and then at a suitable noise intensity, a maximal mean velocity is obtained. After that, further increasing the perturbation strength can only hinder the unidirectional motion. This indicates the occurrence of the velocity-measured SR.

4.5.2. Coupled diffusion with a time-periodic driving

In this last subsection, we give a brief discussion on the coupled diffusion process with a time-dependent periodic driving. The Eq. (150) becomes:

$$\dot{x}(t) = -V_i'(x) + A \sin \Omega t + D_i \xi_i(t), \quad i = 1, 2. \tag{151}$$

Numerical simulations show that there exists a critical driving amplitude A_c such that when $A < A_c$, the system moves unidirectionally to the left, while for $A \geq A_c$, the motion of the system becomes unidirectionally toward the right. Moreover, in both the regimes of the driving amplitude, the unidirectional motion shows velocity-measured SR effect: i.e, the velocity is first increasing with the increase of the driving amplitude until reaching a maximum and then decreasing again with the increase of A. This is shown in Fig. 34(c).

Combining with the discussion of the unidirectional motion in Section 4.4, it is not difficult to understand such a current reversal phenomenon. As has been mentioned in Section 4.4, the interplay of noise and the periodic force in potential V_2 tends to drive the particle moving toward the right. However, without periodic forcing, noise in potential V_2 only plays its
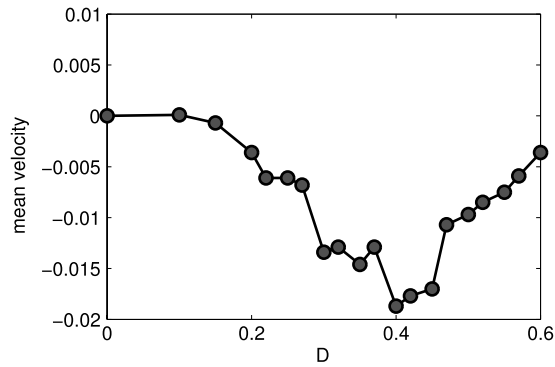
Fig. 33. The mean velocity $\langle \dot{x} \rangle$ of system (150) vs. the noise intensity D under the condition that $D_1 = D_2 = D$.
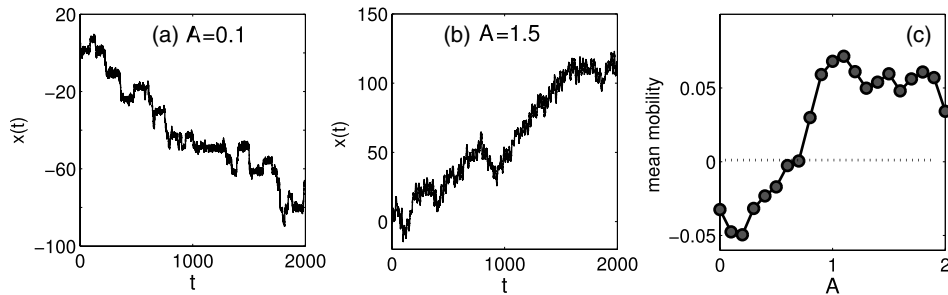
Fig. 34. Trajectories of system (151) for different driving amplitudes A. (a) $A = 0.1$; (b) $A = 1.5$. The mean velocity $\langle \dot{x} \rangle$ as a function of the driving amplitude A is depicted in (c). Here $\omega = 0.25$ and $D = 1.8$.

destructive role. When the periodic forcing is weak, the motion of asymmetric diffusion plays dominant role, which results in a unidirectional motion toward the left. However, when the periodic forcing amplitude increases to a certain value, the cooperation of noise and periodic force becomes dominant. This changes the direction of the system from moving leftward to moving rightward.

4.6. The efficiency of energy transduction in Brownian motors

From the discussions in the previous several sections, we have learned that a multi-state Brownian particle in an asymmetric periodic potential can have a directed motion, even when the total work done by the external force is zero. The molecular motor can thus carry an external load and still move against a resistant force, therefore, does work. It is natural one is interested in the mechanical efficiency of the motor, which has been a topic of great interest for quite long time.

In this section, we shall discuss the efficiency of molecular motors, for both time-independent coupled diffusion and periodically forced time-inhomogeneous Brownian motors. From the general theory of NESS we already had the notions of e.p.r and h.d.r. They are the amount of input energy that is converted into heat and lost to the isothermal environment. However, if the system has a load, at least part of the input energy can be converted into useful work against the load. The focus of the present section, therefore, is the efficiency of this energy conversion.

Analyses in the previous sections have shown that a multi-state Brownian particle can undergo unidirectional movement in a periodic but asymmetric potential even in the absence of any applied macroscopic force or potential gradient. The energy for the movement comes from the chemical state transitions that are coupled to external chemical potential. In fact, such a "Brownian motor" can carry a cargo and against a resistant force (i.e., a load) still moves forward. It can do work! There is a free energy conversion from chemical form to mechanical form. A very important question one is interested is the efficiency of this energy conversion [207,218].

In Section 2.3.2, we have discussed the entropy production: The amount of free energy dissipation which is regarded as being wasted. However, in the case of the Brownian motor with a load, a part of the consumed chemical energy is converted into useful work. The focus of this section, thus, is to discuss the efficiency of such a type of mesoscopic energy utilization. We shall discuss two cases: the time-homogeneous coupled diffusion characterized in terms of Eq. (150) [216] and the one-dimensional time-inhomogeneous Brownian ratchet characterized by Eq. (110) [217].

4.6.1. The efficiency of energy transduction of a Brownian motor with coupled diffusion

For concreteness, we shall again consider the asymmetric potential $V(x) = -V_0(\sin x + 0.25 \sin 2x)$. We have seen in the previous sections that the motion of a Brownian ratchet in such a potential has a net unidirectional bias. Now let us

suppose that the Brownian particle also encounters a resistant force. Intuitively, if the force is not too large, the motion will slow down but will not change the direction. The dynamical equation, and the corresponding FPE, are again described by Eqs. (136) and (139), respectively. We can identify the F term in the equation as the external load.

Applying the same idea in Section 2.3.2, let us consider the Gibbs entropy:

$$S(t) = -k_B T \sum_i \int_0^L p_i(t, x) \ln p_i(t, x) dx \tag{152}$$

where $D^2 = 2k_B T$, where k_B is the Boltzmann constant. For an isothermal Brownian motion in general, the relationship between the entropy production rate (e.p.r), heat dissipation rate (h.d.r.) and the Gibbs entropy can be stated in the following entropy balance equation [49,50]

$$T \cdot \frac{dS(t)}{dt} = e_p - h_d, \tag{153}$$

where e_p is the e.p.r., and h_d is the h.d.r. of the system. In a steady state, the time derivative in Eq. (153) is zero, and the e_p of the system is balanced by the h.d.r.

Carrying out the derivative of $S(t)$ with respect to the time t we have

$$\frac{dS(t)}{dt} = \sum_i k_B T \int_0^L \ln p_i(t, x) \cdot \frac{\partial}{\partial x} J_i(t, x) dx - k_B T \sum_{i,j} \int_0^L p_j(t, x) q_{ji}(x) \ln p_i(t, x) dx. \tag{154}$$

In steady state, the probability density $p_i(t, x)$ and the probability current $J_i(t, x)$ can be replaced by the stationary distribution $\pi_i(x)$ and the current $J_i(x)$, then we have

$$0 = \frac{dS(t)}{dt} = k_B T \sum_i \int_0^L \ln \pi_i(x) \cdot J_i'(x) dx - k_B T \sum_{i,j} \int_0^L \pi_j(x) q_{ji}(x) \ln \pi_i(x) dx. \tag{155}$$

Corresponding to every i in the first term of the equation, we have

$$k_B T \int_0^L \ln \pi_i(x) \cdot J_i'(x) dx = -k_B T \int_0^L \frac{d}{dx} (\ln \pi_i(x)) \cdot J_i(x) dx$$

$$= -\int_0^L [F - V_i'(x)] \cdot J_i(x) dx + \int_0^L \left[F - V_i'(x) - k_B T \cdot \frac{d}{dx} \ln \pi_i(x) \right] \cdot J_i(x) dx. \tag{156}$$

We see that the first term is just the h.d.r on a circle discussed in Section 2, and the second term is the e.p.r arising from the spatial diffusive motion of the particle in state i, denoted as Π_i:

$$\Pi_i = \int_0^L \left[F - V_i'(x) - 2k_B T \cdot \frac{d}{dx} \ln \pi_i(x) \right] \cdot J_i(x) dx. \tag{157}$$

It has three terms, and each has a clear physical interpretation. The first term $\int_0^L F \cdot J_i(x) dx$ describes the energy consumption due to the work done of the motor pulling a load; the second term $\int_0^L 2D_i^{-2}[-V'(x)] \cdot J_i(x) dx$ shows the dissipation of the potential energy during transporting along the trajectory, and the third term $\int_0^L \frac{d}{dx} \ln \pi_i(x) \cdot J_i(x) dx$ is the increment of entropy due to the change in the probability distribution.

Similar to the situation in a Markov chain, the integral in the second term of Eq. (154), in a steady state, can be expressed as:

$$-k_B T \sum_i \sum_j \pi_j(x) q_{ji}(x) \ln \pi_i(x) = k_B T \sum_i \sum_j [\pi_i(x) q_{ij}(x) - \pi_j(x) q_{ji}(x)] \cdot \ln \pi_i(x)$$

$$= \frac{1}{2} k_B T \sum_{i,j} \left[\pi_i(x) q_{ij}(x) - \frac{1}{2} k_B T \pi_j(x) q_{ji}(x) \right] \cdot \ln \frac{\pi_i(x)}{\pi_j(x)}$$

$$= -\frac{1}{2} k_B T \sum_{i \neq j} [\pi_i(x) q_{ij}(x) - \pi_j(x) q_{ji}(x)] \cdot \ln \frac{q_{ij}(x)}{q_{ji}(x)}$$

$$+ \frac{1}{2} \sum_{i \neq j} [\pi_i(x) q_{ij}(x) - \pi_j(x) q_{ji}(x)] \cdot \ln \frac{\pi_i(x) q_{ij}(x)}{\pi_j(x) q_{ji}(x)}, \tag{158}$$

where the first term in the last equality describes the h.d.r of a molecular motor, at position x, when undergoes a chemical transition, while the second term corresponds to the e.p.r of the motor associated with the transition. Let Π_{ij} be the e.p.r. of the motor particle transiting between state i and j, then

$$\Pi_{ij} = \frac{1}{2} k_B T \int_0^L [\pi_i(x) q_{ij}(x) - \pi_j(x) q_{ji}(x)] \ln \frac{\pi_i(x) q_{ij}(x)}{\pi_j(x) q_{ji}(x)} dx. \tag{159}$$

Hence in the steady state, the e.p.r. of the coupled diffusive ratchet is

$$
e_p = \sum_i \Pi_i + \sum_{i \neq j} \Pi_{ij}
$$

$$
= \sum_i \int_0^L \left[F - V_i'(x) - \frac{D_i^2}{2} \cdot \frac{d}{dx} \ln \pi_i(x) \right] \cdot J_i(x) dx
$$

$$
+ \int_0^L \frac{1}{2} k_B T \sum_{i \neq j} [\pi_i(x) q_{ij}(x) - \pi_j(x) q_{ji}(x)] \cdot \ln \frac{\pi_i(x) q_{ij}(x)}{\pi_j(x) q_{ji}(x)} dx. \tag{160}
$$

And the total h.d.r. is

$$
h_d = - \sum_i \int_0^L [F - V_i'(x)] \cdot J_i(x) dx - \frac{1}{2} k_B T \int_0^L \sum_{i \neq j} [\pi_i(x) q_{ij}(x) - \pi_j(x) q_{ji}(x)] \cdot \ln \frac{q_{ij}(x)}{q_{ji}(x)} dx. \tag{161}
$$

As stated in Section 2, the e.p.r e_p is the free energy dissipation in a unit time of a Brownian motor undergoing "uphill" motion against an external load.

During transport, the work done in a unit time by the motor against the load is

$$
W = - \sum_i \int_0^L F \cdot J_i(x) dx. \tag{162}
$$

The rest of the energy is dissipated in the form of entropy production. The total dissipation plus the work done against the outside equals to the total free energy consumption Π (the input power P_{in}), i.e.,

$$
P_{in} = \Pi_{free} = e_p + W. \tag{163}
$$

Eq. (163) is a statement about the conservation of energy: It means that during the unidirectional movements of a molecular motor, the input energy is partly utilized to do useful work against the external load, and the rest is dissipated (i.e., wasted). This equation first appeared in [229] for a chemical model of motor proteins, and more recently, see [216] for a molecular motor which has an internal potential function, and [217] for Brownian ratchet in general. It is important to point out that we have derived the Eq. (163) from the theory of NESS; it is not a supposition based on physical arguments, as had been done in several previous works on motor efficiency.

Now combining the terms (160) and (162) above, we have

$$
e_p + W = \sum_i \int_0^L \sum_j [\pi_j(x) q_{ji}(x) - \pi_i(x) q_{ij}(x)] V_i(x) dx + \frac{1}{2} k_B T \sum_{i \neq j} \int_0^L [\pi_i(x) q_{ij}(x) - \pi_j(x) q_{ji}(x)] \ln \frac{q_{ij}(x)}{q_{ji}(x)} dx. \tag{164}
$$

One sees from Eq. (164) that the total energy supplied to the unidirectional transport by a coupled diffusion ratchet system is only partly from the chemical energy released during the state transition of the enzyme (i.e. the ATPase), represented by the second term in Eq. (164). In addition, though the potential does no work on average, the coupling of the potential and the state transition, which is "driven" externally, also provides energy for the unidirectional motion. The former can be called chemical driving, and the latter, noise-induced force. For molecular motors with internal potential function, the $q_{ij}(x)$ and $V_i(x)$ satisfy the detailed balance condition, then the chemical driving force is the sole energy input [216].

Based on the above discussion, the thermodynamic efficiency of a Brownian motor can thus be expressed as

$$
\eta_{therm} \Delta = \frac{W}{\Pi_{free}} = \frac{W}{e_p + W}. \tag{165}
$$

As the entropy production rate e_p is nonnegative, then for a Brownian motor carrying a load ($W > 0$), we have $0 \leq \eta_{therm} \leq 1$, which means that the consumed energy is partly used to do work and the rest is dissipated. If the motor does not pull a load, then the energy is totally dissipated, which results in a zero efficiency. On the other hand, if the load is equal to the stalling force, then the work done by the motor is also zero. However, the particle is still switching between the different potentials and the e.p.r is nonzero. Hence in this case, the efficiency of the motor is also zero. Therefore, under a suitable amount of load the efficiency reaches a maximum.

We can further unify the notions of Stokes efficiency and thermodynamic efficiency under the same input power:

$$
\eta_{Stokes} \overset{\Delta}{=} \frac{W + \langle \dot{x} \rangle^2}{\Pi_{free}} = \frac{W + \langle \dot{x} \rangle^2}{e_p + W}. \tag{166}
$$
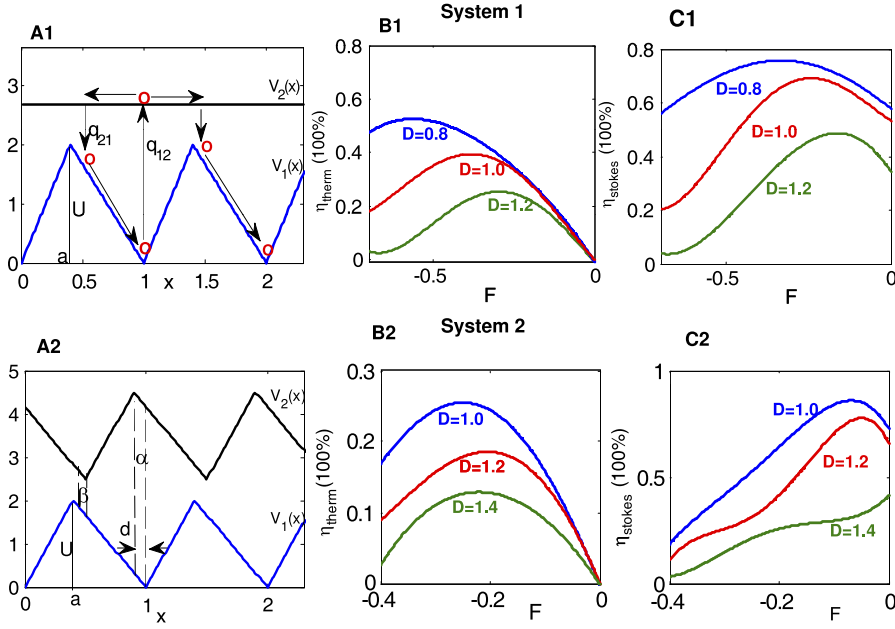
Fig. 35. Computational results from two Brownian ratchets. (A1, A2) show the potential functions used in the computations. (B1, B2) show the thermodynamic efficiency vs. the external load F for different noise intensities. (C1, C2) show the Stokes efficiency vs. the external load F for different noise intensities. (For interpretation of the references to colour in this figure legend, the reader is referred to the web version of this article.)
Source: Reproduced with permission from M. Qian et al., EPL, 84 (2008) 10014.

Without imposing any specific condition on the transition rates and potentials, it is easy to prove that this efficiency measure is bounded by 1. Actually, applying Cauchy–Schwarz inequality and noticing the expression of e_p in Eq. (160), we have

$$
\langle \dot{x} \rangle^2 = \left(\int_0^L \sum_i J_i(x) dx \right)^2 = \left(\int_0^L \sum_i \sqrt{\pi_i(x)} \cdot \frac{J_i(x)}{\sqrt{\pi_i(x)}} dx \right)^2
$$

$$
\leq \int_0^L \sum_i \pi_i(x) dx \cdot \int_0^L \sum_i J_i^2(x)/\pi_i(x) dx
$$

$$
= \int_0^L \sum_i J_i^2(x)/\pi_i(x) dx
$$

$$
\leq e_p
$$

then

$$
\eta_{Stokes} \leq 1.
$$

To illustrate the variation of the efficiency of a motor with increasing load, let us turn to computations. We first consider a simple two-state motor with one periodic and one flat potential in Eq. (136). The potential function is given in Fig. 35A1. We fix the parameters $q_{12} = 3$, $q_{21} = 1$ and $U = 2, a = 0.1, L = 1$. Without any load ($F = 0$), the motor moves to the right. It is shown in Fig. 35B1 and C1 that with the increase of the load F, both η_{therm} and η_{stokes} increase until reaching a maximum, and then decrease with further increasing of the load.

Furthermore, let us consider a two-state motor with two potentials of period $L = 1$ and of equal amplitude U (see Fig. 35A2). Similar to system A in Ref. [218], we suppose that $V_2(x) = V_1(x - \delta) + U_0$, here $\delta = 0.5$, $U_0 = 2.3$. The transition rate of the system obeys $q_{12} = \alpha(x) e^{(V_1 - V_2 + \Delta\mu)/D} + \beta(x) e^{(V_1 - V_2)/D}$, $q_{21} = \alpha(x) + \beta(x)$, where $\alpha(x), \beta(x)$ are the same as in [218].

Employing the e.p.r. formula to calculate the input power, one can see that the curves of η_{therm} vs F for different noise intensities depicted in Fig. 35B2 are similar to those in [218]. Viewing from the Stokes efficiency, we see in Fig. 35C2 that with the increase of external load, η_{stokes} vs F does not always exhibit a bell-shaped curve.

4.6.2. Time-inhomogeneous Brownian ratchet

In the above section, we have discussed the efficiency of a Brownian motion in a time-homogeneous system, moving against an external load. We found that in addition to the chemical driving force in the molecular motor, a system experiencing externally controlled random "flipping" between potential functions also receives an amount of input energy.

This point can be even better studied by considering the system of time-inhomogeneous Brownian ratchet. We shall specifically consider Eq. (121), whose corresponding FPE is

$$\frac{\partial p(t, x)}{\partial t} = -\frac{\partial J(t, x)}{\partial x},$$

(167)

where

$$J(t, x) = (F - V'(x) + A \sin \Omega t) \cdot p(t, x) - \frac{D^2}{2} \frac{\partial p(t, x)}{\partial x}.$$

(168)

The system's Gibbs entropy at time t is

$$S(t) = -\int_0^L p(t, x) \ln p(t, x) dx.$$

(169)

Taking a time-derivative on both sides of the equation, we have

$$\frac{dS(t)}{dt} = -\int_0^L 2D^{-2}[F - V'(x) + A \sin \Omega t] J(t, x) dx$$

$$+ \int_0^L 2D^{-2} \left[F - V'(x) + A \sin \Omega t - \frac{D^2}{2} \cdot \frac{d}{dx} \ln p(t, x) \right]^2 \cdot p(t, x) dx.$$

(170)

Extending the definition of the e.p.r. in steady state to a non-stationary case, we shall call

$$h_d(t) \overset{\triangle}{=} \int_0^L 2D^{-2}[F - V'(x) + A \sin \Omega t] J(t, x) dx$$

(171)

the *instantaneous heat dissipation rate* of system (121) at time t, and

$$e_p(t) \overset{\triangle}{=} \int_0^L 2D^{-2} \left[F - V'(x) + A \sin \Omega t - \frac{D^2}{2} \cdot \frac{d}{dx} (\ln p(t, x)) \right]^2 \cdot p(t, x) dx$$

(172)

the *instantaneous entropy production rate* at time t.

As system (121) is no longer stationary, the e.p.r and the h.d.r. never become constant. Still, we have instantaneous entropy balance equation

$$e_p(t) = \frac{dS(t)}{dt} + h_d(t).$$

(173)

Even though the system does not reach stationarity, one can still define the time-averaged e.p.r as

$$e_p = \lim_{t \to \infty} \frac{1}{t} \int_0^t e_p(s) ds.$$

(174)

For the time-inhomogeneous system with period $T = 2\pi/\omega$, according to Lemma 4.2 in Section 4.3.2, we know that for $\forall s \in [0, T]$, each subprocess $\{x(s + k \cdot T)\}_{k \geq 0}$ asymptotically approaches to a stationary distribution $\nu_s(x) dx$ as time tends to infinite. Here

$$\nu_s(x) dx = \int_0^L \nu_s(y) p(s, s + T; y, x) dy dx.$$

(175)

Eq. (175) shows that $\nu_s(x) dx$ is periodic T-invariant. Hence we can consider a periodic process $\{x(t)\}_{t \geq 0}$ with an initial distribution $\nu_0(x) dx$. Note that the Gibbs entropy $S(t)$ is a bounded function on $[0, +\infty)$ (In fact, we only need to consider the bound of $S(t)$ on interval $[0, T]$). Therefore

$$\lim_{t \to \infty} \frac{1}{t} \int_0^t \frac{dS(t)}{dt} dt = \lim_{t \to \infty} \frac{S(t) - S(0)}{t} = 0.$$

(176)

It follows from Eq. (172), (174) and (176) that for a time-inhomogeneous ratchet:

$$
\begin{aligned}
e_p &= \lim_{t\to\infty} \frac{1}{t} \int_0^t h_d(s)ds \\
&= \lim_{n\to\infty} \frac{1}{nT} \int_0^{nT} h_d(s)ds. \\
&= \lim_{n\to\infty} \frac{1}{nT} \int_0^{nT} dt \int_0^L 2D^{-2}(F - V'(x) + A\sin\Omega t)\cdot J(t,x)dx \\
&= 2D^{-2}\left\{ F\cdot \lim_{n\to\infty} \frac{1}{nT}\int_0^{nT} dt \int_0^L J(t,x)dx - \lim_{n\to\infty}\frac{1}{nT}\int_0^{nT} dt \int_0^L V'(x)J(t,x)dx \right. \\
&\quad \left. + \lim_{n\to\infty}\frac{1}{nT}\int_0^{nT} dt \int_0^L A\sin\Omega t\cdot J(t,x)dx \right\}.
\end{aligned}
\tag{177}
$$

We shall now compute the limits for all above three terms. For the first term, we have

$$
\begin{aligned}
\frac{1}{nT}\int_0^{nT} dt \int_0^L J(t,x)dx &= \frac{1}{nT}\int_0^{nT} dt \int_0^L (F - V'(x) + A\sin\Omega t)p(t,x)dx - \frac{1}{nT}\int_0^{nT} dt \int_0^L \frac{\partial p(t,x)}{\partial x}dx \\
&= \frac{1}{nT}\int_0^{nT} dt \int_0^L (F - V'(x) + A\sin\Omega t)p(t,x)dx \quad (\text{noticing that } p(t,x+L)=p(t,x)) \\
&= \frac{1}{nT}\int_0^{nT} dt \int_0^L (F - V'(x))p(t,x)dx \quad \left(\text{noting } \int_0^L p(t,x)dx = 1, \text{ and } \int_0^{nT} A\sin\omega t dt = 0\right) \\
&= \frac{1}{T}\int_0^T ds \int_0^L (F - V'(x))\cdot \frac{1}{n}\sum_{k=0}^{n-1} p(s+kT,x)dx.
\end{aligned}
$$

Then according to the result in Section 4.3.2, we know that

$$
\lim_{n\to\infty} \frac{1}{T}\int_0^T ds \int_0^L (F-V'(x))\cdot \frac{1}{n}\sum_{k=0}^{n-1} p(s+kT,x)dx = \frac{1}{T}\int_0^T ds \int_0^L (F-V'(x))v_s(x)dx.
$$

It follows from Theorem 4.3 in Section 4.3.2 that

$$
\lim_{n\to\infty} \frac{1}{nT}\int_0^{nT} dt \int_0^L J(t,x)dx = \frac{1}{T}\int_0^T ds \int_0^L (F-V'(x))v_s(x)dx = \langle \dot{x}\rangle.
\tag{178}
$$

For the second term in the last step of Eq. (177), we have

$$
\begin{aligned}
-\frac{1}{nT}\int_0^{nT} dt \int_0^L V'(x)J(t,x)dx &= -\frac{1}{nT}\int_0^{nT} dt \int_0^L J(t,x)dV(x) \\
&= \frac{1}{nT}\int_0^{nT} dt \int_0^L V(x)\cdot \frac{\partial J(t,x)}{\partial x}dx \\
&= -\frac{1}{nT}\int_0^{nT} dt \int_0^L V(x)\cdot \frac{\partial p(t,x)}{\partial t}dx \\
&= -\int_0^L V(x)\left[\frac{1}{nT}\int_0^{nT}\frac{\partial p(t,x)}{\partial t}dt\right]dx \\
&= -\int_0^L V(x)\cdot \frac{p(nT,x)-p(0,x)}{nT}dx.
\end{aligned}
$$

Then

$$
\begin{aligned}
\left|\frac{1}{nT}\int_0^{nT} dt \int_0^L V'(x)J(t,x)dx\right| &\leq \max_{x\in[0,L]}|V(x)|\cdot \frac{1}{nT}\left[\int_0^L p(nT,x)dx + \int_0^L p(0,x)\right] \\
&= \frac{2}{nT}\max_{x\in[0,L]}|V(x)|.
\end{aligned}
$$

Hence

$$
\lim_{n\to\infty} \frac{1}{nT}\int_0^{nT} dt \int_0^L V'(x)J(t,x)dx = 0.
\tag{179}
$$

For the third term in the last step of Eq. (177), we have

$$
\frac{1}{nT}\int_0^{nT}dt\int_0^L A\sin\Omega t\cdot J(t,x)dx = \frac{1}{nT}\int_0^{nT}dt\int_0^L A\sin\Omega t(F-V'(x)+A\sin\Omega t)p(t,x)dx
$$

$$
-\frac{1}{nT}\int_0^{nT}dt A\sin\Omega t\int_0^L \frac{\partial p(t,x)}{\partial x}
$$

$$
= \frac{1}{nT}\int_0^{nT}dt\int_0^L A\sin\Omega t(F-V'(x))p(t,x)dx
$$

$$
+\frac{1}{nT}\int_0^{nT}dt\int_0^L (A\sin\Omega t)^2 p(t,x)dx
$$

$$
= \frac{1}{T}\int_0^T A\sin\Omega s\int_0^L (F-V'(x))\frac{1}{n}\sum_{k=0}^{n-1}p(s+kT,x)dx + \frac{1}{nT}\int_0^{nT}(A\sin\Omega t)^2 dt.
$$

Hence

$$
\lim_{n\to\infty}\frac{1}{nT}\int_0^{nT}dt\int_0^L A\sin\Omega t\cdot J(t,x)dx = \frac{1}{T}\int_0^T A\sin\Omega s ds\int_0^L (F-V'(x))v_s(x)dx + \frac{1}{T}\int_0^T (A\sin(\Omega t))^2 dt. \qquad (180)
$$

Therefore the average e.p.r of the time-inhomogeneous Brownian motor moving against a load is

$$
e_p = 2D^{-2}F\langle\dot x\rangle + 2D^{-2}\left(\frac{1}{T}\int_0^T A\sin\Omega s ds\int_0^L (F-V'(x))v_s(x)dx + \frac{1}{T}\int_0^T (A\sin\Omega t)^2 dt\right), \qquad (181)
$$

in which ζ is the frictional coefficient, $D^2/2 = 1/\zeta$ when $k_BT = 1$. The first two terms are both of the form expressed as a force multiplying a current; while the third term can be regarded as an average power. For $A = 0$, Eq. (181) is just the expression of e_p of time-homogeneous systems mentioned in Eq. (63) in Section 2.4.2.

Therefore the free energy consumption of the time-inhomogeneous Brownian motor is

$$
\Pi = e_p + W
$$

$$
= 2D^{-2}\left[\frac{1}{T}\int_0^T A\sin(\Omega s)ds\int_0^L (F-V'(x))v_s(x)dx + \frac{1}{T}\int_0^T (A\sin\Omega t)^2 dt\right], \qquad (182)
$$

where

$$
W = -2D^{-2}(F\cdot\langle\dot x\rangle). \qquad (183)
$$

Comparing Eqs. (181) and (182), one can see that the coupling of the periodic driving and the asymmetric potential can provide part of the energy for unidirectional transport.

For a time-inhomogeneous Brownian motor, we can still define the efficiency of transport as

$$
\eta = \frac{W}{e_p + W}.
$$

To illustrate the change of the efficiency of a time-inhomogeneous Brownian motor with increasing load, we again give some numerical results. Fig. 36a shows different stationary probability densities corresponding to the processes $\{s+kT\}_{k\geq 0}$ starting from $s\in[0,T]$.

In Fig. 36b, we plot the mean velocity of system (121). The variations of the work done W by the particle and the corresponding efficiency η with the increase of the loaded force F are shown in Fig. 36c and d. One can see similar result to that in the coupled diffusive system (136), i.e., the efficiency reaches a maximum at a suitable load.

5. Conclusions and outlook

In the literature, there are several excellent reviews and books that address the constructive roles of noise in inducing regular oscillations in excitable systems (CR) [132], unidirectional transports in molecular motors (Brownian ratchets) [27] and signal amplifier by the mechanism of stochastic resonance (SR) [26,230]. However, as the review [26] has pointed out, what is still lacking from a physical point of view is a detailed, microscopic (mesoscopic) approach to account for the physical essence of all the noise-induced phenomena. In this report, we have provided a unified theory, i.e. nonequilibrium steady state (NESS), to the phenomena of SR, CR and unidirectional transports.
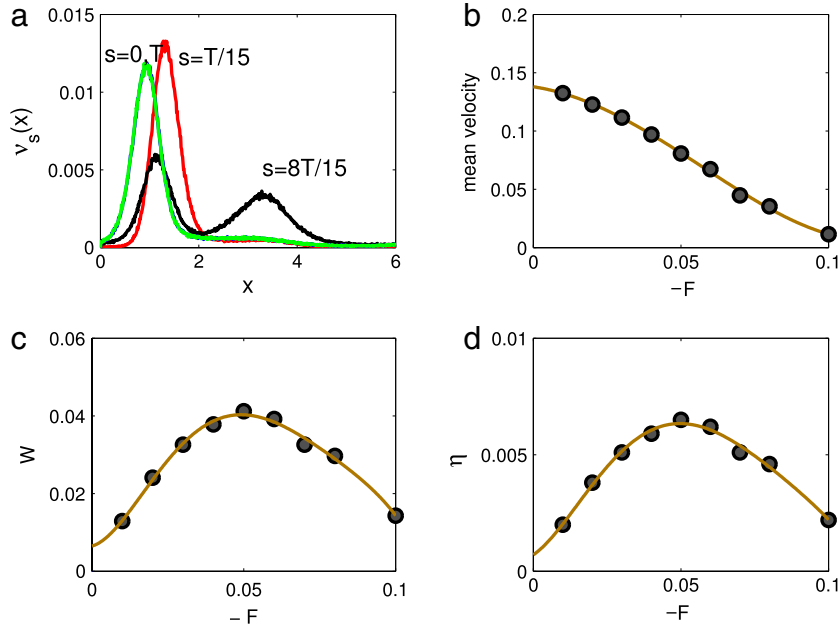
Fig. 36. (a) Stationary probability densities corresponding to the processes $\{x(s+kT)\}_{k \geq 0}$ starting from different values of $s \in [0, T]$. (b) The mean velocity $\langle \dot{x} \rangle$ vs. F. (c) The variations of the work done, W, with the increase of F. (d) The efficiency η vs F for system (121) with the potential given by Eq. (168). Here $V_0 = 1, A = 1.6V_0, \omega = 0.45, D = 0.45, F = -0.07$ for (a). (For interpretation of the references to colour in this figure legend, the reader is referred to the web version of this article.)

For the benefit of our readers, we have presented the mathematical theory of NESS within the framework of stationary Markov processes and continuous diffusion processes on a circle. We ask the readers to bear in mind several key notions which are crucial for understanding the nonequilibrium characteristics of the three phenomena discussed in this report:

(i) The underlying stochastic process is *time irreversible*;

(ii) There are an emergence of *unbalanced circulation* (NBC) due to the break-down of the detailed balance;

(iii) The power spectrum is non-Lorentzian;

(iv) There is a positive entropy production rate.

Unified under the theory of NESS, we have shown that the occurrence of CR in the typical excitable systems such as Adler's phase model, the integrate-and-fire (IF) model and the FitzHugh–Nagumo (FNH) model, is due to the existence of NBC. In the phase model and the IF model, the NBC is characterized by a noise-induced rotation around the circle which also implies a positive e.p.r; in the FHN model, it is represented by the appearance of a stochastic stable limit cycle (SSLC). Interestingly, the concept of SSLC can be clearly quantified by the regularity factor of noise-sustained oscillations (or the quality factor of the power spectrum) which represents a highly localized NBC. Of particular interest is the CR in a single stochastic Hodgkin–Huxley (HH) type neuron with intrinsic channel noise in a membrane patch with finite-size. After a detailed analysis using Gillespie algorithm, we have learned that a single neuron can effectively couple the mesoscopic kinetics of individual channels, with randomly opening and closing of the channel gates, and the macroscopic dynamics of the cell membrane potential, with depolarization and repolarization, to generate spontaneous firings, i.e., CR without any external injected current. We have illustrated in Section 3.2.5 again this is due to the emergence of NBC. This time the NBC is caused by the coupling of passive channel fluctuation with active dynamics of membrane potential. We expected this type of mesoscopic-macroscopic coupled systems, together with the application of NESS theory, will find further applications in biological systems.

Traditionally, SR and CR are usually treated as two different phenomena because the former requires the interplay of noise and a weak external periodic signal while the later does not. However, as we have shown, these two phenomena in fact have the same origin, if one treats the periodically driven SR model as an autonomous system using an embedding-based description. In terms of this embedding method, SR in a classical bistable periodically driven model, which was traditionally explained in the subthreshold regime as the matching of periodically rocking of the two-well potential and the noise-induced hopping between the two potential wells, can now be interpreted from a new perspective. In fact, the two potential wells in the original model, in the subthreshold regime, is equivalent to the two stable limit cycles on the cylinder. Thus the dynamical mechanism of SR can now be explained due to the coherent switching between the two stable limit cycles. Such an embedding method can also quantitatively show that it is the relative position of the stable limit cycle (SLC) to the unstable limit cycle (ULC) as well as the amplitude of the SLC itself that determine the effect of SR. Furthermore, using dynamical theory, the whole parameter regime of (A, ω), the amplitude and the frequency of driving force, can be classified into two regime: One is shown to have two SLCs and therefore is possible for SR to occur, and the other is shown to have

only one SLC and no SR can appear. SR is found to be most significant near the bifurcation curve in the subthreshold regime. It is therefore not surprising to find that SR occurs in the superthreshold regime which had been considered impossible.

Regarding the Brownian ratchet, the same embedding method is also shown to be useful in clarifying the mechanism of unidirectional transport of a Brownian particle in a spatially periodic potential driven by a periodic force in the presence of Gaussian white noise. We have shown the existence of a sequence of SLCs and ULCs of the equivalent dynamical systems on a cylinder, and furthermore elucidated that it is the relative position of the SLC to its two neighboring ULCs, which reflects the break-down of the symmetry, that determines the direction of transport as well as its velocity. In this problem, the NESS theory presented in Section 2 has also found its promising role in clarifying the efficiency of energy transduction by the Brownian motors. We have rigorously shown that the thermodynamic efficiency of a Brownian motor can be explicitly expressed as the work done by the motor over the sum of entropy production rate and the work.

Applying the mathematical theory of NESS to the noise induced phenomena discussed in this report is mainly based on the stochastic theory of Markov processes and diffusion processes on a circle (or cylinder). It should be noted that there are several physical assumptions hidden behind a Markov dynamics for mesoscopic systems such as the separation in time scales between the degrees of freedom associated with a state and those associated with the state transitions, leading to a rapid equilibration of the fast degrees of freedom. For non-Markovian behaviors that sometime observed in condensed phase kinetics, further discussions are required.

Acknowledgments

Appendix A. Mathematical theory of Markov processes

In order to use a Markov process as the mathematical representation for a mesoscopic system in either equilibrium or nonequilibrium states, we give an introductory account of the mathematical theory of Markov processes. We shall only state the key results without giving proofs. Readers who are interested in the full account of the theory are referred to several texts on stochastic processes [231,232].

A.1. Markov chain with discrete time parameter and discrete states

Before discussing a Markov chain with continuous time, we shall first discuss briefly a Markov chain with discrete time. Discrete time is easier to work with, and almost all results on the latter can be translated into the former.

Definition A.1. Suppose that $\{X_n(\omega)\}_{n \in \mathbb{Z}}$ is a stochastic process. It takes values in a finite or denumerable set E. If for $\forall i, j, i_0, i_1, \ldots, i_{n-1} \in E$, we have

$$\Pr\{X_{n+1} = j | X_n = i, X_{n-1} = i_{n-1}, \ldots, X_1 = i_1, X_0 = i_0\} = P\{X_{n+1} = j | X_n = i\}, \tag{A.1}$$

then $\{X_n\}_{n \in \mathbb{Z}}$ is called a Markov chain with the state space E. Furthermore, if $\Pr\{X_{n+1} = j | X_n = i\} = \Pr\{X_1 = j | X_0 = i\}$, then the Markov chain is said to be time-homogeneous.

Eq. (A.1) shows that knowing the state of the system at time n, the probability that the process in state j at time $n + 1$ is independent of the states before time n (memoryless before time n).

For simplicity, we shall assume in the following that the state space of a Markov chain is $E = \{1, 2, \ldots, N\}$, and the process is time-homogeneous.

We call $p_{ij} \stackrel{\Delta}{=} \Pr(X_1 = j | X_0 = i)$ the one-step transition probability of the Markov chain $\{X_n\}_{n \in \mathbb{Z}}$ if it satisfies:

$$p_{ij} \geq 0, \forall i, j \in E; \quad \sum_{j=1}^{N} p_{ij} = 1, \quad \forall i \in E. \tag{A.2}$$

Denote $P \stackrel{\Delta}{=} (p_{ij})$, which is called the one-step transition probability matrix of $\{X_n\}_{n \in \mathbb{Z}}$.

The statistical properties of a Markov chain are determined by its initial distribution $\pi_i \stackrel{\Delta}{=} \Pr\{X_0 = i\}$ and the one-step transition probability matrix $P = (p_{ij})$:

$$\Pr\{X_0 = i_0, X_1 = i_1, \ldots, X_n = i_n\} = \pi_{i_0} p_{i_0 i_1} p_{i_1 i_2} \cdots p_{i_{n-1} i_n}. \tag{A.3}$$

We call $p_{ij}(n) \stackrel{\Delta}{=} \Pr\{X_{m+n} = j | X_m = i\}$ the n-step transition probability of the Markov chain $\{X_n\}_{n \in \mathbb{Z}}$, and $P^n \stackrel{\Delta}{=} (p_{ij}(n))$ is correspondingly called the n-step transition probability matrix. It is not difficult to show that P^n is in fact the nth power of P. Hence we have

Theorem A.2 (*Kolmogorov–Chapman Equation*)**.** *The transition probability matrix P^n satisfies*

$$p_{ij}(m + n) = \sum_k p_{ik}(m)p_{kj}(n). \tag{A.4}$$

i.e.,

$$P^{m+n} = P^n \cdot P^m = P^m \cdot P^n. \quad \square \tag{A.5}$$

Starting from state *i*, if a system has a positive probability reaching state *j*, i.e., $\exists n \geq 1$, s.t. $p_{ij}(n) > 0$, then we call state *j* is reachable from *i*. If *j* is reachable from *i* and *i* is reachable from *j*, then states *i* and *j* are said to be communicative. If starting from *i* the system returns to this state in a finite time with probability 1, i.e.,

$$\Pr \left\{ \bigcup_{n=1}^{n=\infty} \{X_n = i\} \Big| X_0 = i \right\} = 1,$$

then state *i* is said to be *recurrent*.

If any two states of a Markov chain are communicative, then the process is said to be *irreducible*. Obviously, if one state of an irreducible Markov chain is recurrent, then all the states are recurrent.

Theorem A.3 (*The Weak Ergodic Theorem of Markov Chains*)**.** *Let $\{X_n\}_{n\in\mathbb{Z}}$ be a finite-state Markov chain with transition probability matrix P, then the following limit*

$$\lim_{n\to\infty} \frac{1}{n} \sum_{k=0}^{n-1} P^k = L(L = (L_{ij})) \tag{A.6}$$

exists, and $LP = PL = L^2 = L$. $\quad \square$

$1/L_{ij}$ can be understood as the average time of the system starting from state *i* and then coming back to this state. If $L_{ii} > 0$, then state *i* is said to be *positive recurrent*. If $L_{ii} = 0$, then we call state *i zero recurrent*, which means that the average time of the system returning to *i* is infinitely long.

Definition A.4 (*Invariant Distribution*)**.** If there is a vector $\vec{\pi} = (\pi_1, \ldots, \pi_N)$ with $\pi_i \geq 0$ and $\sum_i \pi_i = 1$, such that

$$\vec{\pi}P = \vec{\pi}, \tag{A.7}$$

i.e.,

$$\sum_{i=1}^N \pi_i p_{ij} = \pi_j, \quad \forall j \in E,$$

then $\vec{\pi}$ is called an invariant probability distribution of *P*, or an invariant distribution of the Markov process.

Theorem A.5. *Suppose that a Markov chain $\{X_n\}_{n\geq 0}$ with N states is irreducible, then*
   (1) *it has a unique invariant distribution $\vec{\pi} = (\pi_1, \ldots, \pi_N)$, in which all π_i's are positive.*
   (2) $L = (1, 1, \ldots, 1)^\top (\pi_1, \ldots, \pi_N)$, *which yields that $L_{ii} > 0$, for $\forall i \in E$, i.e., all states are positive recurrent.* $\quad \square$

If a mesoscopic system only changes its states at time $t = 1, 2, \ldots, k, \ldots$, then the evolution of the system with time can be described by a Markov chain $\{\zeta_n(\omega)\}_{n\in\mathbb{Z}}$ with discrete time parameter and discrete states. However, time in a real physical system usually is continuous, hence it is necessary to further discuss Markov processes $\{\xi_t(\omega)\}_{t\in R}$ with continuous time parameter.

A.2. Finite-state Markov chain with continuous time parameter (Q-process)

Let $p_i(t) \overset{\Delta}{=} \Pr\{\xi_t = i\}$ be the probability of a system (say a single enzyme molecule) in state *i* at time *t*, and q_{ij} be the transition probability rate of the particle transiting from state *i* to *j*, then the time evolution of the distribution of a mesoscopic system in state *i* can be described by the following master equation:

$$\frac{dp_i(t)}{dt} = \sum_{j\neq i} \left(-q_{ij}p_i(t) + q_{ji}p_j(t) \right) \overset{\Delta}{=} \sum_{all\ j} q_{ji}p_j(t). \tag{A.8}$$

Let $p_{ij}(t) \overset{\Delta}{=} \Pr\{\xi_t = j|\xi_0 = i\}$. Since $p_{ij}(t) \geq 0$, and $\sum_j p_{ij}(t) = 1$, then

$$q_{ij} = \lim_{t\to 0} \frac{p_{ij}(t)}{t}, \quad i \neq j; \qquad q_i = \lim_{t\to 0} \frac{1 - p_{ii}(t)}{t}, \qquad q_{ii} \overset{\Delta}{=} -q_i.$$

Furthermore, q_{ij} satisfies

(1) $q_{ij} \geq 0, \forall i \neq j; q_{ii} \leq 0$;
(2) $\sum_{j \neq i} q_{ij} = q_i \ (q_i = -q_{ii})$.

Let $P(t) \triangleq (p_1(t), \ldots, p_N(t))$, and $\mathbf{Q} \triangleq \{q_{ij}\}$. We call the matrix Q a Q-matrix and the corresponding stochastic process $\{\xi_t(\omega)\}_{t \in R}$ a Q-process, which is a Markov process with continuous time parameter and discrete states. Equivalently, the master equation (A.8) can be rewritten be as

$$\frac{dP(t)}{dt} = P(t)\mathbf{Q}. \tag{A.9}$$

The trajectory $\{\xi_t(\omega)\}_{t \in R}$ that describes the motion of the system is a function with steps of jumping. For simplicity, we always suppose that it is right continuous, i.e., $\Pr\{\omega; \lim_{t \downarrow t_0} \xi_t(\omega) = \xi_{t_0}(\omega)\} = 1$. Let $\tau = \inf\{t > 0; \xi_t(\omega) \neq \xi_{t_0}(\omega)\}$, which means that conditioning on $\xi_{t_0} = i, \tau$ is the first time that the process jumps out of state i. It is a random variable. Concerning the statistical laws of the transition behavior of the particle, we have the following theorem:

Theorem A.6. *Suppose that a Q-process $\{\xi_t\}_{t \in R}$ is right continuous and $0 < q_i < +\infty$, then*

(1) $\Pr\{\tau \geq t | \xi_0 = i\} = e^{-q_i t}$;
(2) $\Pr\{\xi_\tau = j, \tau \leq s | \xi_0 = i\} = (1 - e^{-sq_i}) \frac{q_{ij}}{q_i} \ (j \neq i, q_i \neq 0)$;
(3) $\Pr\{\xi_\tau = j | \xi_0 = i\} = \frac{q_{ij}}{q_i} \ (j \neq i, q_i \neq 0)$. $\quad \square$

Conclusion (1) reveals that the sojourn time of a mesoscopic particle (i.e., a molecule) residing in state i obeys an exponential distribution. It is easy to calculate that the mean sojourn time of the particle in state i is $1/q_i$. Conclusion (3) states that the probability of the particle transiting from state i to j is q_{ij}/q_i. Based on (1) and (3), Conclusion (2) says that ξ_τ and τ are two conditionally independent random variables under the condition $\xi_0 = i$. These facts are the bases for a computer simulation of a Q-process, known as Gillespie algorithm [178,179].

Definition A.7 (*Communicativity*). A Q-process with finite states is said to be communicative, if

$$\forall i \neq j, \exists i_1, i_2, \ldots, i_s, s.t. \quad q_{ii_1} q_{i_1 i_2} q_{i_2 i_3} \cdots q_{i_{s-1} i_s} q_{i_s j} \neq 0. \tag{A.10}$$

Definition A.8 (*Stationarity*). A Markov chain $\{\xi_t\}_{t \geq 0}$ is said to be stationary, if for $\forall 0 \leq t_1 < t_2 < \cdots < t_k$, and $\forall h > 0$, $(\xi_{t_1}, \xi_{t_2}, \ldots, \xi_{t_k})$ and $(\xi_{t_1+h}, \xi_{t_2+h}, \ldots, \xi_{t_k+h})$ have the same distribution.

The stationarity of a stochastic process means that the statistical properties of the process are invariant with the shift of time.

Proposition A.9. *A Q-process $\{\xi_t\}_{t \geq 0}$ is stationary if and only if its initial distribution $\vec{\pi} = (\pi_1, \ldots, \pi_N)$ is an invariant distribution, i.e, $\vec{\pi}\mathbf{Q} = 0$.* $\quad \square$

Definition A.10 (*Detailed balance*). A stationary Q-process $\{\xi_t\}_{t \in R}$ is said to be in detailed balance, if

$$\pi_i q_{ij} = \pi_j q_{ji}, \quad \forall i \neq j, \tag{A.11}$$

where $\vec{\pi} = (\pi_1, \ldots, \pi_N)$ is the invariant distribution.

Observing a stochastic process is actually viewing the probability characteristics of the process along the time-increasing direction; while its reverse process refers to observing this trajectory along the time-decreasing direction. A natural idea to define a reverse process is to reflect the original process about the zero point in time axis. Denote

$$\xi_t^-(\omega) := \xi_{-t}(\omega), \quad \forall t > 0.$$

We call $\xi^- = \{\xi_t^-(\omega)\}_{t \in R}$ the *reverse process* corresponding to the stationary Q-process $\xi = \{\xi_t(\omega)\}_{t \in R}$.

Obviously, $\{\xi_t^-(\omega)\}_{t \in R}$ is also a Q-process defined on $(\Omega, \mathcal{F}, P)$, with stationary distribution $\tilde{\pi}_i = \Pr\{\xi_t^- = i\} = \pi_i$. Let $\tilde{\mathbf{Q}} = (\tilde{q}_{ij})$ be the corresponding Q-matrix. Suppose that $t_1 < t_2$, i.e. $-t_2 < -t_1$. Since

$$\Pr\{\xi_{t_1}^- = i, \xi_{t_2}^- = j\} = \Pr\{\xi_{-t_1} = i, \xi_{-t_2} = j\} = \Pr\{\xi_{-t_2} = j, \xi_{-t_1} = i\},$$

then

$$\pi_i \tilde{q}_{ij} = \pi_j q_{ji}.$$

Thus the transition probability rate of the reverse process ξ^- is

$$\tilde{q}_{ij} = \frac{\pi_j q_{ji}}{\pi_i}. \tag{A.12}$$

$\tilde{q}_{ij}$ still satisfies the conclusions in Theorem A.6, and $\vec{\pi}\tilde{\mathbf{Q}} = 0$ holds true.

Definition A.11 (*Reversibility*). A Q-process $\{\xi_t(\omega)\}_{t\in R}$ is said to be reversible, if it is stationary and for any $t_1 \le t_2 \le \cdots \le t_k$, $(\xi_{t_1}, \xi_{t_2}, \ldots, \xi_{t_k})$ and $(\xi_{-t_1}, \xi_{-t_2}, \ldots, \xi_{-t_k})$ have the same distribution.

The time reversibility, or simply reversibility, of a stochastic process means that the statistical law of the process is invariant under the reverse of time. Let P^+ and P^- be the probability measures of a stochastic process $\{\xi_t(\omega)\}_{t\in R}$ along the time-increasing and decreasing directions, respectively, then

$$P^- \left(\xi_{t_1} = i_1, \xi_{t_2} = i_2, \ldots, \xi_{t_k} = i_k \right) = P^+ \left(\xi_{t_1}^- = i_1, \xi_{t_2}^- = i_2, \ldots, \xi_{t_k}^- = i_k \right).$$

Proposition A.12. *A stochastic process $\{\xi_t(\omega)\}_{t\in R}$ is reversible if and only if $\forall t > 0$,*

$$P_{[0,t]}^+(\omega) = P_{[0,t]}^-(\omega).$$

This holds true if and only if $\pi_i q_{ij} = \pi_j q_{ji}$, or $\tilde{q}_{ij} = q_{ij}$.   □

A.3. Embedded Markov chain of a Q-process.

Suppose that a Q-process $\{\xi_t(\omega)\}_{t\in R}$ is right continuous. Let

$$t_0(\omega) = 0,$$
$$t_{k+1}(\omega) = \inf\{t > t_k(\omega); \xi_t(\omega) \ne \xi_{t_k}(\omega)\}, \quad k = 0, 1, 2, \ldots$$

and

$$\tau_k(\omega) = t_{k+1}(\omega) - t_k(\omega), \quad k = 0, 1, 2, \ldots$$

then $t_k(\omega)$ is the kth jumping time of ω during time interval $[0, \infty)$, $\tau_k(\omega)$ is the sojourn time of the trajectory in state $\xi_{t_{k-1}}$, they are both random variables. Let

$$\zeta_k(\omega) = \xi_{t_k}(\omega),$$

then $\{\zeta_n(\omega)\}_{n\in\mathbb{Z}}$ is a Markov chain with discrete time parameter and finite states. It has the same state space as that of ξ, and the transition situation of ζ at time $n = 1, 2, \ldots, k, \ldots$ is the same as that of the process ξ at time $t_k(\omega)$, $k = 1, 2, \ldots$. We call $\{\zeta_n(\omega)\}_{n\in\mathbb{Z}}$ an embedded Markov chain of a Q-process $\{\xi_t(\omega)\}_{t\in R}$. It can be seen from Theorem A.6 that the transition probability rate of $\{\zeta_n(\omega)\}_{n\in\mathbb{Z}}$ transferring from state i to j is q_{ij}/q_i. Hence we have

Proposition A.13. *The embedded Markov chain $\{\zeta_n(\omega)\}_{n\in\mathbb{Z}}$ has an invariant distribution $(\widehat{\pi}_1, \ldots, \widehat{\pi}_N): \widehat{\pi}_i = \pi_i q_i / \sum_i \pi_i q_i$, and the transition probability rate of $\{\zeta_n(\omega)\}_{n\in\mathbb{Z}}$ is*

$$\widehat{p}_{ij} = \begin{cases} \dfrac{q_{ij}}{q_i}, & i \ne j; \\ 0, & i = j \end{cases} \tag{A.13}$$

where $(\pi_1, \pi_2, \ldots, \pi_N)$ is the invariant distribution of the Q-process $\{\xi_t(\omega)\}_{t\in R}$.   □

Suppose that the probability space of the Q-process $\{\xi_t(\omega)\}_{t\in R}$ is $(\Omega, \mathcal{F}, P)$, then the embedded Markov chain $\{\zeta_n(\omega)\}_{n\in\mathbb{Z}}$ can be considered as being defined on a subspace $(\widehat{\Omega}, \widehat{\mathcal{F}}, \widehat{P})$ of the space $(\Omega, \mathcal{F}, P)$, here

$$\widehat{\Omega} = \{\omega = \{\omega_n\}_{n\in\mathbb{Z}} : \omega_n \text{ takes values in } \{1, 2, \ldots, N\}\}.$$

The sample path $\omega \in \widehat{\Omega}$ can also be extended to a step-function of $t \in R$, hence $\widehat{\Omega} \subset \Omega$, every trajectory $\omega \in \Omega$ can be sorted as a sequence $(\zeta_1, \zeta_2, \ldots, \zeta_n, \ldots)$ in $\widehat{\Omega}$ according to the observed value of the trajectory at the jumping time. Therefore, we can define a map Θ

$$\Theta : \Omega \longrightarrow \widehat{\Omega},$$
$$\omega \in \Omega \mapsto (\zeta_1, \zeta_2, \ldots, \zeta_n, \ldots) \in \widehat{\Omega}$$

and a probability measure P on $\widehat{\mathcal{F}} :\stackrel{\triangle}{=} \Theta(\mathcal{F})$ by

$$\widehat{P} = P \circ \Theta^{-1}.$$

Appendix B. Background materials on stochastic differential equations

In many applications, one has to deal with a stochastic process with continuous time and continuous states. Usually, such a process is described by a stochastic differential equation (SDE). For simplicity, we consider the following one-dimensional SDE equation:

$$\dot{x}(t) = b(x) + \sigma(x)\xi(t), \tag{B.1}$$

in which $\xi(t)$ is a Gaussian white noise satisfying $\langle \xi(t) \rangle = 0$, $\langle \xi(t)\xi(t') \rangle = \delta(t - t')$, where "$\langle \cdots \rangle$" stands for the expectation. Actually, the white noise is the formal derivative of a Brownian motion $B(t)$ with respect to t, i.e., $\xi(t) = dB(t)/dt$.

B.1. Brownian motion

Since the celebrated work of Einstein in 1905 [233,234][11] and followed by contributions from physicists M. von Smoluchowski, P. Langevin, G.E. Uhlenbeck, L.S. Ornstein [235], and mathematicians N. Wiener, P. Levy, J. Doob and many others, the theory of Brownian motion has become one of the well-established areas of mathematics with wide applications [236,67,237]. There is a large literature, inside and outside mathematics, on Brownian motions and diffusion processes [238]. Here we only present some necessary materials related to stochastic differential equation (B.1). To be consistent with the symbols in probability theory, here we use $E[\cdots]$ to denote the expectation instead of the $\langle \cdots \rangle$.

Definition B.1 (*[237]*)**.** Suppose that there is a free particle moving randomly on a line. The position of the particle at time t is denoted as $B(t, \omega)$. We call the process $\mathbf{B} \triangleq \{B(t, \omega)\}_{t \geq 0}$ a Brownian motion, if it satisfies the following conditions:

(1) The displacements $B(t_i, \omega) - B(s_i, \omega)$ for any finite nonintersect time intervals $(s_i, t_i](t_i > s_i)$ are independent. Here for convenience, we set $B(0) = 0$.

(2) The increment $B(t, \omega) - B(s, \omega)$ $(t > s)$ obeys a normal distribution $N(0, t - s)$ with zero means and variance $t - s$.

(3) For almost all trajectories ω, $B(t, \omega)$ is a continuous function of t.

From (2), one knows that $E[B(t, \omega)] = 0$, and $E[|B(t, \omega) - B(s, \omega)|^2] = |t - s|$. This manifests that the statistical law of a Brownian motion is spatially symmetric, and the mean displacement over $t - s$ time is of order $\sqrt{t - s}$, which suggests that a Brownian motion is non-differentiable with respect to time. In fact, the path characteristics of a Brownian motion can be rigorously characterized in terms of the following two results.

Lemma B.2. *Let $\{B(t, \omega)\}_{t \geq 0}$ be a Brownian motion, then for any fixed time $t \geq 0$ and any time increment $h > 0$, we have*

$$P\left\{\omega; \limsup_{h \to 0^+} \frac{B(t + h, \omega) - B(t, \omega)}{h} = +\infty\right\} = 1,$$

$$P\left\{\omega; \liminf_{h \to 0^+} \frac{B(t + h, \omega) - B(t, \omega)}{h} = -\infty\right\} = 1.$$

The lemma informs us that almost all trajectories of a Brownian motion $B(t)$ have no finite derivative at any time t.

Theorem B.3. *For almost every trajectory ω of a Brownian motion $\{B(t, \omega)\}_{t \geq 0}$, $B(t, \omega)$ is continuous but has no derivative at any fixed time t.*

The term $\xi(t)$ $(= dB(t)/dt)$ in Eq. (B.1) actually makes no sense from a mathematical point of view.

Condition (1) in Definition B.1 indicates that a Brownian motion is a stochastic process with mutually independent increments, hence it is a Markov process. Combining with condition (2), its transition probability can be expressed as

$$p(t; x, y) = \frac{1}{\sqrt{2\pi t}} e^{-\frac{(y-x)^2}{2t}} \tag{B.2}$$

and since $B(0) = 0$, then the distribution density of $\{B(t, \omega)\}_{t \geq 0}$ at time t is

$$p(t, x) = \frac{1}{\sqrt{2\pi t}} e^{-\frac{x^2}{2t}}.$$

One can further deduce from conditions (1) and (2) that any finite-dimensional joint distribution of a Brownian obeys n-dimensional normal distribution. Actually, for any $0 < t_0 < t_1 < \cdots < t_{n-1} < t_n$, it follows from the independence of the increments $B(t_1), B(t_2) - B(t_1), \ldots, B(t_n) - B(t_{n-1})$ that the joint distribution of $B(t_1, \omega), \ldots, B(t_n, \omega)$ is

$$f(t_1, \ldots, t_n; u_1, u_2, \ldots, u_n) = p(t_1, u_1)p(t_2 - t_1, u_2 - u_1) \cdots p(t_n - t_{n-1}, u_n - u_{n-1}).$$

Hence the finite-dimensional distribution of a Brownian motion is

$$P(\omega : B(t_1, \omega) \leq x_1, \ldots, B(t_n, \omega) \leq x_n) = \int_{-\infty}^{x_1} \cdots \int_{-\infty}^{x_n} f(t_1, \ldots, t_n; u_1, u_2, \ldots, u_n)du_1 \cdots du_n$$

$$= \int_{-\infty}^{x_1} \cdots \int_{-\infty}^{x_n} \frac{\exp\left\{-\left(\frac{u_1^2}{2t_1} + \frac{(u_2-u_1)^2}{2(t_2-t_1)} + \cdots + \frac{(u_n-u_{n-1})^2}{2(t_n-t_{n-1})}\right)\right\}}{(2\pi)^{\frac{n}{2}} \sqrt{t_1(t_2 - t_1) \cdots (t_n - t_{n-1})}} du_1 \cdots du_n. \tag{B.3}$$

---

[11] It is now known that the essential idea had been independently developed in Louis Bachelier's Ph.D. thesis "The theory of speculation" in 1900, under the direction of Poincaré.

Definition B.4. For a stochastic process $\{\xi(t, \omega)\}_{t \geq 0}$, if for any $0 < t_1 < t_2 < \cdots < t_n$, the joint distribution of $(\xi_{t_1}, \xi_{t_2}, \ldots, \xi_{t_n})$ obeys a n-dimensional normal distribution, then the process $\{\xi(t, \omega)\}_{t \geq 0}$ is called a Gaussian process.

It follows from Eq. (B.3) that a Brownian motion is a Gaussian process.
Furthermore, we have the following equivalent definition of a Brownian motion (the proof is omitted).

Definition B.4′. A stochastic process $\{B(t, \omega)\}_{t \geq 0}$ with $B(0) = 0$ is called a Brownian motion, if $\{B(t, \omega)\}_{t \geq 0}$ is a Gaussian process with continuous trajectories, and for $\forall s, t > 0$, we have $E[B(t, \omega)] = 0$, $E[B(s)B(t)] = t \wedge s$ (the minimum of t and s).

B.2. Itô and Stratonovich integrals of a stochastic differential equation (SDE)

Since a Brownian motion $\{B(t, \omega)\}_{t \in R}$ has no finite derivative at any time t, Eq. (B.1) is only a formal expression of a noise perturbed system. Rigorously, it should be expressed as the following SDE

$$dx(t) = b(x)dt + \sigma(x)dB(t, \omega), \tag{B.4}$$

or equivalently, an integral equation

$$x(t) - x(0) = \int_0^t b(x(s))ds + \int_0^t \sigma(x(s))dB(s). \tag{B.5}$$

It is worth mentioning that the solution $\{x(t)\}_{t \geq 0}$ to Eq. (B.4) is a Markov process on the Wiener space $(\Omega, \mathcal{F}, \mu)$, where Ω is the space of elementary events with probability measure μ on a σ-algebra $\mathcal{F}$ of sets $A \subseteq \Omega$. So actually, $x(t)$ should be written as $x(t, \omega)$, where the randomness of the trajectory is inherited in $\omega \in \Omega$. In the following, we sometimes write $x(t)$ as $x(t, \omega)$ to emphasize this fact, but often write $x(t)$ for convenience.

We note that for a given sample path ω, $x(s, \omega)$ is a continuous function of s, so the term $\int_0^t b(x(s))ds$ can be considered as a normal integral, but the value of the integral is a random function. But how to deal with the integral $\int_0^t \sigma(x(s))dB(s)$? As a Brownian motion, $\{B(t)\}_{t \geq 0}$ has no derivative with respect to t, nor does it have a finite variance, so we cannot regard this term as a Riemann or a Lebesgue–Stieltjes integral. For this reason, we need to introduce a new method of integration. This was developed by Itô as follows, known as Itô stochastic integral.

Following the same spirit in defining a Riemann integral, we divide the time interval $[a, b]$ into n subintervals:

$$a = t_0 \leq t_1 \leq \cdots \leq t_n = b.$$

Let

$$\triangle_n = \max_{1 \leq i \leq n} (t_{i+1} - t_i)$$

be the maximal length of the subintervals, and

$$S_n(\omega) = \sum_{i=1}^n \sigma(x(t_i, \omega)) (B(t_{i+1}, \omega) - B(t_i, \omega)) \tag{B.6}$$

be the summation associated with the given partition.

If for every ω, the limit of $S_n(\omega)$ exists as $\triangle_n \to 0$, then naturally, we can define such a limit as the integral of $\sigma(x(t, \omega))$ with respect to $\mathbf{B} = \{B(t, \omega)\}_{t \geq 0}$. However, because $\{B(t, \omega)\}_{t \geq 0}$ has no finite variance, in general we cannot be sure that a limit exists for the sequence $\{S_n(\omega)\}_{n \geq 0}$ with every ω. As a matter of fact, for most of the trajectories ω, $\{S_n(\omega)\}_{n \geq 0}$ may not have a limit. Because of this, let us consider an alternative limit in a different sense.

Definition B.5. If a limit $S(\omega)$ exists for the sequence $\{S_n(\omega)\}_{n \geq 0}$ defined by (B.6) in the mean-square sense as $n \to \infty$, i.e.,

$$\lim_{n \to \infty} E\left[|S_n(\omega) - S(\omega)|^2 \right] = 0, \tag{B.7}$$

then $S(\omega)$ is called an Itô stochastic integral of the function $\sigma(x)$ with respect to a Brownian motion $\mathbf{B}$ in time interval $[a, b]$, denoted as

$$S(\omega) = \int_a^b \sigma(x(s))dB(s) = \ell.i.m._{t \to \infty} S_n(\omega). \quad (\text{Itô}) \tag{B.8}$$

Here $\ell.i.m.$ means "limit in mean square", i.e., Eq. (B.7).

Remark 1. According to the relationship between the convergences in mean-square sense and in probability measure, one knows that if formula (B.7) holds true, then $\forall \varepsilon > 0$,

$$\lim_{n \to \infty} \Pr\{\omega : |S_n(\omega) - S(\omega)| \geq \varepsilon\} = 0, \tag{B.9}$$

(B.9) means that the probability of the set formed by those ω whose $S_n(\omega)$ and $S(\omega)$ are not sufficiently close is small when n is large. Considering every ω as an trajectory, then (B.9) means that the probability of those trajectories whose $S_n(\omega)$ does not approach to $S(\omega)$ could be as small as possible.

Remark 2. In the definition of Itô integral, we take $\sigma(x(t_i))$, which is the value of $\sigma(x(t))$ at the left point of the interval $[t_i, t_{i+1})$, as an approximation of σ on $[t_i, t_{i+1})$. It should be kept in mind that one can no longer take the value of σ at any point in the interval as an approximation. Actually, if we take the value of σ at the middle point of the interval $[t_i, t_{i+1})$ as an approximation, then it corresponding to a different type of integral, known as Stratonovich stochastic integral. Its precise definition is given below.

Definition B.6. Let

$$\widetilde{S}_n(\omega) = \sum_{i=1}^{n} \sigma\left(\frac{x(t_i) + x(t_{i+1})}{2}\right) (B(t_{i+1}, \omega) - B(t_i, \omega)). \tag{B.10}$$

If there exists a random variable $\widetilde{S}(\omega)$, such that $\{\widetilde{S}_n(\omega)\}_{n \geq 0}$ converges to $\widetilde{S}(\omega)$ in mean-square sense, i.e.,

$$\lim_{n \to \infty} E|\widetilde{S}_n(\omega) - \widetilde{S}(\omega)|^2 = 0, \tag{B.11}$$

then $\widetilde{S}(\omega)$ is called a Stratonovich stochastic integral of $\sigma(x)$ with respect to a Brownian motion **B** on interval $[a, b]$, which is denoted as

$$\widetilde{S}(\omega) = \int_a^b \sigma(x(s))dB(s) = \ell.i.m_{n \to \infty}\widetilde{S}_n(\omega). \quad \text{(Stratonovich)} \tag{B.12}$$

The stochastic integrals given by Definitions B.5 and B.6 are different; each has its own advantage. The Itô integral can be easily implemented in numerical simulations, while the Stratonovich integral shows a much clear physical meaning. In the following, we mainly follow Itô's approach.

We shall mention some important properties of Itô stochastic integral. Similar to the Riemann integral, stochastic integral exhibits properties such as linearity and additivity of the integral with respect to the interval. In addition, it has the following two distinct properties:

(i)

$$E\left[\int_a^b \phi(t, \omega)dB(t, \omega)\right] = 0, \tag{B.13}$$

(ii)

$$E\left[\int_a^b \phi(t, \omega)dB(t, \omega) \cdot \int_a^b \psi(t, \omega)dB(t, \omega)\right] = \int_a^b E[\phi(t, \omega)\psi(t, \omega)]dt. \tag{B.14}$$

More specifically,

$$E\left[\left|\int_a^b \phi(t, \omega)dB(t, \omega)\right|^2\right] = \int_a^b E\left[|\phi(t, \omega)|^2\right]dt. \tag{B.15}$$

In the above equations, both $\phi(t, \omega)$ and $\psi(t, \omega)$ are stochastic processes that only depend on the past of the Brownian motion, and both their Itô stochastic integrals are assumed to exist.

B.3. Method of numerical integrations of a SDE

In computer simulations, we need to discretize the time. Based on Itô stochastic integral, the SDE (B.4) can be approximated by the following difference scheme

$$x(t + \Delta t) - x(t) = b(x(t))\Delta t + \sigma(x(t))\Delta B(t, \omega), \tag{B.16}$$

where $\Delta B(t, \omega) = B(t + \Delta t, \omega) - B(t, \omega)$.

Considering the time interval $[0, T]$, let $0 = t_0 < t_1 < \cdots < t_n = T$ be a partition, and denote $\Delta t_i = t_{i+1} - t_i$, then Eq. (B.16) yields an iterative relation

$$x(t_{i+1}) = x(t_i) + b(x(t_i))\Delta t_i + \sigma(x(t_i))\Delta B(t_i). \tag{B.17}$$

One knows that a Brownian motion is a stochastic process with independent increments. The variance of the increment is $E[B(t_{i+1}) - B(t_i)]^2 = t_{i+1} - t_i$, which roughly shows $\Delta B(t_i)$ to be on the order of $\sqrt{\Delta t_i}$, and $\Delta B(t_i)/\sqrt{\Delta t_i}$ obeys normal distribution $N(0, 1)$. Hence, Eq. (B.17) can be equivalently rewritten as

$$x(t_{i+1}) = x(t_i) + b(x(t_i))\Delta t_i + \sigma(x(t_i))\frac{\Delta B(t_i)}{\sqrt{\Delta t_i}}\sqrt{\Delta t_i}. \tag{B.18}$$

Eq. (B.18) is the basis for numerical simulations of a SDE. One only needs to produce n normally distributed random numbers $\Delta B(t_i)/\sqrt{\Delta t_i}$, then the trajectory of the SDE (B.4) can be simulated according to the iterated equation (B.18). The difference to a deterministic differential equation is that even starting from the same initial condition $(t_0, x(0))$, each simulation of SDE gives a different trajectory, it is a different realization of the stochastic process.

B.4. Diffusion processes and Fokker–Planck equations

One can either study the dynamical behavior of a stochastic process by numerical simulations, or one can investigate the statistical law of the process via its probability density function. Suppose that the transition probability of a stochastic process $\{x(t, D)\}_{t\geq 0}$ is $P(s, t; x, \omega)$, in which $s < t$, D is a measurable set in $\mathcal{F}$. Let $O_\varepsilon(x) = \{y \in R : |y - x| < \varepsilon\}$ be a small neighborhood of x. The process is called a diffusion process, if for any fixed $\varepsilon > 0$, the probability of the particle escape away from this neighborhood in a sufficiently short time is $o(t - s)$, i.e.,

$$P(s, t; x, O_\varepsilon^c(x)) = o(t - s), \quad \text{for } t - s \to 0.$$

It can be proved that the solution $\{x(t, \omega)\}_{t\geq 0}$ to Eq. (B.4) is a diffusion process.

According to the iterated Eq. (B.16) and the Definition B.1, we can estimate that

$$\lim_{h\to 0^+} E\left[\frac{x(t + h) - x(t)}{h}\bigg| x(t) = x\right] = b(x) + \lim_{h\to 0^+}\frac{1}{h}\sigma(x)E\{(B(t + h) - B(t))|x(t) = x\}$$
$$= b(x),$$

and

$$\lim_{h\to 0^+} E\left[\frac{(x(t + h) - x(t))^2}{h}\bigg| x(t) = x\right] = \lim_{h\to 0^+} b^2(x) \cdot h + 2\lim_{h\to 0^+} b(x)\sigma(x)E\left[(B(t + h) - B(t))|x(t) = x\right]$$
$$+ \lim_{h\to 0^+}\sigma^2(x)E\left[\frac{(B(t + h) - B(t))^2}{h}\bigg| x(t) = x\right]$$
$$= \sigma^2(x).$$

Furthermore, it follows from the diffusive properties that

$$b(x) = \lim_{h\to 0^+} E\left[\frac{x(t + h) - x(t)}{h}\bigg| x(t) = x\right]$$
$$= \lim_{h\to 0^+}\frac{1}{h}\int_{|y-x|\leq 1}(y - x)P(h, x; dy); \tag{B.19}$$

$$\sigma^2(x) = \lim_{h\to 0^+} E\left[\frac{(x(t + h) - x(t))^2}{h}\bigg| x(t) = x\right]$$
$$= \lim_{h\to 0^+}\frac{1}{h}\int_{|y-x|\leq 1}(y - x)^2P(h, x; dy); \tag{B.20}$$

$b(x)$ is called the drifting coefficient, and $\sigma^2(x)$ is called the diffusion coefficient.

One can also obtain from Eq. (B.16) that for $k > 2$,

$$\lim_{h\to 0^+}\frac{1}{h}\int_{|y-x|\leq 1}(y - x)^k P(h, x; dy) = 0.$$

Eqs. (B.19) and (B.20) provide intuitively the physical meanings of $b(x)$ and $\sigma^2(x)$. More rigorously they can be obtained via Itô stochastic integral provided that the functions $b(x)$ and $\sigma(x)$ satisfy certain conditions. In the following, we will prove Eqs. (B.19) and (B.20) for the case when $b(x)$ and $\sigma(x)$ are smooth and bounded. Readers who are unfamiliar with or not interested in the rigorous mathematic treatment can skip this part.

According to Itô integral, we have

$$\lim_{h\to 0^+} E\left[\frac{x(t+h)-x(t)}{h}\bigg| x(t)=x\right] = \lim_{h\to 0^+} E\left[\frac{1}{h}\int_t^{t+h} b(x(s))ds\bigg| x(t)=x\right]$$
$$+ \lim_{h\to 0^+} E\left[\frac{1}{h}\int_t^{t+h}\sigma(x(s))dB(s)\bigg| x(t)=x\right].$$

By the dominated convergence theorem and the continuous property of the trajectory, the first term of the above equation is

$$\lim_{h\to 0^+} E\left[\frac{1}{h}\int_t^{t+h} b(x(s))ds\bigg| x(t)=x\right] = E\left[\lim_{h\to 0^+}\frac{1}{h}\int_t^{t+h} b(x(s))ds\bigg| x(t)=x\right]$$
$$= b(x).$$

By the property of the stochastic integral (see Eq. (B.13)) and the independence of the increments of a Brownian motion, the second term is

$$\lim_{h\to 0^+} E\left[\frac{1}{h}\int_t^{t+h}\sigma(x(s))dB(s)\bigg| x(t)=x\right] = 0.$$

Hence

$$\lim_{h\to 0^+} E\left[\frac{x(t+h)-x(t)}{h}\bigg| x(t)=x\right] = b(x).$$

Similarly, according to the dominated convergence theorem, we have

$$\lim_{h\to 0^+} E\left[\frac{(x(t+h)-x(t))^2}{h}\bigg| x(t)=x\right] = E\left[\lim_{h\to 0^+}\frac{1}{h}\left(\int_t^{t+h} b(x(s))ds\right)^2\bigg| x(t)=x\right]$$
$$+ 2E\left[\lim_{h\to 0^+}\frac{1}{h}\left(\int_t^{t+h} b(x(s))ds\int_t^{t+h}\sigma(x(s))dB(s)\right)\bigg| x(t)=x\right]$$
$$+ E\left[\lim_{h\to 0^+}\frac{1}{h}\left(\int_t^{t+h}\sigma(x(s))dB(s)\right)^2\bigg| x(t)=x\right]$$
$$= \lim_{h\to 0^+}\frac{1}{h}E\left[\int_t^{t+h}\sigma(x(s))dB(s)\right]^2$$

(the integrals of the first and second terms are both)$o(h)$

$$= \lim_{h\to 0^+}\frac{1}{h}\int_t^{t+h} E[\sigma^2(x(s))]ds$$

(by the property of Itô integral, Eq. (B.14))

$$= \sigma^2(x).$$

Similar to the case of master equation of a Q-process, there is a partial differential equation, i.e., Fokker–Planck equation, for the time evolution of the probability density function of the diffusion process defined by the SDE (B.1). There is some differences, however, between the form of the Fokker–Planck equation obtained according to Itô integration and that according to Stratonovich integration. Taking the probability density $p(t, x)$ for example, we have the following Fokker–Planck equations (also known as Kolmogorov forward equation):

The Itô form:

$$\frac{\partial}{\partial t}p(t,x) = -\frac{\partial}{\partial x}(b(x)p(t,x)) + \frac{1}{2}\frac{\partial^2}{\partial x^2}\left(\sigma^2(x)p(t,x)\right)$$
$$= -\frac{\partial}{\partial x}(\widetilde{b}(x)p(t,x)) + \frac{1}{2}\frac{\partial}{\partial x}\left(\sigma^2(x)\cdot\frac{\partial}{\partial x}p(t,x)\right) \tag{B.21}$$

where $\widetilde{b}(x) = b(x) - \sigma(x)\sigma'(x)$.

Physicists and engineers prefer to use the following Stratonovich form of the Fokker–Planck equation [19].

The Stratonovich form:

$$\frac{\partial}{\partial t}p(t,x) = -\frac{\partial}{\partial x}(b(x)p(t,x)) + \frac{1}{2}\frac{\partial}{\partial x}\left(\sigma(x)\cdot\frac{\partial}{\partial x}(\sigma(x)p(t,x))\right). \tag{B.22}$$

When the diffusion coefficient $\sigma^2(x)$ is independent of the position x, then Eqs. (B.21) and (B.22) are the same. Both expressions are important. The proof of these equations can be found in general texts on stochastic processes. Since the proofs are not particularly relevant for applications, we shall omit them.

Appendix C. Dynamics of a periodically driven phase model without noise

In this Appendix, we give a mathematical analysis of the dynamical behaviors of system (90):

$$\dot{x} = b - \sin x + y, \qquad \dot{y} = -\omega z, \qquad \dot{z} = \omega y, \tag{C.1}$$

for $b < 1$ in the cases $A < 1 - b$ and $A > 1 - b$, respectively [122].

C.1. Case 1: $A \leq 1 - b$

Due to the periodicity of $\sin x$, we only need to consider $x \in (-\pi/2, 3\pi/2]$. Let

$$G_1 : \{(t, x)|t \in R, -\pi/2 < x \leq \pi/2\},$$
$$G_2 : \{(t, x)|t \in R, \pi/2 < x \leq 3\pi/2\}$$

be two ring-shaped regions on the cylinder E^2. Obviously, there is no equilibrium point in G_1 and G_2. Any orbit moving along the boundary of G_1 will eventually enter G_1 and any orbit moving along the boundary of G_2 will eventually leave G_2. So by Poincaré–Bendixson theorem on a cylinder, at least one stable limit cycle (SLC) lies in region G_1 and at least one unstable limit cycle (ULC) lies in G_2.

There exists at most one SLC in G_1 and at most one ULC in G_2. Otherwise, if there are two limit cycles in G_1, then the corresponding solutions to (C.1) can be written as:

$$LC_1 : \begin{cases} x_1 = f_1(t), \\ y_1 = A \cos \omega t, \\ z_1 = A \sin \omega t. \end{cases}$$

$$LC_2 : \begin{cases} x_2 = f_2(t), \\ y_2 = A \cos \omega t, \\ z_2 = A \sin \omega t. \end{cases}$$

Obviously, LC_1 and LC_2 should have the same periodicity $T = \frac{2\pi}{\omega}$.

It follows from Eq. (C.1) that

$$\dot{x}_2(t) - \dot{x}_1(t) = \sin x_1 - \sin x_2.$$

Then

$$[x_2(t) - x_1(t)] - [x_2(0) - x_1(0)] = \int_0^t (\sin x_1 - \sin x_2) dt.$$

Suppose that $x_1 < x_2$. Since $x_1, x_2 \in (-\frac{\pi}{2}, \frac{\pi}{2})$, then $\sin x_1 - \sin x_2 < 0$. As a result, $[x_2(T) - x_1(T)] - [x_2(0) - x_1(0)] < 0$. This contradicts the fact that $x_1(t), x_2(t)$ are two periodic solutions to Eq. (C.1). Therefore, there is only one SLC in region G_1. Similarly, only one ULC can exist in G_2.

C.2. Case 2: $A > 1 - b$

Firstly, let us investigate the situation for $\omega \gg 1$. We introduce the following transformation:

$$\Gamma : \begin{cases} \xi = e^x y, \\ \eta = e^x z. \end{cases}$$

Obviously, the transformation Γ is a homeomorphism. It maps a ring-shaped region on E^2 to a ring-shaped region on ξ–η plane and maps a cycle $C : x = x_c$ on E^2 to a circle $C' : \xi^2 + \eta^2 = A^2 e^{2x_c}$ on the ξ–η plane. The inverse transformation of Γ can be expressed as:

$$\Gamma^{-1} : \begin{cases} x = \dfrac{1}{2} \ln \left(\dfrac{\xi^2}{A^2} + \dfrac{\eta^2}{A^2} \right), \\[2mm] y = \xi \left(\dfrac{\xi^2}{A^2} + \dfrac{\eta^2}{A^2} \right)^{-\frac{1}{2}}, \\[2mm] z = \eta \left(\dfrac{\xi^2}{A^2} + \dfrac{\eta^2}{A^2} \right)^{-\frac{1}{2}}. \end{cases}$$

So we only need to study the dynamics of the following equivalent system:

$$\begin{cases} \dfrac{d\xi}{dt} = \dot{x}\xi - \omega\eta, \\[2mm] \dfrac{d\eta}{dt} = \dot{x}\eta + \omega\xi, \end{cases} \tag{C.2}$$

where $\dot{x} = b - \sin(\frac{1}{2} \ln \frac{\xi^2 + \eta^2}{A^2}) + \xi (\frac{\xi^2}{A^2} + \frac{\eta^2}{A^2})^{-1/2}$.

Let $t = \frac{s}{\omega}$, then

$$\begin{cases} \dfrac{d\xi}{dt} = -\eta + \dfrac{1}{\omega}\dot{x}\xi, \\ \dfrac{d\eta}{dt} = \xi + \dfrac{1}{\omega}\dot{x}\eta. \end{cases} \tag{C.3}$$

To judge the existence of limit cycles of system (C.3) for $\omega \gg 1$, we cite the following Lemma without proof [239]:

Lemma C.1. *Let*

$$\begin{cases} \dot{x} = -y + \lambda f_1(x, y), \\ \dot{y} = x + \lambda f_2(x, y) \end{cases} \tag{C.4}$$

be a perturbation of a linear dynamical system

$$\begin{cases} \dot{x} = -y, \\ \dot{y} = x. \end{cases} \tag{C.5}$$

Suppose that the equilibrium point $(0, 0)$ *of Eq.* (C.5) *is still the unique equilibrium point of system* (C.4)*, but no longer of central type for* $\lambda \neq 0$*. Let*

$$\Phi(r) = \int_0^{2\pi} [x f_1(x, y) + y f_2(x, y)] dt,$$

where $x = r \sin t, y = r \cos t$*, then*

(1) *For* $\lambda \ll 1$*, the necessary condition for Eq.* (C.4) *to have a closed orbit near the orbit* $L_{r_0} : x = r_0 \sin t, y = r_0 \cos t$ *of Eq.* (C.5) *is* $\Phi(r_0) = 0$*.*

(2) *If* $r_0 > 0$, $\Phi(r_0) = 0$ *and* r_0 *is not the extreme point of* $\Phi(r_0)$*, then for* $\lambda \ll 1$*, Eq.* (C.4) *has a closed orbit near* L_{r_0}*.*

(3) *If* $\Phi(r_0) = \cdots = \Phi^{(2k)}(r_0) = 0$*, and* $\Phi^{(2k+1)}(r_0) < 0$*, then for* $\lambda \ll 1$*, Eq.* (7) *has a limit cycle near* L_{r_0}*. It is stable for* $\lambda > 0$ *and unstable for* $\lambda < 0$*.* □

For Eq. (6), let $\xi = r \sin s, \eta = r \cos s, f_1 = \xi \dot{x}, f_2 = \eta \dot{x}$, we have

$$\Phi(r) = \frac{2\pi r}{\omega} \left[b - \sin \left(\ln \frac{r}{A} \right) \right].$$

The roots of $\Phi(r) = 0$ are: $r_0 = 0$ (discarded), $r_1 = A \exp(\arcsin b)$ and $r_2 = A \exp(\pi - \arcsin b)$, the corresponding derivatives are: $\Phi'(r_1) = -\frac{2\pi}{\omega}\sqrt{1 - b^2} < 0$ and $\Phi'(r_1) = \frac{2\pi}{\omega}\sqrt{1 - b^2} > 0$.

According to Lemma C.1, we know that for $\omega \gg 1$, system (C.3) has a SLC at $\xi = r_1 \sin s, \eta = r_1 \cos s$ and a ULC at $\xi = r_2 \sin s, \eta = r_2 \cos s$. Except these two limit cycles, no other limit cycle exists for $x \in (-3\pi/2, \pi/2]$. Correspondingly, system (C.1) has a unique SLC at $x = \arcsin b$ and a unique ULC at $x = \pi - \arcsin b$ in $(-3\pi/2, \pi/2]$.

Now let us consider the situation for $\omega \ll 1$. Here we take the case $1 - b < A < 1 + b$ for example to prove the nonexistence of the limit cycle. Let $H_k : \{(z, y, x) | 2k\pi - \pi/2 < x \leq 2k\pi + 3\pi/2\}$ be a ring-shaped region of system (C.1) on the cylinder ($k \in \mathbb{Z}$). If there is a limit cycle, obviously it could not interact with both H_k and H_{k+1}. Otherwise, it contradicts the direction of the vector fields. So the limit cycle can only exist in the region H_k, hence its amplitude is smaller than 2π.

Let $\{(z(t), y(t), x(t))\}_{t \geq 0}$ be any limit cycle in H_k, $a = (A - (1 - b))/2$, and

$$F(t) = \sin \omega t - \frac{1 - b + a}{A} \omega t.$$

Then $F(0) = 0$, $F'(t) = \omega[\cos \omega t - (1 - b + a)/A]$. If $t \in \left(0, \frac{1}{\omega} \arccos \frac{1-b+a}{A}\right]$, then $F'(t) \geq 0$. For a sufficiently small $\omega \left(0 < \omega < \frac{a}{2\pi} \cdot \arccos \frac{1-b+a}{A}\right)$, we can select $t_1 \in \left(\frac{2\pi}{a}, \frac{1}{\omega} \arccos \frac{1-b+a}{A}\right)$, such that $t_1 a > 2\pi$. Then $F(t_1) \geq 0$, i.e.,

$$\frac{\sin \omega t_1}{\omega t_1} \geq \frac{1 - b + a}{A}.$$

So for these ω, we have

$$\begin{aligned} x(t_1) - x(0) &= b t_1 - \int_0^{t_1} \sin x(s) ds + A \cdot \frac{\sin \omega t_1}{\omega} \\ &> t_1 \left(b - 1 + A \cdot \frac{\sin \omega t_1}{\omega t_1} \right) \\ &> t_1 \left(b - 1 + A \cdot \frac{1 - b + a}{A} \right) \\ &= t_1 a > 2\pi. \end{aligned}$$

This contradicts the fact that any periodic solution can only lie in the region H_k with amplitude smaller than 2π. So for $\omega \ll 1$, and $1 - b < A < 1 + b$, system (C.1) has no limit cycle on the cylinder.

References

[1] W. Pauli, Pauli Lectures on Physics: Thermodynamics and the Kinetic Theory of Gas, vol. 3, The MIT Press, Cambridge, MA, 1973.
[2] W. Pauli, Pauli Lectures on Physics: Statistical Mechanics, vol. 4, The MIT Press, Cambridge, MA, 1973.
[3] J. Gibbs, Elementary Principles of Statistical Mechanics, Dover, New York, 1960.
[4] R.H. Fowler, Statistical Mechanics, Cambridge Univ, UK, 1936.
[5] F. Reif, Fundamentals of Statistical and Thermal Physics, McGraw Hill, New York, 1965.
[6] T.L. Hill, Statistical Mechanics: Principles and Applications, Dover, New York, 1987.
[7] E. Schrödinger, What is Life? Cambridge University Press, 1944.
[8] M.C. Mackey, Time's Arrow: The Origins of Thermodynamic Behavior, Dover, 2003.
[9] G. Nicolis, I. Prigogine, Self-organization in Nonequilibrium Systems: From Dissipative Structures to Order Through Fluctuation, Wiley, New York, 1977.
[10] D.Q. Jiang, M. Qian, M.P. Qian, Mathematical Theory of Nonequilibrium Steady States, in: Lecture Notes in Mathematics, vol. 1883, Springer-Verlag, Berlin, 2004.
[11] A.N. Kolmogorov, Math. Ann. 112 (1936) 155.
[12] M. Vellela, H. Qian, J. R. Soc. Interface 6 (2009) 925.
[13] G.N. Lewis, Proc. Natl. Acad. Sci. USA 11 (1925) 179.
[14] A. Goldbeter, Biochemical Oscillations and Cellular Rhythms: The Molecular Bases of Periodic and Chaotic Behaviour, Cambridge University Press, 2004.
[15] G. Buzsáki, Rhythms of the Brain, Oxford University Presss, 2006.
[16] E.M. Sevick, R. Prabhakar, S. Williams, D.J. Searles, Ann. Rev. Phys. Chem. 59 (2008) 603.
[17] R.K.P. Zia, B. Schmittmann, J. Stat. Mech. Theory Exp. (2007) P07012.
[18] H. Risken, The Fokker–Planck Equation: Methods of Solutions and Applications, Springer-Verag, New York, 1996.
[19] N.G. van Kampen, Stochastic Processes in Physics and Chemistry, North-Holland, Amsterdam; New York, 1992.
[20] C. Gardiner, Handbook of Stochastic Methods: For Physics, Chemistry and the Natural Sciences, 2nd ed., Springer-Veralg, New York, 1996.
[21] J. Keizer, Statistical Thermodynamics of Nonequilibrium Processes, Springer, New York, 1987.
[22] J. Ross, Thermodynamics and Fluctuations far from Equilibrium, Springer, New York, 2008.
[23] C. Fall, E. Marland, J. Wagner, J.J. Tyson (Eds.), Computational Cell Biology, Springer-Verlag, New York, 2002.
[24] H. Haken, Synnergetics: An Introduction: Nonequilibrium Phase Transitions and Self-organization in Physics, Chemistry, and Biology, 1977.
[25] H. Haken, Advanced Synergetics: Instability Hierachies of Self-organizing Systems and Devices, Springer-Verlag, Berlin, New York, 1983.
[26] L. Gammaitoni, P. Hänggi, P. Jung, F. Marchesoni, Rev. Modern Phys. 70 (1998) 223.
[27] F. Jülicher, A. Ajdari, J. Prost, Rev. Mod. Phys. 69 (1997) 1269.
[28] W. Horsthemke, R. Lefever, Noise-Induced Transitions: Theory, Apllications in Physics, Chemistry, and Biology, Springer Series in Synergetics, vol. 15, Springer-Verlag, Berlin, 1984.
[29] R.B. Laughlin, D. Pines, J. Schmalian, B. Stojkovic, P.G. Wolynes, Proc. Natl. Acad. Sci. 97 (2000) 32.
[30] N. van Kampen, Statistical Physics, in: Proc. of Int. Con., North-Holland, Budapest, Amsterdam, 1975, pp. 25–29.
[31] Y. Murayama, Mesoscopic Systems, Wiley-VCH, 2001.
[32] M. Doi, S. Edwards, The Theory of Polymer Dynamics, Oxford Univ. Press, Clarendon, UK, 1999.
[33] F. Reif, Statistical Physics: Berkeley Physics Course, 1967.
[34] M. Toda, R. Kubo, N. Saitô, Statistical Physics I, Equilibrium Statistical Mechanics, 2nd ed., Springer-Verlag, Berlin, Heidelberg, 1991.
[35] R. Kubo, M. Toda, N. Hashitsume, Statistical Physics II, Nonequilibrium Statistical Mechanics, 2nd ed., Springer-Verlag, Berlin, Heidelberg, 1991.
[36] J.R. Knowles, Annu. Rev. Biochem. 49 (1980) 877.
[37] H.A. Kramers, Physica 7 (1940) 284.
[38] H. Qian, Protein Science 11 (2002) 1.
[39] F.W. Sears, G. Salinger, Thermodynamics, Kinetic Theory, and Statistical Thermodynamics, 3rd ed., Addison-Wesley, 1986.
[40] K. Denbigh, The Principles of Chemical Equilibrium, Cambridge University Press, London, 1981.
[41] A.B. Koudriavtsev, W. Linert, R.F. Jameson, The Law of Mass Action, Springer-Verlag, Berlin, New York, 2001.
[42] L. Boltzmann, in: F. Hasenöhrl (Ed.), Wissenschaftliche Abhandlungen, English translation in S. Brush, Kinetic theory, vol. 2. p. 88, volume I, Chelsea (reprinted), New York, 1872, pp. 316–402.
[43] H. Qian, E.L. Elson, Biophys. Chem. 101 (2002) 565.
[44] L. Onsager, Phys. Rev. 37 (1931) 405.
[45] S.C. Kou, X.S. Xie, Phys. Rev. Lett. 93 (2004) 180603.
[46] H. Qian, H. Wang, Eur. Phys. Lett. 76 (2006) 15.
[47] H. Wang, H. Qian, J. Math. Phys. 48 (2007) 013303.
[48] H. Qian, Phys. Rev. E 63 (2001) 042103.
[49] H. Qian, Phys. Rev. E 64 (2001) 022101.
[50] H. Qian, Phys. Rev. E 65 (2002) 021111.
[51] P. Glansdorff, I. Prigogine, Thermodynamic Theory of Structure, Stability and Fluctuations, Wiley-Interscience, London, 1971.
[52] D. Ruelle, J. Statist. Phys. 85 (1996) 1.
[53] D. Ruelle, Commun. Math. Phys. 189 (1997) 365.
[54] C. Maes, F. Redig, A.V. Moffaert, J. Math. Phys. 41 (2000) 1528.
[55] H. Qian, J. Phys. Chem. B. 110 (2006) 15063.
[56] H. Qian, Ann. Rev. Phys. Chem. 58 (2007) 113–142.
[57] G.E. Crooks, Phys. Rev. E 60 (1999) 2721.
[58] J.L. Lebowitz, H. Spohn, J. Statist. Phys. 95 (1999) 333.
[59] M. Qian, M.P. Qian, X.J. Zhang, Phys. Lett. A. 309 (2003) 371.
[60] D.Q. Jiang, M. Qian, F.X. Zhang, J. Math. Phys. 44 (2003) 4176.
[61] H. Qian, M. Qian, Phys. Rev. Lett. 84 (2000) 2271.
[62] S.H. Strogatz, Nonlinear Dynamics and Chaos, Perseus Books Group, 2001.
[63] K.H. Kim, H. Qian, Phys. Rev. Lett. 93 (2004) 120602.
[64] M.P. Qian, D. Wang, Ergodic Theory Dynam. Systems 20 (2000) 547.
[65] K.D. Elworthy, Stochastic Differential Equations on Manifolds, Cambridge University Press, Cambridge, New York, 1982.
[66] S.R. deGroot, P. Mazur, Non-Equilibrium Thermodynamics, Dover Publications, 2011.
[67] I. Karatzas, S.E. Shreve, Brownian Motion and Stochastic Callulus, 2nd ed., Springer-Verlag, New York, 1991.
[68] M. Qian, Z.D. Wang, Commun. Math. Phys. 206 (1999) 429.
[69] J.F. Lindner, B.K. Meadows, W.L. Ditto, M.E. Inchiosa, A.R. Bulsara, Phys. Rev. Lett. 75 (1995) 3.
[70] J.F. Lindner, B.K. Meadows, W.L. Ditto, M.E. Inchiosa, A.R. Bulsara, Phys. Rev. E 53 (1996) 2081.
[71] A.S. Pikovsky, J. Kurths, Phys. Rev. Lett. 78 (1997) 775.
[72] J. Paulsson, O.G. Berg, M. Ehrenberg, Proc. Natl. Acad. Sci. USA 97 (2000) 7148.
[73] J.M.G. Vilar, J.M. Rubi, Phys. Rev. Lett. 86 (2001) 950.

[74] M. Samoilov, S. Plyasunov, A. Arkin, Proc. Natl. Acad. Sci. USA 102 (2005).
[75] M.L. Bishop, H. Qian, Biophys. J. 98 (2010) 1.
[76] D. Honga, W.M. Saidelb, S. Manc, J.V. Martin, J. Theoret. Biol. 245 (2007) 726.
[77] Y. Chen, M.P. Qian, J.S. Xie, J. Math. Phys. 48 (2007).
[78] R. Benzi, A. Sutera, A. Vulpiani, J. Phys. A 14 (1981) 453.
[79] R. Benzi, G. Parisi, A. Sutera, A. Vulpiani, Tellus 34 (1982) 10.
[80] C. Nicolis, G. Nicolis, Tellus 33 (1981) 225.
[81] C. Nicolis, Tellus 34 (1982) 1.
[82] S. Fauve, F. Helslot, Phys. Lett. A 97 (1983) 5.
[83] B. McNamara, K. Wiesenfeld, R. Roy, Phys. Rev. Lett. 60 (1988) 2626.
[84] I.K. Kaufman, McClintock, Phys. Rev. E 57 (1998) 78.
[85] R.N. Mantegna, B. Spagnolo, Phys. Rev. E 49 (1994) R1792.
[86] R.N. Mantegna, B. Spagnolo, Nuovo Cimento D 17 (1995) 873.
[87] M.L. Spano, M. Wun-Fogle, W.L. Ditto, Phys. Rev. A 46 (1992) 5253.
[88] F. Vaudelle, J. Gazengel, et al., J. Opt. Soc. Am. B 15 (1998) 2674.
[89] K.P. Singh, G. Ropars, M. Brunel, F. Bretenaker, A.L. Floch, Phys. Rev. Lett. 87 (2001).
[90] V.N. Chizhevsky, G. Giacomelli, Phys. Rev. A 71 (2005) 011801.
[91] M. Misono, T. Kohmoto, M. Kunitomo, Y. Fukuda, Phys. Rev. E 67 (2003) 061102.
[92] A. Joshi, M. Xiao, Phys. Rev. A 74 (2006) 013817.
[93] M. Grifoni, P. Hänggi, Phys. Rev. E 54 (1996) 1390.
[94] S.F. Huelga, M.B. Plenio, Phys. Rev. A 62 (2000) 052111.
[95] D.S. Leonard, L.E. Reichl, Phys. Rev. E 49 (1994) 1734.
[96] Z. Hou, H. Xin, Phys. Rev. E 60 (1999) 6329.
[97] A. Zaikin, J. García-Ojalvo, R. Báscones, E. Ullner, J. Kurths, Phys. Rev. Lett. 90 (2003) 030601.
[98] A. Longtin, J. Stat. Phys. 70 (1993) 309.
[99] J.K. Douglass, L. Wilkens, E. Pantazelou, F. Moss, Nature 365 (1993) 337.
[100] J.E. Levin, J.P. Miller, Nature 380 (1996) 165.
[101] A.A. Faisal, L.P.J. Selen, D.M. Wolpert, Nat. Rev. Neurosci. 9 (2008) 292.
[102] J. Dunkel, S. Hilbert, L. Schimansky-Geier, P. Hänggi, Phys. Rev. E 69 (2004) 056118.
[103] T. Wellens, V. Shatokhin, A. Buchleitner, Rep. Progr. Phys. 67 (2004) 45.
[104] H.E. Plesser, T. Geisel, Phys. Rev. E 59 (1999) 7008.
[105] P.L. Gong, J.X. Xu, Phys. Rev. E 63 (2001) 031906.
[106] S.G. Lee, S. Kim, Phys. Rev. E 72 (2005) 061906.
[107] S.G. Lee, A. Neiman, S. Kim, Phys. Rev. E 57 (1998) 3292.
[108] O.V. Sosnovtseva, D. Setsinsky, A. Fausboll, E. Mosekilde, Phys. Rev. E 66 (2002) 041901.
[109] Y. Yu, W. Wang, J. Wang, F. Liu, Phys. Rev. E 63 (2001) 021907.
[110] K. Pakdaman, S. Tanabe, T. Shimokawa, Neural Netw. 14 (2001) 895.
[111] G. Schmid, I. Goychuk, P. Hänggi, Europhys. Lett. 56 (2001) 22.
[112] J.P. Baltanes, J.M. Casado, Physica D 122 (1998) 231.
[113] B. Lindner, L. Schimansky-Geier, Phys. Rev. E 60 (1999) 7270.
[114] V.A. Makarov, V.I. Nekorkin, M.G. Velarde, Phys. Rev. Lett. 86 (2001) 3431.
[115] A.M. Lacasta, F. Saguěs, J.M. Sancho, Phys. Rev. E 66 (2002) 045105.
[116] S. Wu, W. Ren, K. He, Z. Huang, Phys. Lett. A 279 (2001) 347.
[117] H. Gu, M. Yang, L. Li, Z. Liu, W. Ren, NeuroReport 13 (2002) 1657.
[118] P.L. Gong, J.X. Xu, S.J. Hu, Chaos Solitons Fractals 13 (2002) 885.
[119] B. Lindner, L. Schimansky-Geier, A. Longtin, Phys. Rev. E 66 (2002) 031916.
[120] J.F. Feng, B. Tirozzi, Phys. Rev. E 61 (2000) 4207.
[121] K. Wiesenfeld, D. Pierson, E. Pantazelou, C. Dames, F. Moss, Phys. Rev. Lett. 72 (1994) 2125.
[122] M. Qian, G.X. Wang, X.J. Zhang, Phys. Rev. E 62 (2000) 6469.
[123] J.M. Casado, Phys. Lett. A 291 (2001) 82.
[124] H. Treutlein, K. Schulten, Euro. Biophys. J. 13 (1986) 355.
[125] G. Hu, T. Ditzinger, C.Z. Ning, H. Haken, Phys. Rev. Lett. 71 (1993) 807.
[126] Y.D. Chen, Biophys. J. 13 (1973) 1276.
[127] H.S. Hahn, A. Nitzan, P. Ortoleva, J. Ross, Proc. Natl. Acad. Sci. 71 (1974) 4067.
[128] J.D. Murray, Mathematical Biology, Springer-Verlag, Berlin, Heidelberg, 1989.
[129] A. Neiman, P.I. Saparin, L. Stone, Phys. Rev. E 56 (1997) 270.
[130] Z. Liu, Y.C. Lai, Phys. Rev. Lett. 86 (2001) 4737.
[131] L.Q. Zhu, Y.C. Lai, Z. Liu, A. Raghu, Phys. Rev. E 66 (2002) 015204.
[132] B. Lindner, J. García-Ojalvob, A. Neimand, L. Schimansky-Geiere, Phys. Rep. 392 (2004) 321.
[133] A. Bulsara, L. Gammaitoni, Phys. Today 49 (1996) 39.
[134] R. Benzi, A. Sutera, A. Vulpiani, J. Phys. A 18 (1985) 2239.
[135] N. Sungar, J.P. Sharpe, S. Weber, Phys. Rev. E 62 (2000) 1413.
[136] H. Gang, H. Haken, X. Fagen, Phys. Rev. Lett. 77 (1996) 1925.
[137] M. Locher, G.A. Johnson, E.R. Hunt, Phys. Rev. Lett. 77 (1996) 4698.
[138] H.S. Wio, Phys. Rev. E 54 (1996) R3075.
[139] J.J. Brey, A. Prados, Phys. Lett. A 216 (1996) 240.
[140] J.M.G. Vilar, J.M. Rubi, Phys. Rev. Lett. 78 (1997) 2886.
[141] J. Xiao, G. Hu, H. Liu, Y. Zhang, Eur. Phys. J. B 5 (1998) 133.
[142] A. Kovaleva, Phys. Rev. E 74 (2006) 011126.
[143] M.H. Choi, R.F. Fox, P. Jung, 57, (1998), 6335.
[144] T. Zhou, F. Moss, Phys. Rev. A 41 (1990) 4255.
[145] T. Zhou, F. Moss, P. Jung, Phys. Rev. A 42 (1990) 3161.
[146] L. Gammaitoni, F. Marchesoni, E. Menichella-Saetta, S. Santucci, Phys. Rev. Lett. 62 (1989) 349.
[147] C. Presilla, F. Marchesoni, L. Gammaitoni, Phys. Rev. A 40 (1989) 2105.
[148] F. Apostolico, L. Gammaitoni, F. Marchesoni, S. Santucci, Phys. Rev. E 55 (1997) 36.
[149] L. Alfonsi, L. Gammaitoni, S. Santucci, A.R. Bulsara, Phys. Rev. E 62 (2000) 299.
[150] G. Hu, G. Nicolis, C. Nicolis, Phys. Rev. A 42 (1990) 2030.
[151] T. Ditzinger, C. Ning, G. Hu, Phys. Rev. E 50 (1994) 3508.
[152] R. Adler, Proc. Inst. Radio Engr. 34 (1946) 351–357.
[153] R. Adler, Proc. IEEE 61 (1973) 1380–1385.

[154] A. Bulsara, E.W. Jacobs, T. Zhou, J. Theoret. Biol. 152 (1991) 531.
[155] J.E. Levin, J.P. Miller, Nature 380 (1996) 165.
[156] P. Cordo, J.T. Inglis, S. Verschueren, J.J. Collins, et al., Nature 383 (1996) 769.
[157] M.D. McDonnell, D. Abbott, Plos Comp. Biol. 5 (2009) e1000348.
[158] N. Brunel, M.C. van Rossum, Biol. Cybern. 97 (2007) 337.
[159] E.M. Izhikevich, Dynamical Systems in Neuroscience: The Geometry of Excitability and Bursting, The MIT Press, Cambridge, Massachusetts. London, England, 2007.
[160] J.F. Feng, Neural Networks 14 (2001) 955.
[161] D. Brown, J.F. Feng, S. Feerick, Phys. Rev. Lett. 82 (1999) 4731.
[162] J.M. Fellous, M. Rudolph, A. Destexhe, T.J. Sejnowski, Neurosci. 122 (2003) 811.
[163] J.F. Feng, D. Brown, Neural Comput. 12 (2000) 671.
[164] X.J. Zhang, G.Q. You, T.P. Chen, J.F. Feng, Neural Comput. 21 (2009) 3079.
[165] M. Vellela, H. Qian, Proc. Roy. Soc. A: Math. Phys. Eng. Sci. 466 (2010) 771.
[166] S.K. Han, T.G. Yim, D.E. Postnov, O.V. Sosnovtseva, Phys. Rev. Lett. 83 (1999) 1771.
[167] T.L. Hill, O. Kedem, J. Theoret. Biol. 10 (1966) 399.
[168] T.L. Hill, Free Energy Transduction and Biochemical Cycle Kinetics, Springer-Verlag, New York, 1995.
[169] H.M. Fishman, Proc. Natl. Acad. Sci. USA. 70 (1973) 876.
[170] N. Geva-Zatorsky, N. Rosenfeld, S. Itzkovitz, R. Milo, A. Sigal, E. Dekel, T. Yarnitzky, Y. Liron, P. Polak, G. Lahav, U. Alon, Molec. Syst. Biol. 0033 (2006) 1744.
[171] A. Ciliberto, B. Novak, J.J. Tyson, Cel. Cyc. 4 (2005) 488.
[172] H. Qian, J. Math. Chem. 27 (2000) 219.
[173] C.C. Chow, J.A. White, Biophys. J 71 (1996) 3013.
[174] E. Neher, B. Sakmann, Nature 260 (1976) 799.
[175] H. Lecar, R. Nossal, Biophys. J. 11 (1971) 1048.
[176] H. Lecar, R. Nossal, Biophys. J. 11 (1971) 1068.
[177] R. Fox, Y.N. Lu, Phys. Rev. E 49 (1994).
[178] D.T. Gillespie, J. Phys. Chem. 81 (25) (1977) 2340.
[179] D.T. Gillespie, J. Comput. Phys. 22 (1976) 403.
[180] D.T. Gillespie, Annu. Rev. Phys. Chem. 58 (2007) 35–55.
[181] B. Sengupta, S.B. Laughlin, J.E. Niven, Phys. Rev. E 81 (2010) 011918.
[182] J.H. Goldwyn, N.S. Imennov, M. Famulare, E. Shea-Brown, Phys. Rev. E 83 (2011) 041908.
[183] X.J. Zhang, J. Phys. A: Math. & Gen. 37 (2004) 7473.
[184] P. Jung, P. Hänggi, Phys. Rev. A 44 (1991) 8032.
[185] F. Apostolico, L. Gammaitoni, F. Marchesoni, S. Santucci, Phys. Rev. E 55 (1997) 36.
[186] P. Jung, Phys. Rep. 175 (1993).
[187] P. Jung, P. Hänggi, Europhys. Lett. 8 (1989) 505.
[188] P. Jung, P. Hänggi, Ber. Bunsenges. Phys. Chem. 95 (1991) 311.
[189] X.J. Zhang, G.X. Wang, Phys. A 331 (2004) 467.
[190] M. Qian, X.J. Zhang, Phys. Rev. E 65 (2001) 011101.
[191] M. Qian, X.J. Zhang, Phys. Rev. E 65 (2002) 031110.
[192] P. Hadley, M.R. Beasley, K. Wiesenfeld, Phys. Rev. B 38 (1988) 8712.
[193] Y. Kuramoto, Chemical Oscillator, Waves and Turbulence, Springer, New York, 1984.
[194] H.G. Schuster, Nonlinear Dynamics and Neuronal Network, VCH, Weinheim, 1991.
[195] C. Tang, K. Wiesenfeld, P. Bak, S. Coppersmith, P. Littlewood, Phys. Rev. Lett. 58 (1987) 1161.
[196] H.E. Plesser, T. Geisel, Phys. Rev. E 59 (1999) 7008.
[197] R.D. Astumian, Science 276 (1997) 917.
[198] A.F. Huxley, Prog. Biophys. Biophys. Chem. 7 (1957) 257.
[199] T.L. Hill, Prog. Biophys. Mol. Biol. 28 (1974) 267–340.
[200] J. Howard, Mechanics of Motor Proteins and the Cytoskele, Sinauer Associates, Sunderland, MA., 2001.
[201] B. Alberts, D. Bray, J. Lewis, M. Raff, K. Roberts, J.D. Watson, The Molecular Biology of the Cell, Garland, New York, 1994.
[202] P. Reimann, Phys. Rep. 361 (2002) 57.
[203] J. Klafter, M. Urbakh (Eds.), Molecular Motors (J. Phys. Cond. Matt.), vol. 17, IoP Pub., UK, 2005.
[204] A.B. Kolomeisky (Ed.), Physical Chemistry of Biomolecular Motors and Machines (Phys. Chem. Chem. Phys.), vol. 11, RSC Pub., UK, 2009.
[205] A.R. Bug, B.J. Berne, Phys. Rev. Lett. 59 (1987) 948.
[206] A. Ajdari, J. Prost, C. R. Acad. Sci. Paris 315 (1992) 1635.
[207] R.D. Astumian, M. Bier, Phys. Rev. Lett. 72 (1994) 2652.
[208] J. Prost, J.F. Chauwin, L. Peliti, Phys. Rev. Lett. 72 (1994) 2652.
[209] R. Bartussek, P. Hänggi, J.G. Kissner, Europhys. Lett. 28 (1994) 459.
[210] M.O. Magnasco, Phys. Rev. Lett. 71 (1993) 1477.
[211] H. Qian, J. Phys. Cond. Matt. 17 (2005) S3783.
[212] P. Jung, J.G. Kissner, P. Hänggi, Phys. Rev. Lett. 76 (1996) 3436.
[213] J. Mateos, Phys. Rev. Lett. 84 (2000) 258.
[214] M. Barbi, M. Salerno, Phys. Rev. E 62 (2000) 1988.
[215] H.X. Zhou, Y.D. Chen, Phys. Rev. Lett. 77 (1996) 194.
[216] H. Qian, Phys. Rev. E 69 (2004) 012901.
[217] M. Qian, X.J. Zhang, R.J. Wilson, J. Feng, Eurphys. Lett. 84 (2008) 10014.
[218] A. Parmeggiani, F. Jülicher, A. Ajdari, J. Prost, Phys. Rev. E 60 (1999) 2127.
[219] I. Derényi, M. Bier, R.D. Astumian, Phys. Rev. Lett. 83 (1999) 903.
[220] D. Suzuki, T. Munakata, Phys. Rev. E 68 (2003) 021906.
[221] V. Berdichevsky, M. Gitterman, Physica A 249 (1998) 88–95.
[222] M. Qian, Y. Wang, X.J. Zhang, Chin. Phys. Lett. 20 (2003) 810–812.
[223] N. Wax, Selected Papers on Noise and Stochastic Process, in: Lecture Notes in Mathematics, vol. 426, Springer, New York, 1974.
[224] D. Freedman, Brownian motion and diffusion, Holden-Day, San Francisco, 1971.
[225] P. Walters, An Introduction to Ergodic Theory, Springer-Verlag, New York, 1982.
[226] C.M. Arizmendi, F. Family, Physica A 232 (1996) 119.
[227] O. Yevtushenkov, S. Flach, K. Richter, Phys. Rev. E 61 (2000) 7215.
[228] I. Derényi, M. Bier, R.D. Astumian, Phys. Rev. Lett. 83 (1999) 903.
[229] H. Qian, Biophy. Chem. 83 (2000) 35.
[230] M.D. McDonnell, N.G. Stocks, C.E.M. Pearce, D. Abbott, Stochastic Resonance: From Suprathreshold Stochastic Resonance to Stochastic Signal Quantisation, Cambridge University Press, 2008.
[231] K.L. Chung, Markov Chains With Stationary Transition Probabilities, Springer, 1967.

[232] S. Karlin, H.M. Taylor, A First Course in Stochastic Processes, Academic Press, 1975.
[233] A. Eistein, Ann. Physik 17 (1905) 549.
[234] A. Eistein, Ann. Physik 19 (1906) 371.
[235] G.E. Uhlenbeck, L.S. Ornstein, Phys. Rev. 36 (1930) 823.
[236] A. Einstein, Investigations on Theory of the Brownian Movement, Dover, New York, 1956.
[237] F.B. Knight, Essentials of Brownian Motion and Diffusion, Amer. Math. Soc. (1981).
[238] A.N. Borodin, P. Salminen, Handbook of Brownian Motion: Facts and Formulae, Birkhäuser, 2002.
[239] J. Zhang, B. Feng, The Geometric Theory of Ordinary Differential Equations and Bifurcation Problems, 3rd ed., Peking University Press, Beijing, 1997, (in Chinese).